TNO Institute of Environmental
and Energy Technology

Laan van Westenenk 501
P.O. Box 342
7300 AH Apeldoorn
The Netherlands

Telex 39395 tnoap nl
Phone +31 55 49 34 93
Fax +31 55 41 98 37

TNO-report

Results of Sexbierum Wind Farm; double wake measurements at 1.5 D, 2.5 D and 4 D

Reference number 93-271
File number 112324-22420
Date July 1993
NP

St-code
C19.3

Author
J.W. Cleijne

Keywords
- wind energy
- full-scale measurements
- wake effects

Intended for
Participants JOUR-0064
Participants JOUR-0087

Summary

In the framework of the JOULE-0064 'Full-scale Measurements in Wind Turbine Arrays' in the period between November 1992 - January 1993 measurements have been performed in the Sexbierum Wind Farm. The aim of the measurements is to provide data for the validation of wake and wind farm models, which are being developed simultaneously, and to provide input data for wind turbine load calculation programmes.

The campaign concerned measurement of the wind speed, turbulence and shear stress behind two wind turbines in line, which were at an inter-distance of 5 rotor diameters. The wind speed sensors were mounted on three masts at 1.5, 2.5 and 4 rotor diameters behind the second machine, respectively.

A database has been compiled containing 1-minute averaged values of the measured quantities. The database was analysed using a two-dimensional bin analysis with respect to the undisturbed wind direction and wind speed.

The analysis contains horizontal and vertical profiles of the:
- U-,V-, and W-component of the wind in the wake;
- turbulence intensities in three directions and turbulent kinetic energy in the wake;
- shear stresses u'v', u'w' and v'w' in the wake.

These quantities are presented both in dimensional and in non-dimensionalized form.

With the data base a useful set of data is created for the validation of wake and wind farm models.

Table of contents

List of symbols

a_{hub}	Weibull scale factor at hub height
c_P	Power coefficient
D	Rotor diameter
H	Hub height
I	Turbulence intensity (e.g. u'/U)
k	turbulent kinetic energy per unit mass $^1/_2(u'^2+v'^2+w'^2)$
k_{hub}	Weibull shape factor
M_{72}	Meteo mast 7, height 2 (= hub height)
P	Turbine Power
T_{36}	Turbine 36
T_{37}	Turbine 37
T_{38}	Turbine 38
U	wind speed component along the undisturbed wind
u'	rms value of turbulent velocity fluctuations in U-directions
u'v'	U-V component of turbulent shear stress
u'w'	U-W component of turbulent shear stress
U_0	undisturbed wind speed
$u_{0'}$	undisturbed U-component of turbulent velocity fluctuations
V	wind speed component perpendicular to the undisturbed wind direction
v'	rms value of turbulent velocity fluctuations in V-directions
v'w'	V-W component of turbulent shear stress
W	vertical wind speed component
w'	rms value of turbulent velocity fluctuations in W-directions
z	height
z_0	roughness height
δ	wind direction
κ	Von Kármán constant
λ	tip speed ratio
ρ	air density

suffix

max	maximum value
min	minimum value
0	undisturbed conditions

1 Introduction

Between November 1992 and January 1993 a detailed measuring campaign was carried out in the Sexbierum Wind Farm in order to collect experimental data on the wind speed, turbulence intensity and shear stresses in the wakes of two wind turbines in line. This report gives the results of the measurements and of the bin analysis of the data. Further, it describes the measuring conditions and the geometry of the wind farm and the turbines. Two other campains have been carried out and were reported. [Cleijne, 1992] describes measurements in the wake of 2 machines in line at 4 diameters behind the second turbine. [Cleijne, 1993] reports the measurements in the wake of a single turbine. The purpose of this report is to document the results of the analysis and to pass the information to the participants in the project Wake and Wind Farm Modelling (JOUR-0087), who will use it for the development and validation of wake models.

The measuring campaign is part of the CEC JOULE project 'Full-Scale measurements in Wind Turbine Arrays' (JOUR-0064). The project aims at collecting full-scale data for the purpose of:
- validation of wake and wind farm models;
- providing input data for load calculations.

To this end long term measurements and short term campaigns are carried out in various wind farms within the CEC.

In the Sexbierum wind farm the following quantities are monitored:
- fast rate wind speed data in wakes;
- wind turbine power;
- fatigue loads on various components, such as blades, hub and shaft.

In The Netherlands KEMA and TNO jointly carry out the measurements and the analysis of the wake data. KEMA is responsible for the measurements and pre-processing of the data; TNO is responsible for the experimental set-up and the analysis of the data.

Chapter 2 describes the experimental set-up of the measurements. It gives details on wind farm lay-out, properties of the wind turbines and measuring sensors and procedures. Chapter 3 describes the data analysis procedure, which has been applied and chapter 4 describes the results of the analysis.

2 Experimental set-up

2.1 Sexbierum wind farm

2.1.1 Lay-out

The Dutch Experimental Wind Farm at Sexbierum is located in the Northern part of The Netherlands at approximately 4 km distance of the seashore. The wind farm is located in flat homogeneous terrain, mainly grassland used by farmers for the grazing of cows. In the direct vicinity of the wind farm only a few scattered farms are found.

The wind farm has a total of 5.4 MW installed capacity consisting of 18 turbines of 300 kW rated power each. The wind turbines are placed in a semi-rectangular grid of 3×6 rows at inter-distances of 5 rotor diameters along one major grid line and at an inter-distance of 8 diameters perpendicular to this grid line (see figure 2.1). The direction of the rows is at 353° with the North.

Around the wind farm there are 7 meteorological masts, which enables the measurement of the undisturbed wind conditions for every wind direction. Further, the pressure and temperature are measured. Masts 4 and 6 are parallel to the prevailing wind direction and have wind sensors at 3 heights. The other 5 masts have sensors at hub height. Turbine T36 has been instrumented to study the wake effects on the wind turbine loads.

The prevailing wind direction in the wind farm is along the line T18 to T36. The wind climate at hub height is given by Weibull frequency distribution with scale factor a_{hub}=8.6 m/s and shape factor k_{hub}=2.1. The average wind speed is 7.6 m/s.

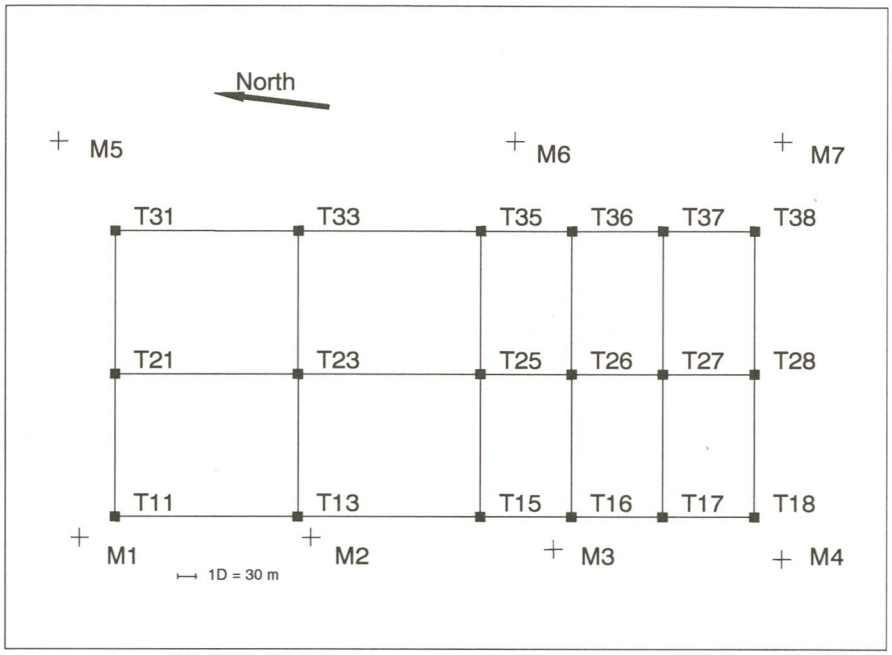

Figure 2.1 Lay-out of Sexbierum Wind Farm

2.1.2 Turbines

The wind turbines in the wind farm are HOLEC machines with three WPS 30/3 blades and with a rated power of 310 kW. The rotor diameter is 30.1 m, the hub height is 35 m. The turbines contain synchronous generators and operate at variable speed. In order to obtain maximum efficiency the tip speed ratio is kept constant up to a wind speed of 10 m/s. Above this wind speed the power is limited to 310 kW. Above 13 m/s the power is limited by means of pitch control. The machines have a cut-in wind speed of 5 m/s; a rated wind speed of 14 m/s and a cut out wind speed of 20 m/s.

The control computer of the turbine takes care of these action and also takes care of yawing. The input data for the yawing actions comes from the wind farm control computer.

Results of Sexbierum Wind Farm; double wake measurements at 1.5 D, 2.5 D and 4 D

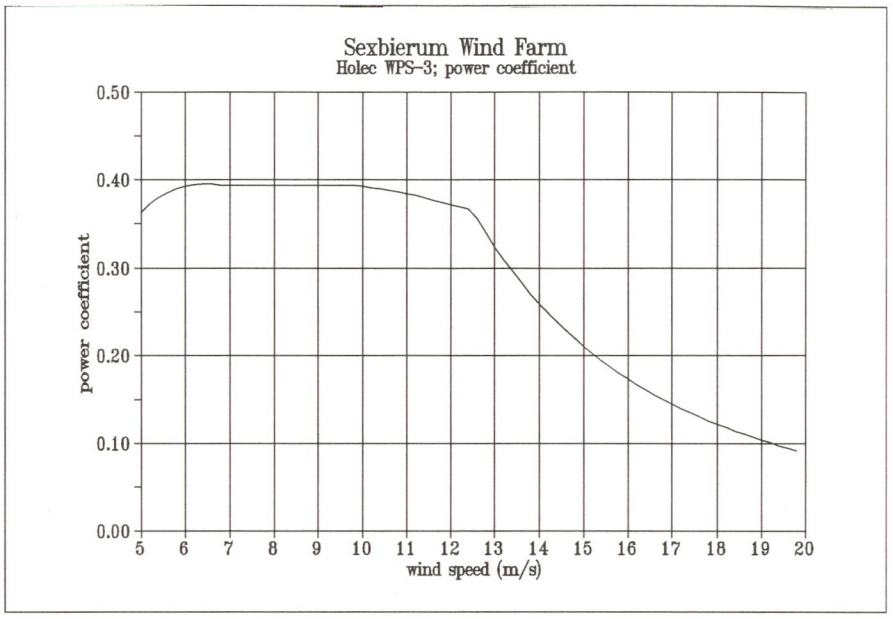

Figure 2.2 Calculated power coefficient of HOLEC WPS-30 wind turbine

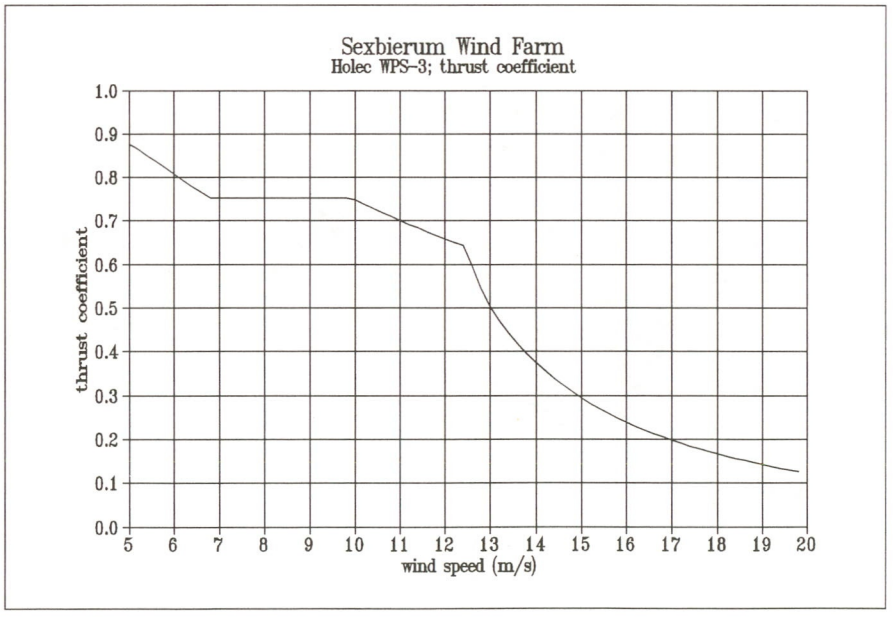

Figure 2.3 Calculated thrust coefficient of HOLEC WPS-30 wind turbine

Figure 2.2 gives the calculated power coefficient; figure 2.3 gives the calculated thrust coefficient of the wind turbine. In Annex A1 more detailed data can be found on the HOLEC wind turbine.

2.1.3 Data acquisition

The data-acquisition system and instrumentation of the wind farm serves the following purposes:
- monitoring and control of the wind farm;
- detailed measurements of the wake structure inside the farm;
- wake effects on the mechanical loads on the turbines;
- wake effects on the aggregate wind farm power;
- electrical behaviour of the wind farm.

For this purpose the wind farm has a central computer, which takes care of monitoring and control of the wind farm and a data-acquisition system consisting of measuring computers and data elaboration computers (see figure 2.4).

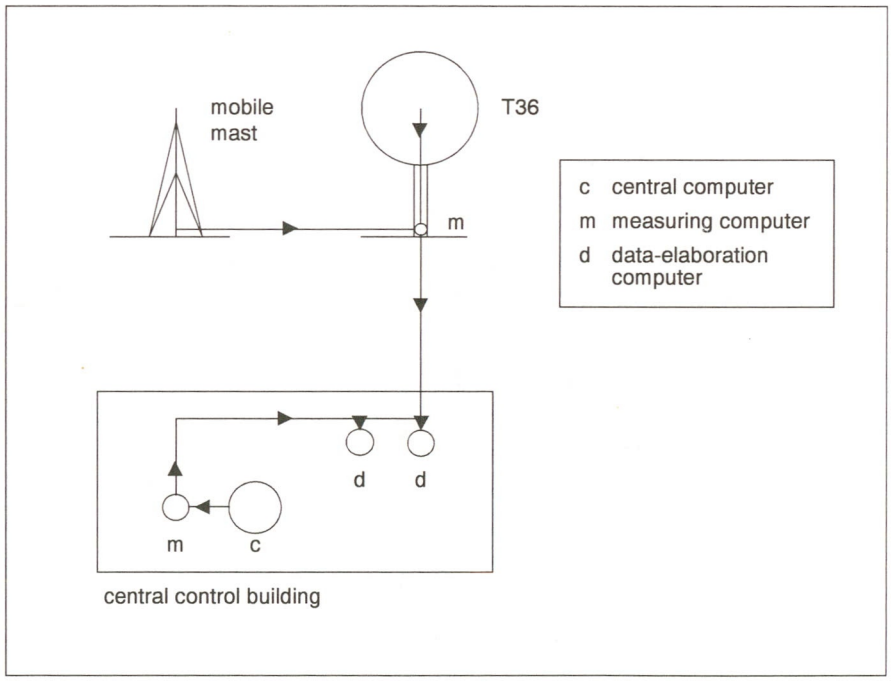

Figure 2.4 The data-acquisition system of the Sexbierum wind farm

The signals from the extra-instrumented turbine T36 are sampled at 32 Hz by a measuring computer inside the tower. The signals from the mobile measuring masts are also connected to this computer and sampled at 4 Hz.

Signals with respect to the electrical behaviour of the wind farm are sampled at 32 Hz by a measuring computer in the central control building. This computer is connected to the central computer which supplies at 1 Hz the following data:
- undisturbed wind speed and wind direction from the stationary wind masts;
- air pressure and temperature;
- status of each wind turbine.

All acquired data are passed to the two central data elaboration computers in the central control building. The data can be processed on-line using a statistical software or can be stored on tape or optical data for further processing off-line.

2.1.4 Instrumentation

Meteorological masts
The wind farm is surrounded by 7 fixed wind measurement towers. The locations of the towers are given in figure 2.1. Each tower has a wind anemometer and a wind vane at 35 m (hub height). The towers 4 and 6 have also wind sensors at 20 m and 50 m height. At mast 3 the temperature and the air pressure are measured. The signals from the meteorological tower are sampled at a rate of 1 Hz.

Instrumentation of turbines
Turbine T36 (see figure 2.1) has been extra instrumented. It contains sensors for the measurements of mechanical loads in the blades, the hub, the tower and the drive train. Sensors have been mounted for measurement of the pitch angle, blade position and nacelle direction. Further, various electrical signals are measured. The signals are sampled at a 32 Hz sampling rate. A complete list of the measured signals is given in annex A2.

Mobile wind measuring masts
There are three mobile masts in the wind farm for detailed wake measurements. It is possible to install the masts at any place inside the wind farm enabling detailed wind measurements of the wake structure.

One mast is equipped with 3-component propeller anemometers at 47 m, 35 m and 23 m, respectively. At heights of 41 m and 29 m two extra cup anemometers have been mounted. The other two masts contain 3-component propeller anemometers at 35 m. The signals from the mobile masts are sampled at a 4 Hz sampling rate.

The 3-component propeller anemometer consists of three light-weight carbon fibre propellers mounted on a pyramid-shaped rig at angles of 30° relative to each other. Combination of the three anemometer signals gives the X, Y and Z components of the wind. The sensor was calibrated in a wind tunnel and yields reliable results within a cone of approximately 30° relative to the sensor centre-line.

2.2 Measuring campaign

2.2.1 Description

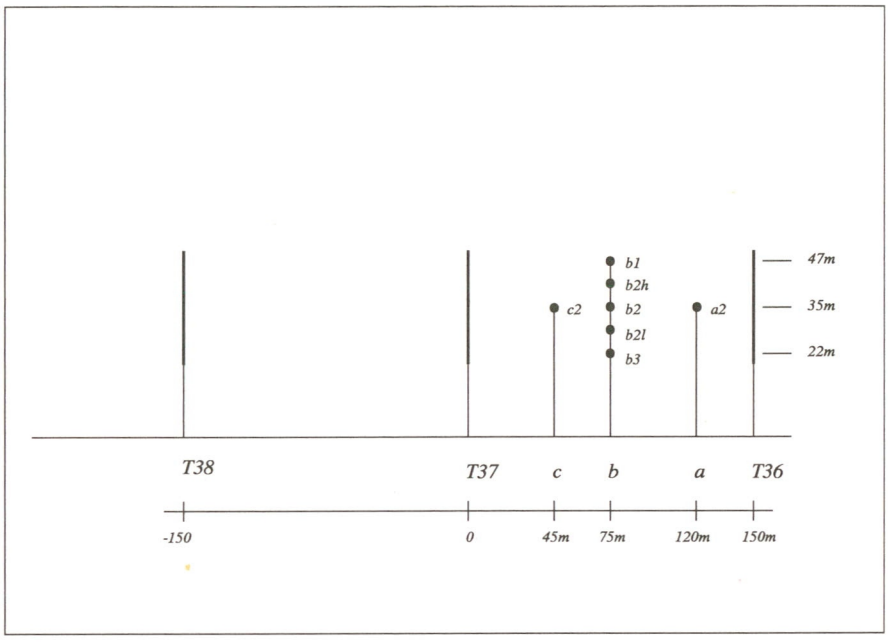

Figure 2.5 Experimental set-up during the measuring campaign

Between November 1992 and January 1993 measurements have been made in the double wake of T38 and T37 (see figure 2.5). In the indicated direction the distance between the turbines is 150 m, i.e. 5 rotor diameters.

Table 2.1 Overview of the measured and stored data

Sensor	Signal
a2..c2	U, V, W, U_{max}, U_{min}, V_{max}, V_{min}, W_{max}, W_{min}, u'^2, v'^2, w'^2, u'v', u'w', v'w'
b2l, b2h	U, u', U_{max}, U_{min}
P38	P, σ_P, P_{max}, P_{min}
wvel72	U_0, u'_0, U_{0max}, U_{0min}
wdir72	δ_0, $\sigma_{\delta 0}$, δ_{0max}, δ_{0min}

The measured data were stored on hard disk and every day a back-up was made on magnetic tape. Later, the tapes were pre-processed off-line into 1-minute averaged samples.

2.2.2 Observations

During the campaign no serious problems arose. From the previous measuring compaigns it was known that the measurements at the meteorological masts were disturbed by the presence of a lightning rod on top of the masts. The magnitude of the disturbance has been estimated on the basis of wind speed measurements at mast M4. The windspeeds measured at level 3 were corrected for height using a logarithmic profile and compared with the wind speed measurement at level 1.

Figure 2.6 presents the results of this comparison. At wind directions around 180 degrees an underprediction of 5% is found, while wind speeds are 5% overpredicted at a wind direction of 200 degrees, approximately.

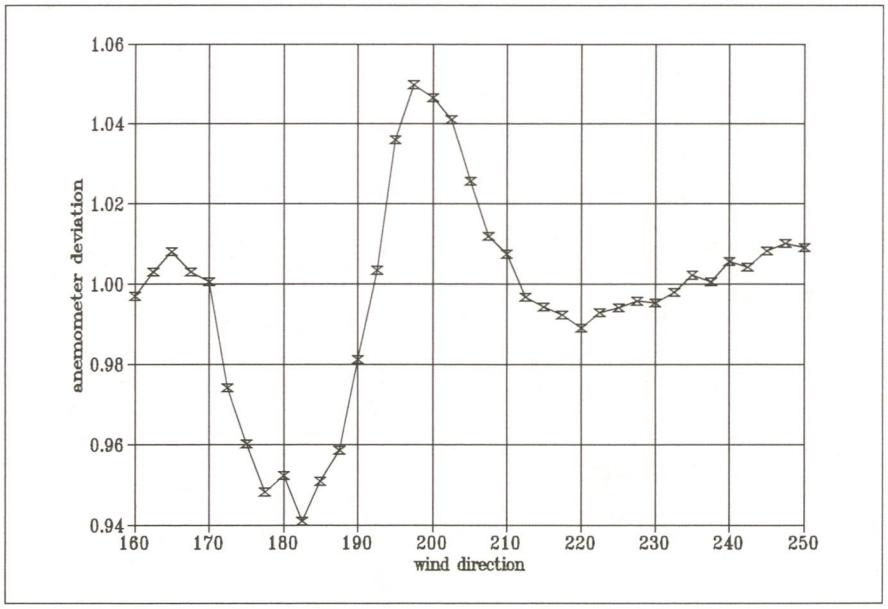

Figure 2.6 Disturbance of top anemometers by lightning rod

The dated presented in the next chapter have not been corrected for this effect, since the exact wind directions for which the deviations occur at mast M72 are not known.

The effects on the measurement results are twofold:
- Measured quantities are sometimes stored in a bin too high or too low according to the deviation in the undisturbed wind measurements.
- Quantities non-dimensionalized with U_0 or u'_0 may deviate due to these disturbances.

3 Analysis

3.1 Pre-processing and resulting database

A first data-reduction and quality control of the measured data was done during pre-processing of the data. The 1 Hz and 4 Hz time series of the measured quantities were manipulated in order to obtain time series of 1-minute averages of various quantities such as the wind speed, the turbulent velocities and the shear stress. Table 2.1 gives an overview of the time series contained in the data base. The 1-minute data have served as the working data base. The chosen format makes it possible to combine the 1-minute averages into samples with multiple-minute averages. Annex A3 gives the statistical operations used for the data manipulation.

3.2 Time averaging

Before the data base was further analysed, the samples were combined to obtain 3-minutes averaged quantities. Considerations for selecting a period of 3 minutes were the following:

- **stationarity of the data**
  It is common practice to assume a spectral gap for wind velocity data between 10 minutes and 1 hour. Shorter averaging periods will result in non-stationary data;

- **coherence between undisturbed wind signal and wake signal**
  Meteorological mast 7 and the mobile masts are 350 m apart, assuming a wind speed of 8 m/s, this corresponds to a delay of 45 seconds, approximately. In order to obtain a reasonable coherence between the wake wind data and the undisturbed wind data it is necessary to use an averaging period of more than this period.

- **effect of slow wind direction variations**
  If the averaging period is chosen too long, slow variations in the wind direction will blur the details of the wake.

- **number of available records**
  Longer averaging periods result in less samples. A 3-minutes averaging period resulted in a database with 1444 samples.

- **effect on wind turbines**
  Power curves for wind turbines are most often determined using averaging periods of 10 minutes; Wind fluctuations shorter than 1 minute are most important for the determination of wind turbine loads. Slower fluctuations are absorbed by the control system.

The wake deficit profiles are hardly affected by the averaging period. However, non-linear signals, such as turbulent velocities and shear stresses are indeed affected by the changing averaging period. Longer averaging periods result in higher turbulent velocities, for instance. Nevertheless, it is not easy to select an optimum averaging period. Taking into account the arguments listed above, it was decided to analyse the data on the basis of 3-minutes averaged samples.

3.3 Frame of reference

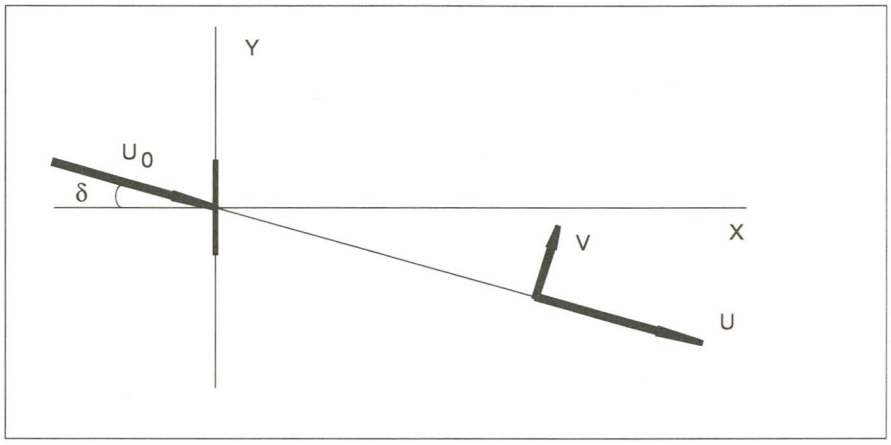

Figure 3.1 Definition of the frame of reference

Besides scalar quantities, such as the wind turbine power and the total turbulent kinetic energy k, also vector quantities (wind vector) and tensor quantities (turbulent co-variance matrix) had to be analysed. Therefore it was necessary to define a proper frame of reference for the presentation of the data. It was decided to couple the frame of reference of the wake data to the co-ordinate system of the undisturbed wind. The definition of the frame of reference is given in figure 3.1. The undisturbed wind direction is given with respect to the line connecting the turbines T38 and T36, defined as 0 degrees. The u-component is parallel to the undisturbed wind, the v-component is perpendicular to the undisturbed wind in the horizontal plane. The w-component is in the vertical direction. u,v and w define a right-handed co-ordinate system. This conforms to the normal meteorological definitions. Before the 3-minutes samples were bin-sorted, they were converted first to the above given coordinate system, using the co-ordinate transformation formulas given in Annex A3.

During the analysis of the data it showed that the sensor used to measure the undisturbed wind direction had a misalignment of 5°. Prior to the analysis, the undisturbed wind direction and the other measured quantities have been corrected for this misalignment.

3.4 Bin-sorting

The 3-minutes samples were sorted into different bands of undisturbed wind speed and wind direction. Between 5 m/s and 12 m/s a bin width of 1 m/s was used; above 12 m/s the bin width was taken equal to 2 m/s. The selected wind direction bin width was 2.5°.

For each bin the mean value, variance, minimum and maximum values of the measured quantities were determined and saved in separate files. Together with these quantities the number of samples in the bin, the average undisturbed wind speed and the average wind direction were saved.

Since the wind turbines operate at constant tip speed ratio in the interval 6-10 m/s, it was expected that the wake effects would not vary much over this speed range. A selected number of bin analyses has been made using a single wind speed bin of 5-10 m/s.

3.5 Dimensionless quantities

Except in dimensional form the results are also presented in a non-dimensionalized form.
First, the measured quantities have been non-dimensionalized with the undisturbed wind speed:
- U/U_0, V/U_0, W/U_0;
- u'/U_0, v'/U_0, w'/U_0, k/U_0^2, u'/u'_0;
- $u'v'/U_0^2$, $u'w'/U_0^2$, $v'w'/U_0^2$.

Second the quantities have been non-dimensionalized using local parameters:
- V/U, W/U;
- u'/U, v'/U, w'/U, k/U;
- u'v'/k, u'w'/k, v'w'/k.

In the next chapter the results of the analysis are presented.

4 Results

This chapter contains the results of the analysis performed on the double wake data described in the previous chapters. First, the undisturbed wind conditions during the measuring period are described. Secondly, the power output of the turbine in the free-stream (T38) is given. The next sections describe the results of the wind measurements on the mobile measuring masts. Successively, the wind speed, the turbulence levels and the shear stresses in the wake are treated for a selected number of cases. A comprehensive overview of the analysis results can be found in annex A4.

4.1 Undisturbed wind conditions

This section describes the undisturbed wind conditions at the Sexbierum wind farm during the described measuring period.

Figure 4.1 gives the wind speed distribution during the measuring period. It shows that the majority of the data has been found between 6 and 8 m/s. The mean wind speed during the measuring period was 9.2 m/s. The figure also shows that the wind direction distribution is non-symmetrical about the axis. Figure 4.2 shows the frequency distribution during the measuring campaign.

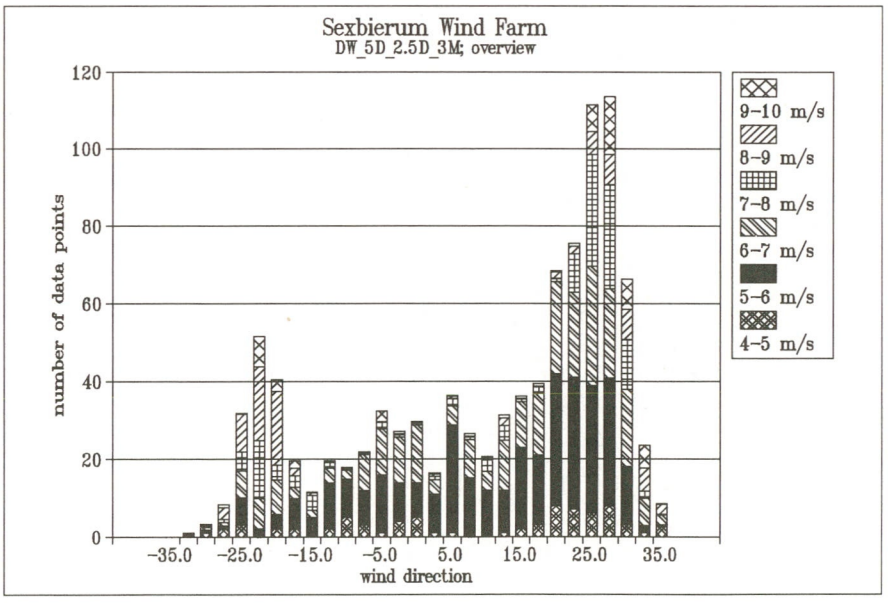

Figure 4.1 Overview of available data

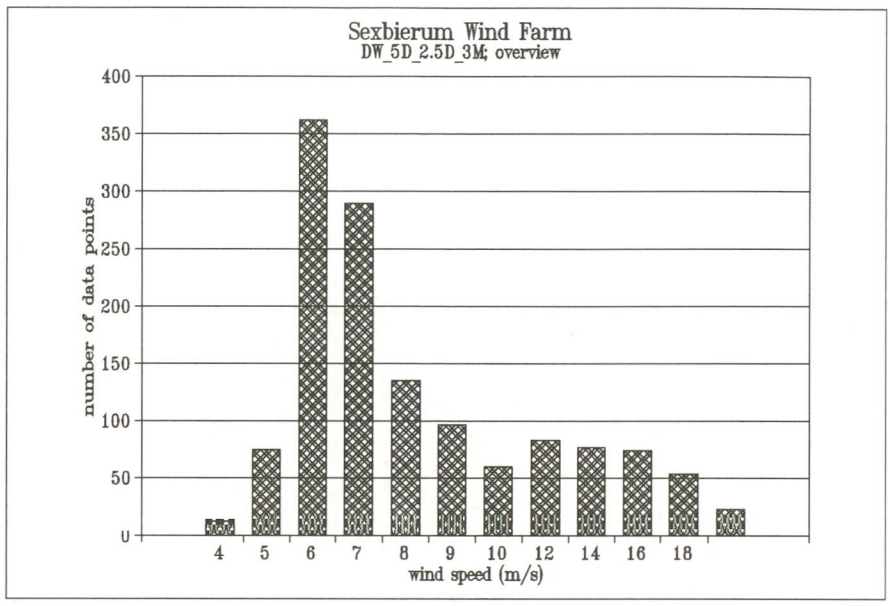

Figure 4.2 Frequency distribution of the wind speed during the measuring campaign

According to [Cleijne, 1992] the roughness length upstream of turbine T38 is equal to $z_0=0.045\pm0.07$ m.

4.2 Wind turbine power

4.2.1 Free-stream power curve; power coefficient

Figure 4.3 gives the power curve of turbine T38 using data from all available wind directions. Further, the figure shows the power coefficient of T38 derived from the power curve [Cleijne, 1992].

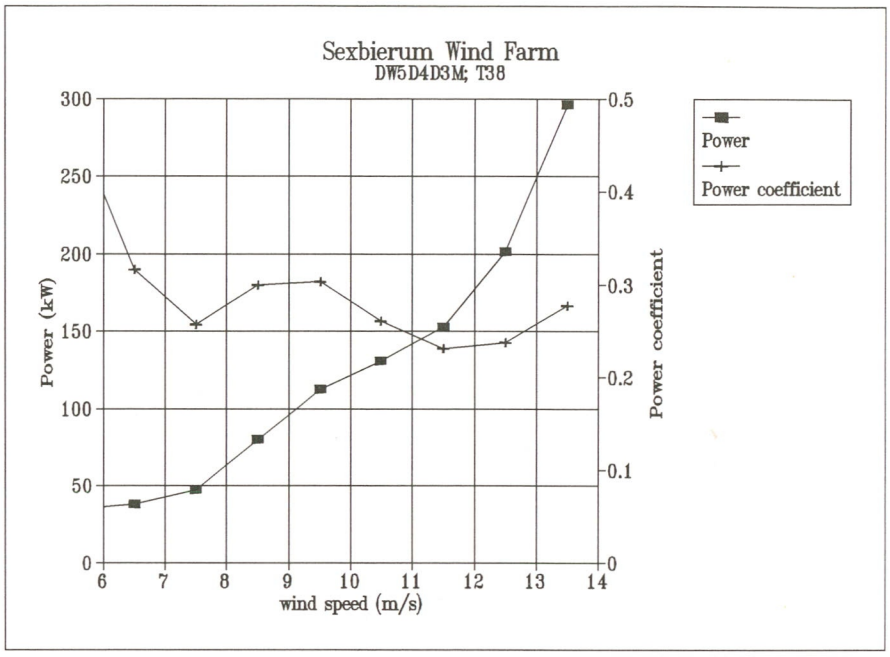

Figure 4.3 Power curve and power coefficient of wind turbine T38, based on 3-minutes averages

The figure shows that the power coefficient is more or less constant in the range between 6 and 10 m/s, which is brought about by the machine's control strategy.

4.3 Wake deficit

4.3.1 Wake deficit per bin

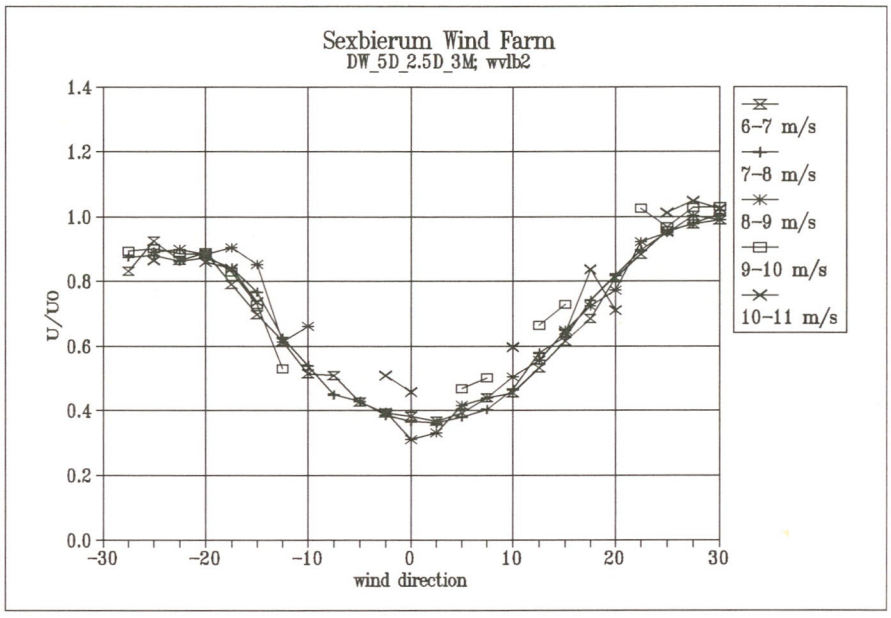

Figure 4.4 Wind speed ratio U/U_0 at sensor b2 as a function of the undisturbed wind direction

Figure 4.4 shows the wind speed ratio U/U_0 at sensor b2 as a function of the undisturbed wind direction for the wind speed classes between 6 m/s and 11 m/s. The graphs of U/U_0 of the other sensors have been gathered in annex A4.

The figure shows that the wind speed ratio U/U_0 is almost equal for the depicted wind speed classes, which can be explained by the fact that the wind turbines operate at constant tip speed ratio between 6 and 10 m/s. In this range the thrust or axial force is therefore almost constant.

At the wake centre-line U/U_0 reaches a minimum of 0.45, approximately. At an undisturbed wind direction of 20-25 degrees the edge of the wake is observed and U/U_0 is equal to unity. This means that the double wake is approximately 2 diameters wide. Overspeeding ($U/U_0>1$) which is sometimes seen at the wake edge, can not be observed in this case. The wake profile is asymmetrical due to disturbance of the upstream wind conditions at mast 72, brought about by a lightning rod mounted on top of the mast.

4.3.2 Aggregated results

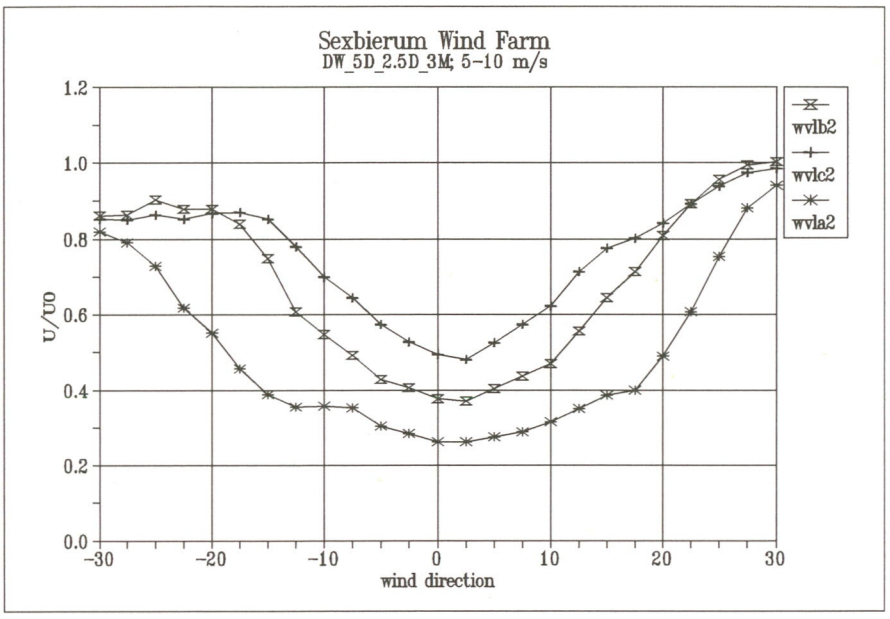

Figure 4.5 Wind speed ratio U/U_0 as a function of wind direction for sensors b2, c2 and a2

Figure 4.5 shows the aggregated results in the wind speed range of 5-10 m/s for the three sensors b2, c2, a2 at hub height. Sensor a2 is at 1.5 D behing T37; sensor b2 at 2.5 D and sensor c2 at 4D.
At x = 1.5 D the wind speed ratio is U/U_0 = 0.35; at x = 2.5 D a value of U/U_0 = 0.38 is found and at x = 4 D the wind speed ratio is 0.48.
Clearly, the flattened profile at x = 1.5 D develops in a more pronounced profile downstream.

With the undisturbed wind direction changing, the wake configuration changes. At 0 degrees the wakes are fully immersed, but for larger angles the wakes only partially overlap. However, at one particular wind direction the three sensors give the wind speed at different positions in the wake, but for identical wake configurations.

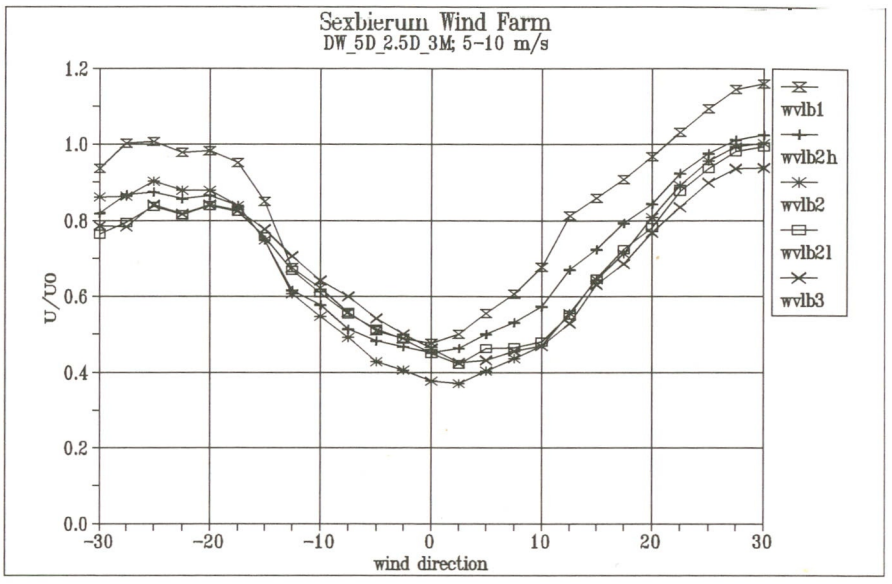

Figure 4.6 Wind speed ratio U/U_0 as a function of wind direction for sensors b1, b2h, b2, b2l and b3

Figure 4.6 gives the ratio U/U_0 at the 5 sensors mounted at different heights on mast b. The figure clearly reveals that the wake profiles are almost identical in shape at the given heights, with the lowest values of U/U_0 at hub height. However, the figure also shows that the profiles are asymmetrical. For negative wind directions the measured profiles coincide, while for positive wind directions they are clearly different in magnitude. The effect is caused by systematic errors in the undisturbed wind measurement at mast M7 as described in section 2.2.2.

4.4 Turbulence intensity

4.4.1 Turbulence intensity data per bin

In this section we show the results of the analysis on the measured turbulence in non-dimensional form.

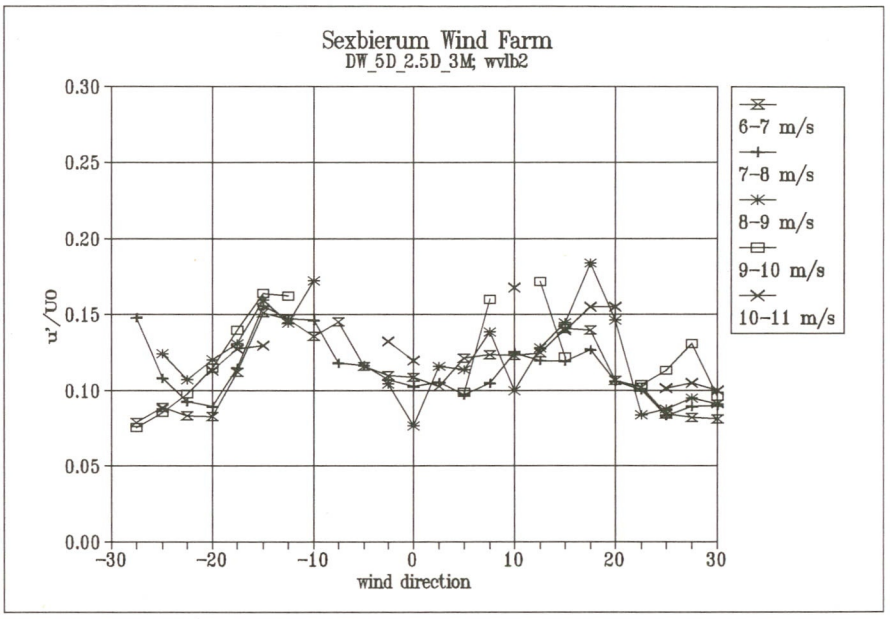

Figure 4.7 Turbulence intensity u'/U_0 as a function of wind direction at sensor b2

Figure 4.7 shows the turbulence intensity (non-dimensionalized with U_0) of the horizontal wind component for sensor b2 as a function of the wind direction. Figures 4.8 and 4.9 show the lateral and vertical turbulence intensity. The figures show that the turbulence intensity increases towards the centre of the wake. Unlike the lateral and the vertical turbulence intensity, the u-component shows peaks at a wind direction of approximately 15 degrees, which corresponds with the locus of the maximum wind speed gradient (see figure 4.4), which corresponds with maximum turbulence production.
Although the figures show some scatter, it seems that the turbulence intensity scales with U_0.

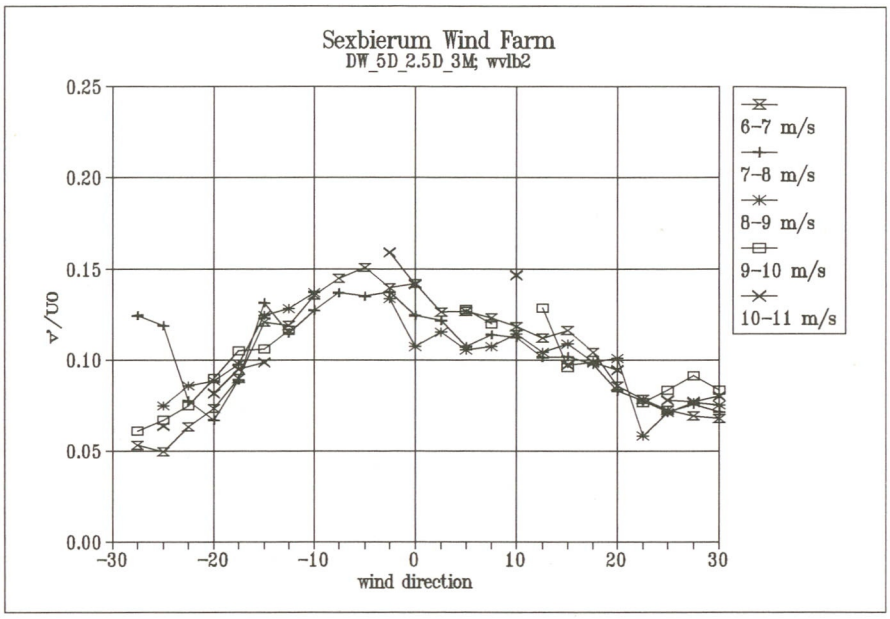

Figure 4.8 Lateral turbulence intensity v'/U_0 as a function of wind direction at sensor b2

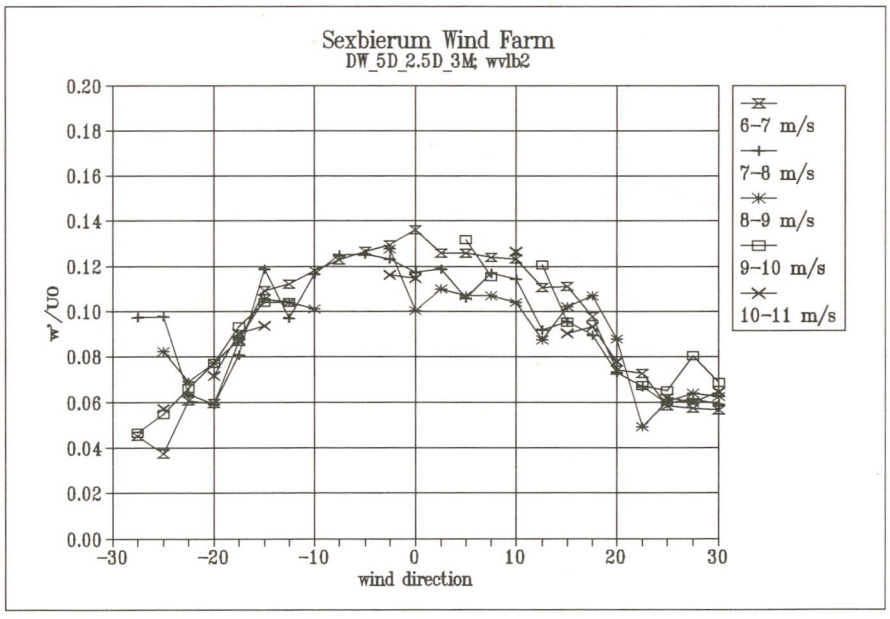

Figure 4.9 Vertical turbulence intensity w'/U_0 as a function of wind direction at sensor b2

Figure 4.10 shows the turbulent kinetic energy k (non-dimensionalized with U_0) as a function of the wind direction. The behaviour of k is roughly the same as that of the components of the turbulence.

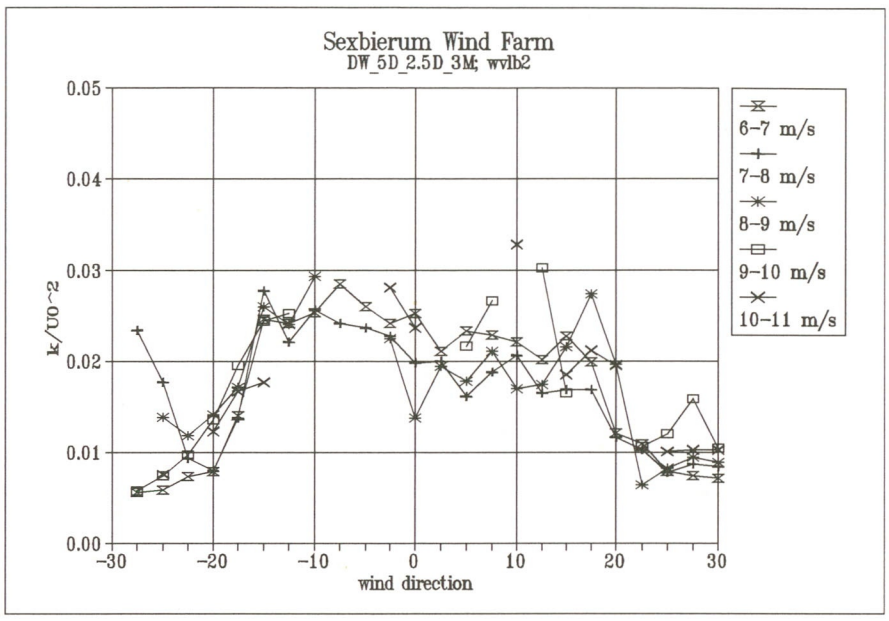

Figure 4.10 Turbulent kinetic energy k/U_0^2 as a function of wind direction at sensor b2

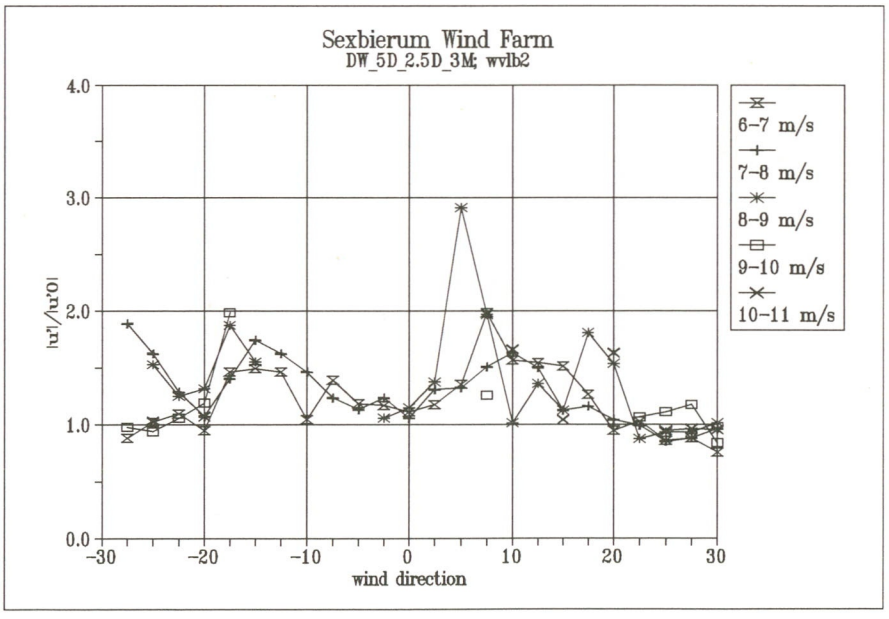

Figure 4.11 Ratio of wake turbulence and undisturbed turbulence u'/u_0' as a function of wind direction at sensor b2

In figure 4.11 the ratio u'/u'_0 is given as a function of the wind direction. The figure shows that the turbulence level is increased in distinct peaks, although the graph contains considerable scatter (due to scatter in u'_0). The turbulence level is increased with the factor 1.5 - 1.8, approximately.

4.4.2 Aggregated results

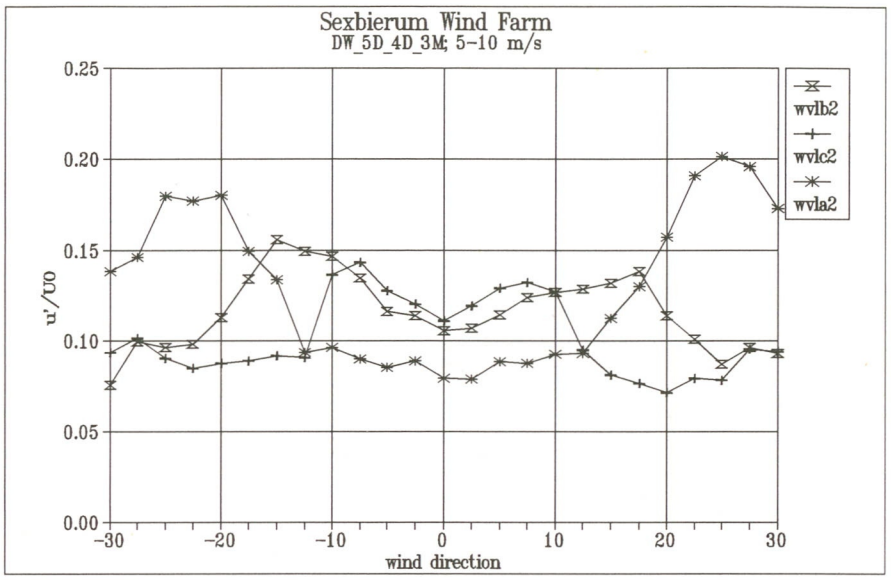

Figure 4.12 Aggregated turbulence intensity u'/U_c at different distances behind the rotor (wvla2: x = 1.5 D; wvlb2: x = 2.5 D; wvlc2: x = 4 D)

Figure 4.12 shows the development of the turbulence intensity behind wind turbine T38. At 1.5 D two distinct turbulence peaks are visible, which are connected by a flat plateau. The turbulence peaks reflect the developing shear layers, while the flat plateau reflects the potential core, where the wind speed is uniformly lower.
Further downstream, at 2.5 D and 4 D the shear layers diffuse and the peaks in the turbulence levels decrease.

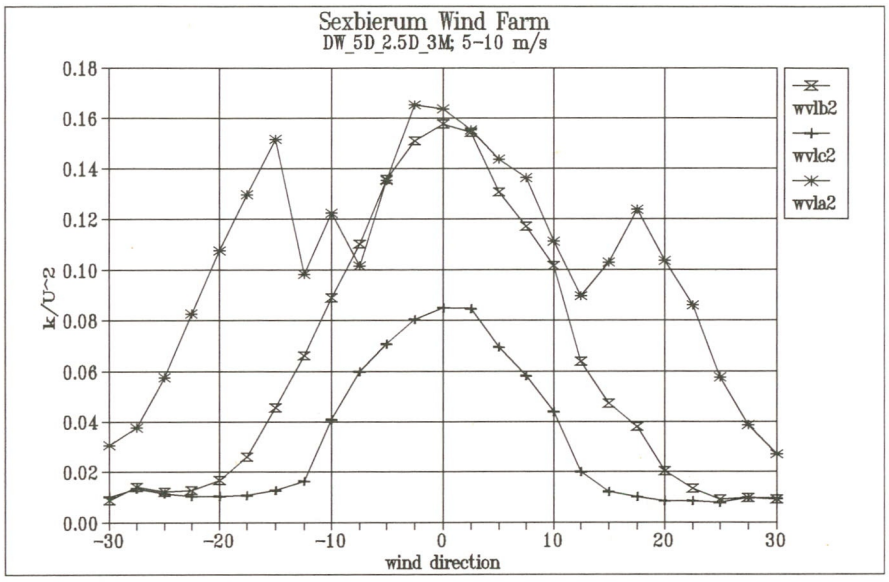

Figure 4.13 Aggregated turbulent kinetic energy k non-dimensionalized with the local windspeed U at x = 1.5 D (wvla2); x = 2.5 D (wvlb2) and x = 4D (wvlc2)

Figure 4.13 shows the development of the turbulent kinetic energy non-dimensionalized with the local wind speed U as a function of the downstream distance. At x = 1.5 D (wvla2) the turbulent kinetic energy displays two clear peaks at approximately half the wake width. At larger distances these peaks have disappeared due to turbulent diffusion. At x = 1.5 D we find a maximum value for $k/U^2 \approx 0.17$; at x = 2.5 D a maximum value of $k/U^2 \approx 0.16$ is found and x = 4D we find a value of 0.08, approximately.

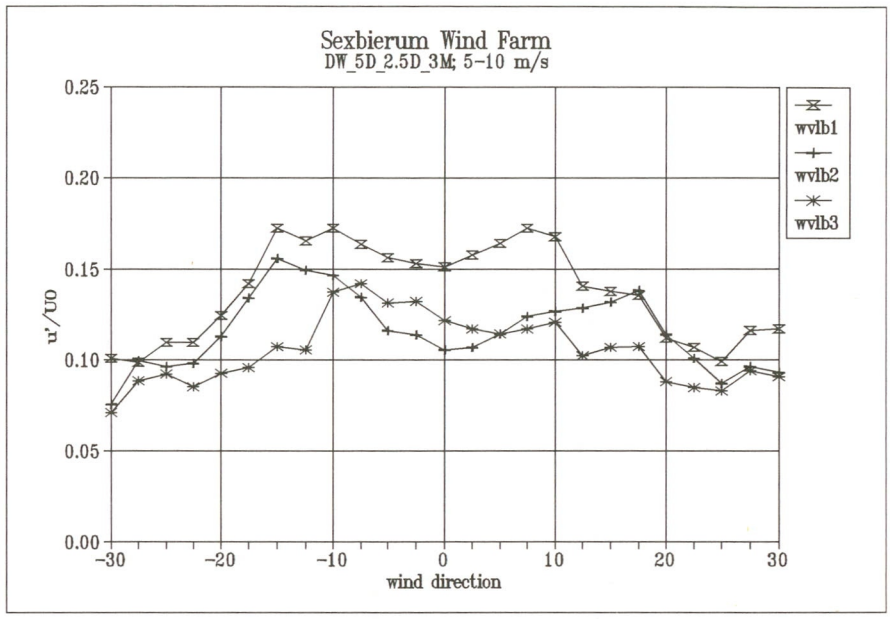

Figure 4.14 Aggregated turbulence intensity u'/U_0 as a function of wind direction at mast b

Figure 4.14 depicts the turbulence intensity u'/U_0 at mast b for the positions 1, 2 and 3. Clearly, the turbulence intensity is the highest at the top-most sensor $u'/U_0 = 0.17$ and lowest at the bottom-most sensor $u'/U_0 = 0.14$. This corresponds well to what is expected. As production of turbulence is related to the wind velocity gradient, the highest turbulence is expected where the gradients are at maximum. At the highest sensor position the boundary layer wind velocity gradient is increased by the presence of the wake, while the wake decreases the gradient at the lowest sensor position (see figure 4.21).

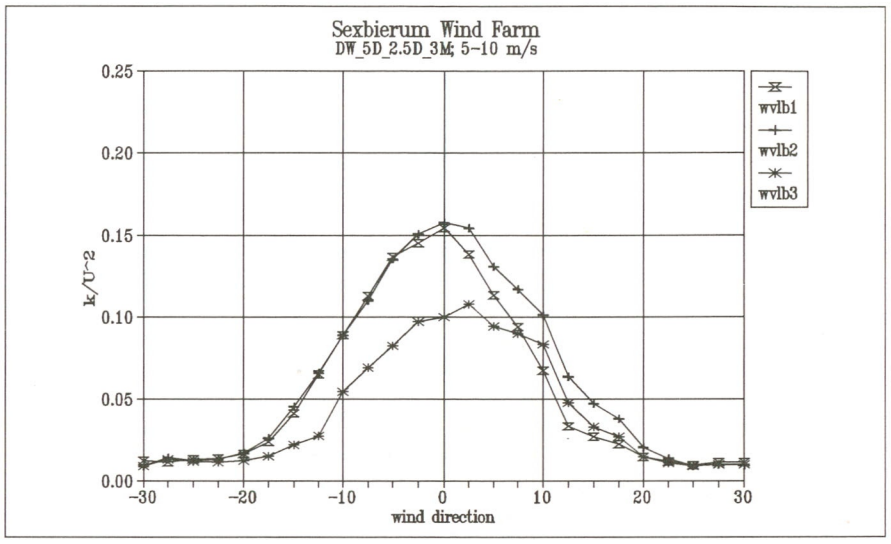

Figure 4.15 Turbulent kinetic energy non-dimensionalized with local velocity as a function of wind direction

Figure 4.15 depicts the turbulent kinetic energy non-dimensionalized with the local wind speed. The curves have a more or less Gaussian shape and the lowest value k/U^2 is found at the bottom most sensor.

4.5 Shear stress

4.5.1 Shear stress per bin

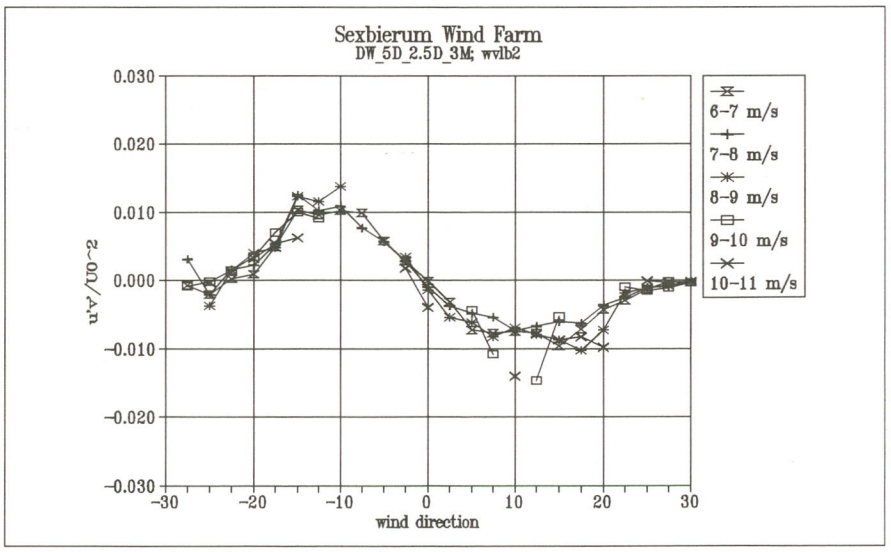

Figure 4.16 Shear stress $u'v'/U_0^2$ as a function of wind direction at sensor b2

The Reynolds-stress u'v' is the turbulent shear stress which is the driving force for the recovery of the wake deficit in horizontal direction. Figure 4.16 shows the shear stress u'v' non-dimensionalized with the undisturbed wind speed U_0 against the undisturbed wind. Starting from the right side of the figure (positive wind directions) and going to the negative wind directions it shows that at the edge of the wake $u'v'/U_0^2$ is equal to zero and then shows a minimum of -0.010. At 0° wind direction it goes through zero, it then shows a maximum of 0.01 before it relaxes again to 0 at the left edge of the wake. Generally speaking this is expected, since it is generally assumed that the shear stress is proportional to the local wind shear, i.e. the horizontal wind gradient. The fact that the curves return to zero at the edge of the wake, and that they cross the x-axis at 0° wind directions gives confidence in the quality of the data. Scaling of the data with U_0 seems to be successful.

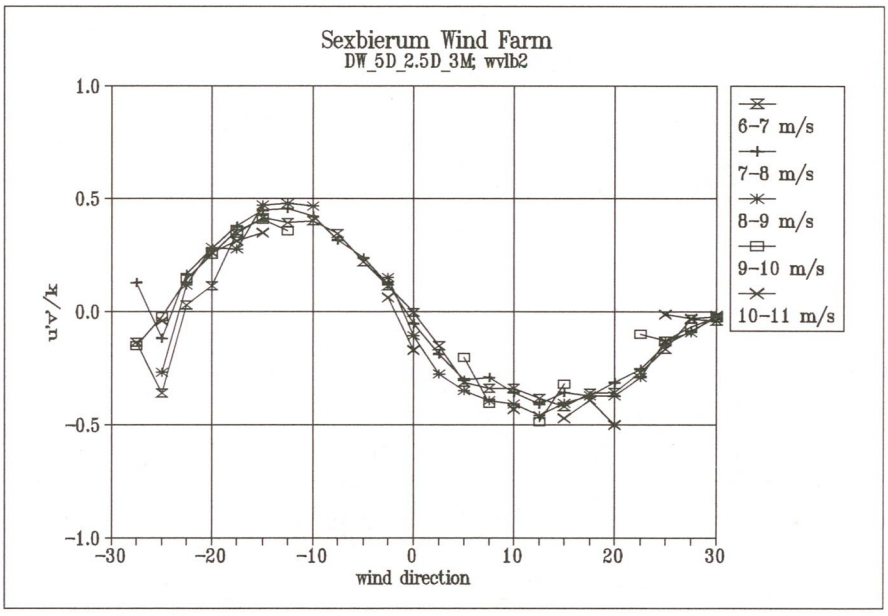

Figure 4.17 Shear stress u'v' non-dimensionalized with the local turbulent kinetic energy as a function of wind direction at sensor b2

The profile for u'v' shows to be asymmetrical. This is consistent with the measurements of the turbulence intensity and the horizontal wind profile. Figure 4.17 shows that if the shear stress is not non-dimensionalized with the undisturbed wind speed, but with a local quantity such as k, the asymmetry partly disappears. The asymmetry is caused by the disturbance of the measurement of wind speed U_0 by the presence of a lightning rod on top of the measuring mast.

4.5.2 Aggregated results

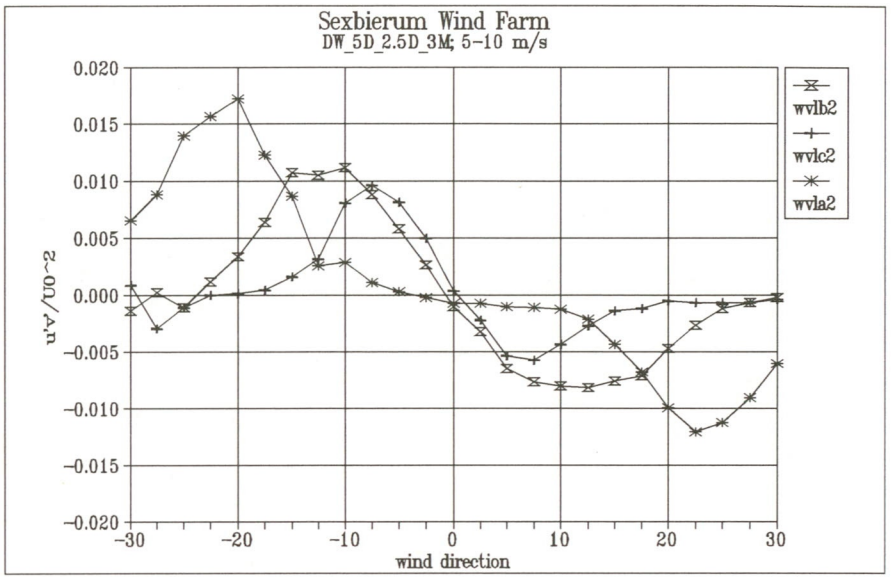

Figure 4.18 Non-dimensionalized shear stresses $u'v'/U_o^2$ as a function of wind direction in wind speed bins 5-10 m/s
Distance x = 1.5 D: wvla2
x = 2.5 D: wvlb2
x = 4.0 D: wvlc2

Figure 4.18 shows the horizontal shear stress as a function of wind direction at 3 different downstream distances x = 1.5 D; x = 2.5 D and x = 4.0 D.
At 1.5 D downstream the wind turbine the ring-shaped shear layer can be recognized, (shear maximum at -20°; shear minimum at +22.5°), which has not diffused to the centre of the wake yet,
At the positions further downstream (wvlb2, wvlc2) turbulent diffusion causes the shear layers to extend across the wake completely. With the relaxation of the wake the maximum values of $u'v'/U_o^2$ decrease with increasing distance.

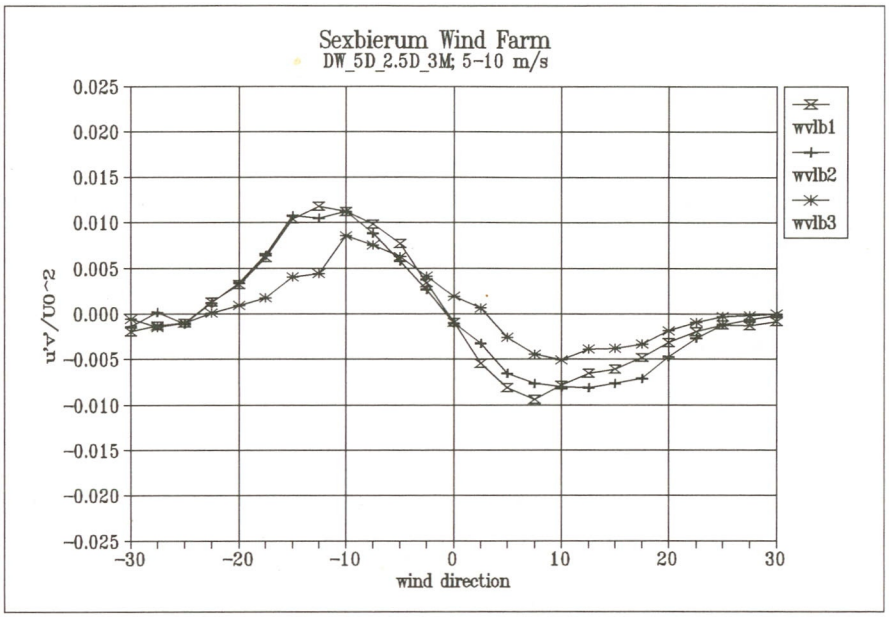

Figure 4.19 Shear stress $u'v'/U_0^2$ as a function of wind direction for sensors b1, b2 and b3

Figure 4.19 shows the non-dimensional shear-stress $u'v'/U_0^2$ for the three sensors at mast b as a function of the undisturbed wind direction. Eddy-viscosity theory for turbulence assumes that the turbulent shear stress is proportional to the local shear. This is clearly reflected in the curves of figure 4.19. Outside the wake no horizontal wake effect is present and hence the horizontal wind gradient is zero. At the maximum gradient dU/dy shear stress reaches a maximum, after which it decreases zero, where the wind speed shows a minimum. For larger wind directions the shear shows a similar behaviour but of an opposite sign.

The shape and the magnitude of the shear stress curves compare well with results of wind tunnel tests [Smith].

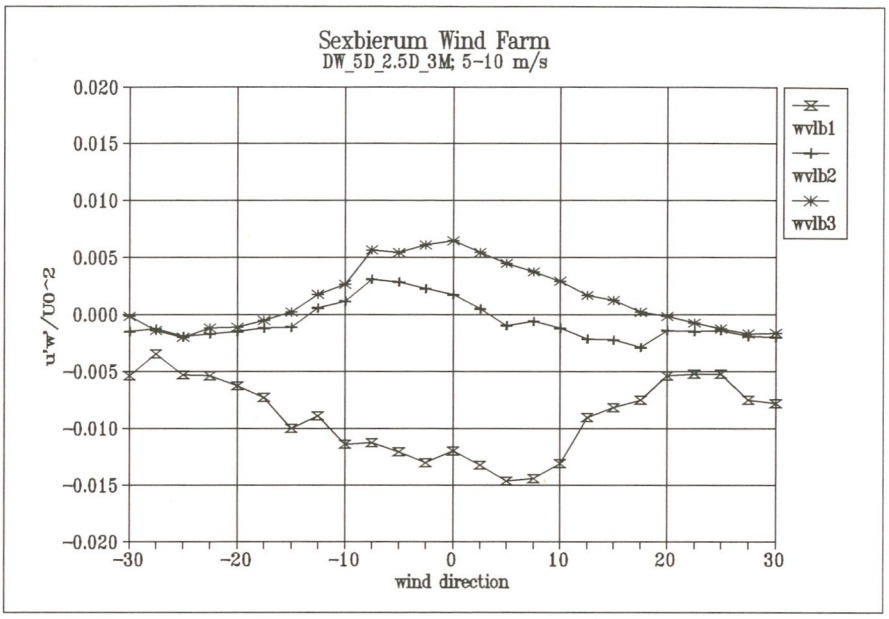

Figure 4.20 Shear stress $u'w'/U_0^2$ as a function of wind direction for sensors b1, b2 and b3

Figure 4.20 shows the non-dimensional turbulent shear stress $u'w'/U_0^2$ as a function of the wind direction at the three sensor positions b1, b2, b3. The graphs show quite a distinct behaviour from the horizontal shear.
The shear stress u'w' is proportional to the vertical wind speed gradient dU/dz. Outside the wake the u'w' is negative corresponding to the shear stress in the atmospheric boundary layer. Traversing through the wake at the top position b1, the vertical gradient increases with the increasing wake effect and so u'w' becomes more negative (figure 4.21). At the bottom sensor b3 the situation is different. When the wind direction changes the wake effect becomes stronger; the wind gradient and hence u'w' changes sign.

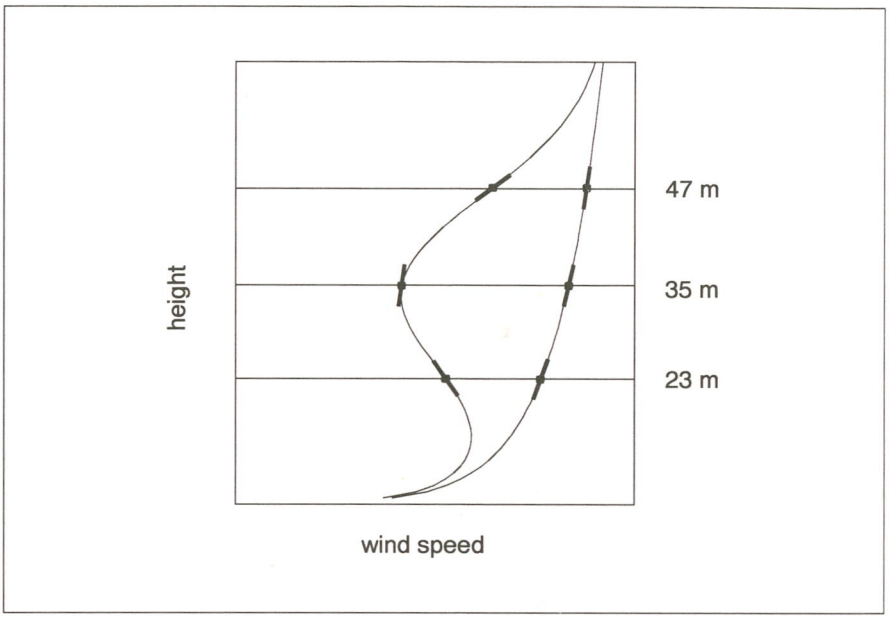

Figure 4.21 Change of the vertical wind gradient under influence of the wake deficit

4.6 Reproducibility

The present measurement campaign includes measurements at x = 4 D. In a previous campaign described in [Cleijne, 1992] measurements were also taken at this position, which makes it possible to get an idea about the reproducibility of the measurements. The measurements were taken under similar conditions.

Figure 4.22 depicts the wind speed ratio and the horizontal shear stress recorded during the two campaigns. Clearly, the measurements almost overlap, showing a very good reproducibility.

Results of Sexbierum Wind Farm; double wake measurements at 1.5 D, 2.5 D and 4 D

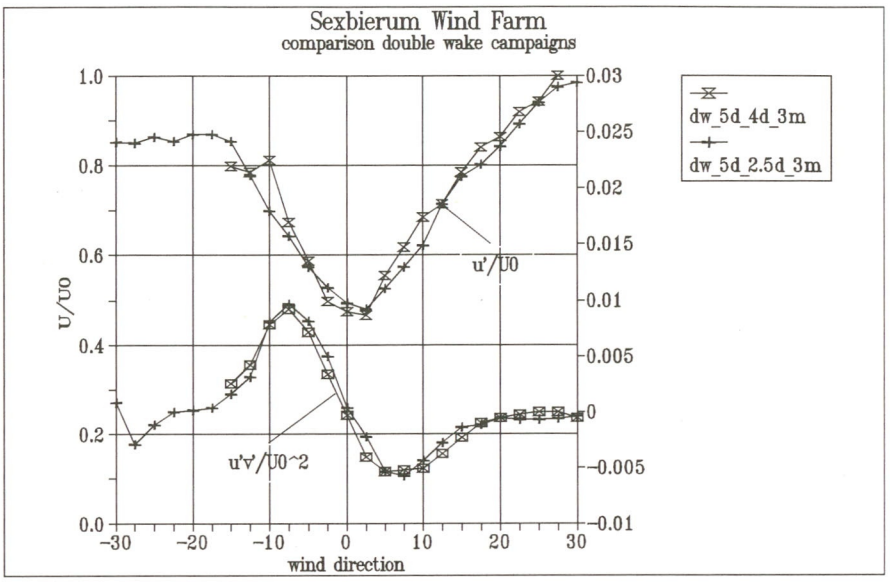

Figure 4.22 Comparison of wind speed ratio and horizontal shear stress measurements at x = 4 D in two different measuring campaigns
DW-5D-4D-3M: March 92 - April 92
DW-5D-2.50-3M: November 92 - January 93

5 Conclusions and recommendations

The measurement campaign in the wake of two wind turbines in line has resulted in a useful data base for the validation of wake and wind farm models and for input to wind turbine load calculation programs.

The data base is built up of 1444 3-minute samples containing data on undisturbed wind conditions, wind speed components, turbulence and shear stress data. The data base has been analysed with respect to the undisturbed wind conditions, i.e. with respect to wind speed and wind direction outside the wind farm.

The wake deficit at various measuring positions downstream the second turbine has been determined at x = 1.5 D; x = 2.5 D and x = 4 D. The measurements do not show the shape of the individual wakes of the upstream turbines clearly, but give a picture of one single merged wake. The horizontal wake profile at x = 1.5 D has a horizontal plateau near the centre-line corresponding to the so-called potential core.

The u-component of the turbulence intensity shows peaks at the maximum wind speed gradient. The vertical and lateral components of the turbulence intensity lack such a peaked shape.

The shear stresses have been measured succesfully. The course of the individual shear stresses can be explained qualitatively by making some simple assumptions about the wind speed gradient in the wake.

Results of turbulence intensity and horizontal shear stress at a down-stream distance of x = 1.5 D show a narrow shear layer, between the undisturbed outer flow and the inner potential core with lower wind speed. Inside the potential core turbulence and shear stress are not influenced.

The analysis of the wake measurement has been affected by disturbance of the upstream wind speed measurements. A lightning rod on top of the meteorological mast causes deviations in the wind speed measurements in the order of 5%.

The reproducibility of the measurements has been checked by comparing measuring results of two different campaigns, measured at the same downstream position. The reproducibility of the results shows to be very good.

6 References

[1] Beljaars, A.C.M.;
The measurement of gustiness at routine wind stations - A review;
WMO-instruments and observing methods, report no. 31, Geneva 1987.

[2] Bendat, J.S., A.G. Piersol;
Random data; Analysis and Measurement procedures; 2nd edition;
Wiley, 1986.

[3] Bulder, B.H., J.G. Schepers;
Calculation data base of the WPS-30 wind turbine;
ECN report ECN-CX--91-053, September 1991.

[4] Cleijne, J.W.;
Local wind speed distribution around the SEP experimental wind farm (in Dutch);
TNO report 91-421; Apeldoorn, January 1992.

[5] Cleijne, J.W.;
Results of Sexbierum Wind Farms; double wake measurements - revised.
TNO report 92-388, Apeldoorn, November 1992.

[6] Cleijne, J.W.;
Results of Sexbierum Wind Farms; single wake measurements.
TNO report 93-082, Apeldoorn, March 1993.

[7] Crespo, A.;
2nd progress report JOUR-0087 'Wake and wind farm modelling';
May, 1992.

[8] Panofsky, H.A., J.A. Dutton;
Atmosperic Turbulence, models and methods for engineering applications;
Wiley, 1984.

[9] Smith, D.;
An experimental and theoretical investigation of wind turbine wakes in arrays and complex terrain;
Ph.D. Thesis, NP-TEC, 1991.

[10] Strong winds in the atmospheric boundary layer: part 2 discrete gust speeds;
Engineering Sciences Data Item 83045;
ESDU, November 1983.

[11] Taylor, G.J.;
Full-Scale Measurements in Wind Turbine Arrays JOUR-0064;
Kick-off document, 1990.

[12] Toussaint, P., H.K. Hutting, J.W. Cleijne, M. Mortier;
Results from operation and research of the experimental wind farm of the Dutch Electricity Generating Board;
Proceedings EWEA special topic conference '92, Herning, 1992.

7 Authentication

Name and address of the principal
Commission of the European Community
contract JOUR-0064

Names and functions of the cooperators
Ir. J.W. Cleijne - research engineer

Names of establishments to which part of the research was put out to contract
-

Date upon which, or period in which, the research took place
January 1992 - November 1992

Signature

Ir. J.W. Cleijne
project manager

Approved by

Ir. N.J. Duijm
section manager
wind engineering

Annex A1 Specification of the holec WPS-30/3 wind turbine

Type		:	HAWT
Rotor		:	upwind
Number of blades		:	3
Blade material		:	steel
Rotor diameter		:	30.1 m
Blade root radius		:	1.14 m[1)]
Blade profiles		:	NACA 230xxx series
Mass of one blade		:	1800 kg
Mass of blade foot		:	1360 kg
Mass of rotor (incl. hub)		:	15400 kg
First flap-wise			
Own-frequency		:	3.35 Hz
Rotor rotation direction		:	clockwise (looking downwind)
Tilt angle		:	5.5°
Cone angle		:	0.0°
Tower material		:	steel
Tower diameter	-base	:	3.2 m
	-top	:	1.32 m
Tower height		:	35 m
Distance rotor-tower		:	1.67 m (at hub height)
Rated Power		:	310 kW
Rated wind speed		:	14 m/s
Cut-in wind speed		:	5 m/s
Cut-out wind speed		:	20 m/s
Generator		:	synchronous with DC link
Control		:	variable speed/ variable pitch

1) The blade root is defined to be the position of the outer bearing of the blade, see figure 5 the blade lay-out

Annex A2 Specification of the extra instrumentation on turbine T36

Channels

blades and hub
8 strain gauges on each blade
4 strain gauges on the hub
strain gauges on the joint between hub and blades

rest of turbine
torque on the main shaft
torque on the fast shaft
bending moments in N-S and E-W directions 6 m below the tower top
bending moments in N-S and E-W directions 4 m above the tower base
pitch angle
blade position
nacelle direction

Electrical and control signals
field voltage of the generator
field current of the generator
voltage of all 3 phases of the generator
current of all 3 phases of the generator
frequency of the generator
set point field current
set point DC current
set point pitch angle
DC voltage
DC current turbine
DC current converter
voltage of all phase of the 10 kV grid connection

All above signals are sampled at a 32 Hz rate

Annex A3 Data transformation and averaging

A3.1 Co-ordinate transformation

The various quantities are measured in a frame of reference fixed to the wind farm, having co-ordinates X, Y and Z. X is horizontal, Y is horizontal and perpendicular to X, and Z points vertically upwards. X, Y, Z form a right handed co-ordinate system.

Scalar quantities, vectors, as well as tensor quantities (Reynolds-stresses) are measured in the fixed frame of reference. For analysis purposes these quantities need to be transformed to the wind frame of reference U, V, W. U is in the direction of the average undisturbed wind speed, V is perpendicular to the wind and W is vertical. Again a right handed frame of reference is used. For a definition of the two coordinate systems see figure 3.2. The directions of X and U are at an angle δ. The transformation from the fixed co-ordinate system to the wind co-ordinate system is hence a simple rotation about the Z-axis over an angle δ. The transformation matrix is given by:

$$\Delta_{ij} = \begin{bmatrix} \cos\delta & -\sin\delta & 0 \\ \sin\delta & \cos\delta & 0 \\ 0 & 0 & 1 \end{bmatrix}$$

Scalars are insensitive to a rotation of the frame of reference and thus need not to be transformed. However the components of a vector are affected by a rotation of the frame of reference. The components in the wind frame of reference are found by applying the following expression:

$$U_{wind,\,i} = \sum_{j=1}^{3} \Delta_{ij} \cdot U_{x,\,j}$$

The components of a tensor are changed according to the following transformation formula

$$T_{ij}' = \sum_{k=1}^{3} \sum_{l=1}^{3} \Delta_{ik} T_{kl} \Delta_{lj}^{T}$$

A3.2 Merging of 1-minute records to obtain multiple-minute averages

The data-base consists of records with one-minute averages of the measured quantities. However, for further analysis it is necessary to use multiple-minute records (for instance 3-minutes averages as was done in this report). It is possible to obtain averages over several minutes, combining subsequent records without losing accuracy using the formulas given below.

A distinction is made between linear averaged quantities (wind speed, power, wind direction, etc.) and non-linear quantities, such as the variance of the given quantities.

Linear averaged quantities
Subsequent records are simply averaged arithmetically to obtain the multiple-minute averaged value:

$$\mu_M = \frac{1}{M} \sum_{m=1}^{M} \mu_m$$

μ_M denotes the overall mean, μ_m denotes the means of the separate records.

Quadratic averaged quantities
Co-variance and variance mean values cannot be found by simply averaging their record values, but should be corrected for the variance and covariance of the record means.

The overall covariance is found in the following way:

$$(u'_i u'_j)_M = \frac{1}{M} \sum_{m=1}^{M} (u'_i u'_j)_m = \frac{1}{M} \sum_{m=1}^{M} (\mu_{i,m} - \mu_{i,M})(\mu_{j,m} - \mu_{j,M})$$

μ_m and μ_M are as defined before. $(u_i'u_j')_M$ denotes the overall average of the co-variance. $(u_i'u_j')_m$ denotes the average of the co-variance in record m.
Calculating the average variance is a special case of this expression and is found by taking equal i and j.

$$\sigma^2_{i,M} = \frac{1}{M} \sum_{m=1}^{M} \sigma^2_{i,m} + \frac{1}{M} \sum_{m=1}^{M} (\mu_{i,m} - \mu_{i,M})^2$$

$\sigma_{i,M}$ denotes the overall variance of the i-component, $\sigma_{i,m}$ denotes the variance of record m.

Results of Sexbierum Wind Farm; double wake measurements at 1.5 D, 2.5 D and 4 D Annex 4 - Figures

Reference number 93-271
File number 112324-22420
Date July 1993
NP

Author
J.W. Cleijne

Intended for
Participants JOUR-0064
Participants JOUR-0087

Annex A4 Figures

In this annex a comprehensive overview is given of the analysis results. The results are given in the following order:

1. Results of sensor a2
2. Results of sensor b1
3. Results of sensor b2h
4. Results of sensor b2
5. Results of sensor b2l
6. Results of sensor b3
7. Results of sensor c2
8. Vertical profiles
9. Horizontal profiles

A4.1 Sensor a2

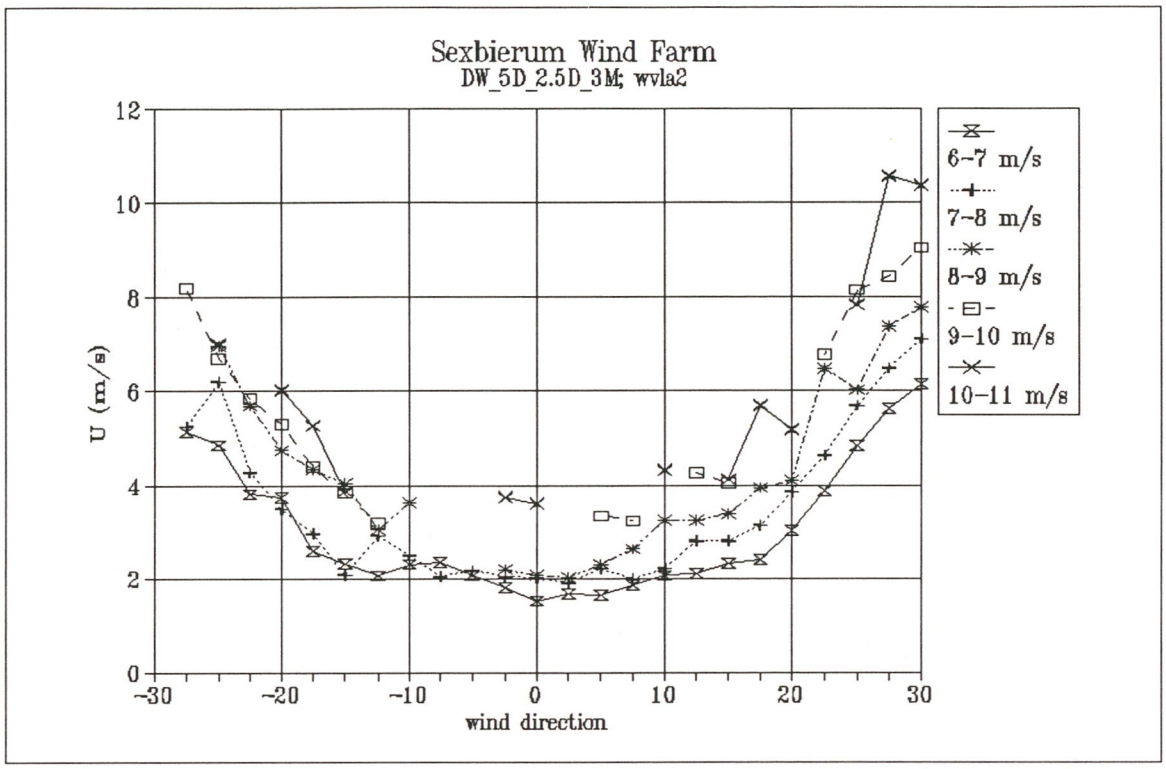

Figure 1 Horizontal wind speed U as a function of wind direction and wind speed bin

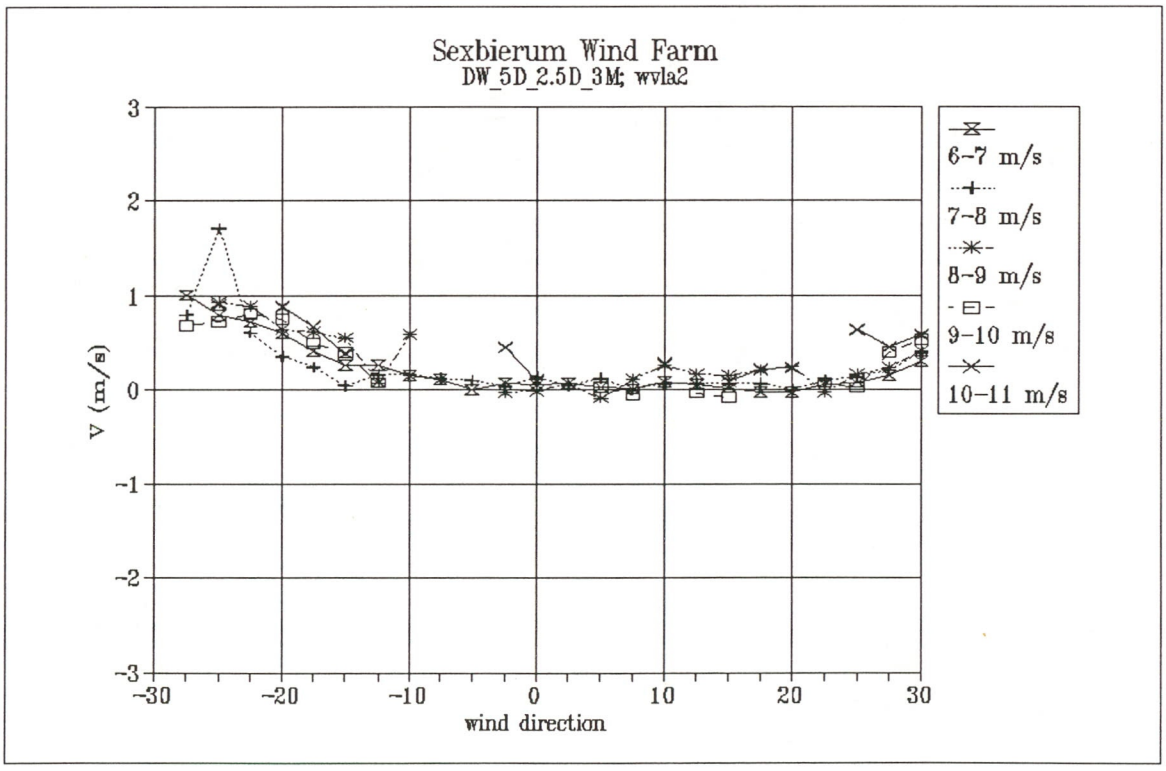

Figure 2 Lateral wind speed V as a function of wind direction and wind speed bin

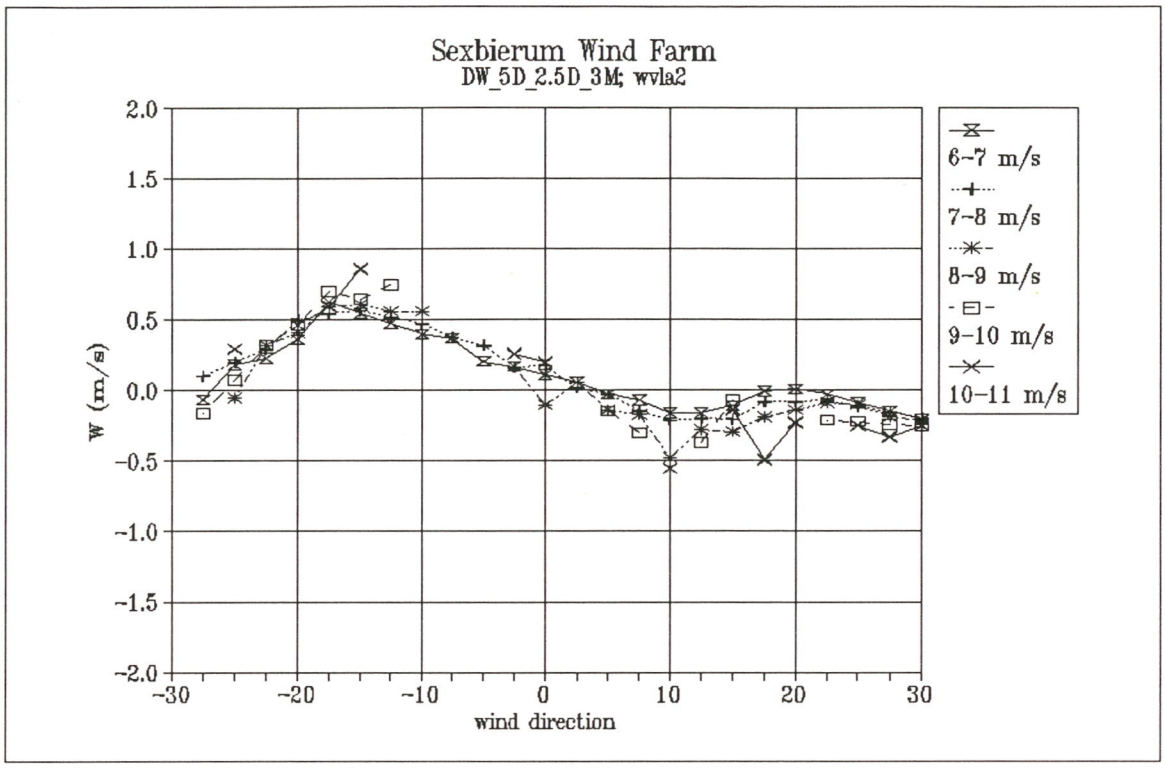

Figure 3 *Vertical wind speed W as a function of wind direction and wind speed bin*

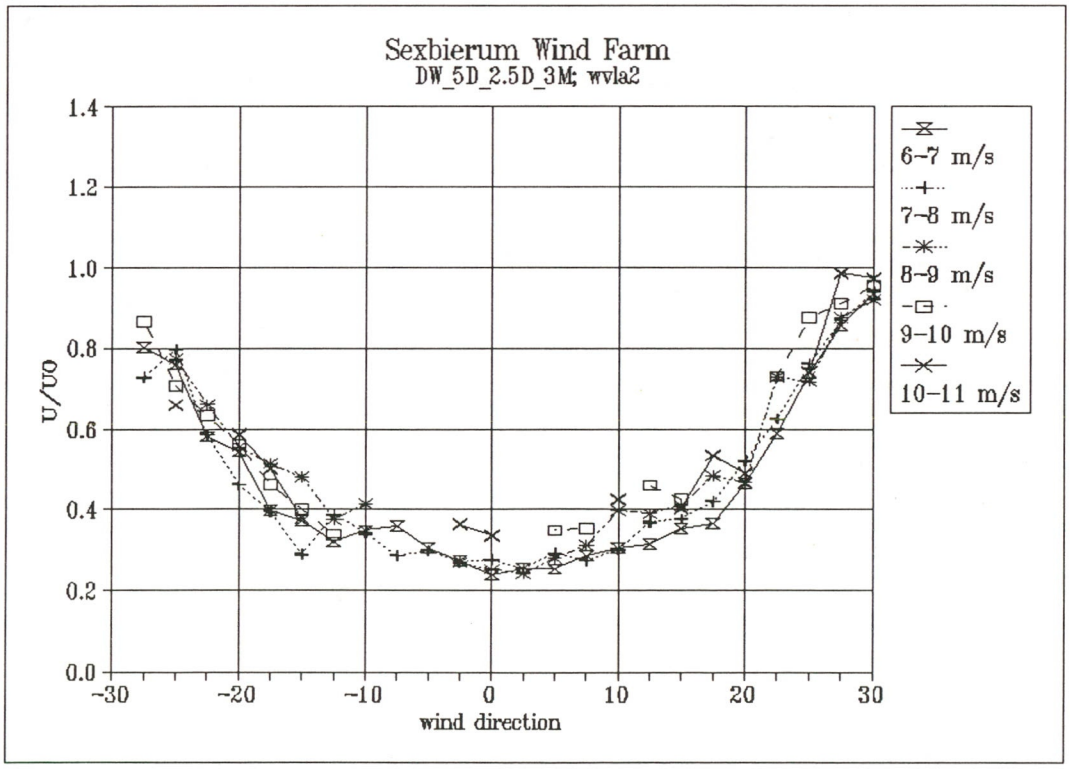

Figure 4 *Wake deficit U/U_0 as a function of wind direction and wind speed bin*

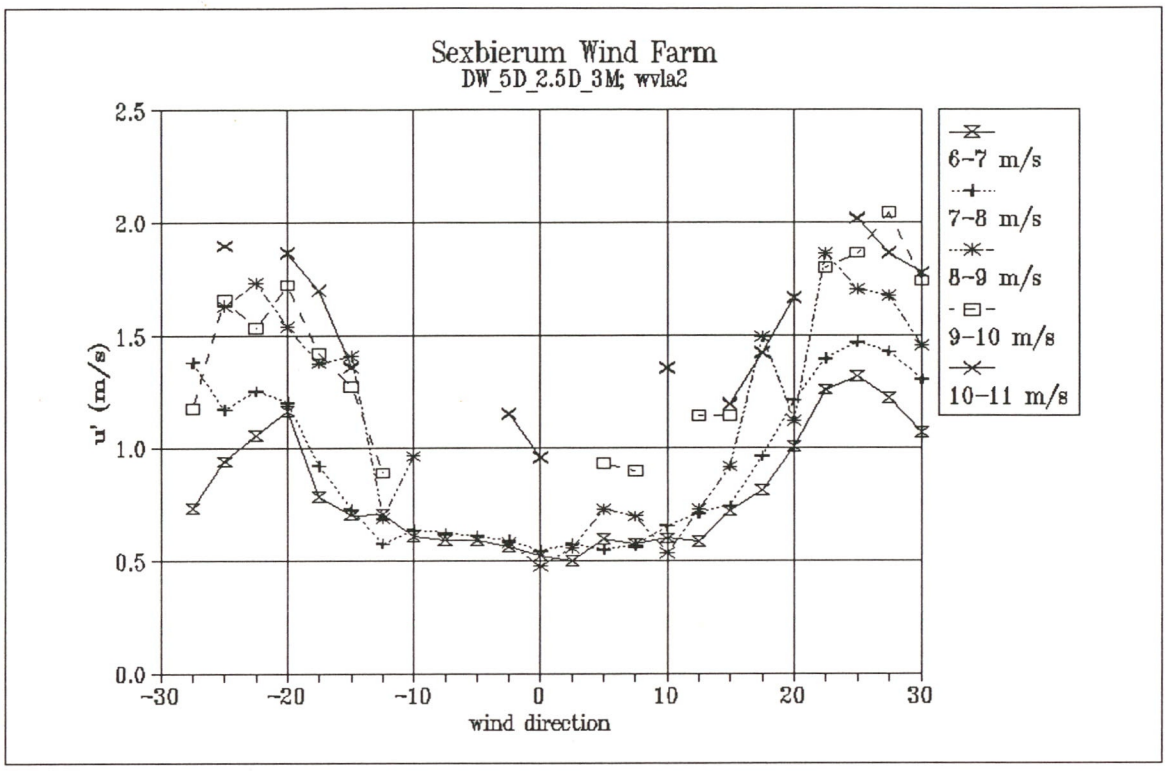

Figure 5 Longitudinal turbulent fluctuations u' as a function of wind direction and wind speed bin

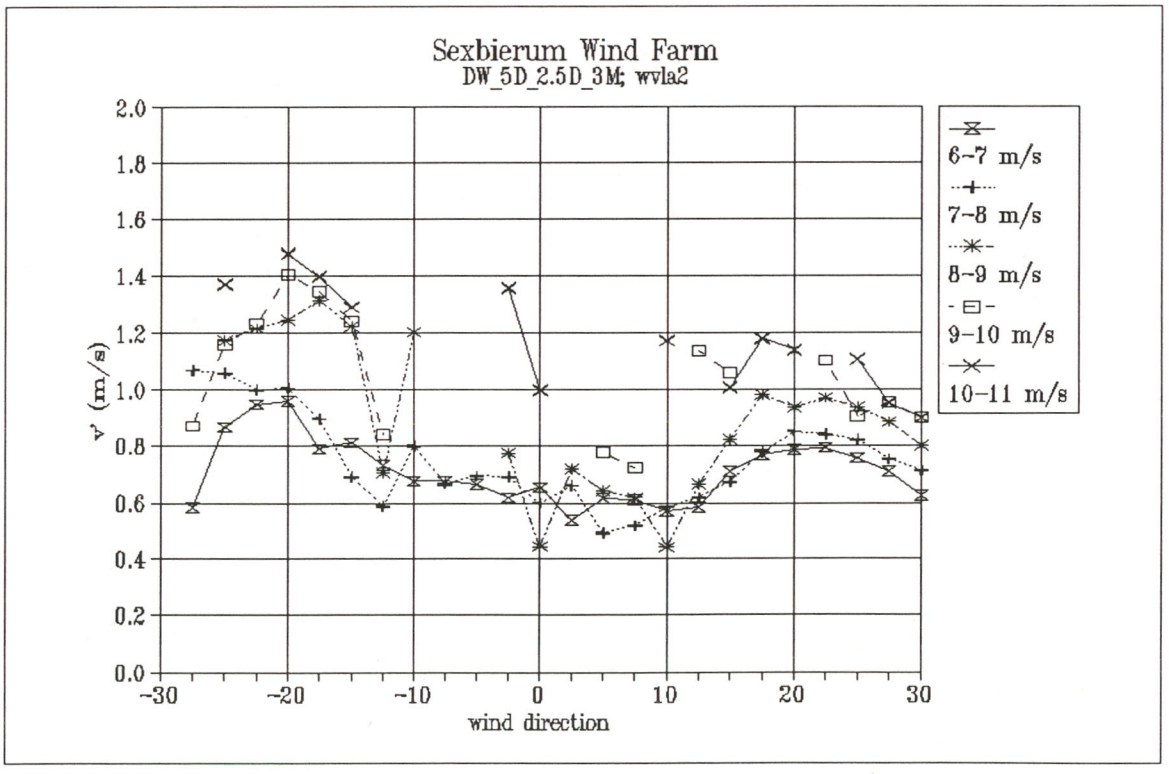

Figure 6 Lateral turbulent fluctuations v' as a function of wind direction and wind speed bin

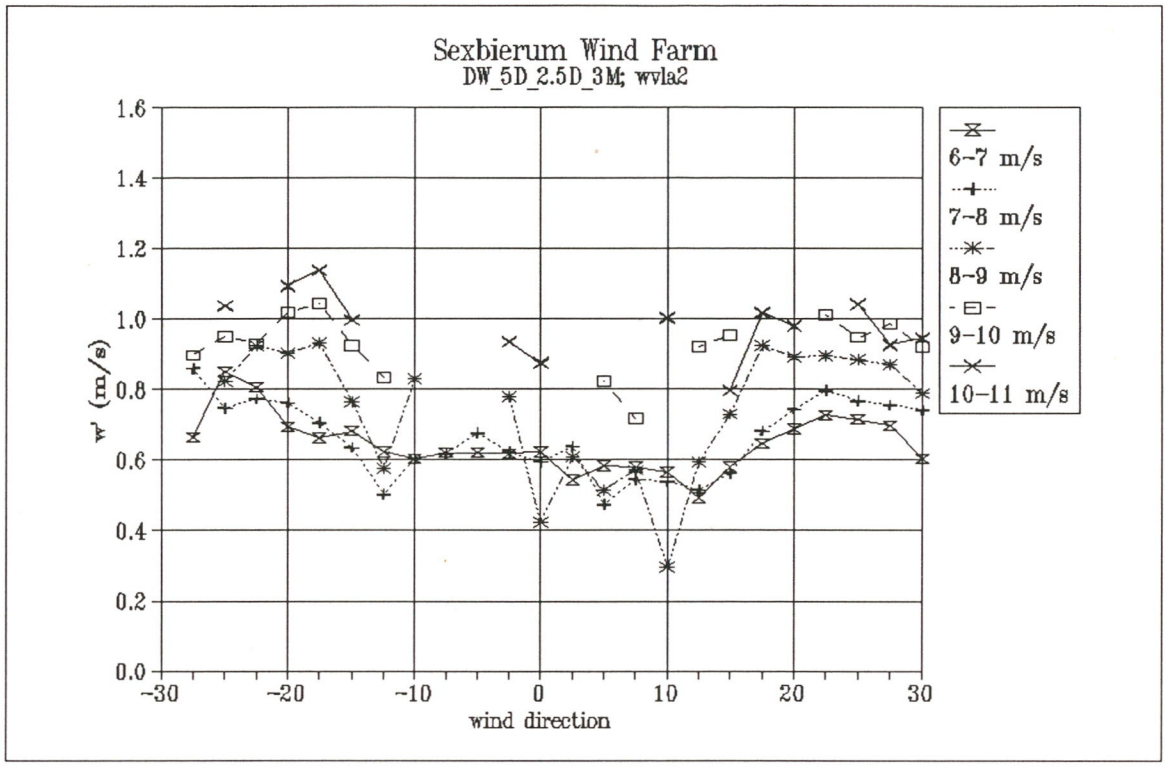

Figure 7 Vertical turbulent fluctuations w' as a function of wind direction and wind speed bin

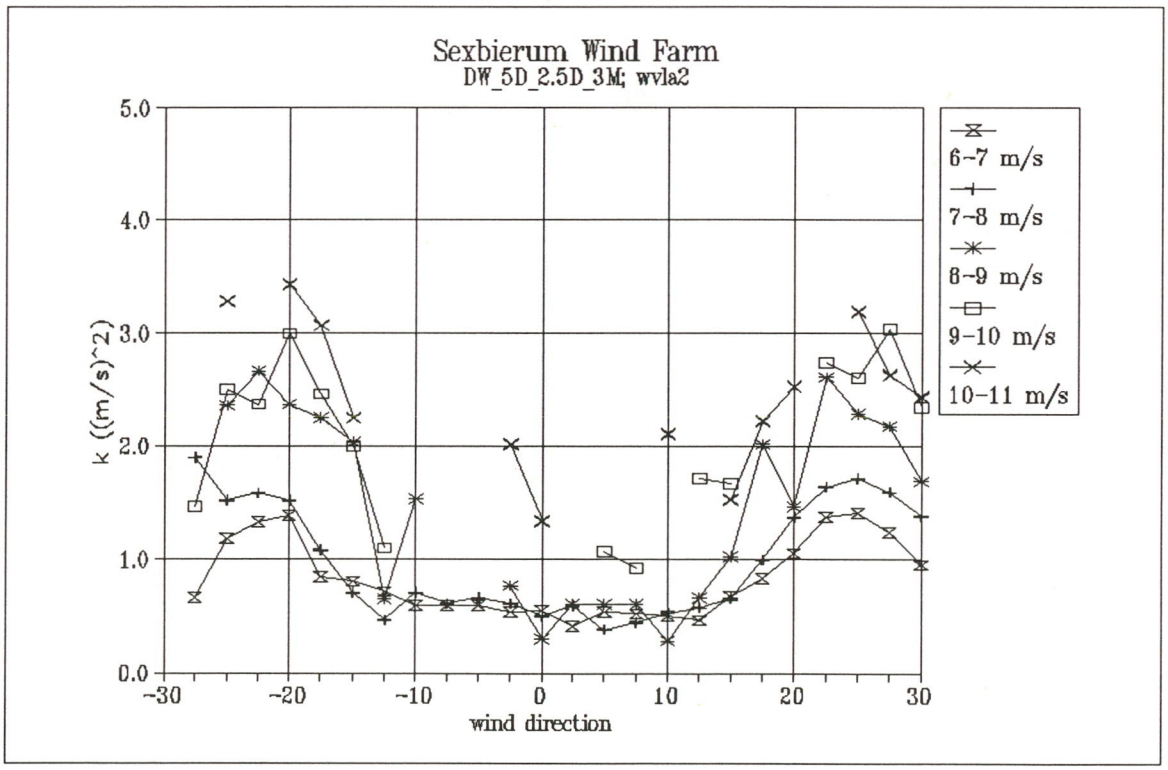

Figure 8 Turbulent kinetic energy per unit mass as a function of wind direction and wind speed bin

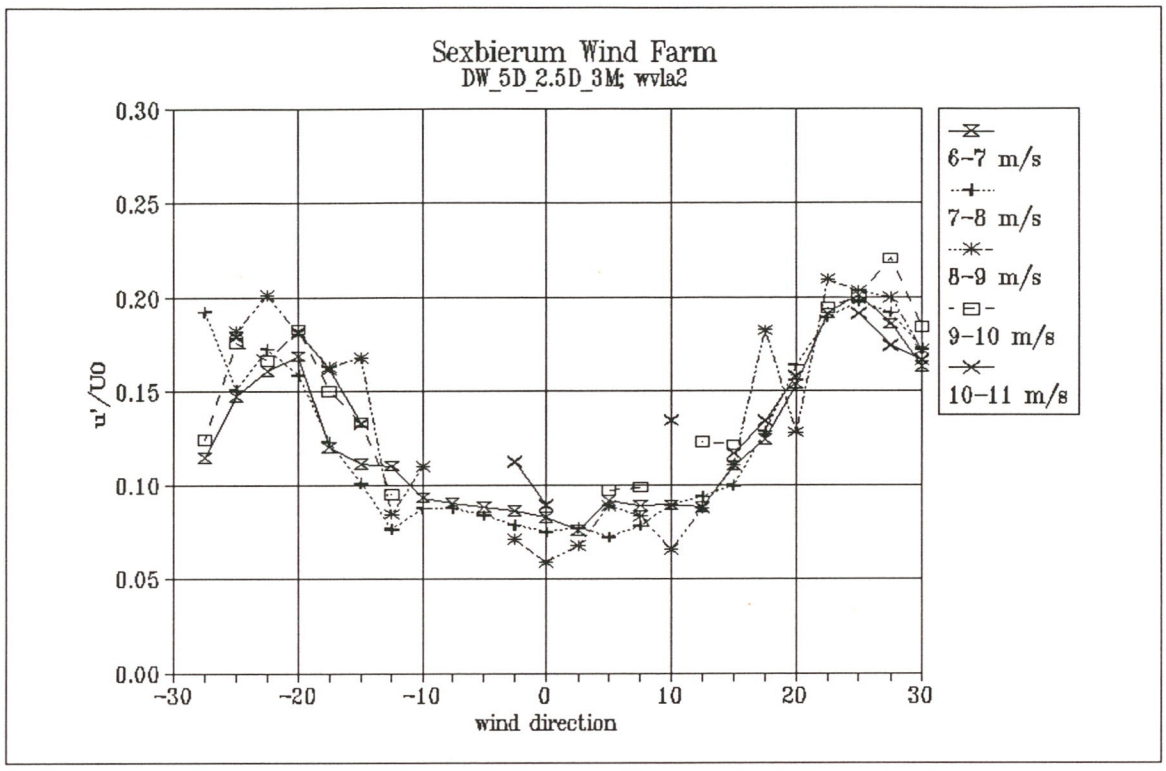

Figure 9 *Non-dimensionalized longitudinal turbulent fluctuations u'/U_0 as a function of wind direction and wind speed bin*

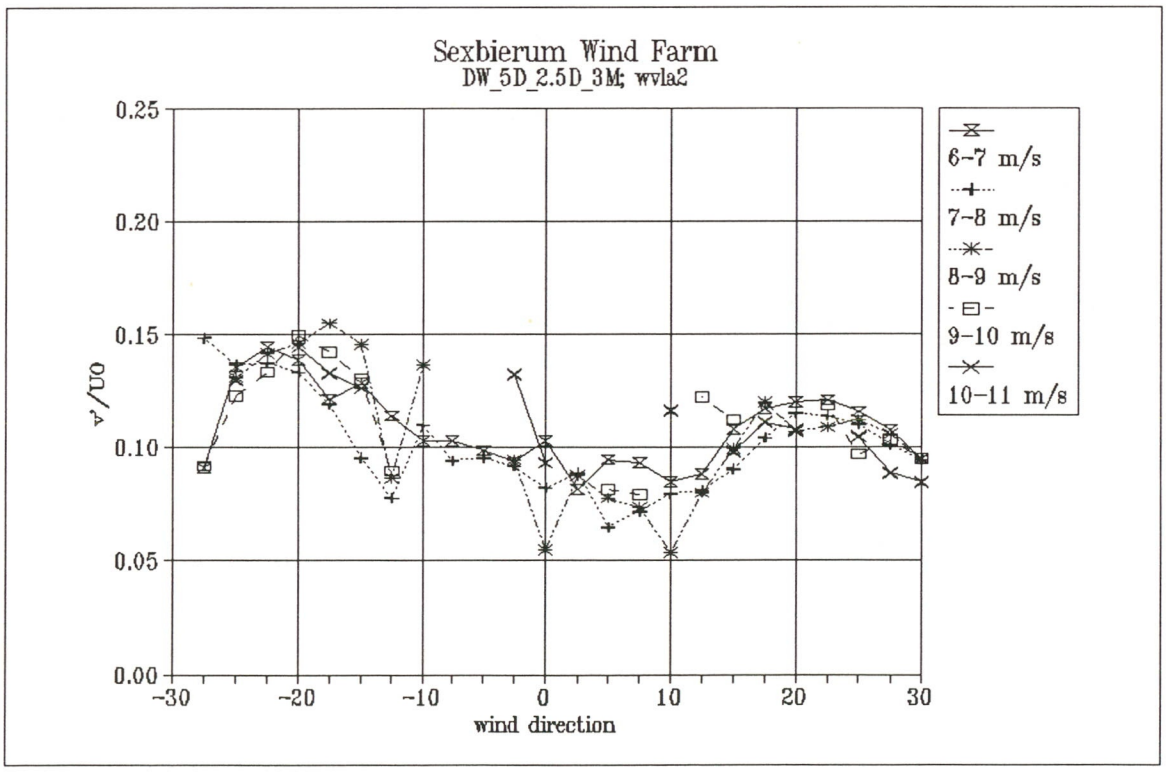

Figure 10 *Non-dimensionalized lateral turbulent fluctuations v'/U_0 as a function of wind direction and wind speed bin*

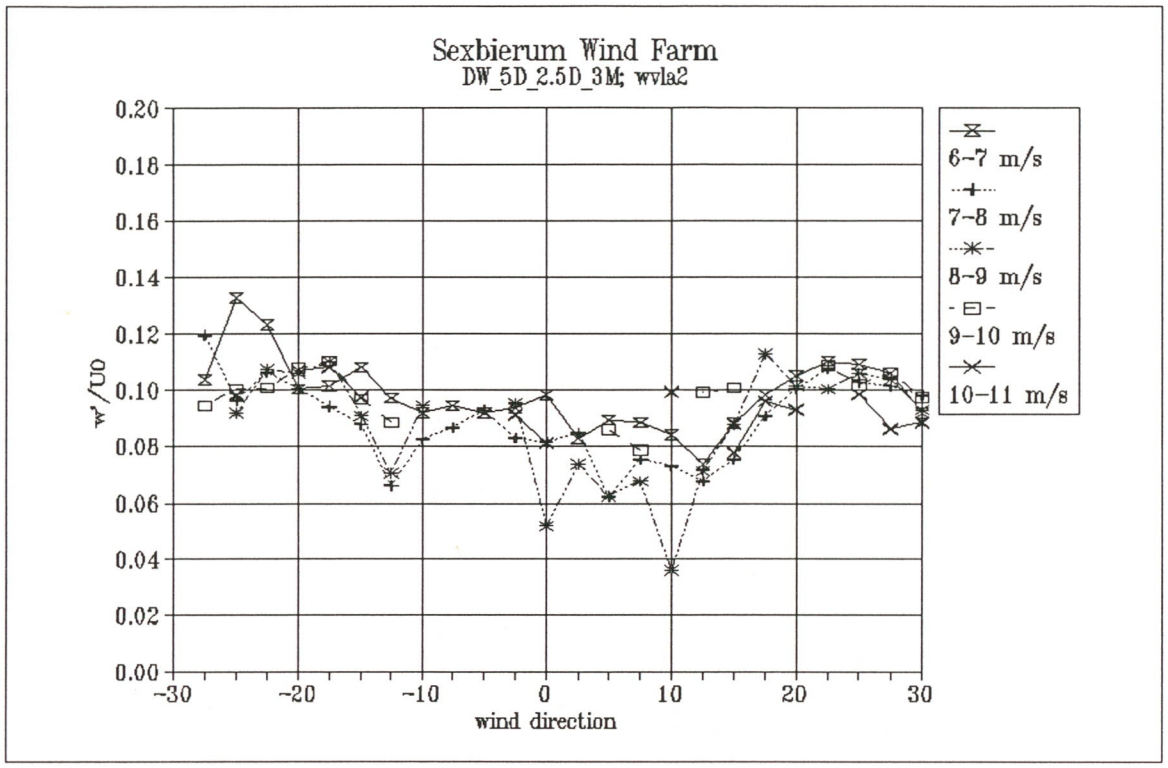

Figure 11 *Non-dimensionalized vertical turbulent fluctuations w'/U_0 as a function of wind direction an wind speed bin*

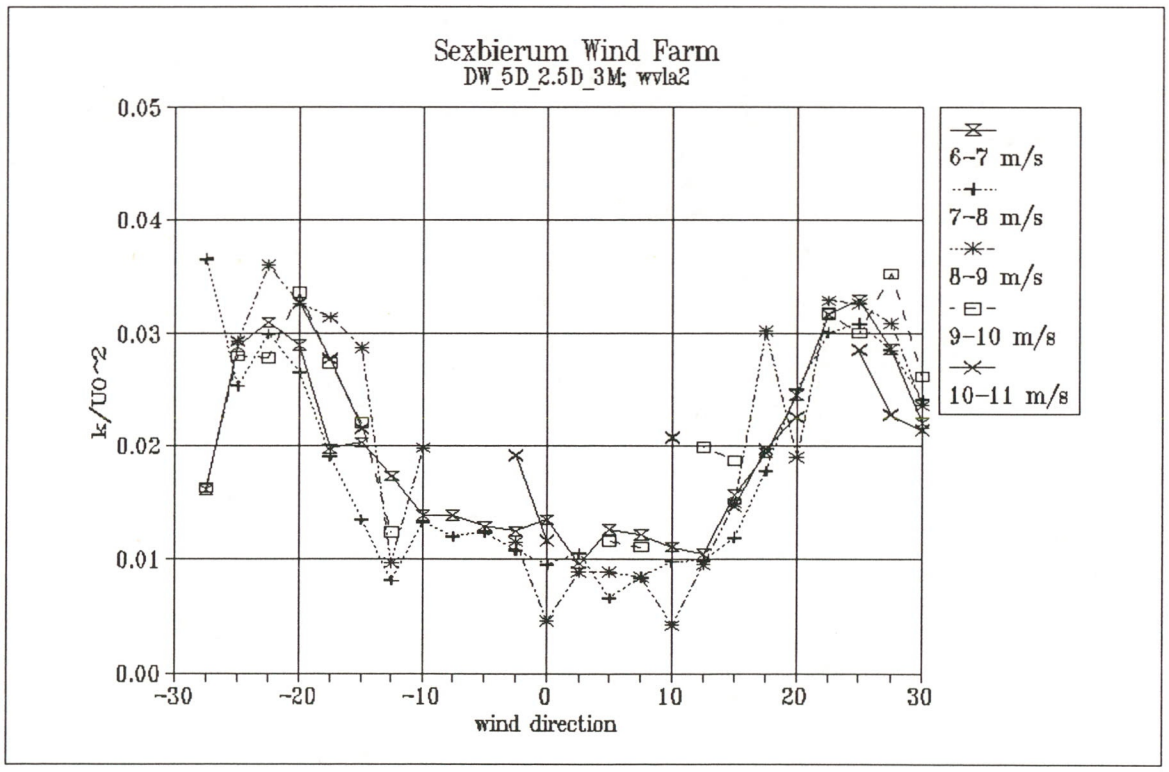

Figure 12 *Non-dimensionalized turbulent kinetic energy k/U_0^2 as a function of wind direction and wind speed bin*

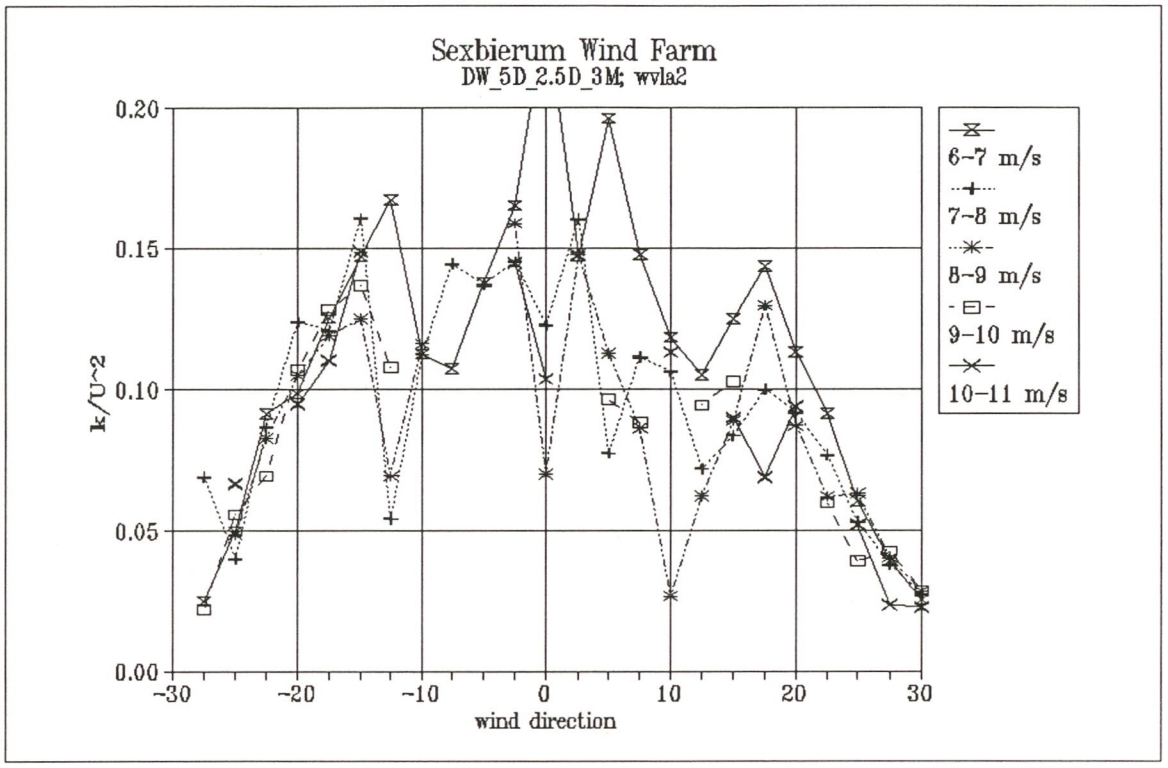

Figure 13 Non-dimensionalized turbulent kinetic energy k/U^2 as a function of wind direction and wind speed bin

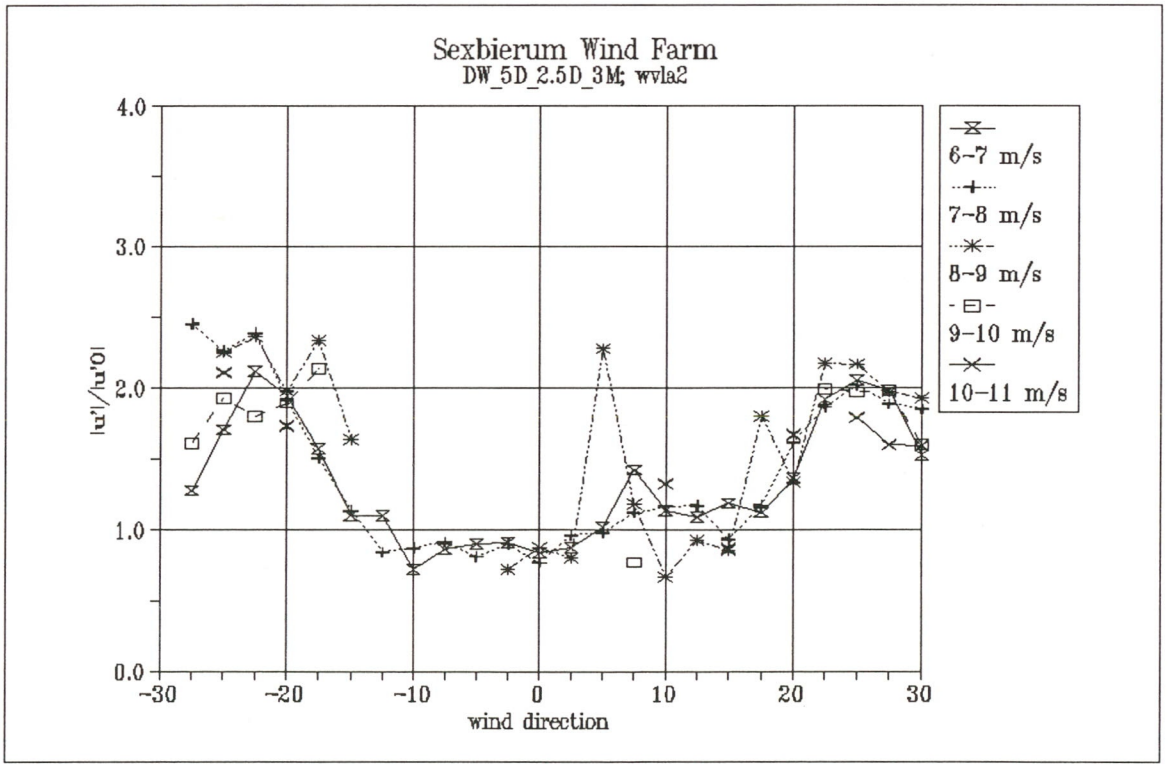

Figure 14 Longitudinal turbulence enhancement u'/u'_0 as a function of wind direction and wind speed bin

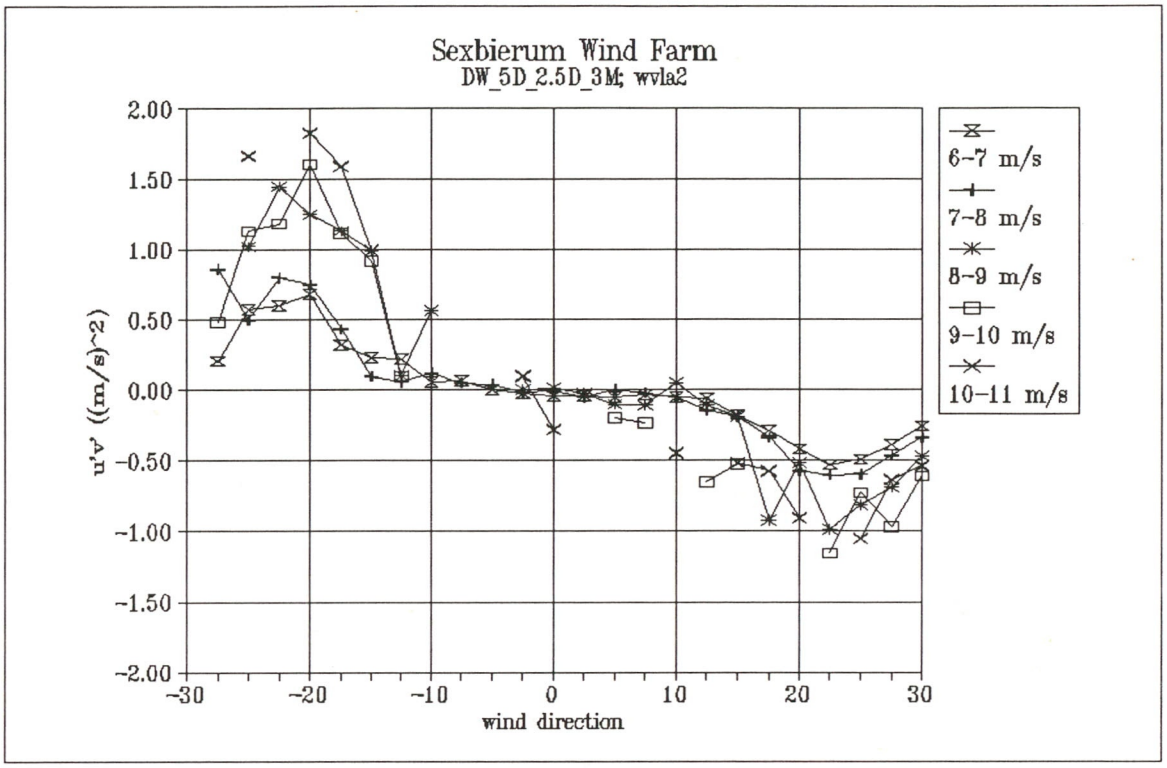

Figure 15 Shear stress u'v' as a function of wind direction and wind speed bin

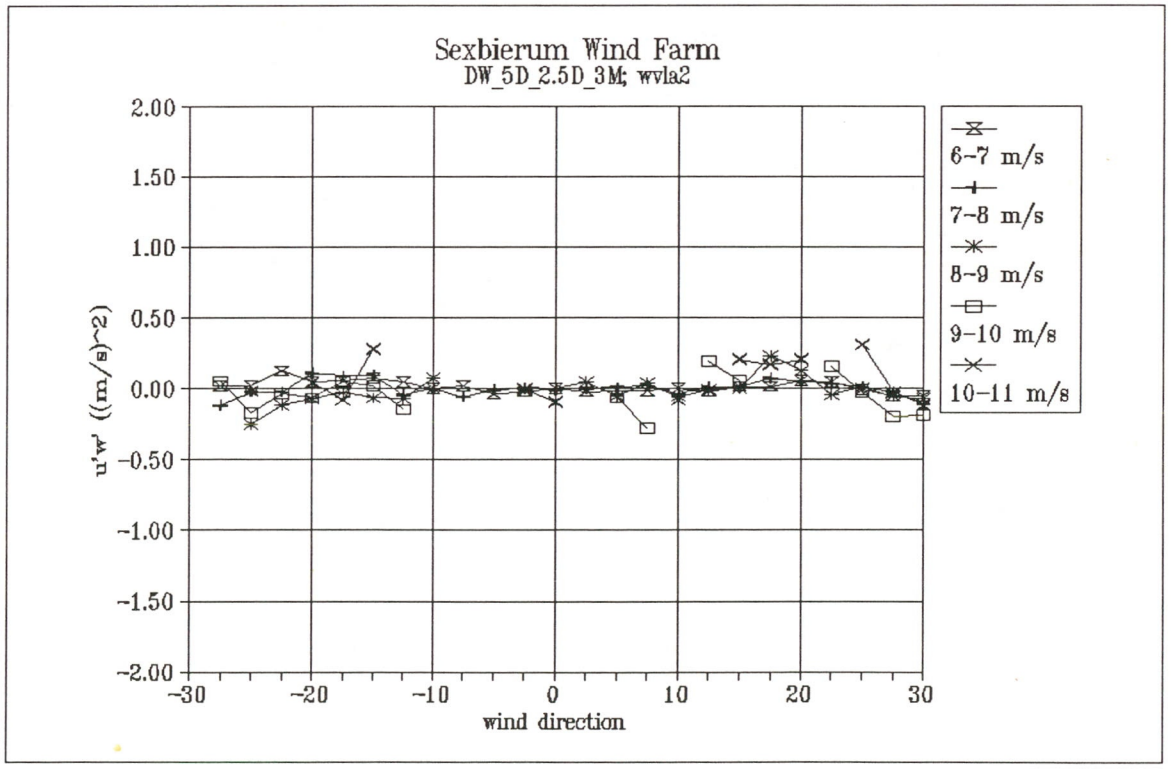

Figure 16 Shear stress u'w' as a function of wind direction and wind speed bin

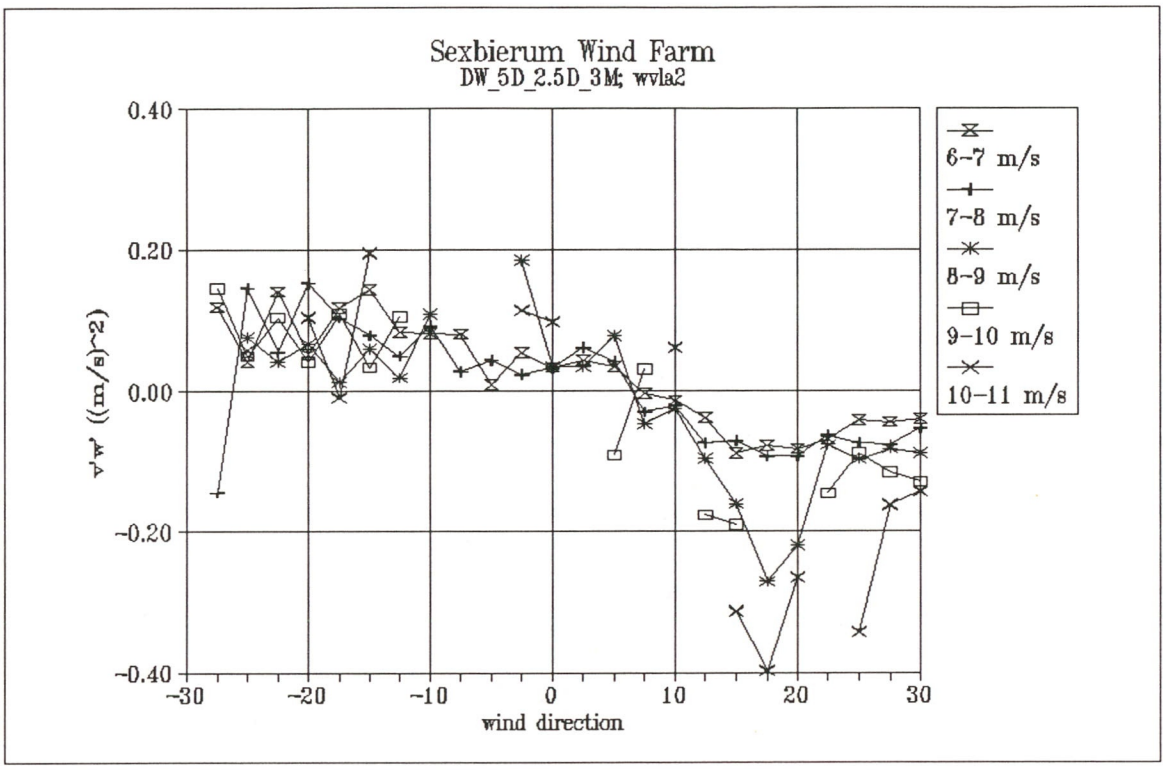

Figure 17 Shear stress v'w' as a function of wind direction and wind speed bin

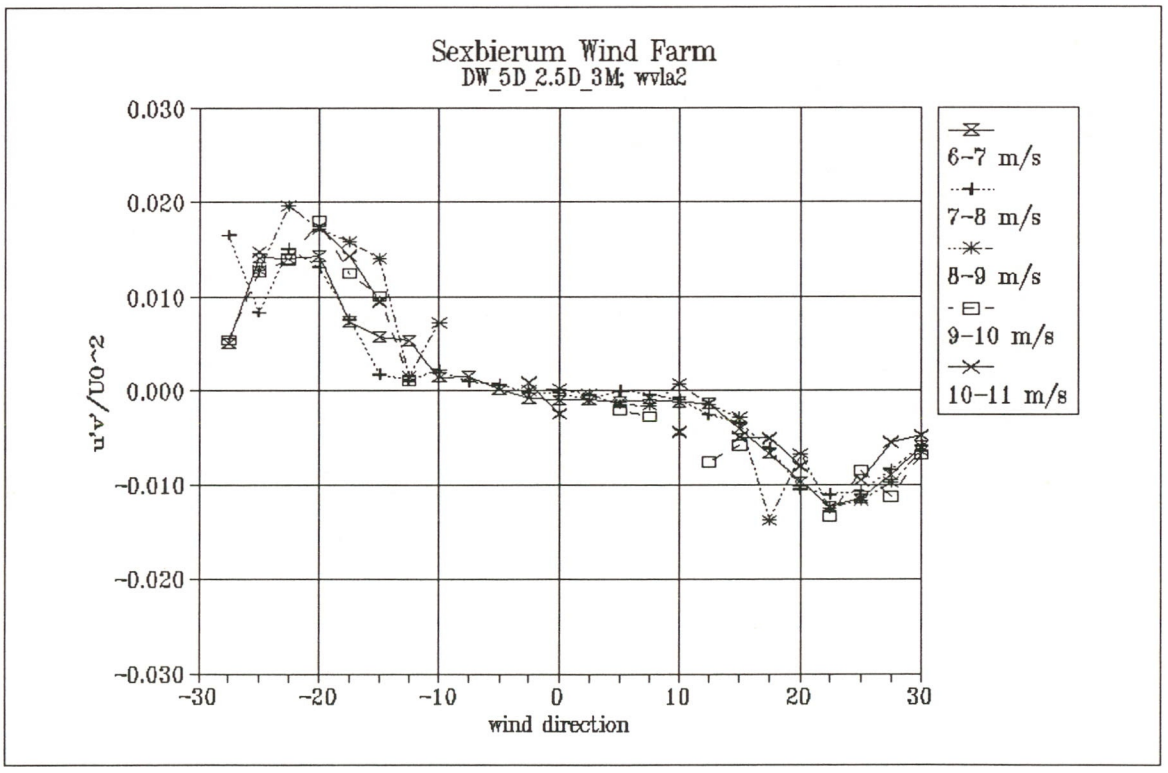

Figure 18 Non-dimensionalized shear stress $u'v'/U_0^2$ as a function of wind direction and wind speed bin

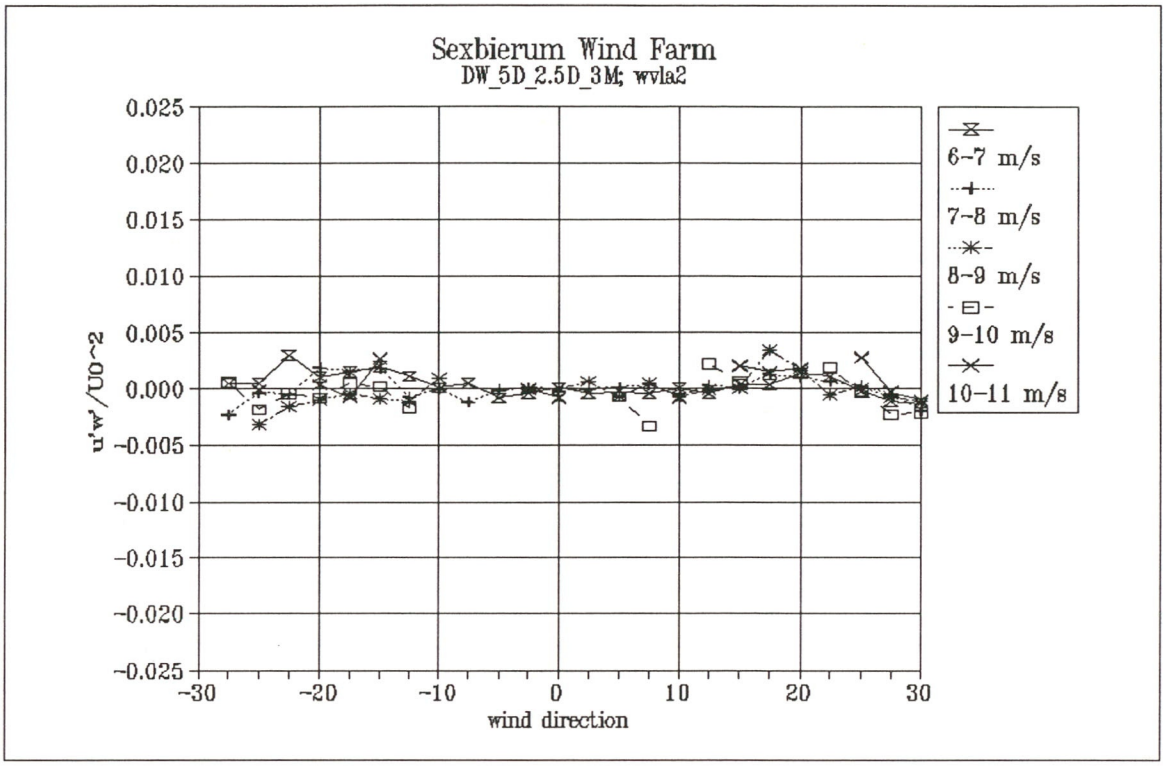

Figure 19 Non-dimensionalized shear stress $u'w'/U_0^2$ as a function of wind direction and wind speed bin

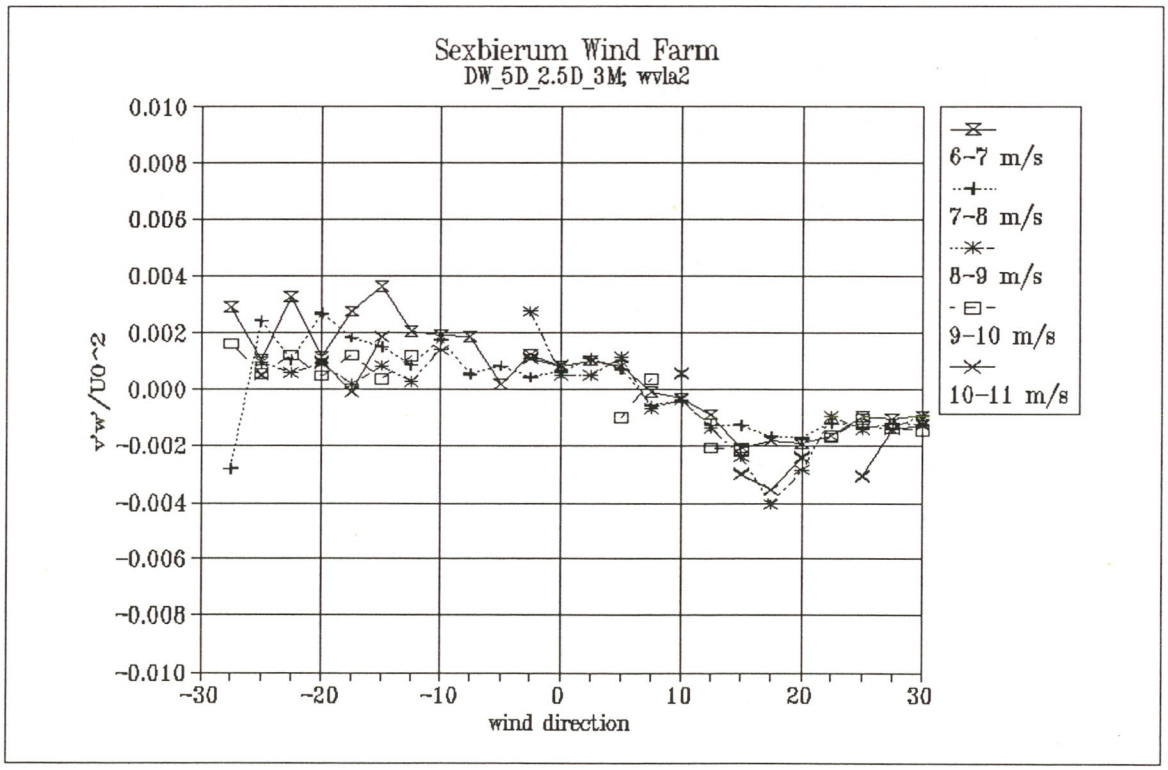

Figure 20 Non-dimensionalized shear stress $v'w'/U_0^2$ as a function of wind direction and wind speed bin

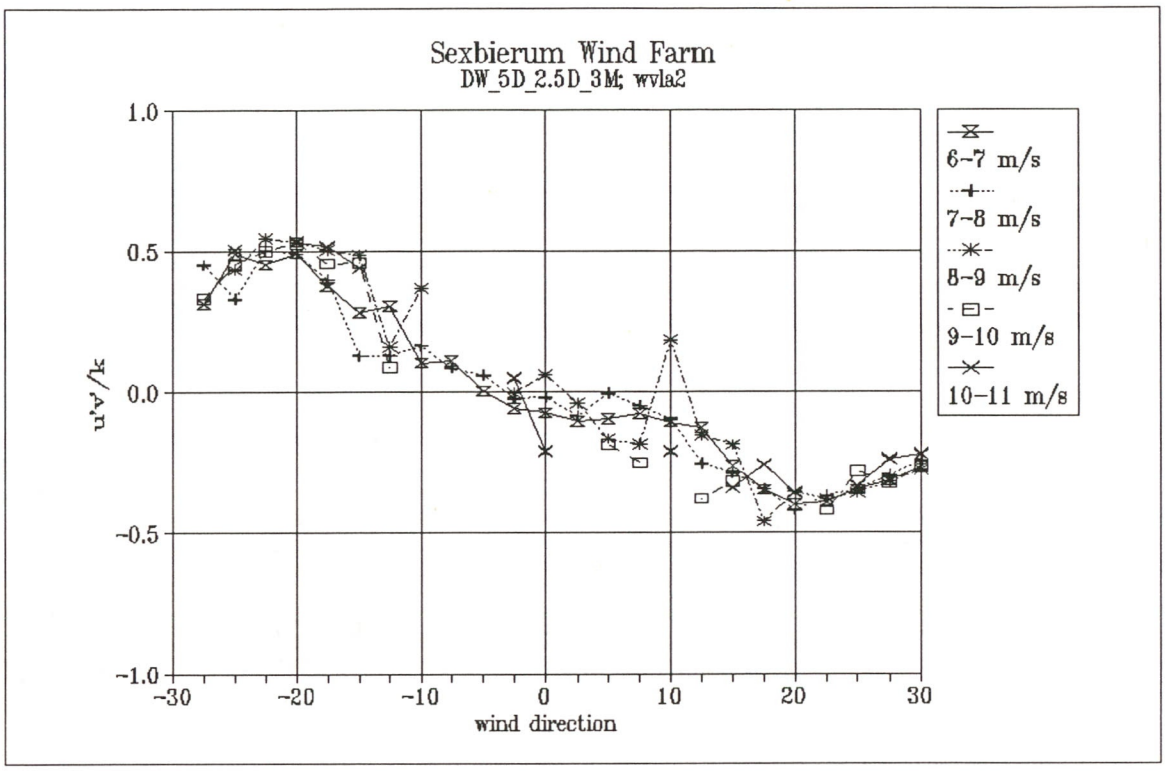

Figure 21 Non-dimensionalized shear stress u'v'/k as a function of wind direction and wind speed bin

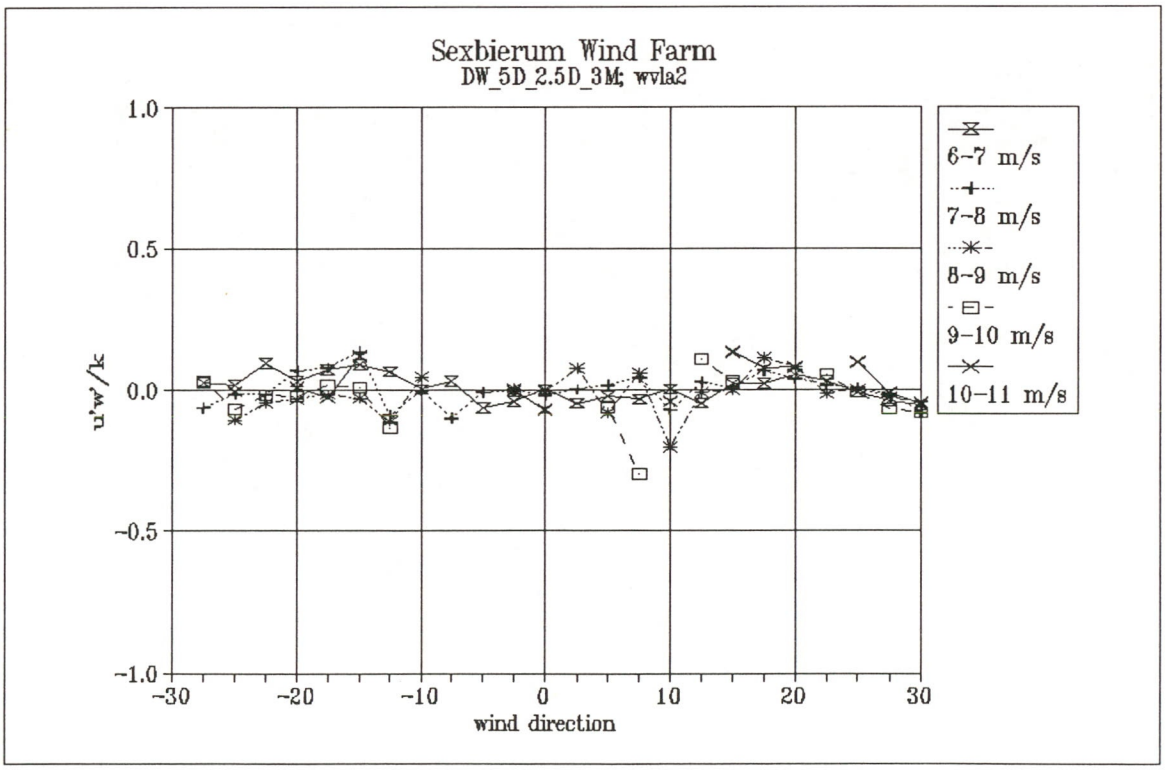

Figure 22 Non-dimensionalized shear stress u'w'/k as a function of wind direction and wind speed bin

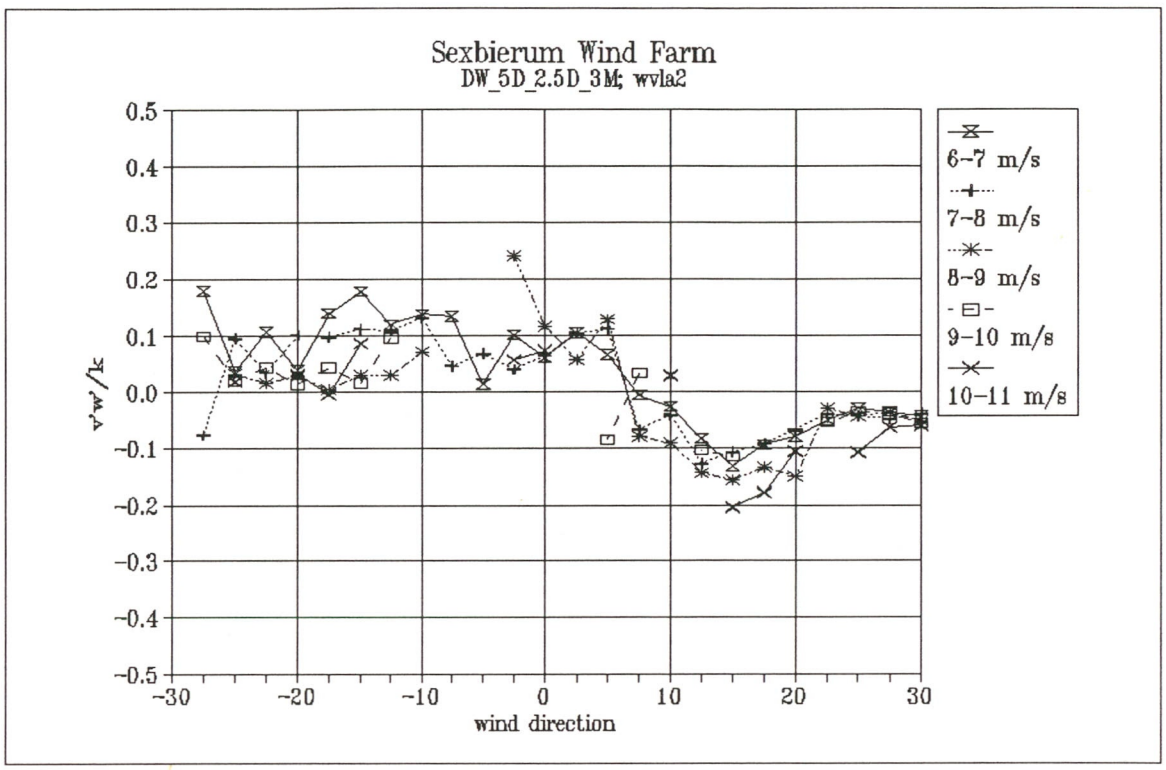

Figure 23 Non-dimensionalized shear stress v'w'/k as a function of wind direction and wind speed bin

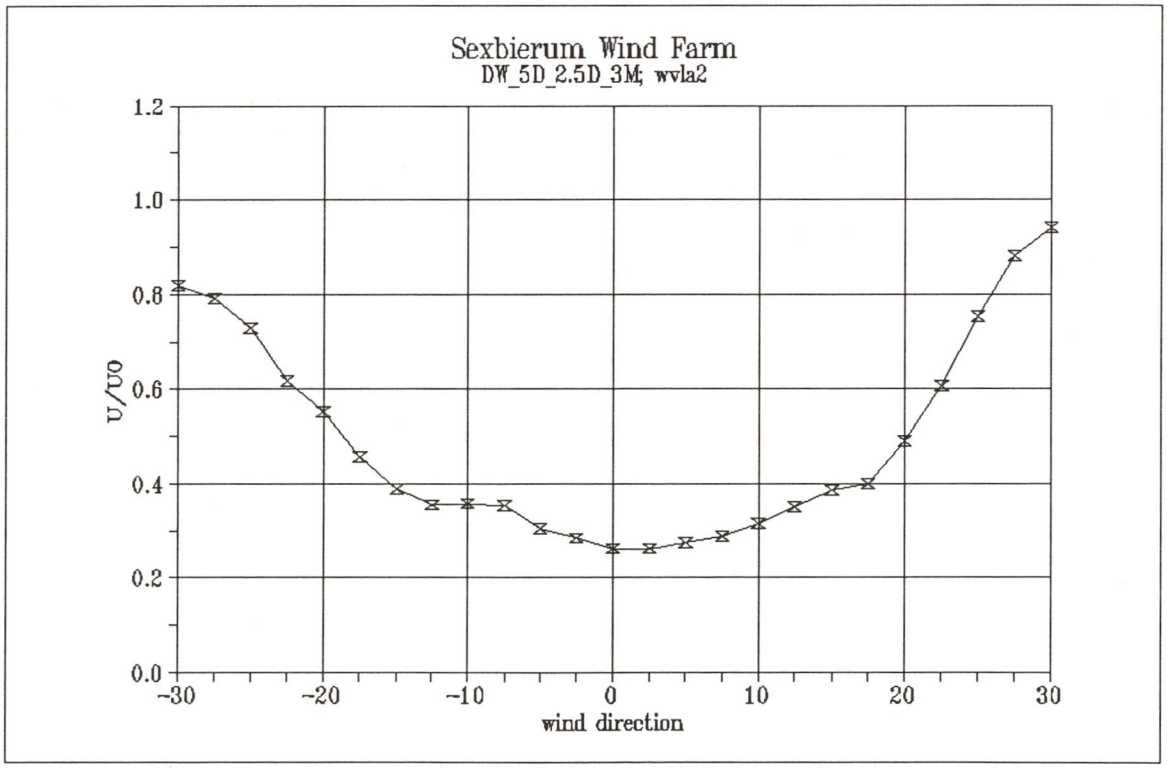

Figure 24 Wake deficit U/U_0 as a function of wind direction in the wind speed bin 5-10 m/s

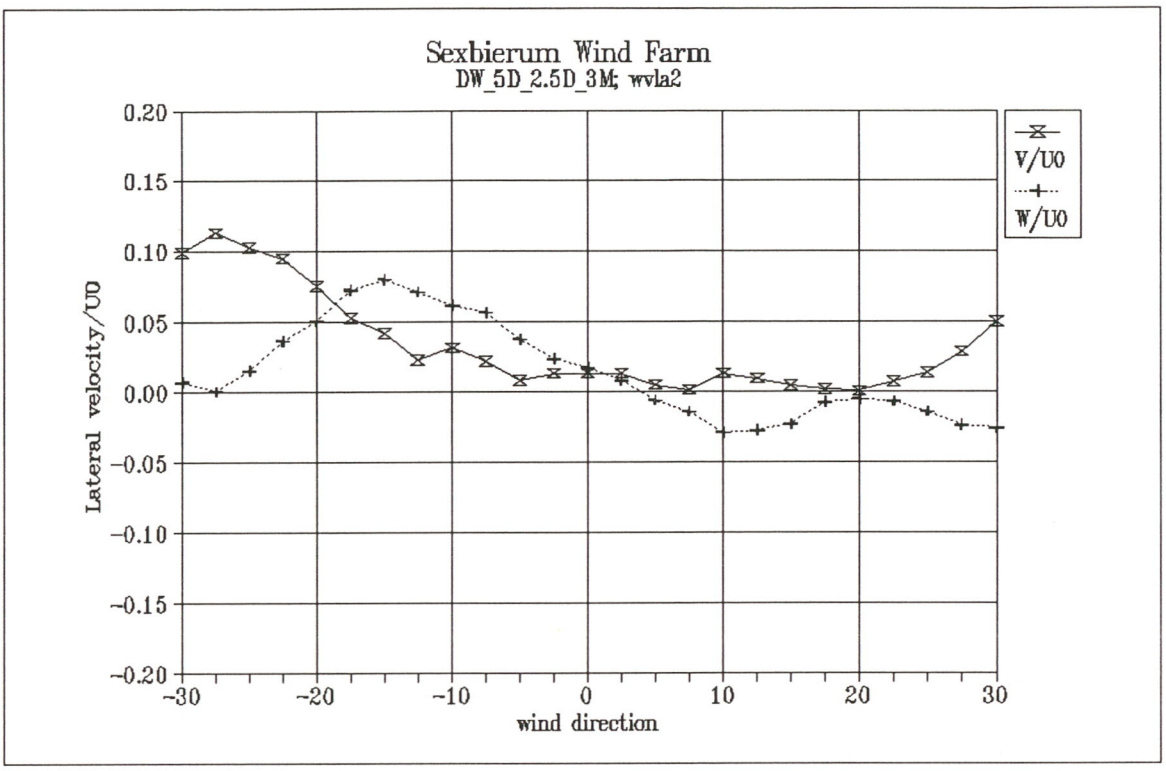

Figure 25 Lateral and vertical wind speed V/U_0 and W/U_0 as a function of wind direction in the wind speed bin 5-10 m/s

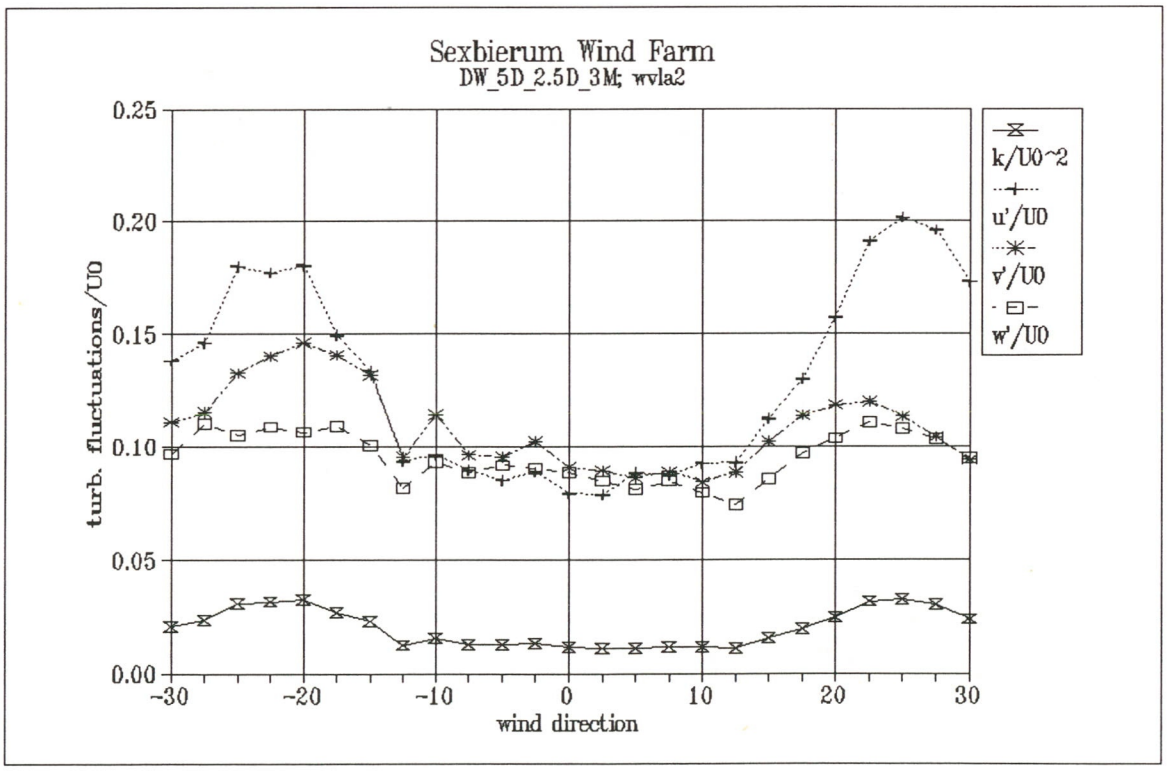

Figure 26 Turbulent fluctuations as a function of wind direction in the wind speed bin 5-10 m/s, non-dimensionalized with U_0

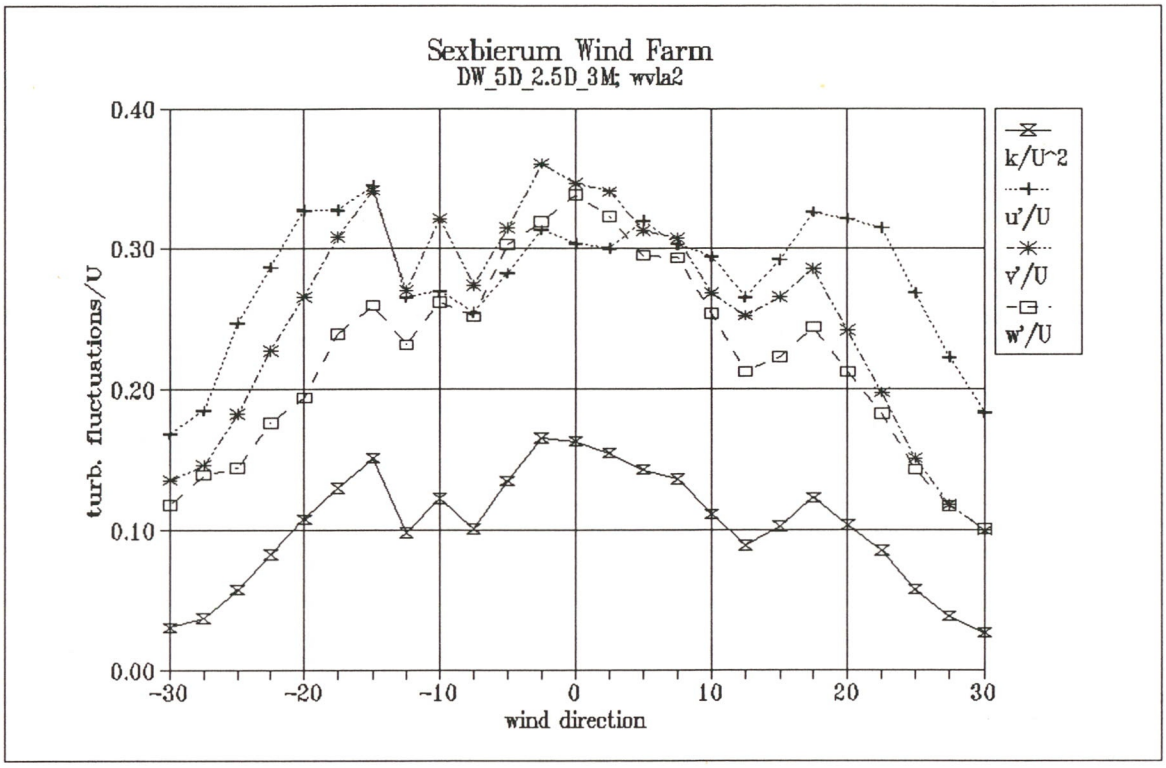

Figure 27 Turbulent fluctuations as a function of wind direction in the wind speed bin 5-10 m/s, non-dimensionalized with U

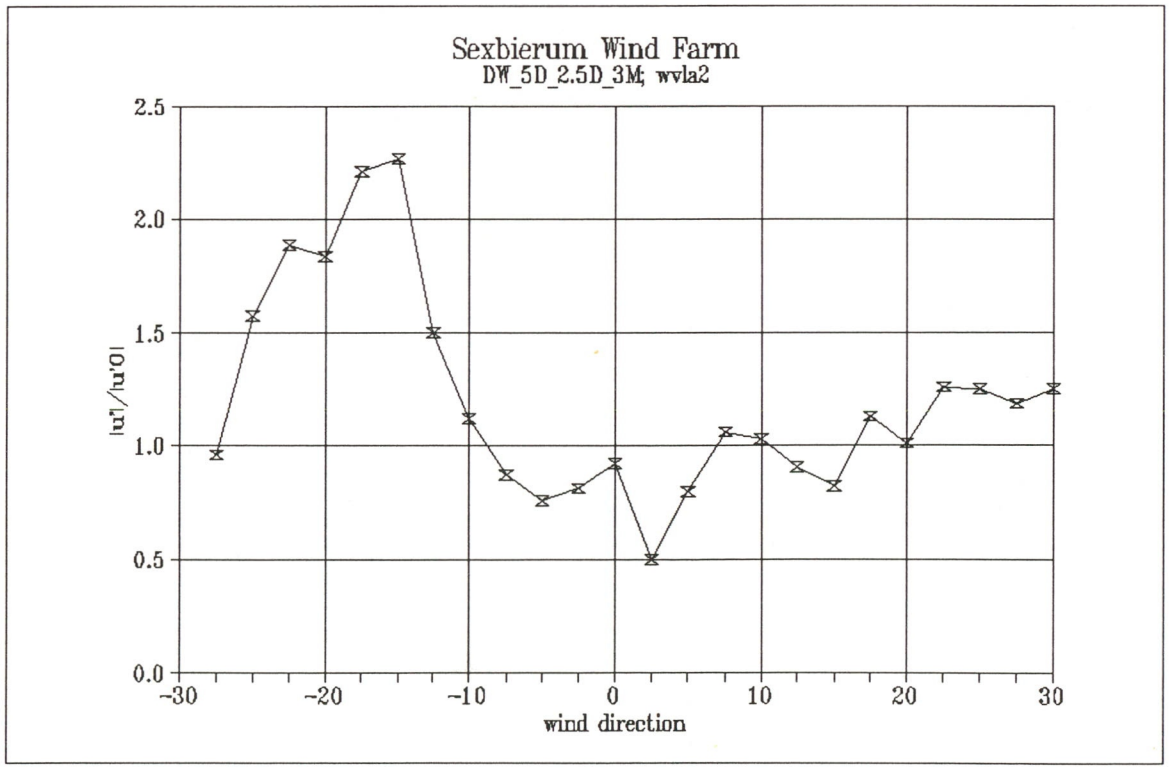

Figure 28 Longitudinal turbulence enhancement u'/u'_0 as a function of wind direction in the wind speed bin 5-10 m/s

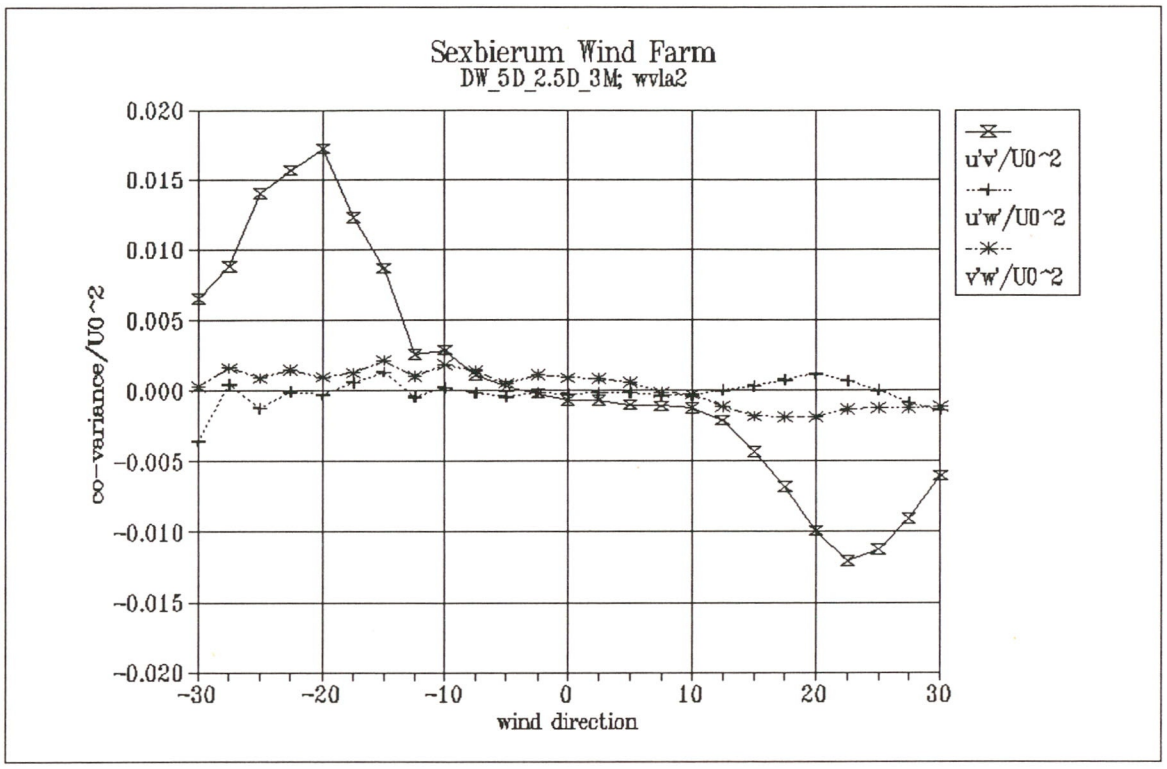

Figure 29 *Non-dimensionalized shear stresses $u'v'/U_0^2$; $u'w'/U_0^2$; $v'w'/U_0^2$ as a function of wind direction in the wind speed bin 5-10 m/s*

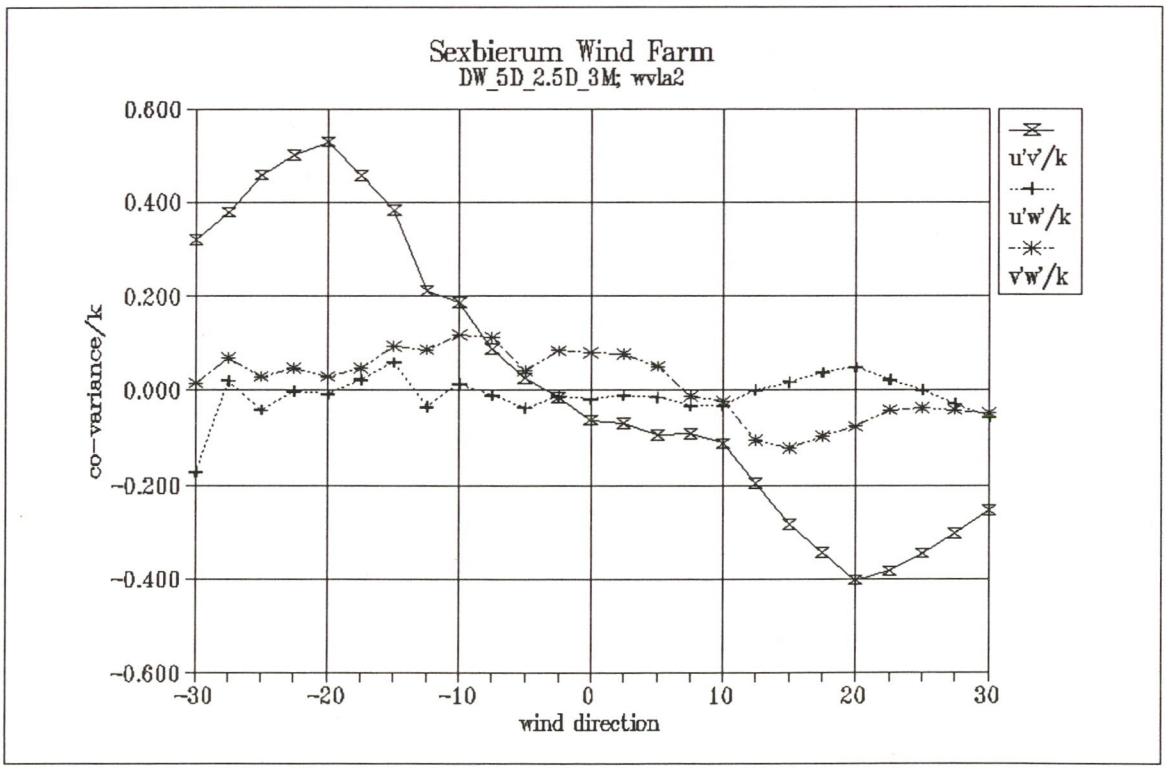

Figure 30 *Non-dimensionalized shear stresses u'v'/k; u'w'/k; v'w'/k as a function of wind direction in the wind speed bin 5-10 m/s*

A4.2 Sensor b1

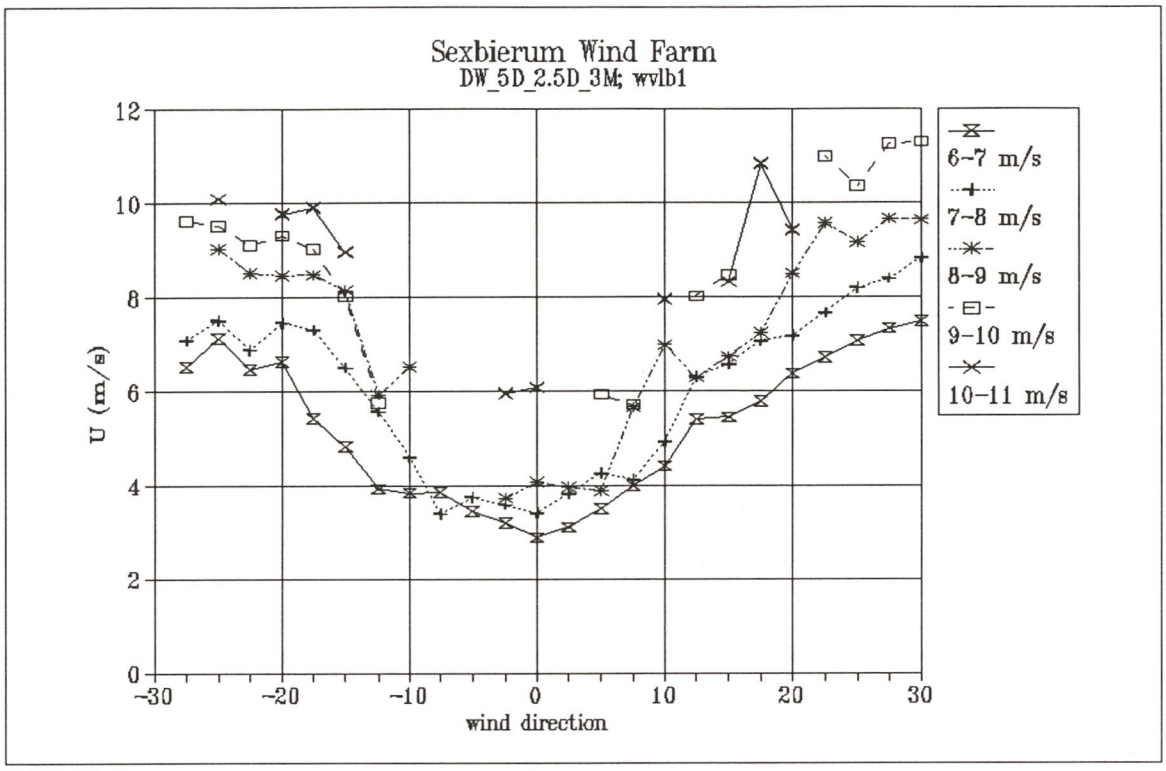

Figure 1 Horizontal wind speed U as a function of wind direction and wind speed bin

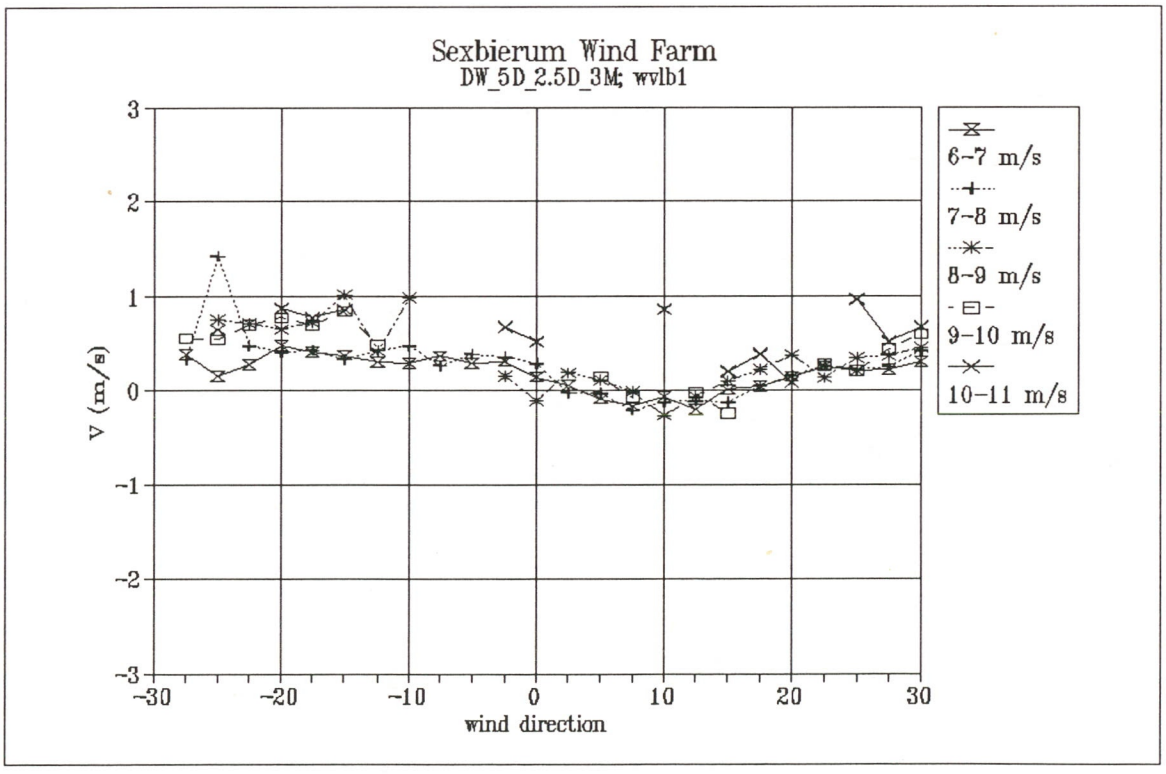

Figure 2 Lateral wind speed V as a function of wind direction and wind speed bin

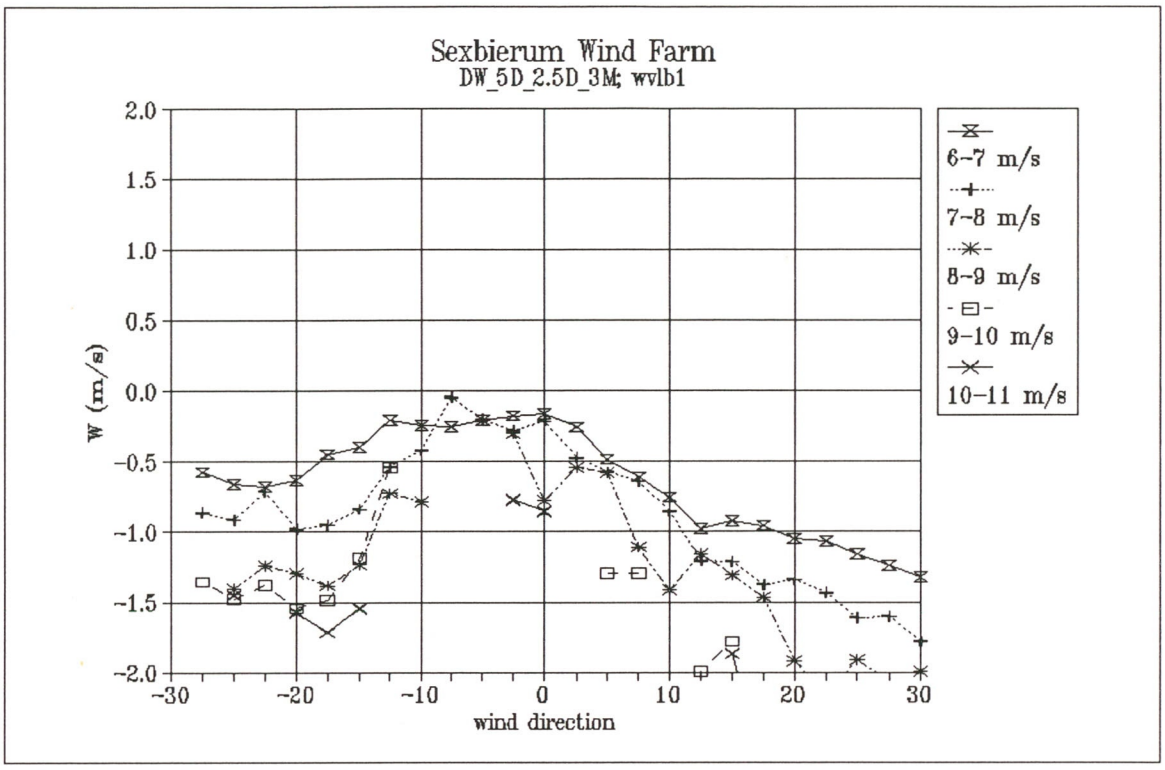

Figure 3 *Vertical wind speed W as a function of wind direction and wind speed bin*

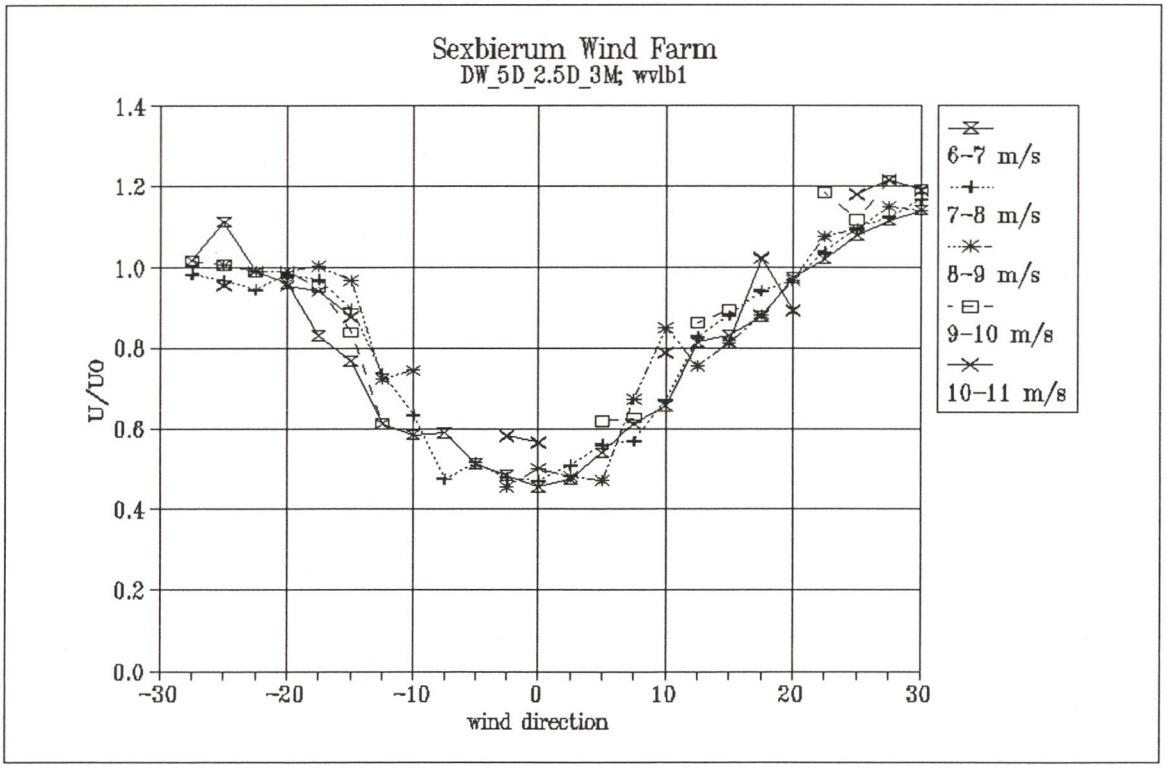

Figure 4 *Wake deficit U/U_0 as a function of wind direction and wind speed bin*

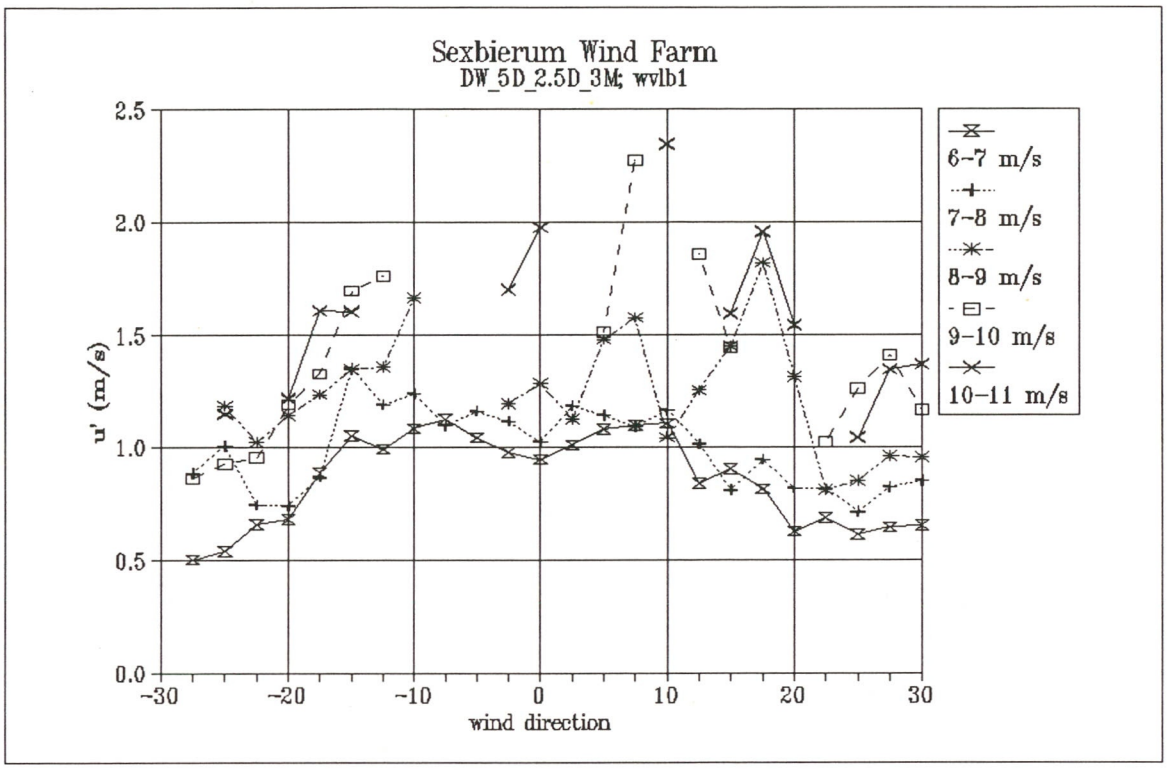

Figure 5 Longitudinal turbulent fluctuations u' as a function of wind direction and wind speed bin

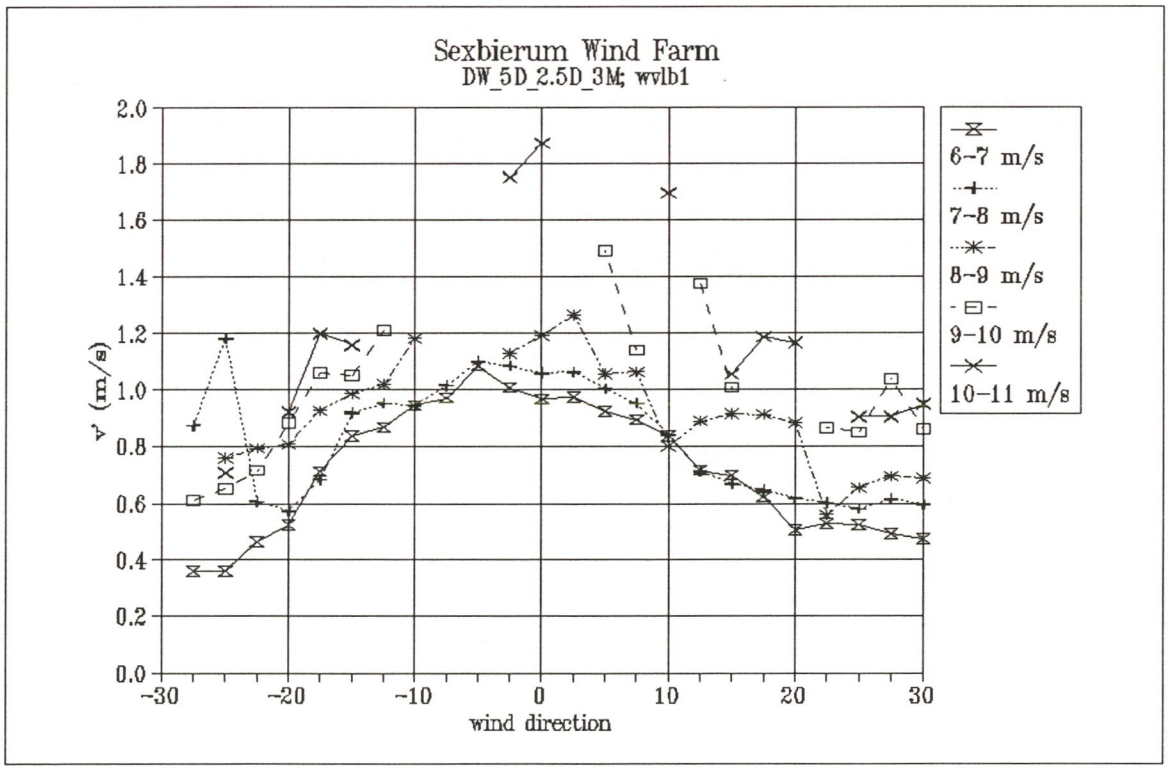

Figure 6 Lateral turbulent fluctuations v' as a function of wind direction and wind speed bin

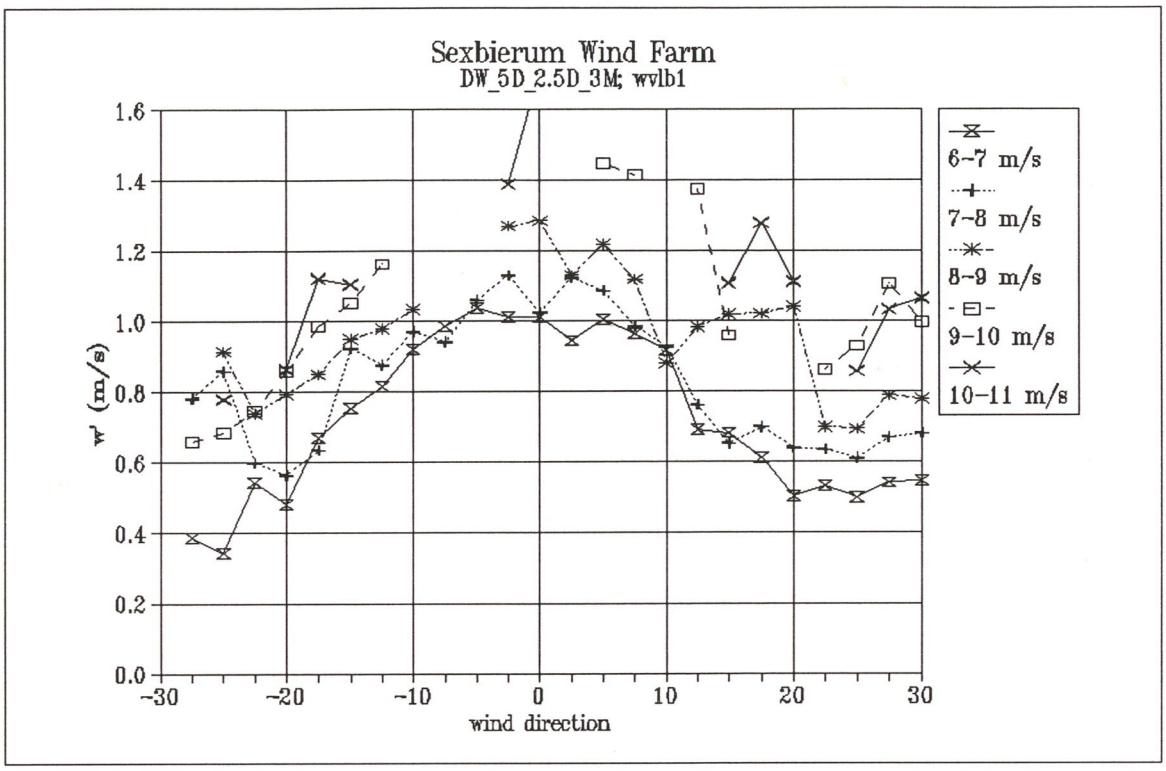

Figure 7 Vertical turbulent fluctuations w' as a function of wind direction and wind speed bin

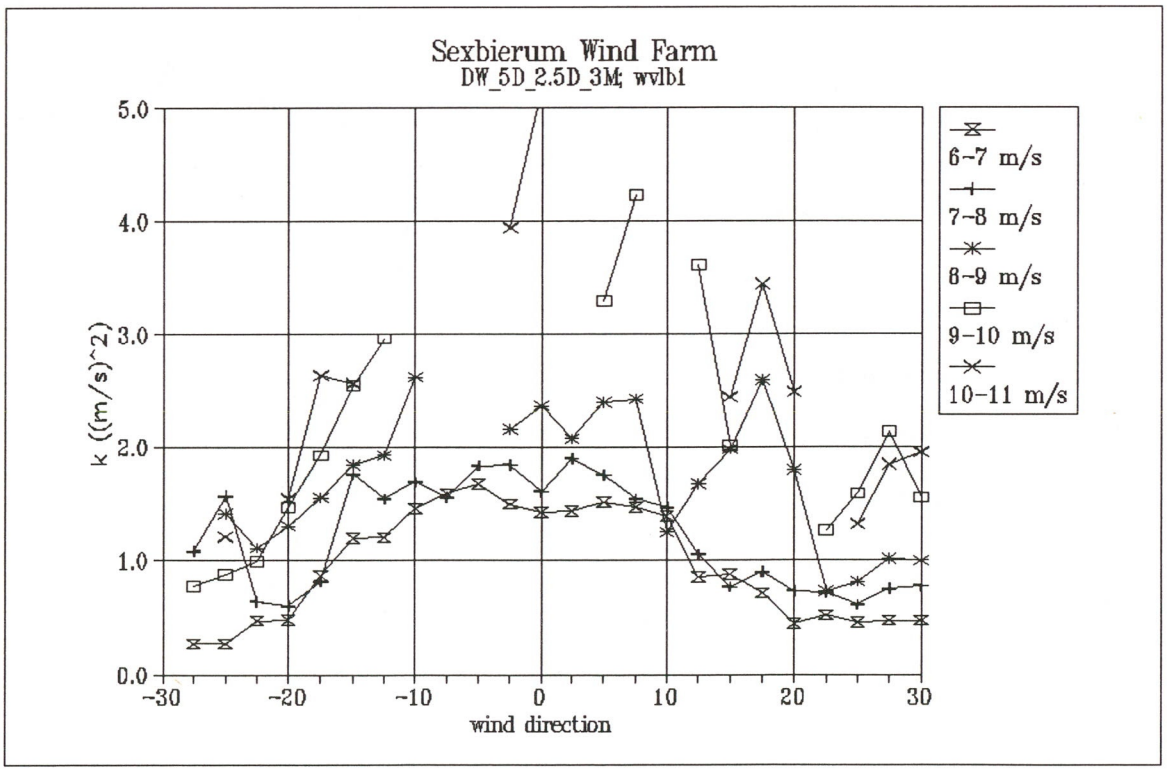

Figure 8 Turbulent kinetic energy per unit mass as a function of wind direction and wind speed bin

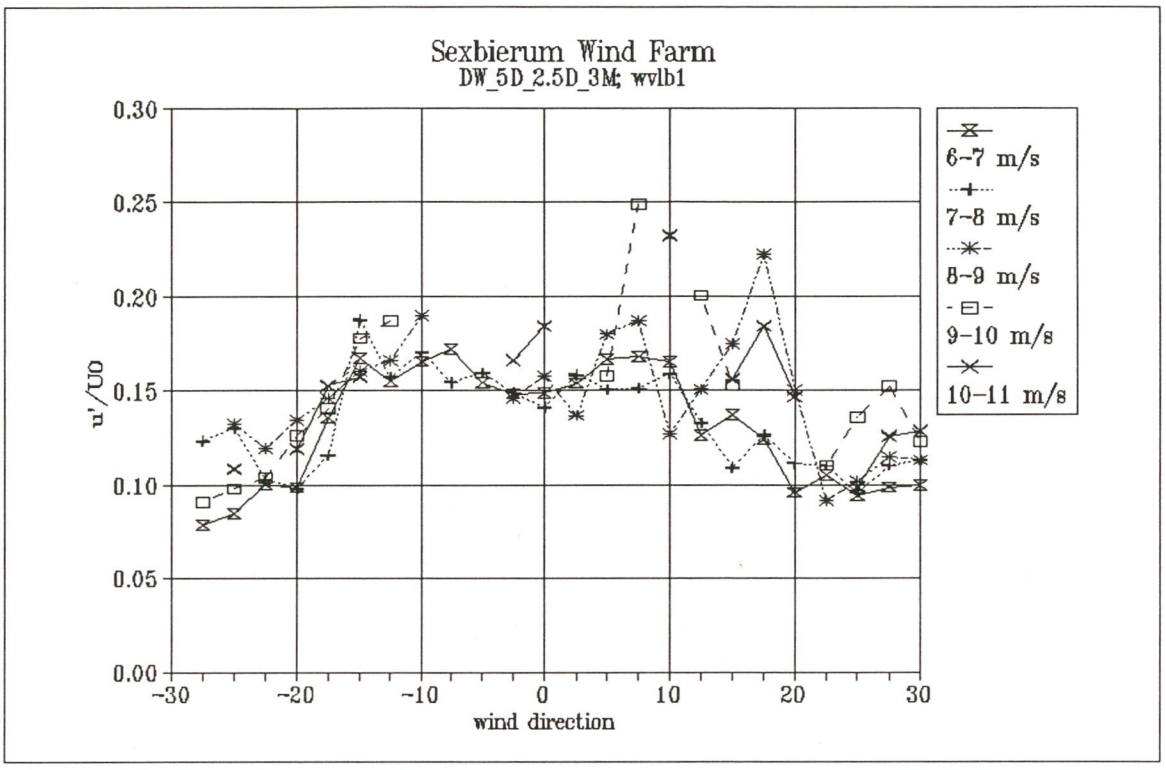

Figure 9 *Non-dimensionalized longitudinal turbulent fluctuations u'/U_0 as a function of wind direction and wind speed bin*

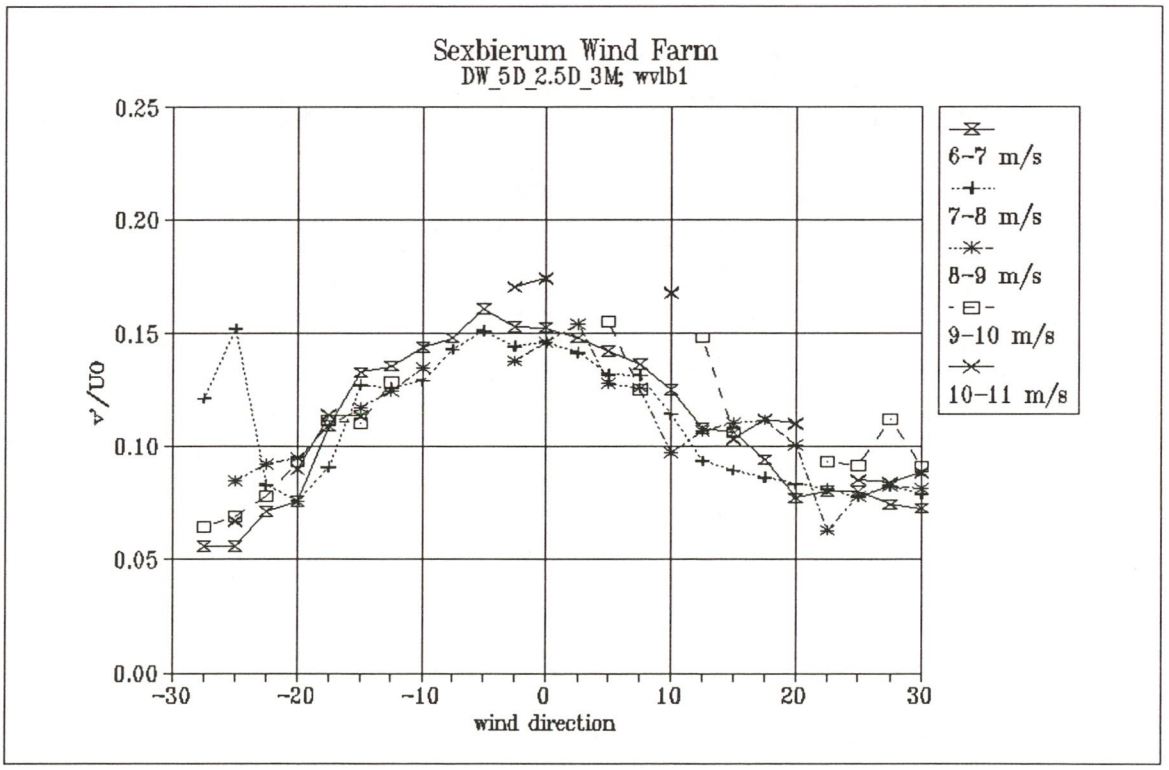

Figure 10 *Non-dimensionalized lateral turbulent fluctuations v'/U_0 as a function of wind direction and wind speed bin*

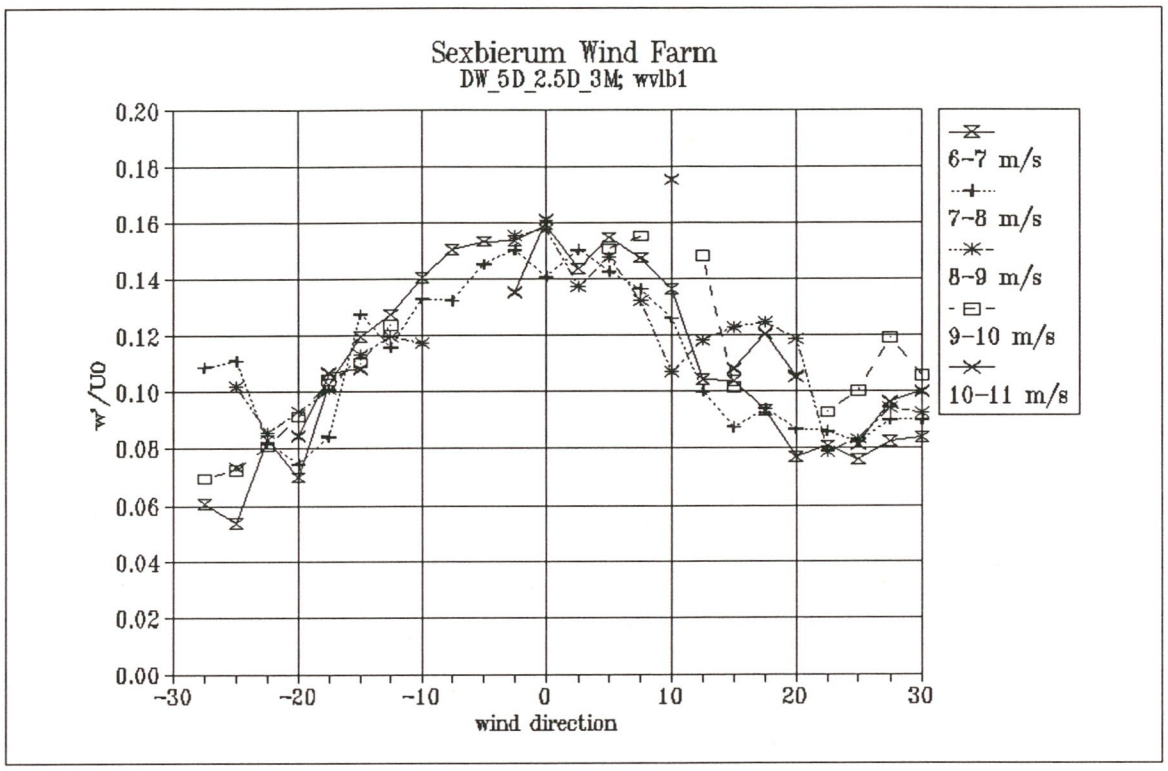

Figure 11 *Non-dimensionalized vertical turbulent fluctuations w'/U_0 as a function of wind direction and wind speed bin*

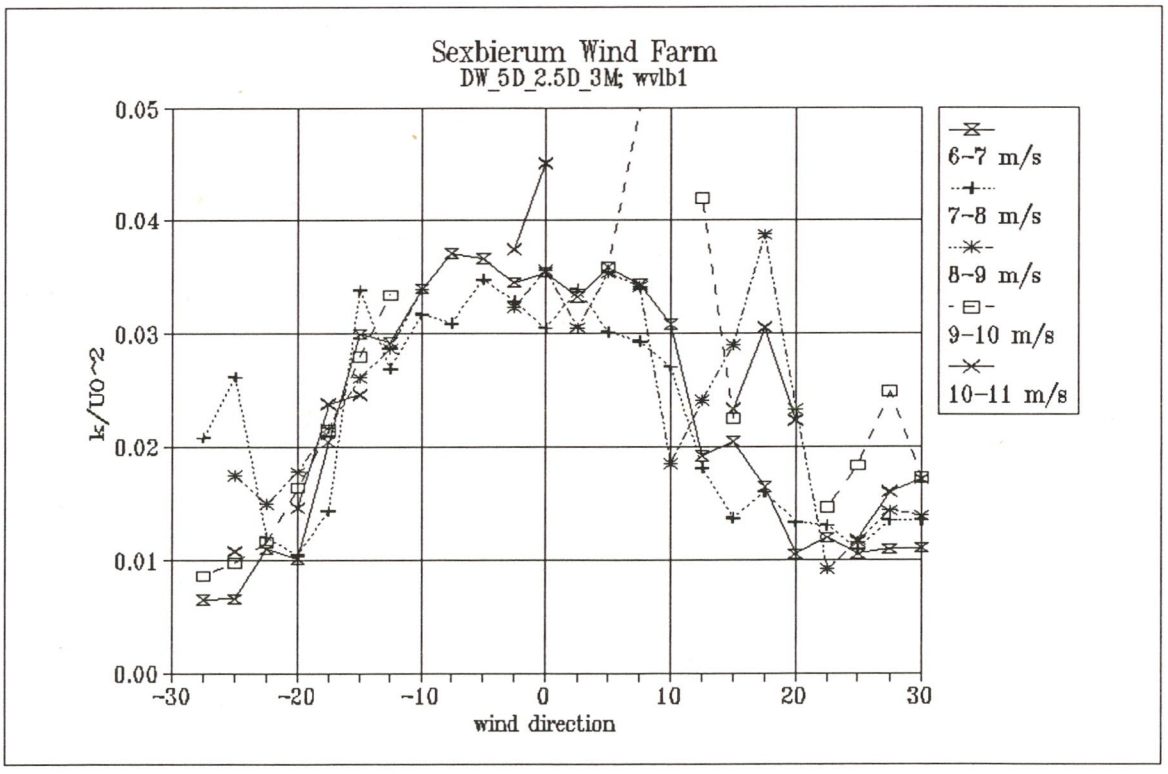

Figure 12 *Non-dimensionalized turbulent kinetic energy k/U_0^2 as a function of wind direction and wind speed bin*

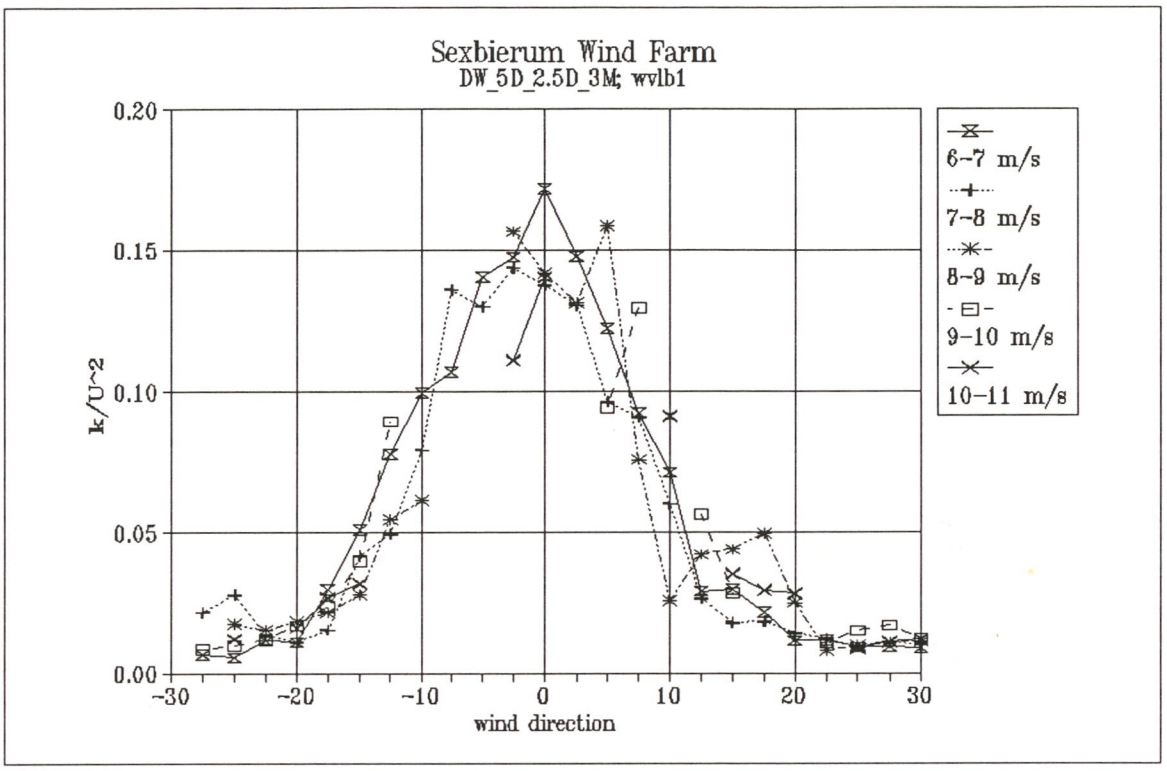

Figure 13 Non-dimensionalized turbulent kinetic energy k/U^2 as a function of wind direction and wind speed bin

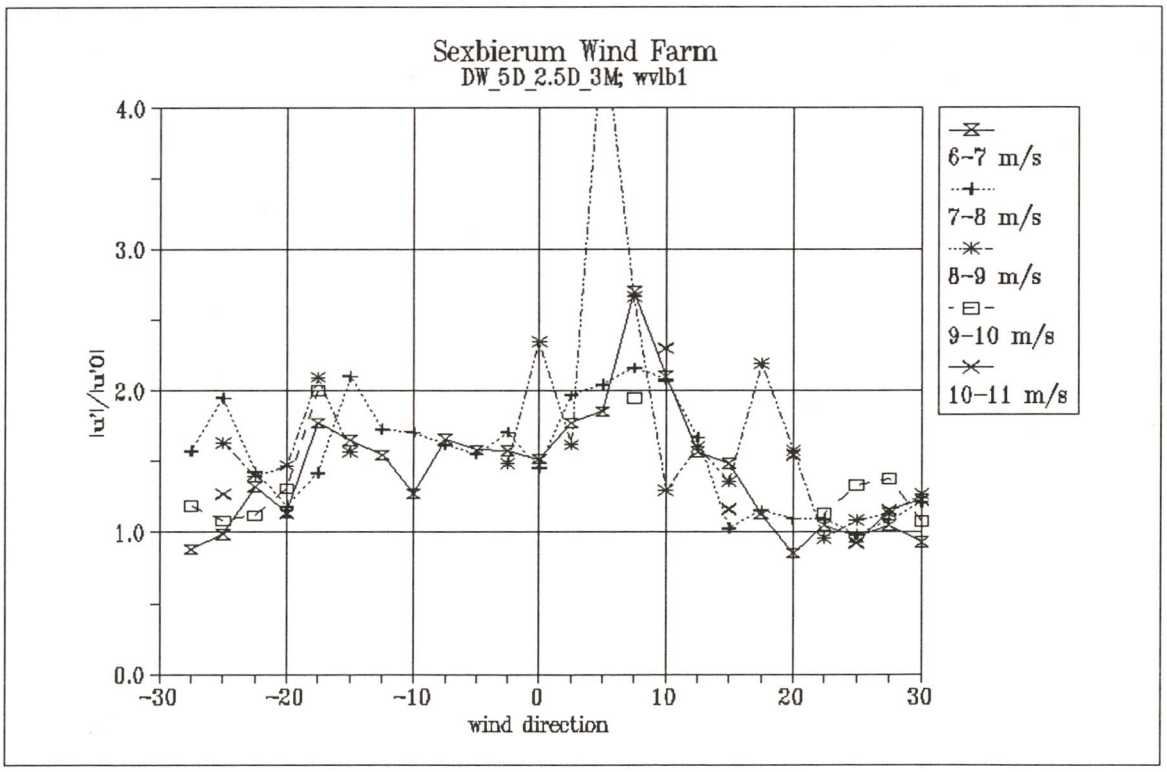

Figure 14 Longitudinal turbulence enhancement u'/u'_0 as a function of wind direction and wind speed bin

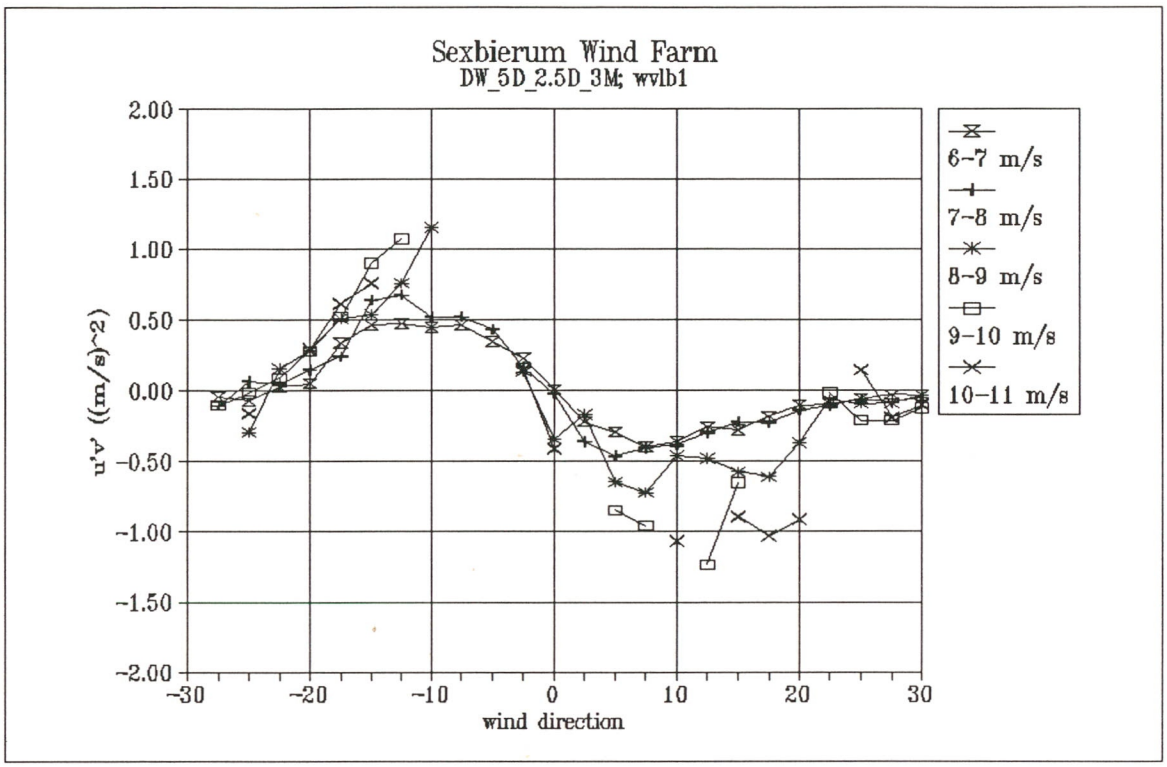

Figure 15 Shear stress u'v' as a function of wind direction and wind speed bin

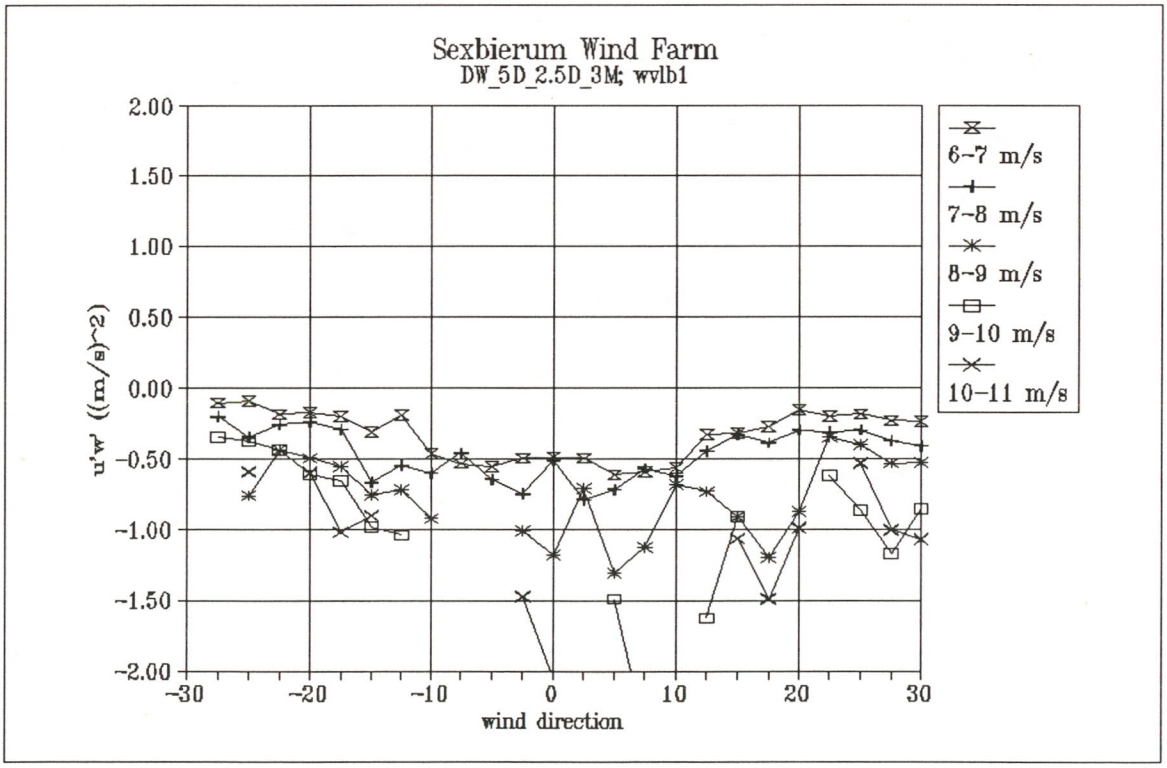

Figure 16 Shear stress u'w' as a function of wind direction and wind speed bin

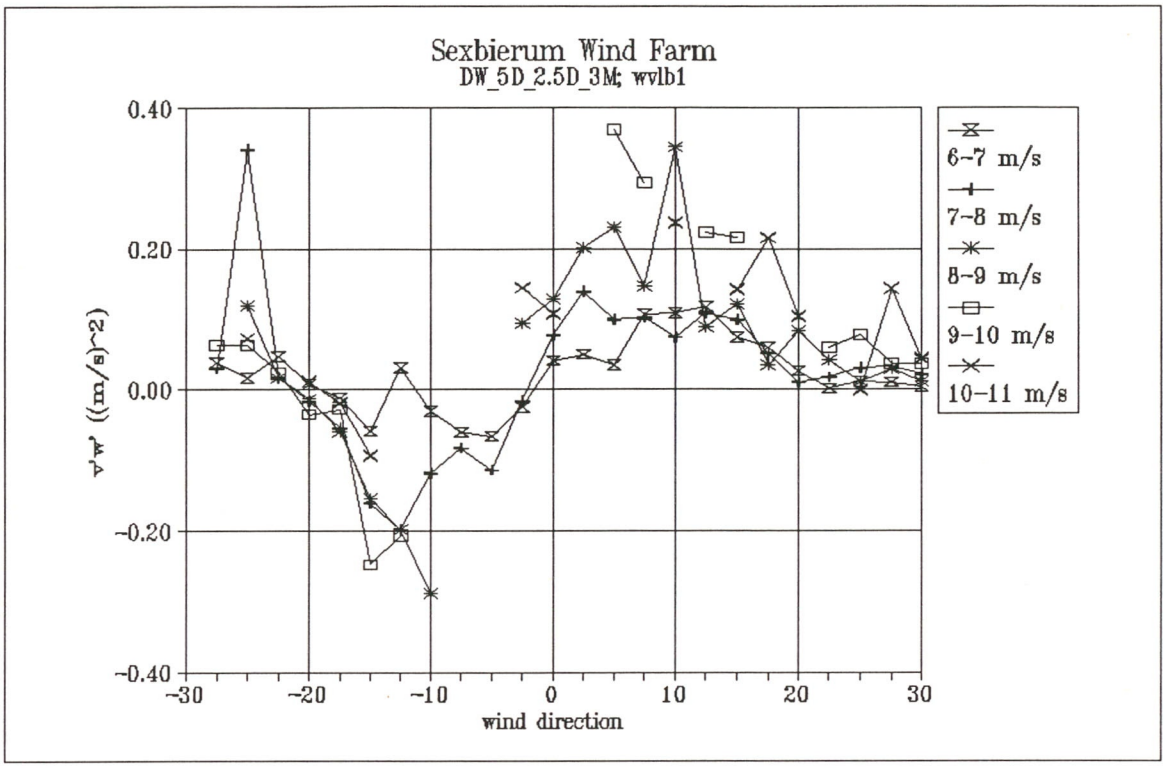

Figure 17 Shear stress v'w' as a function of wind direction and wind speed bin

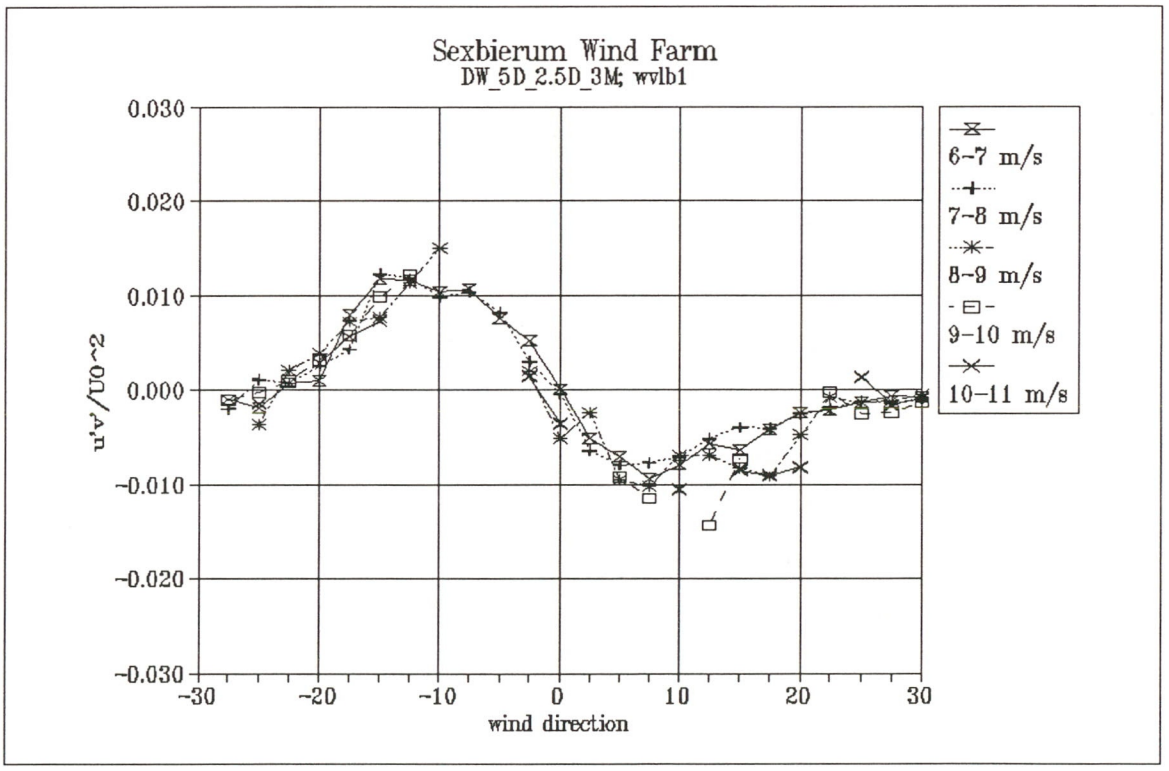

Figure 18 Non-dimensionalized shear stress $u'v'/U_0^2$ as a function of wind direction and wind speed bin

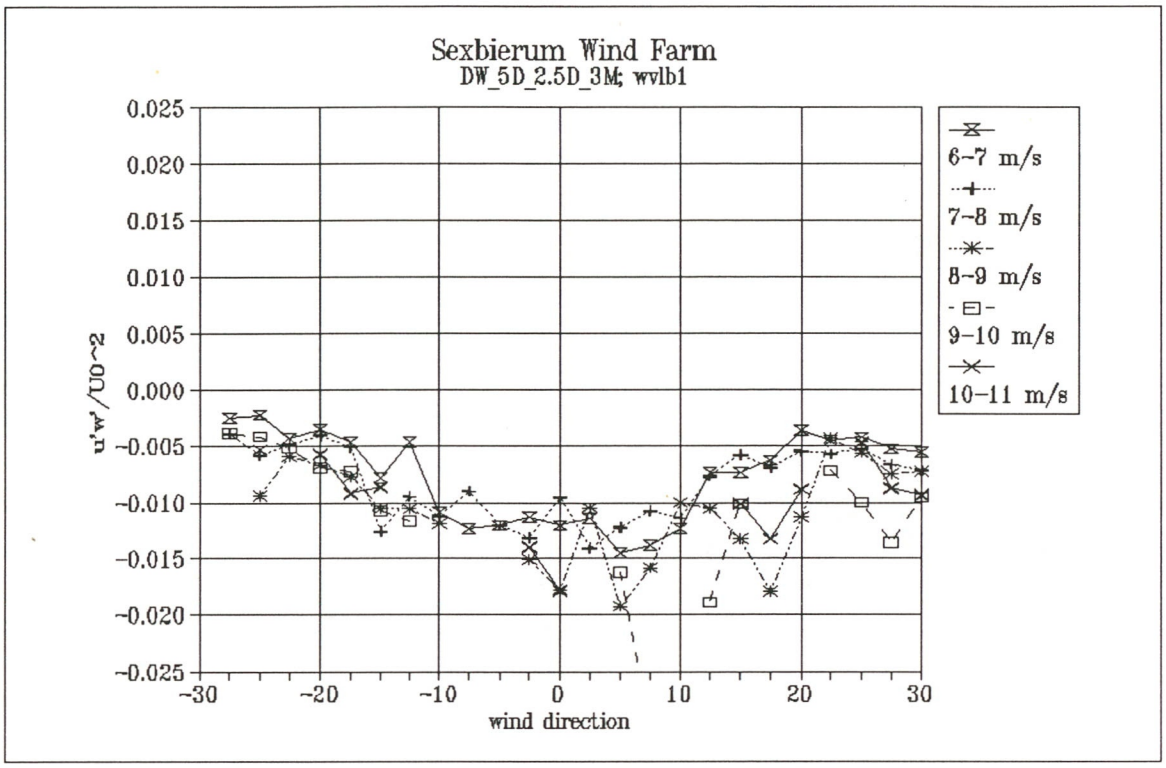

Figure 19 Non-dimensionalized shear stress $u'w'/U_0^2$ as a function of wind direction and wind speed bin

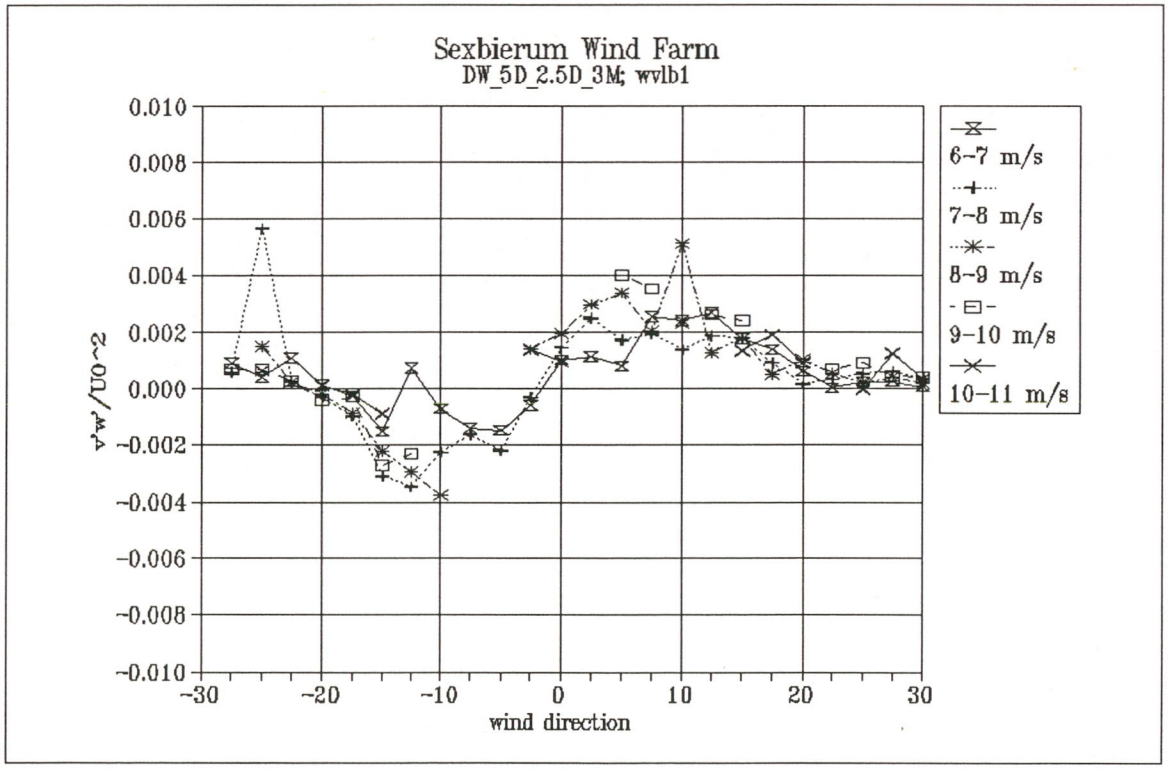

Figure 20 Non-dimensionalized shear stress $v'w'/U_0^2$ as a function of wind direction and wind speed bin

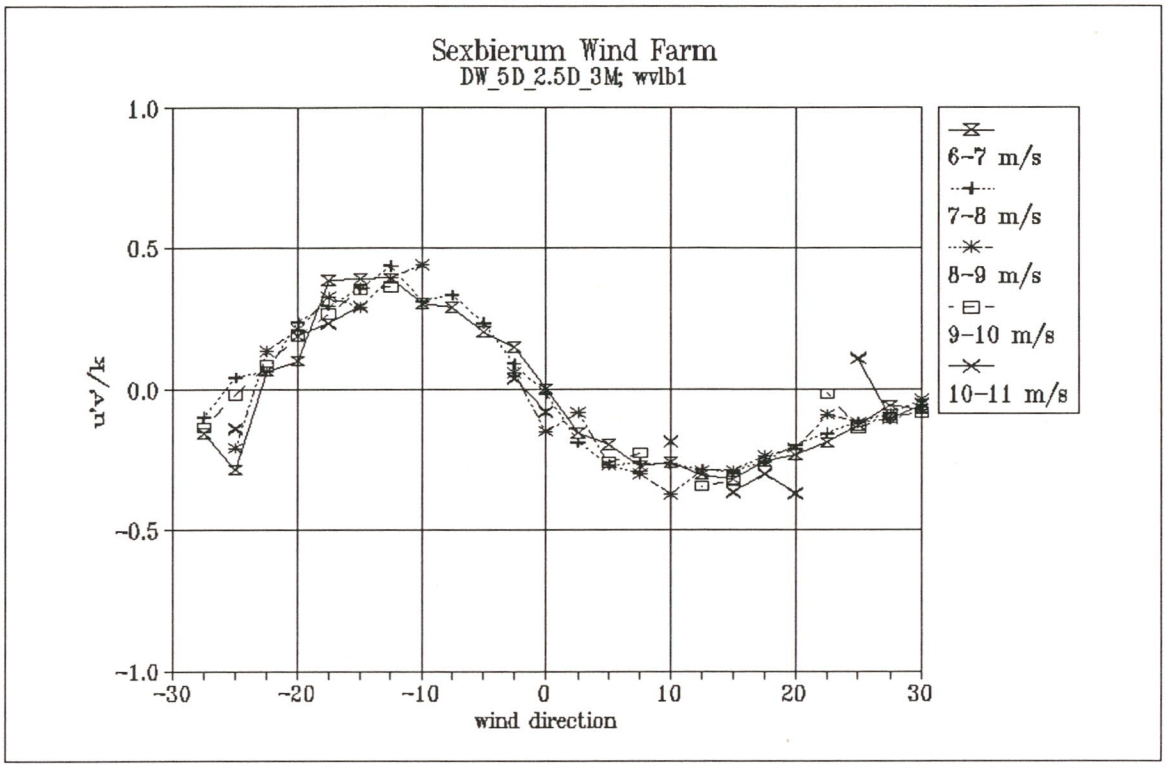

Figure 21 Non-dimensionalized shear stress u'v'/k as a function of wind direction and wind speed bin

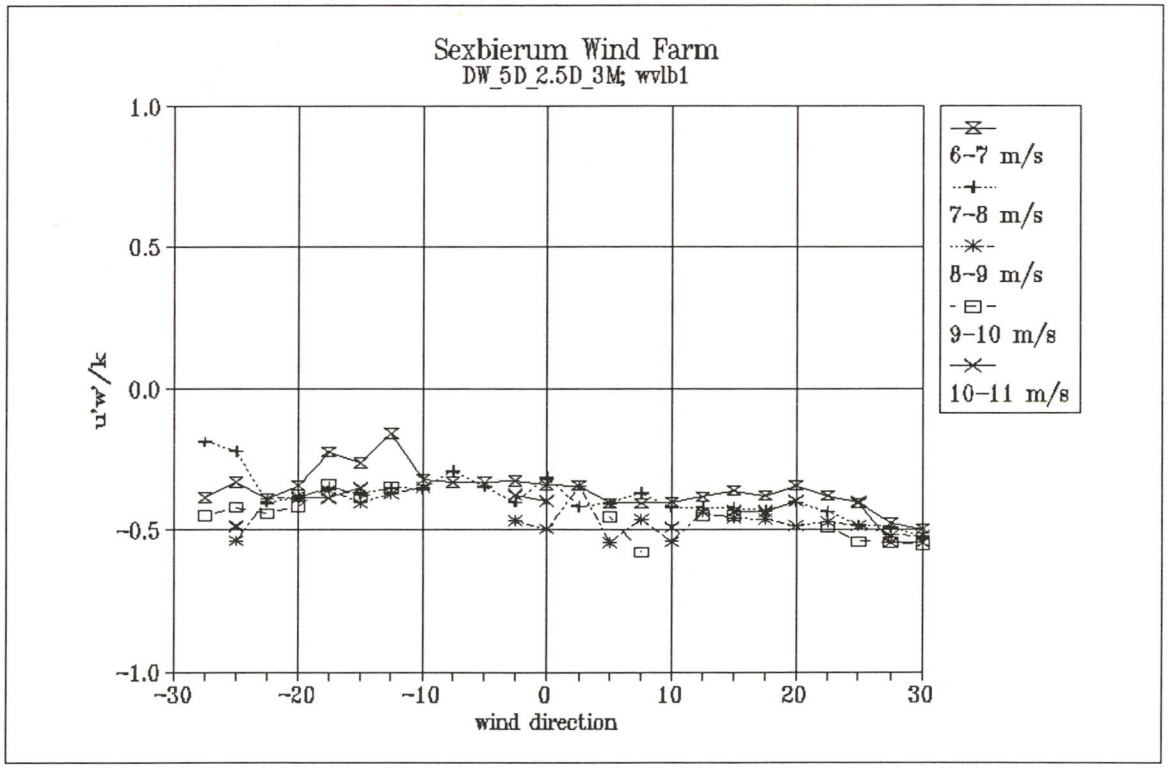

Figure 22 Non-dimensionalized shear stress u'w'/k as a function of wind direction and wind speed bin

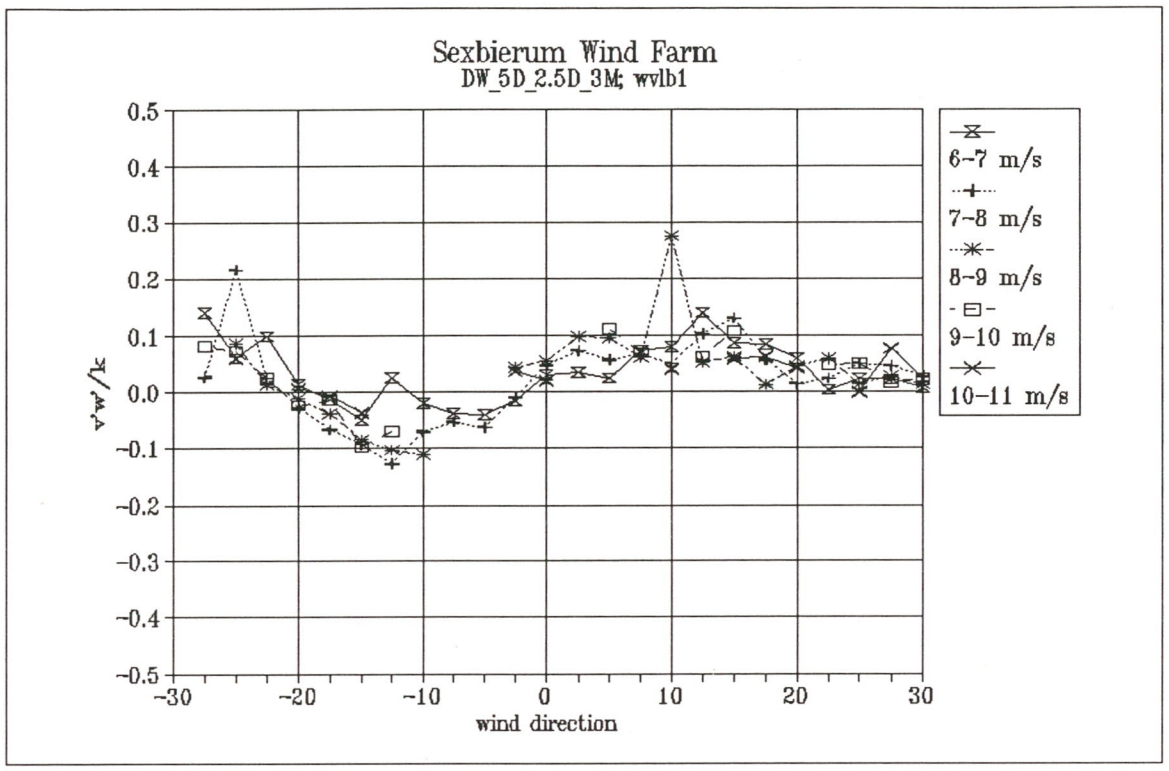

Figure 23 Non-dimensionalized shear stress v'w'/k as a function of wind direction and wind speed bin

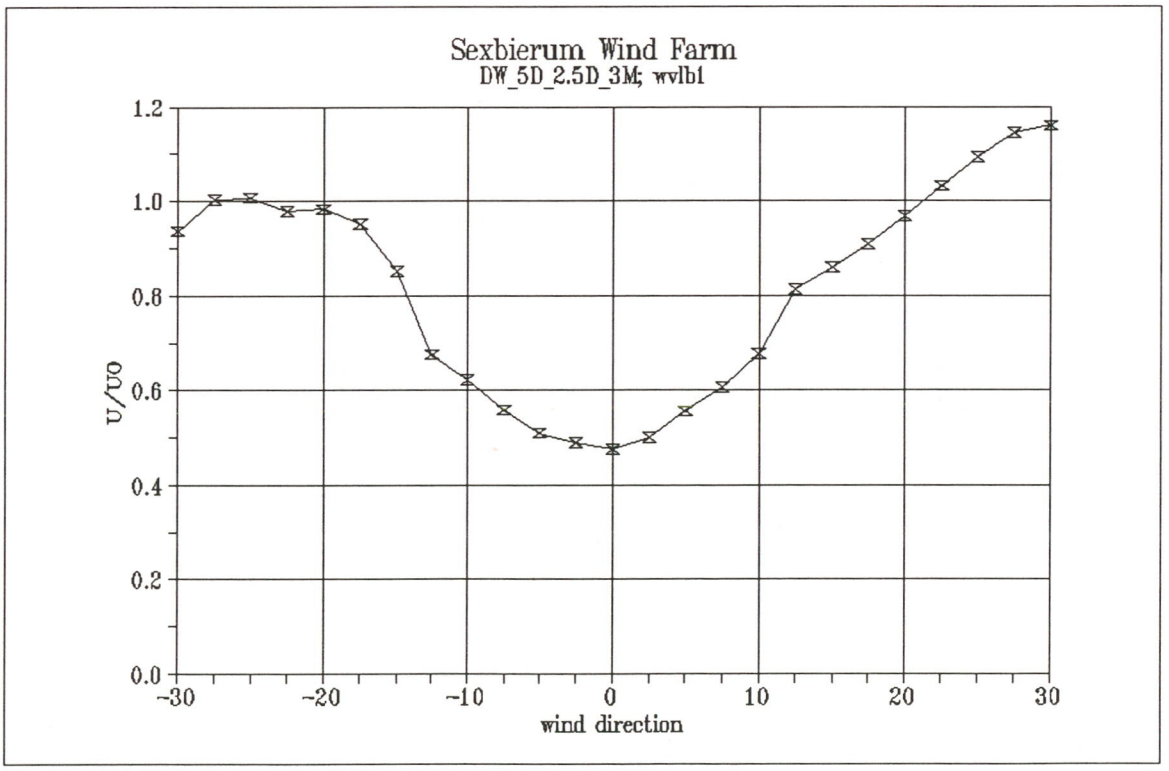

Figure 24 Wake deficit U/U_0 as a function of wind direction in the wind speed bin 5-10 m/s

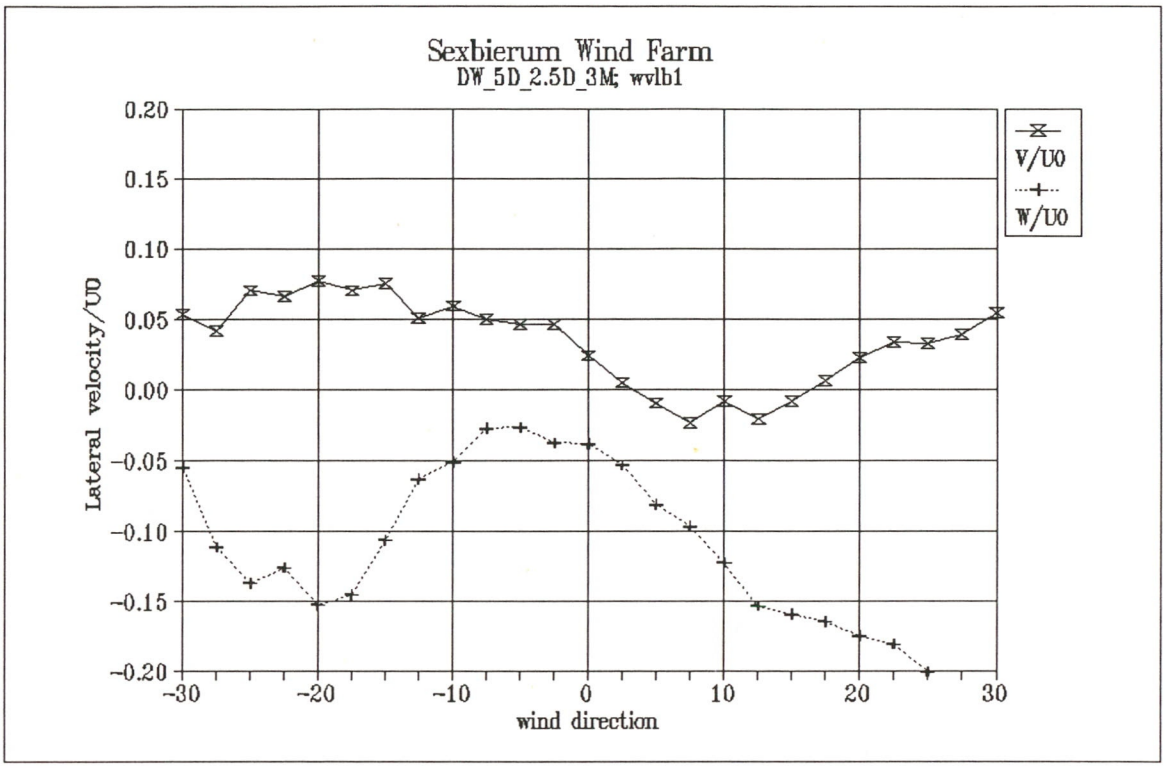

Figure 25 Lateral and vertical wind speed V/U_0 and W/U_0 as a function of wind direction in the wind speed bin 5-10 m/s

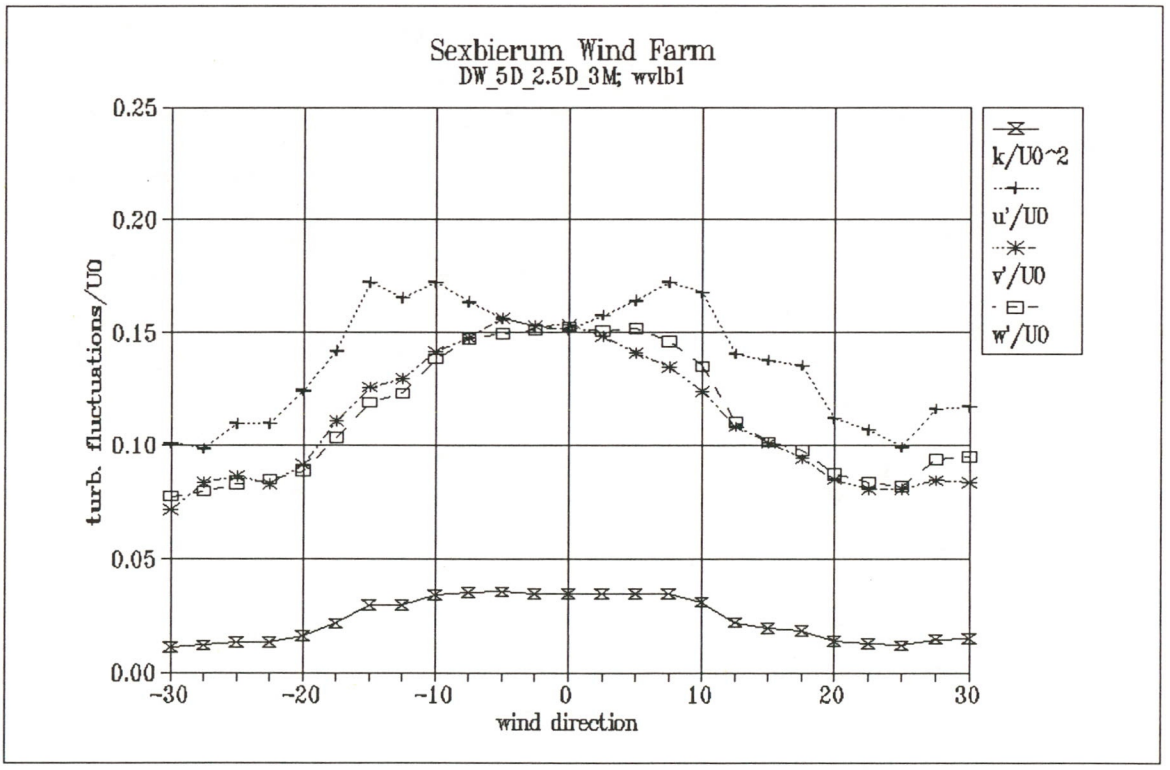

Figure 26 Turbulent fluctuations as a function of wind direction in the wind speed bin 5-10 m/s, non-dimensionalized with U_0

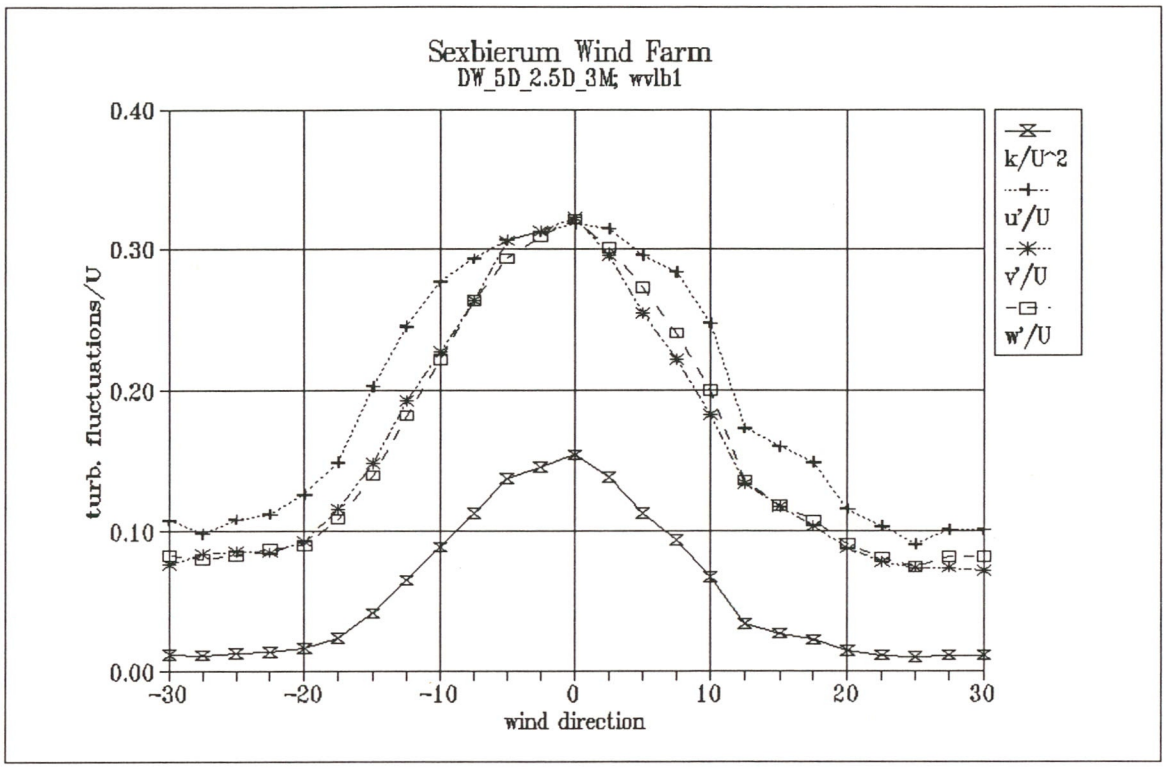

Figure 27 Turbulent fluctuations as a function of wind direction in the wind speed bin 5-10 m/s, non-dimensionalized with U

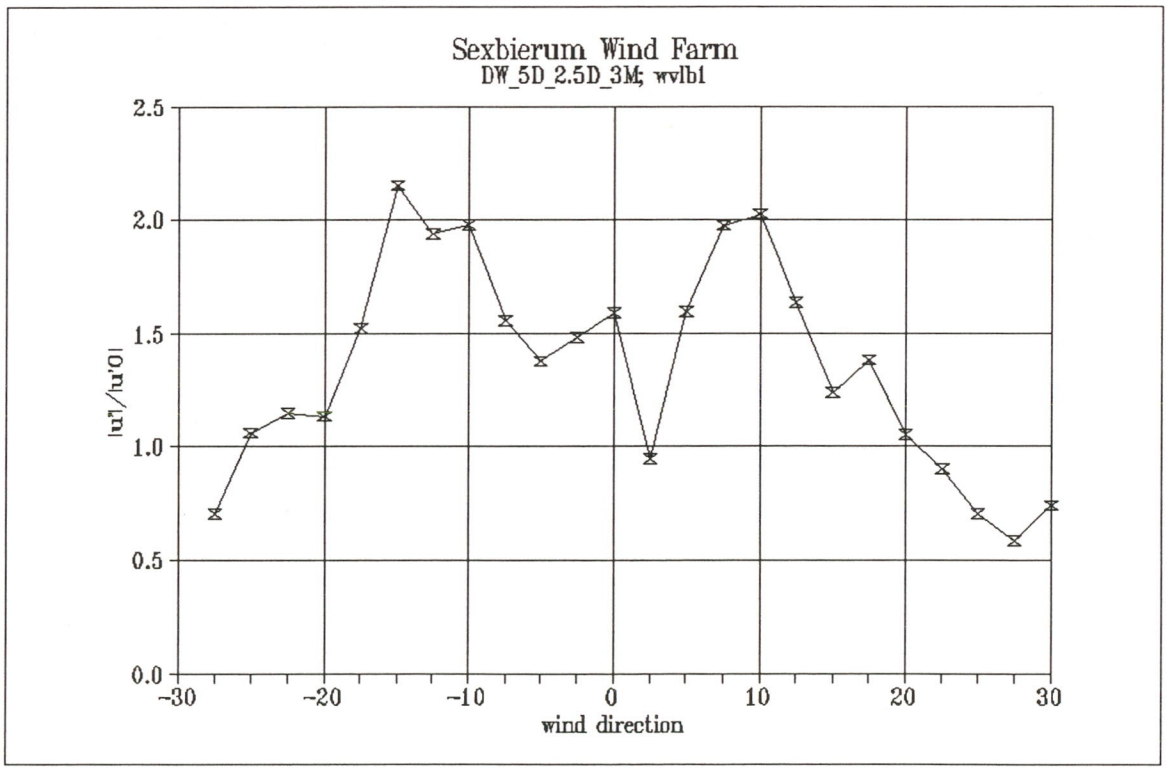

Figure 28 Longitudinal turbulence enhancement u'/u'_0 as a function of wind direction in the wind speed bin 5-10 m/s

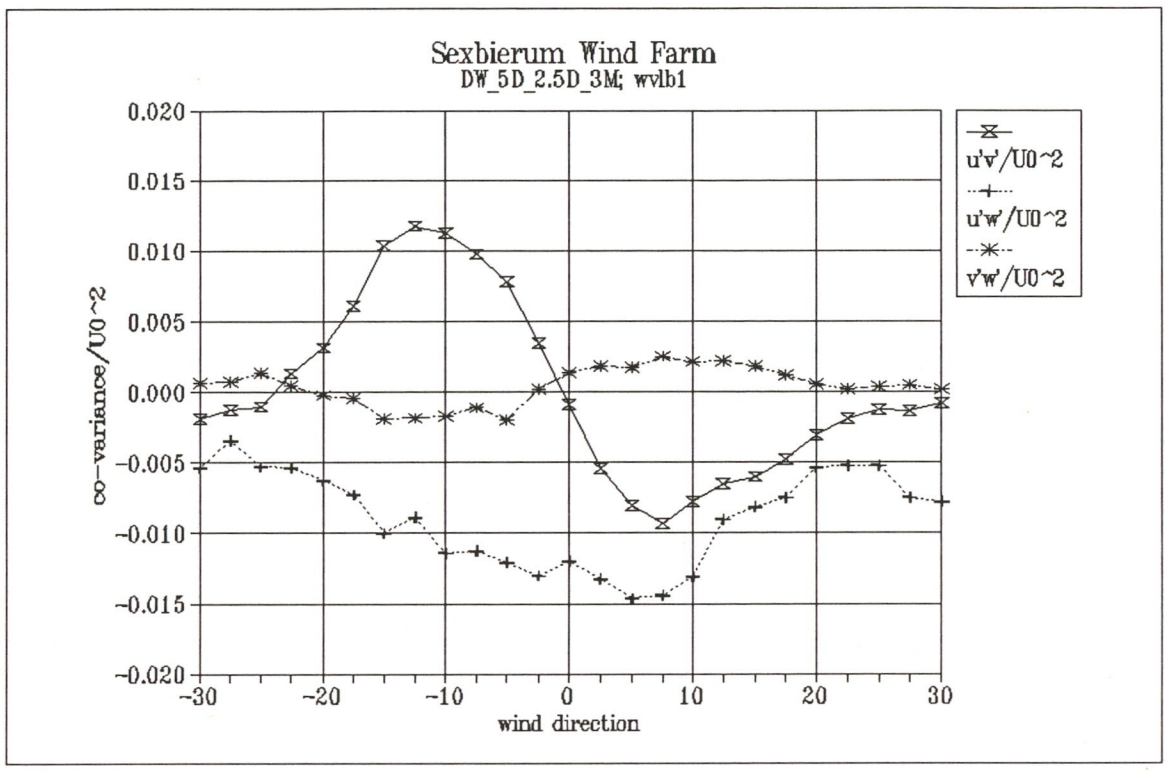

Figure 29 Non-dimensionalized shear stresses $u'v'/U_0^2$; $u'w'/U_0^2$; $v'w'/U_0^2$ as a function of wind direction in the wind speed bin 5-10 m/s

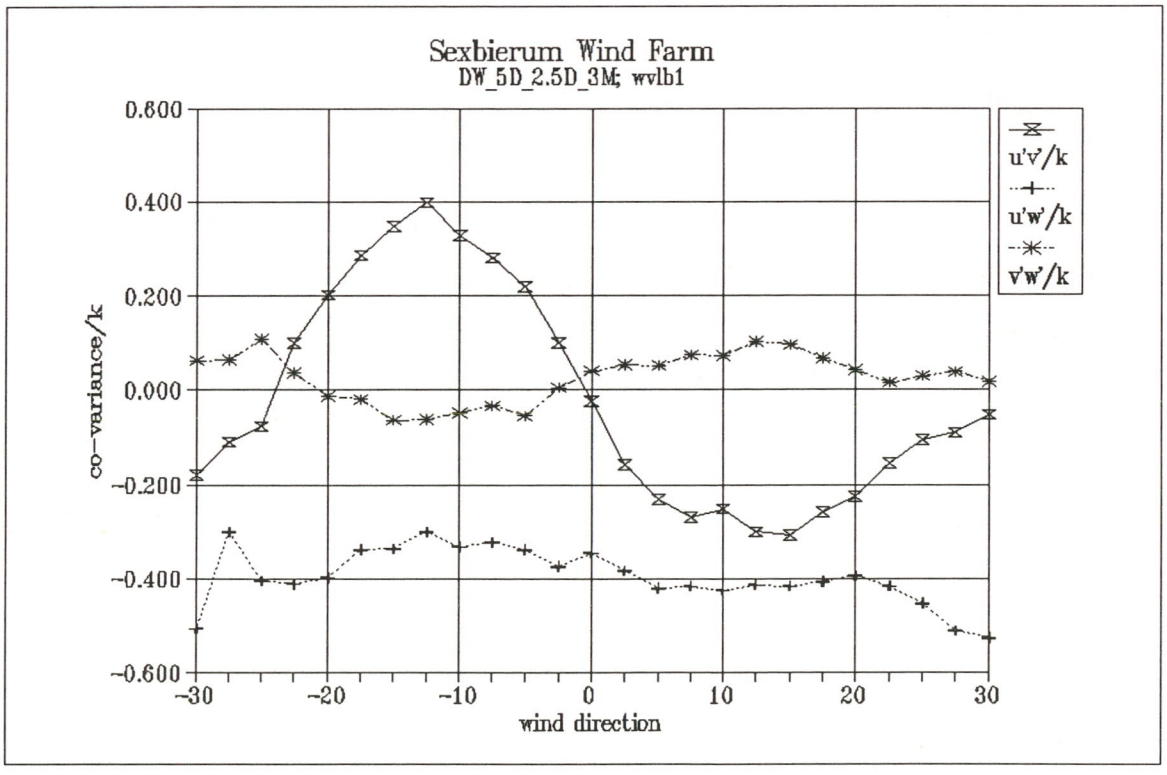

Figure 30 Non-dimensionalized shear stresses u'v'/k; u'w'/k; v'w'/k as a function of wind direction in the wind speed bin 5-10 m/s

A4.3 Sensor b2h

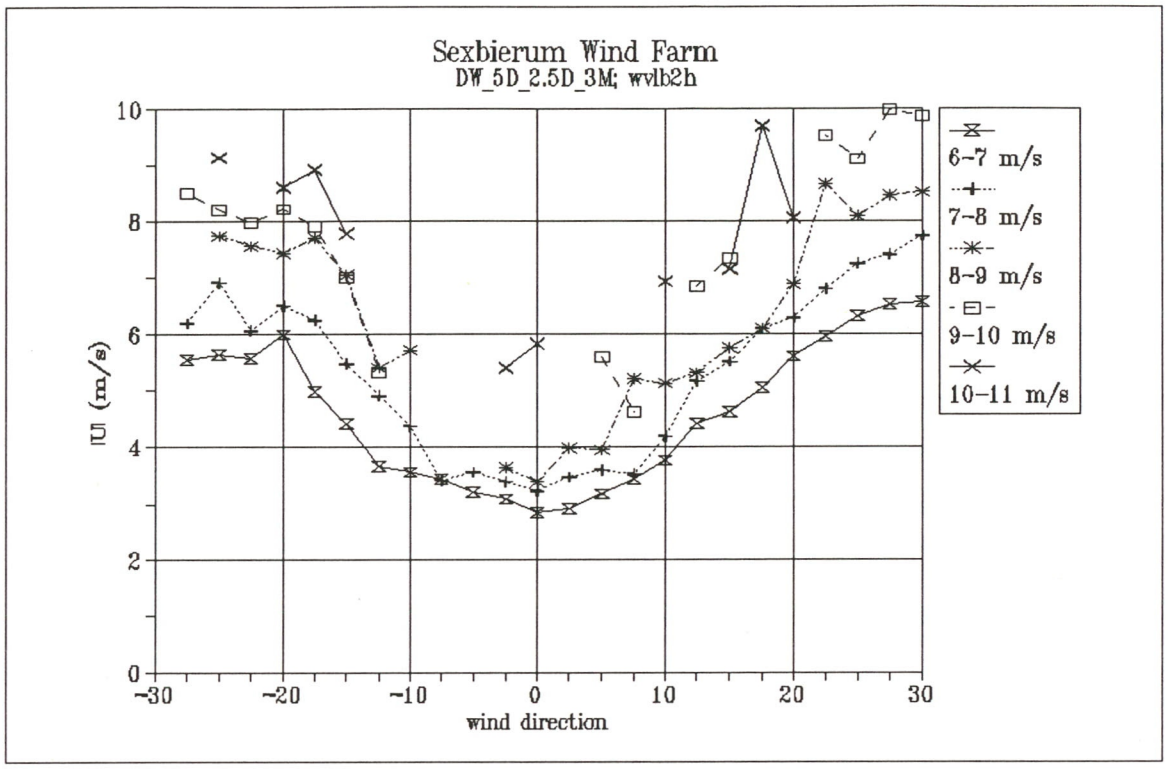

Figure 1 *Wind speed U as a function of wind direction and wind speed bin*

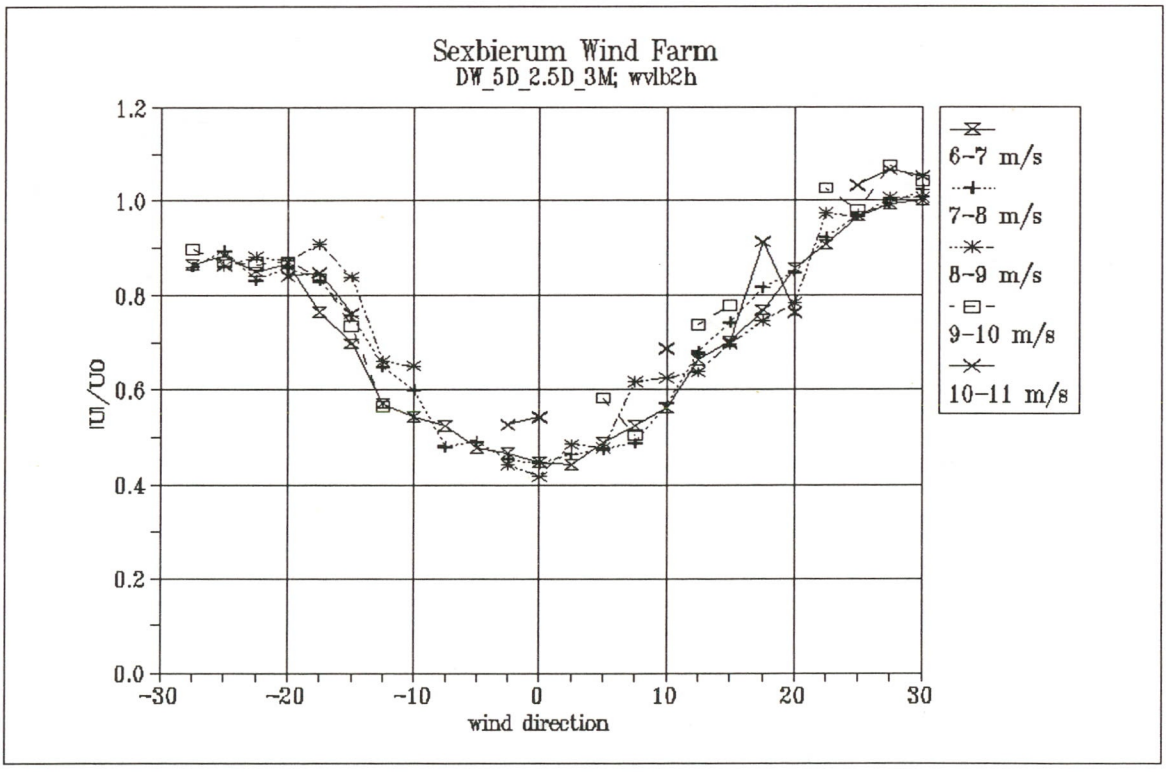

Figure 2 *Wake deficit U/U_0 as a function of wind direction and wind speed bin*

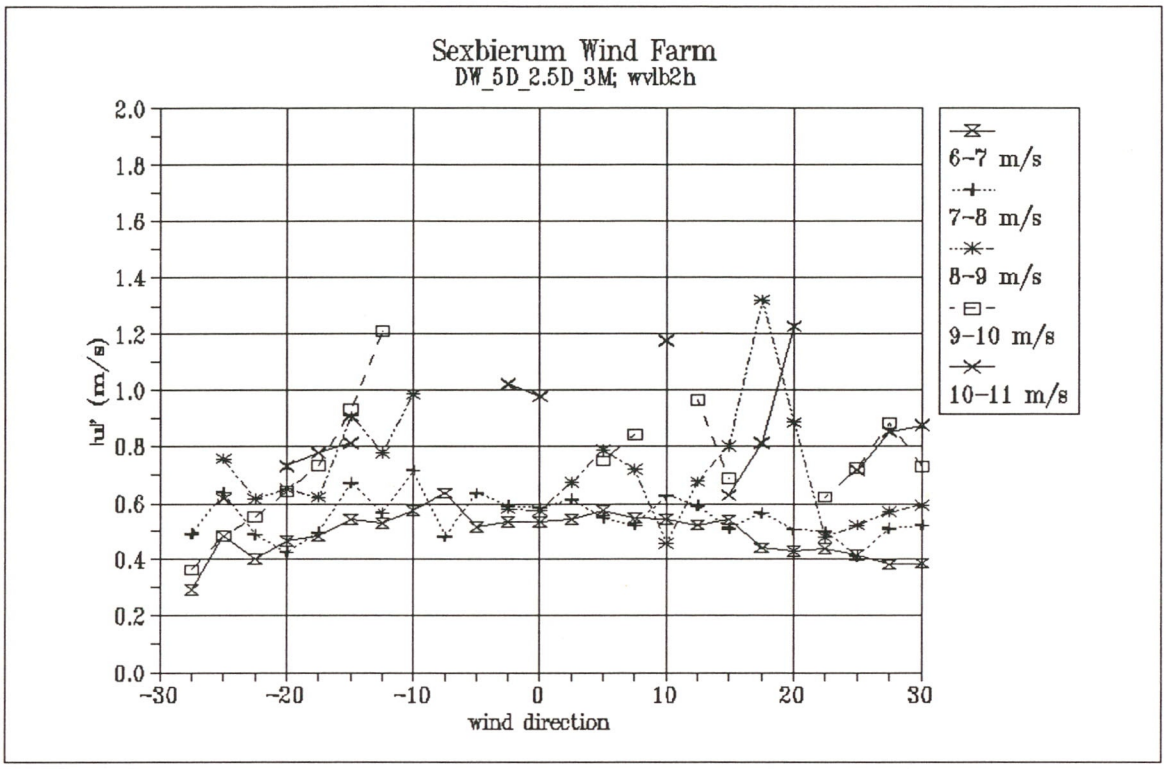

Figure 3 Turbulent fluctuations u' as a function of wind direction and wind speed bin

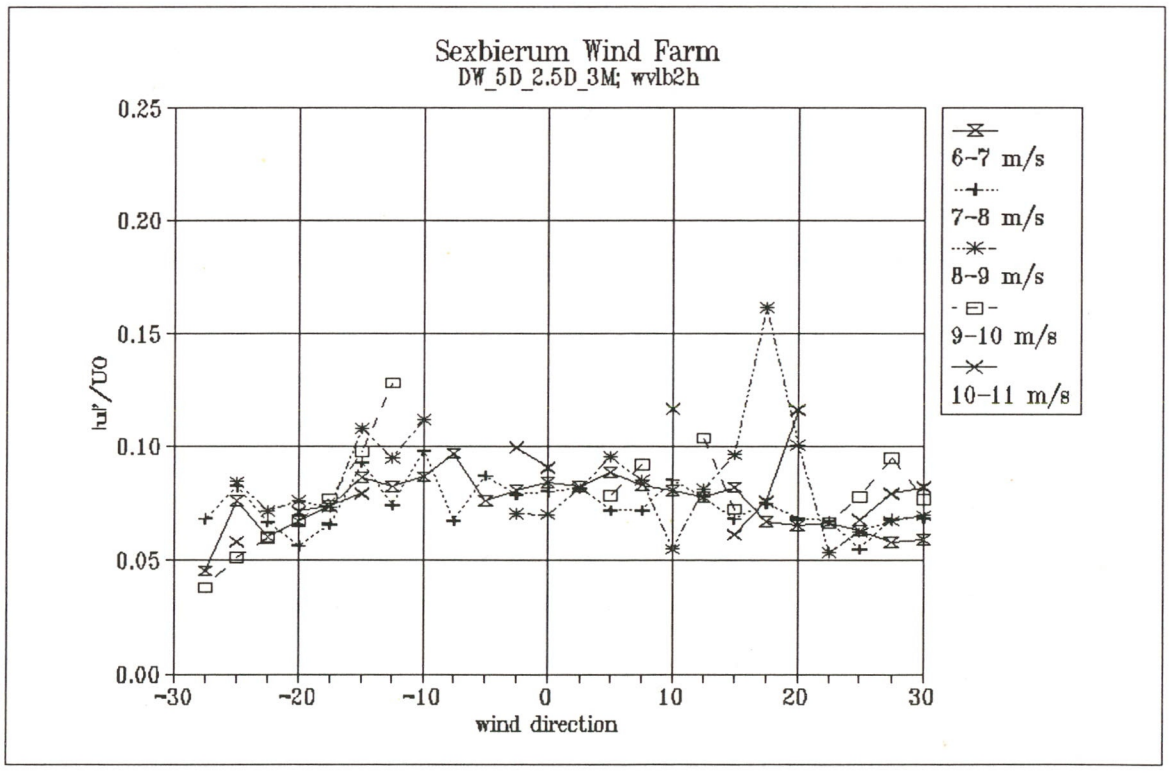

Figure 4 Non-dimensionalized turbulent fluctuations u'/U_0 as a function of wind direction and wind speed bin

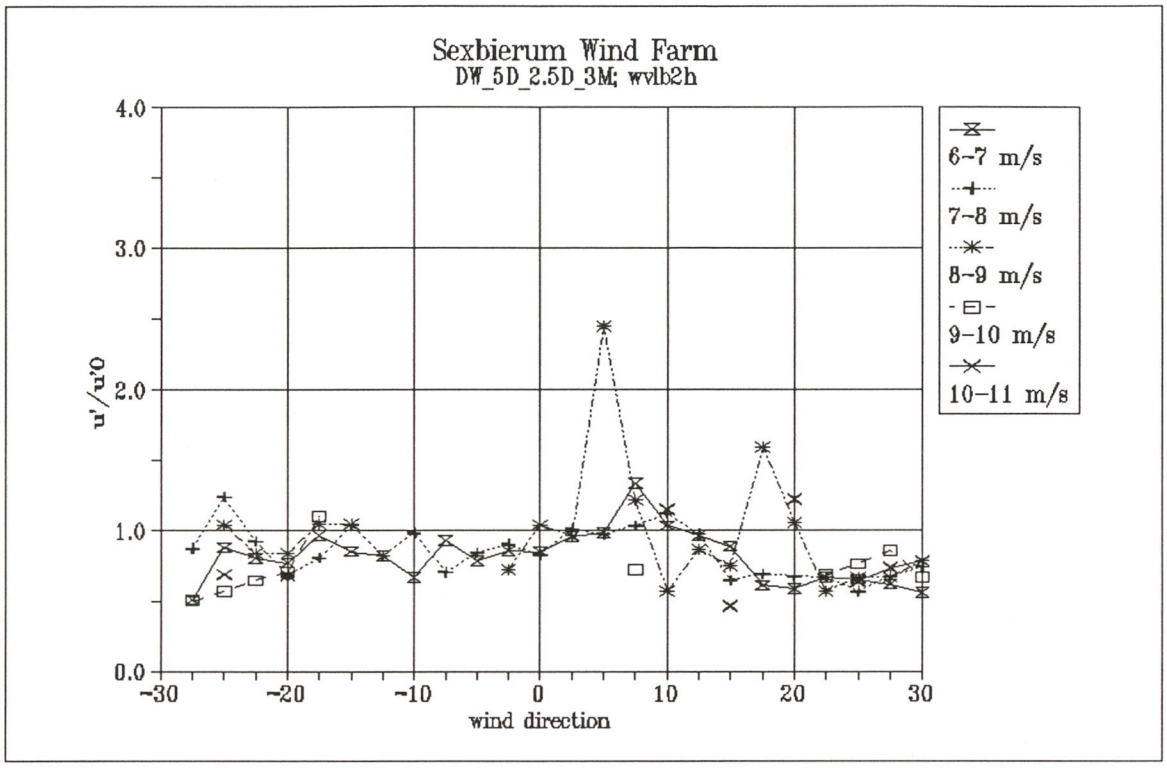

Figure 5 Turbulence enhancement u'/u'_0 as a function of wind direction and wind speed bin

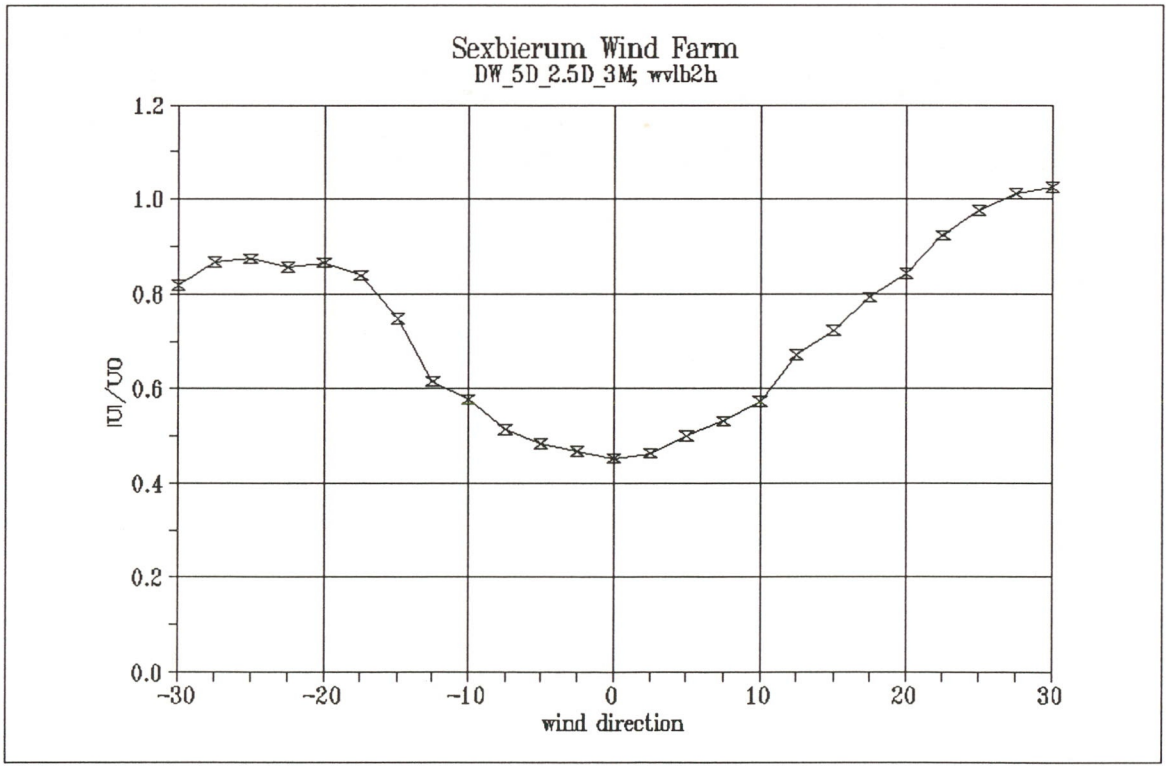

Figure 6 Wake deficit U/U_0 as a function of wind direction in the wind speed bin 5-10 m/s

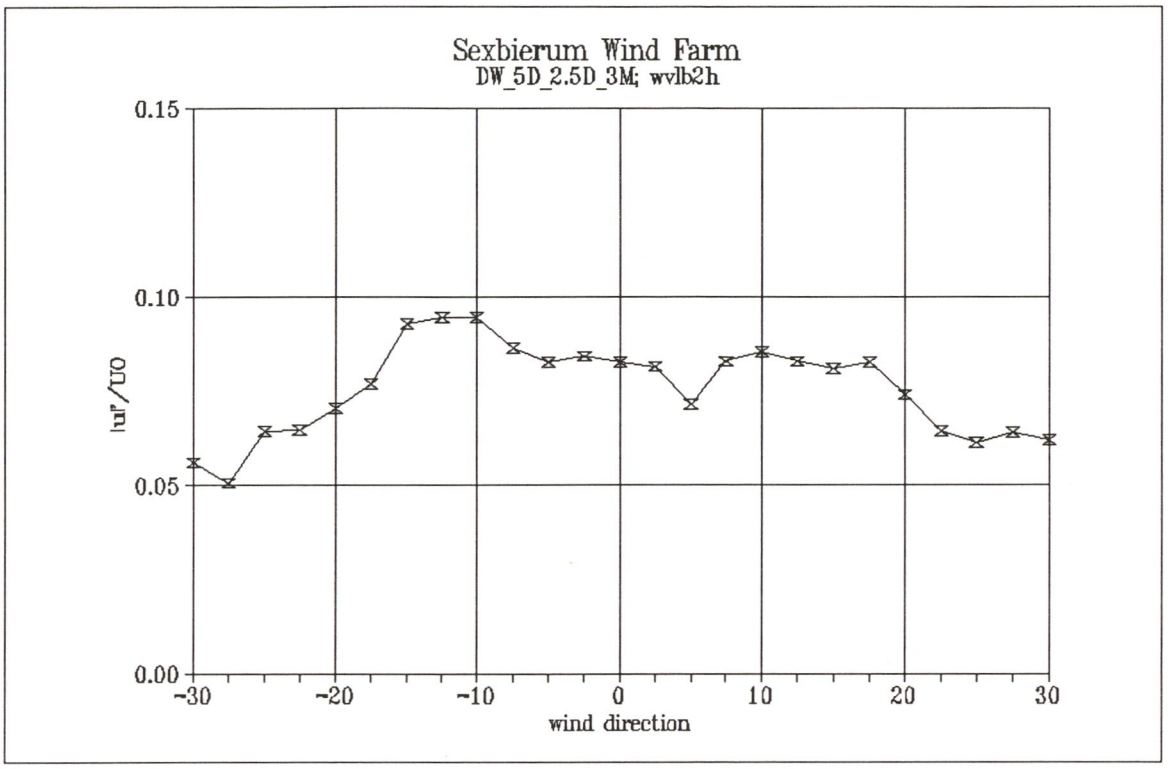

Figure 7 *Non-dimensionalized turbulent fluctuations u'/U_0 as a function of wind direction in the wind speed bin 5-10 m/s*

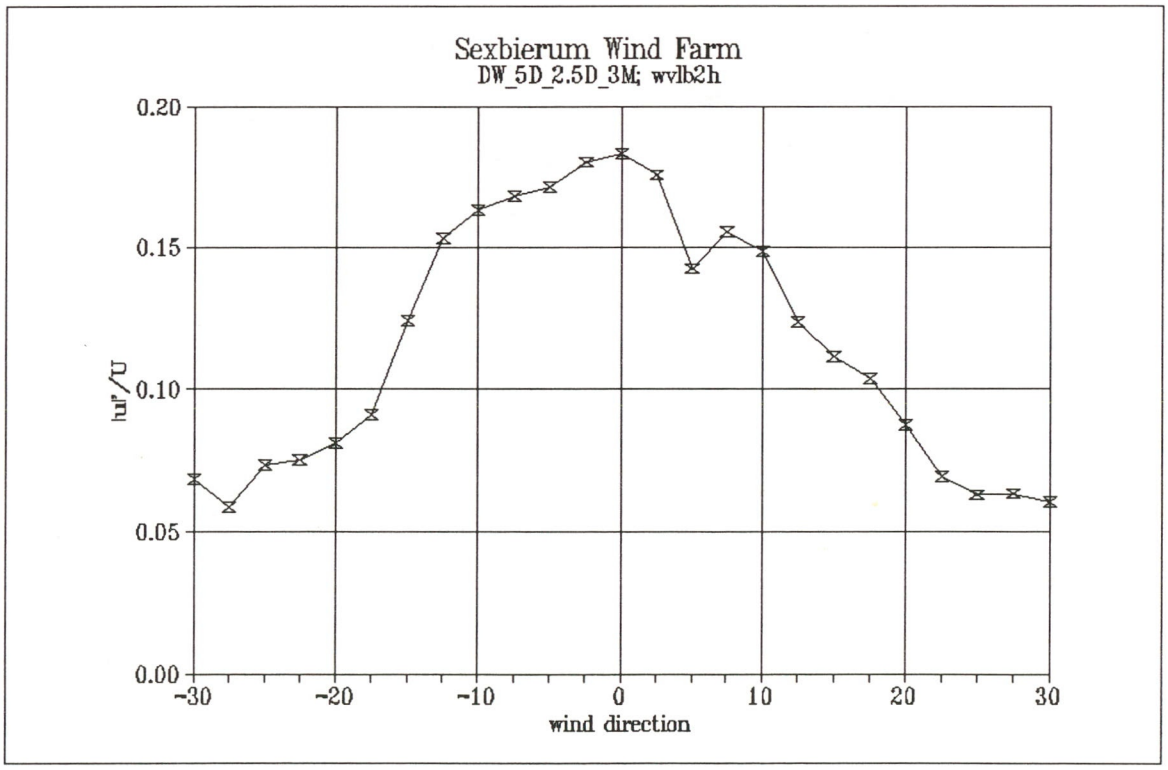

Figure 8 *Non-dimensionalized turbulent fluctuations u'/U as a function of wind direction in the wind speed bin 5-10 m/s*

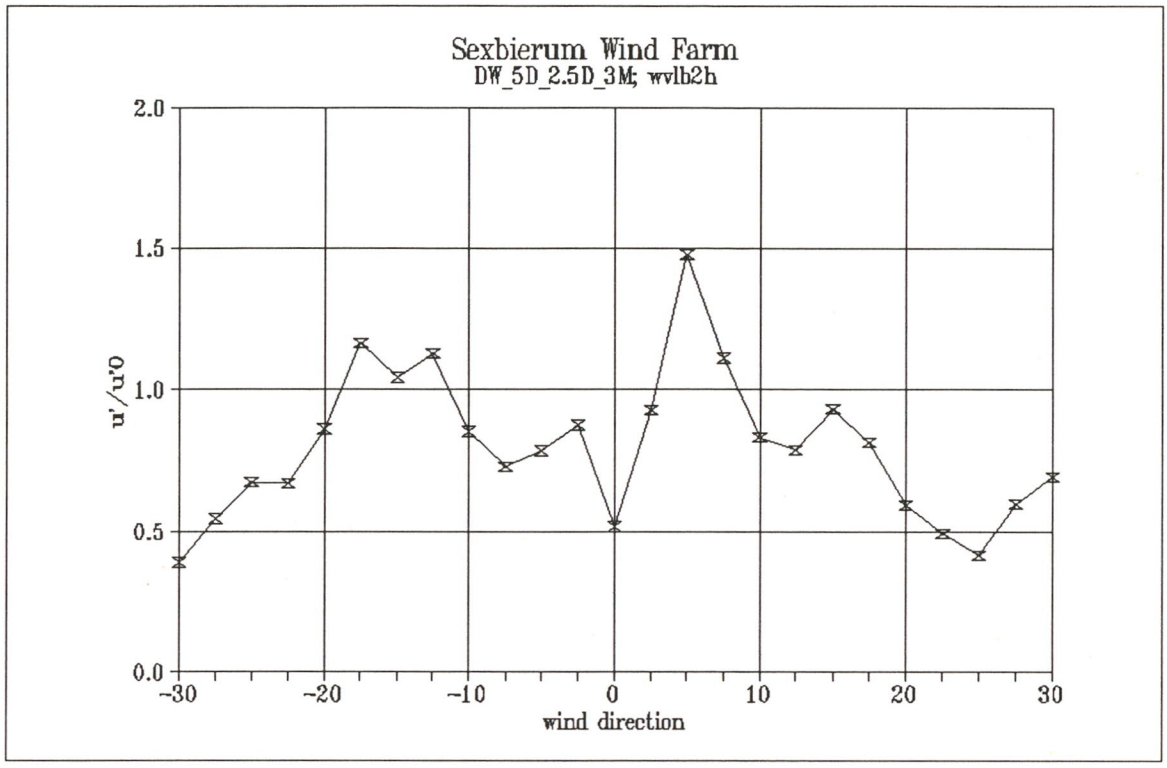

Figure 9 Turbulence enhancement u'/u'_0 as a function of wind direction in the wind speed bin 5-10 m/s

A4.4 Sensor b2

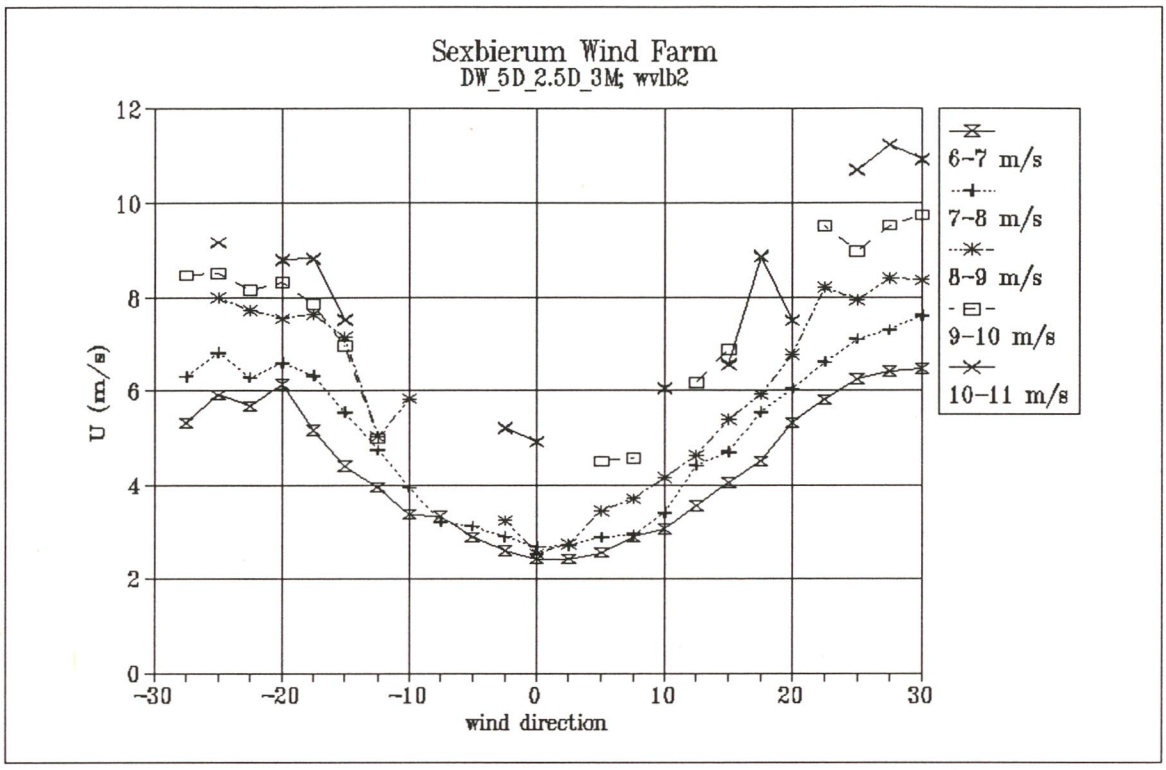

Figure 1 Horizontal wind speed U as a function of wind direction and wind speed bin

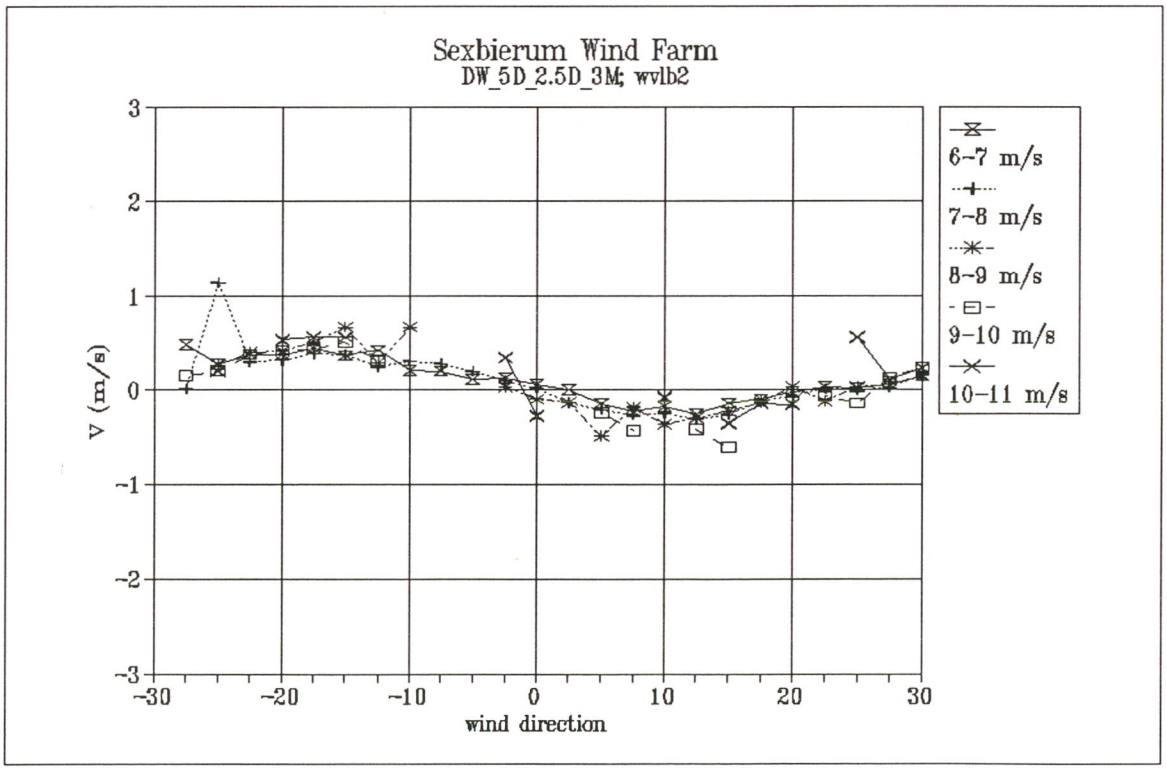

Figure 2 Lateral wind speed V as a function of wind direction and wind speed bin

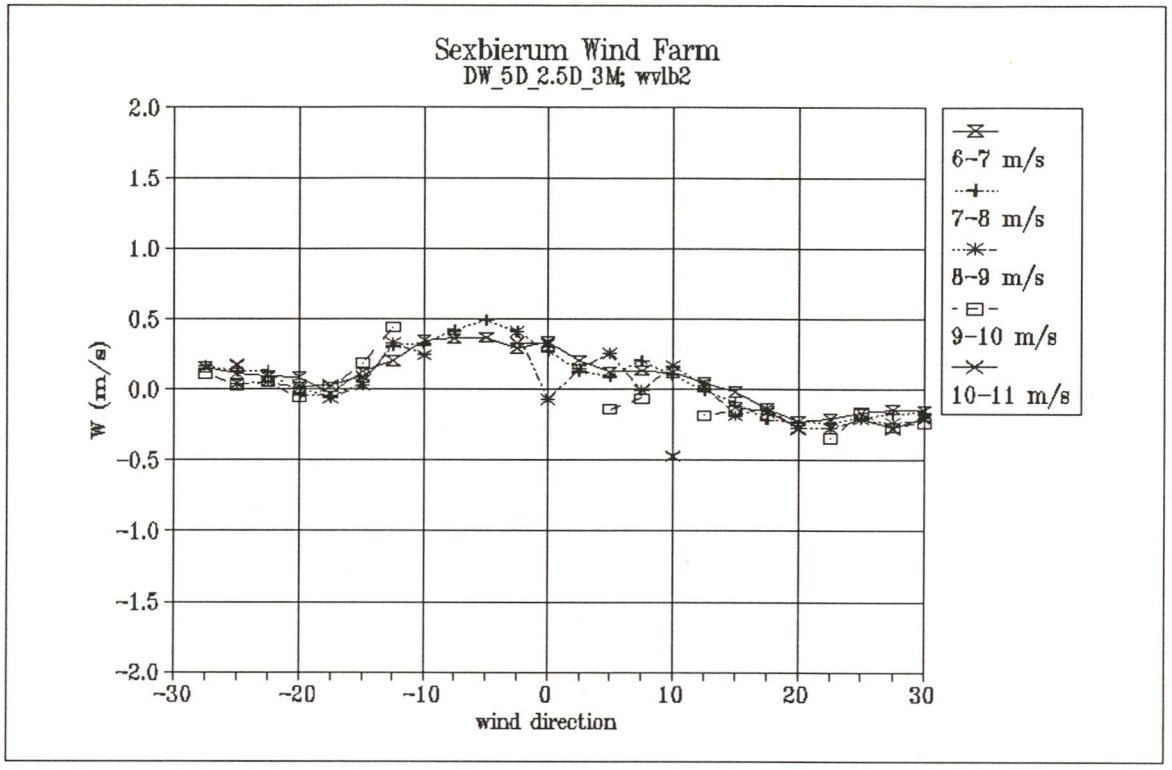

Figure 3 Vertical wind speed W as a function of wind direction and wind speed bin

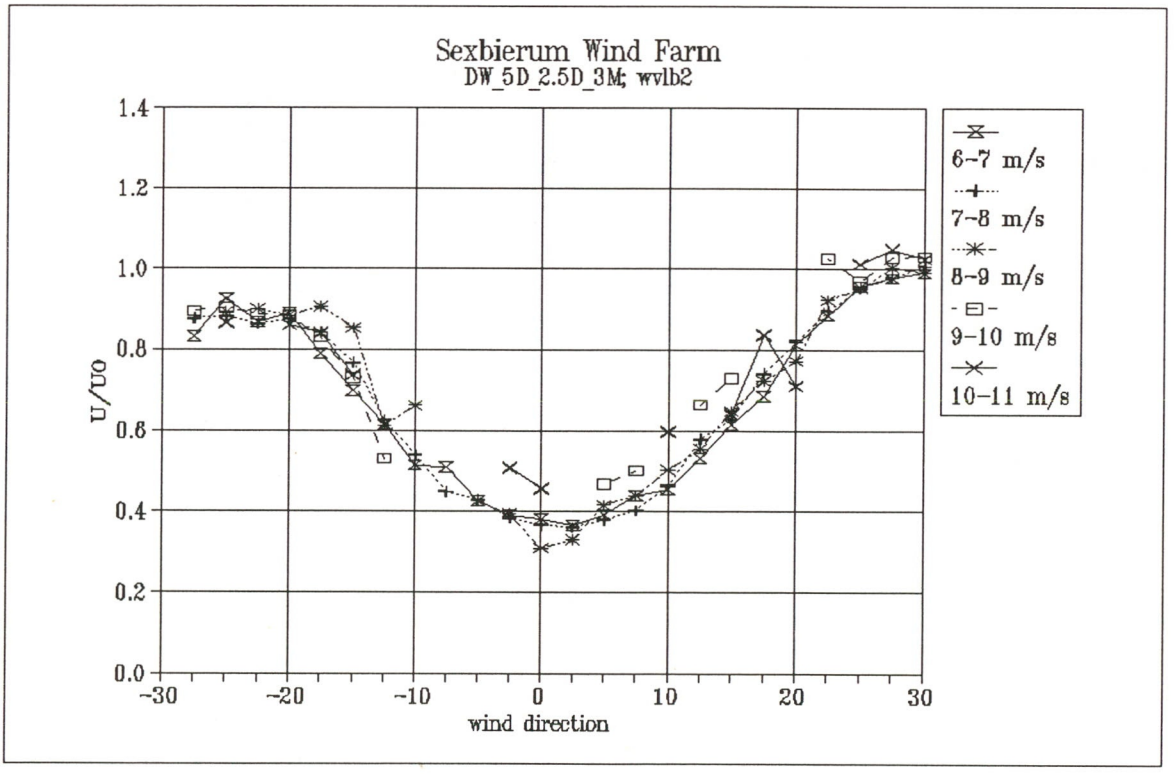

Figure 4 Wake deficit U/U_0 as a function of wind direction and wind speed bin

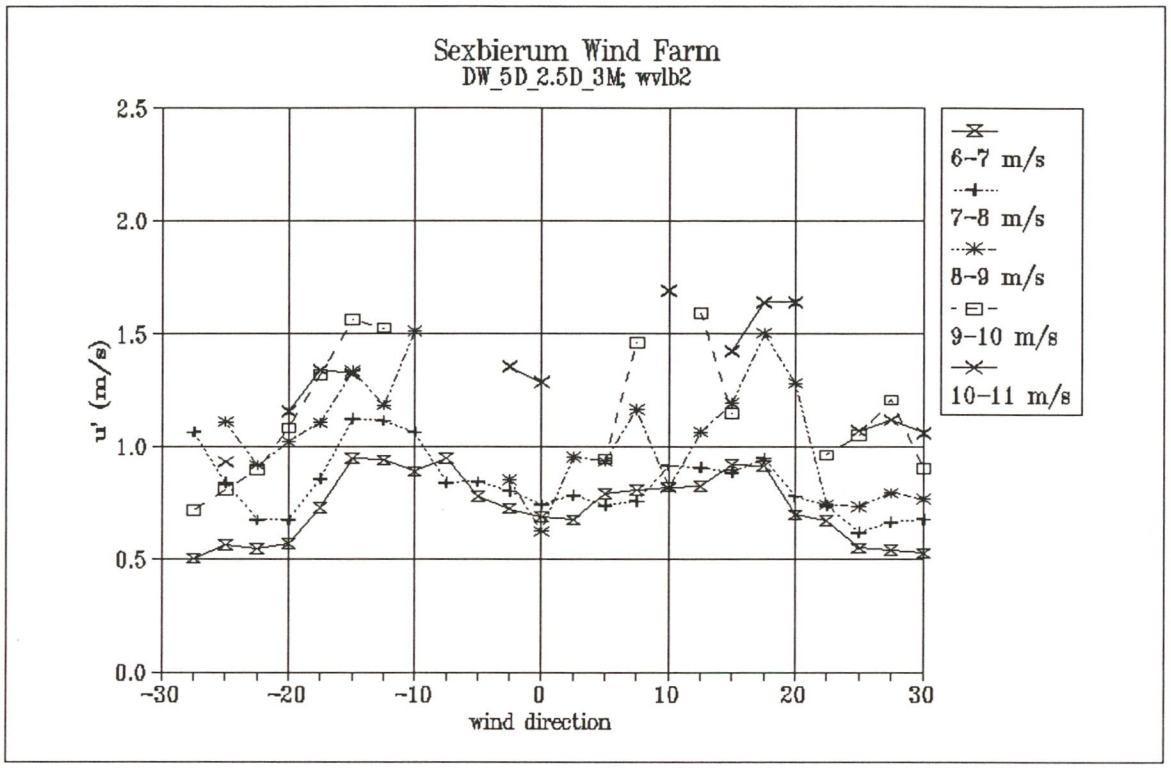

Figure 5 Longitudinal turbulent fluctuations u' as a function of wind direction and wind speed bin

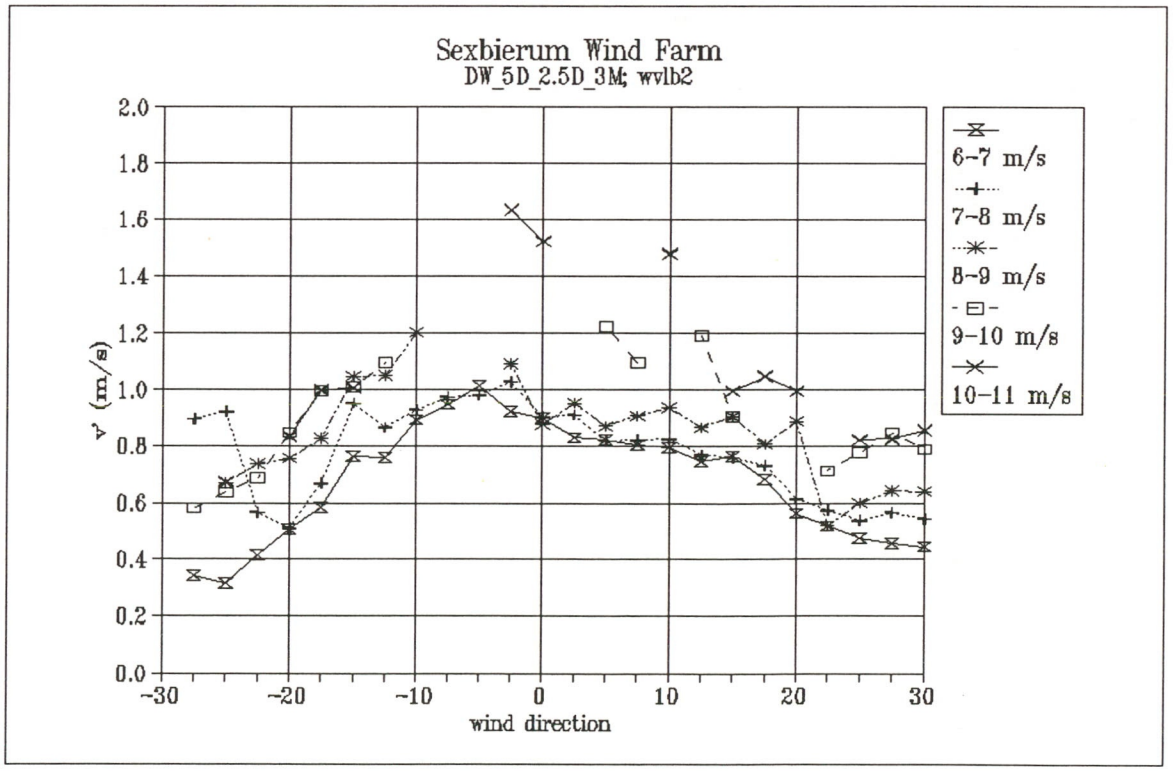

Figure 6 Lateral turbulent fluctuations v' as a function of wind direction and wind speed bin

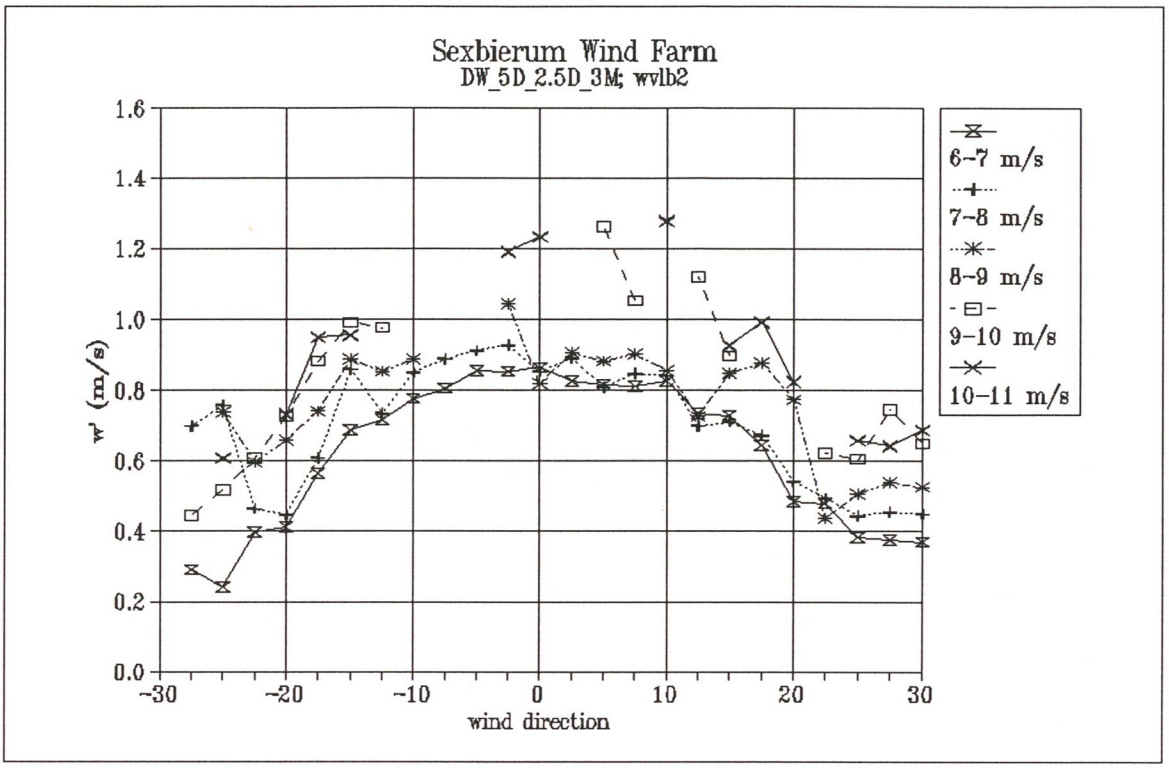

Figure 7 Vertical turbulent fluctuations w' as a function of wind direction and wind speed bin

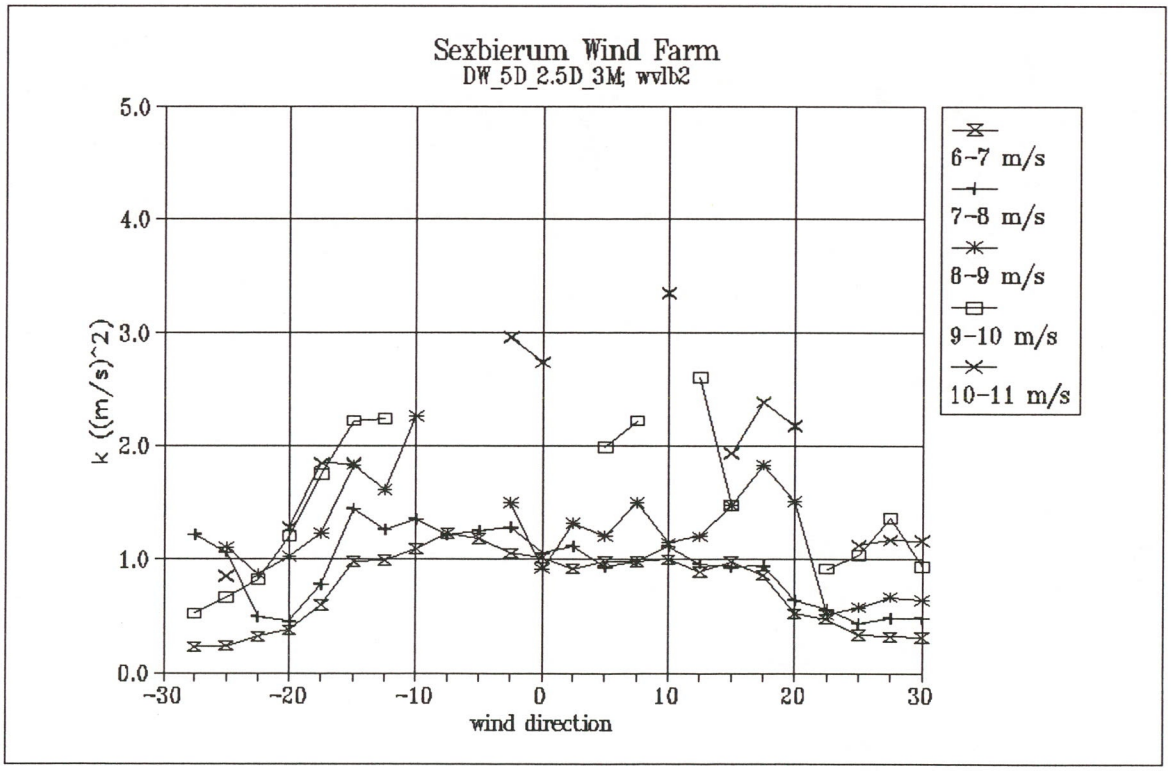

Figure 8 Turbulent kinetic energy per unit mass as a function of wind direction and wind speed bin

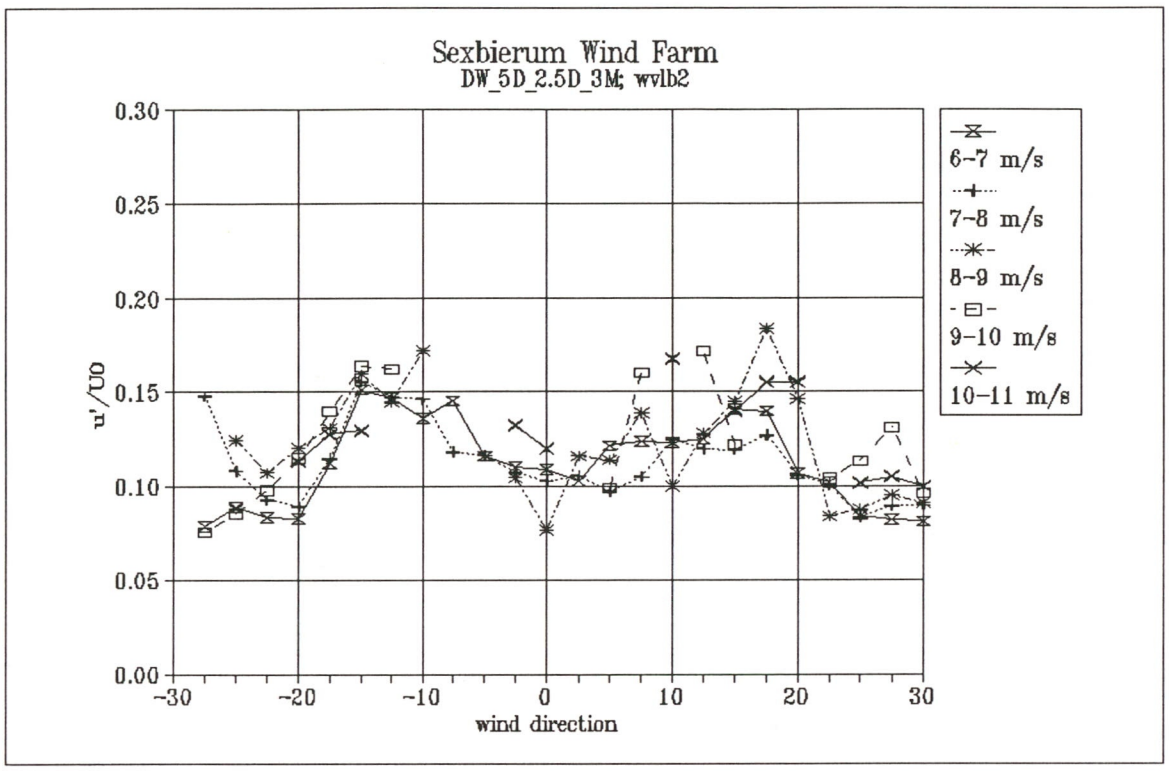

Figure 9 *Non-dimensionalized longitudinal turbulent fluctuations u'/U_0 as a function of wind direction and wind speed bin*

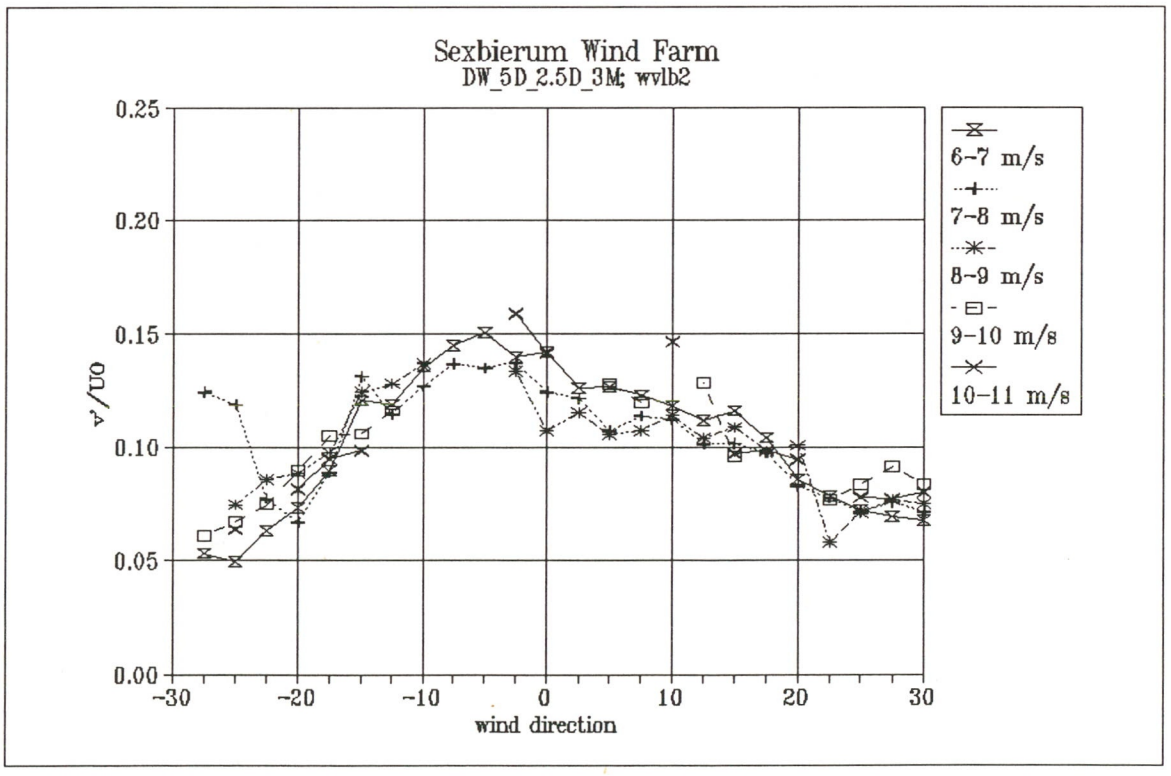

Figure 10 *Non-dimensionalized lateral turbulent fluctuations v'/U_0 as a function of wind direction and wind speed bin*

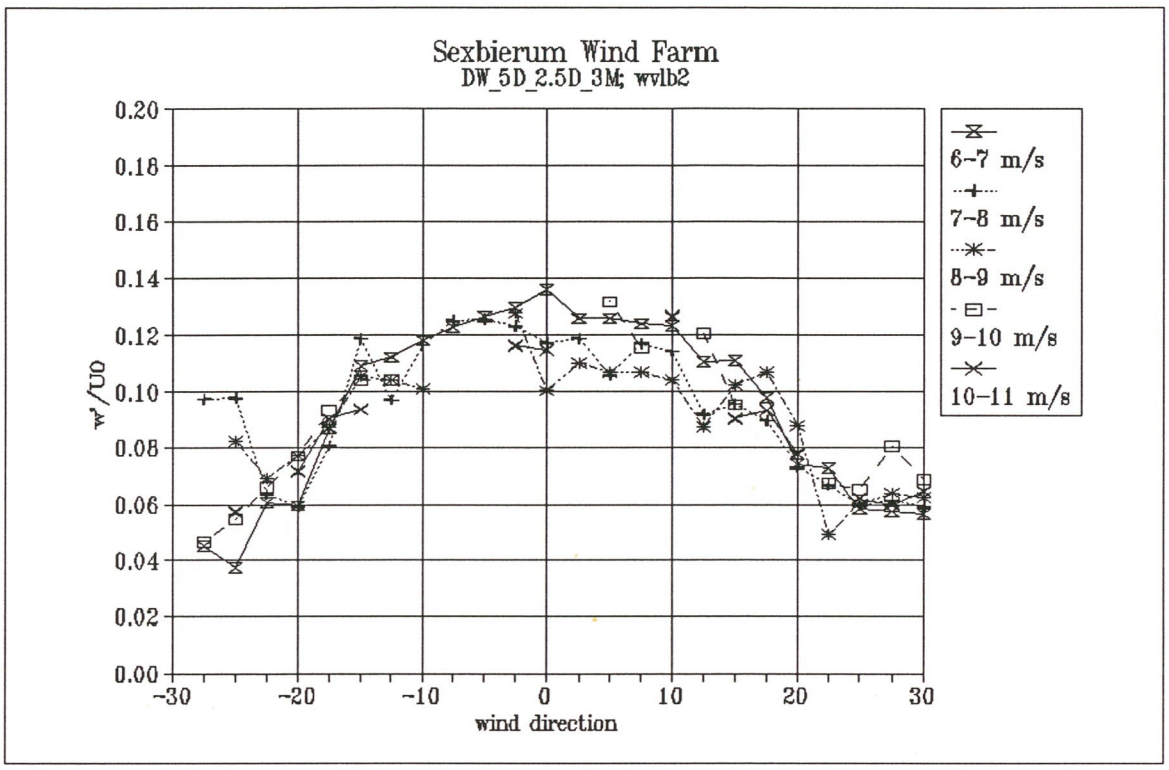

Figure 11 *Non-dimensionalized vertical turbulent fluctuations w'/U_0 as a function of wind direction and wind speed bin*

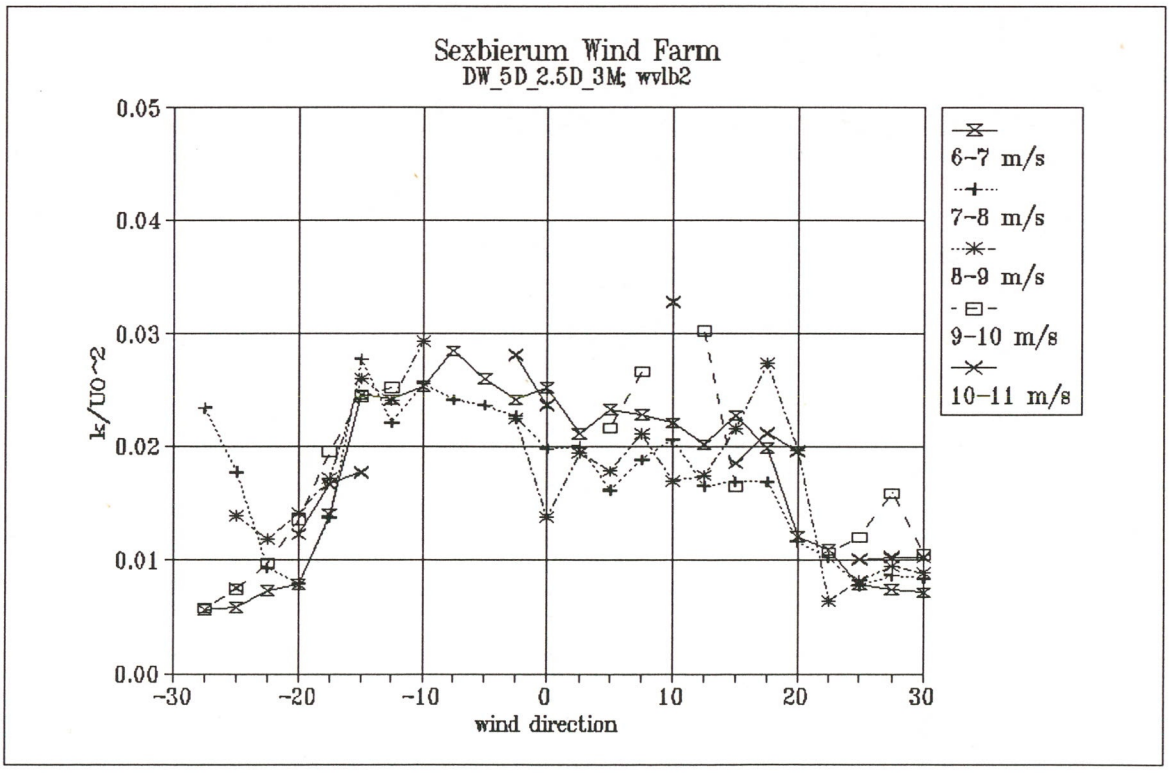

Figure 12 *Non-dimensionalized turbulent kinetic energy k/U_0^2 as a function of wind direction and wind speed bin*

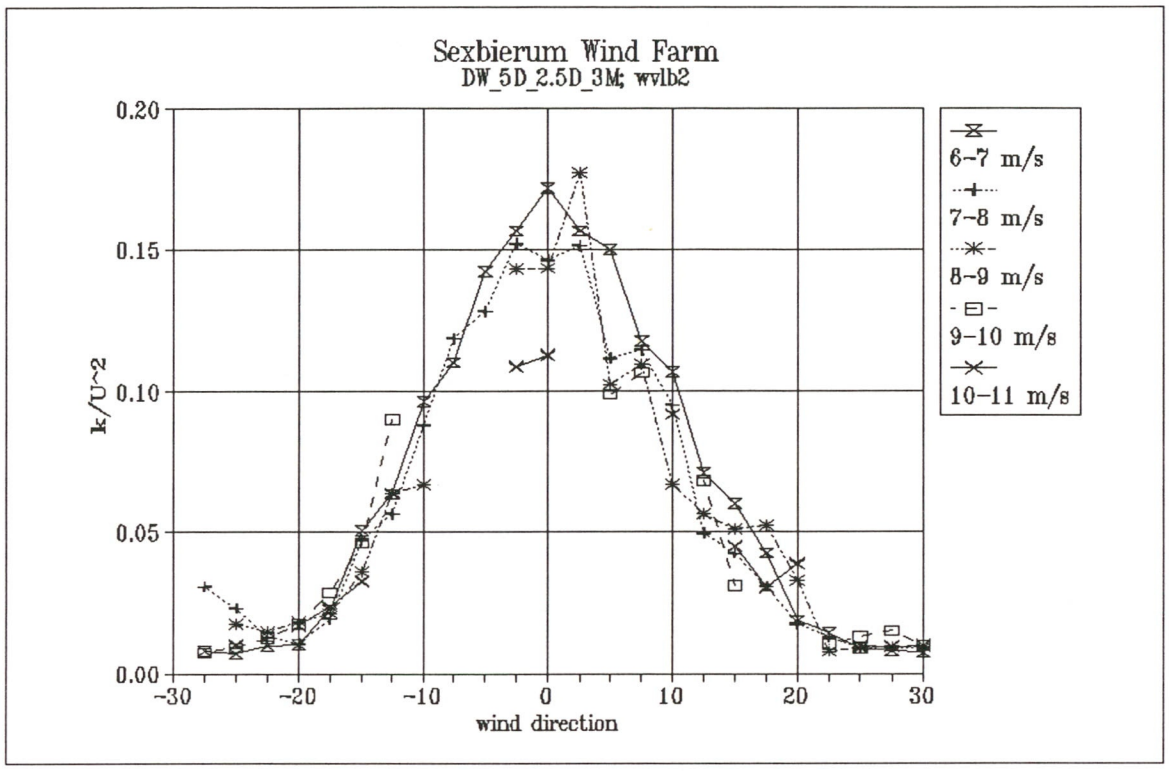

Figure 13 Non-dimensionalized turbulent kinetic energy k/U^2 as a function of wind direction and wind speed bin

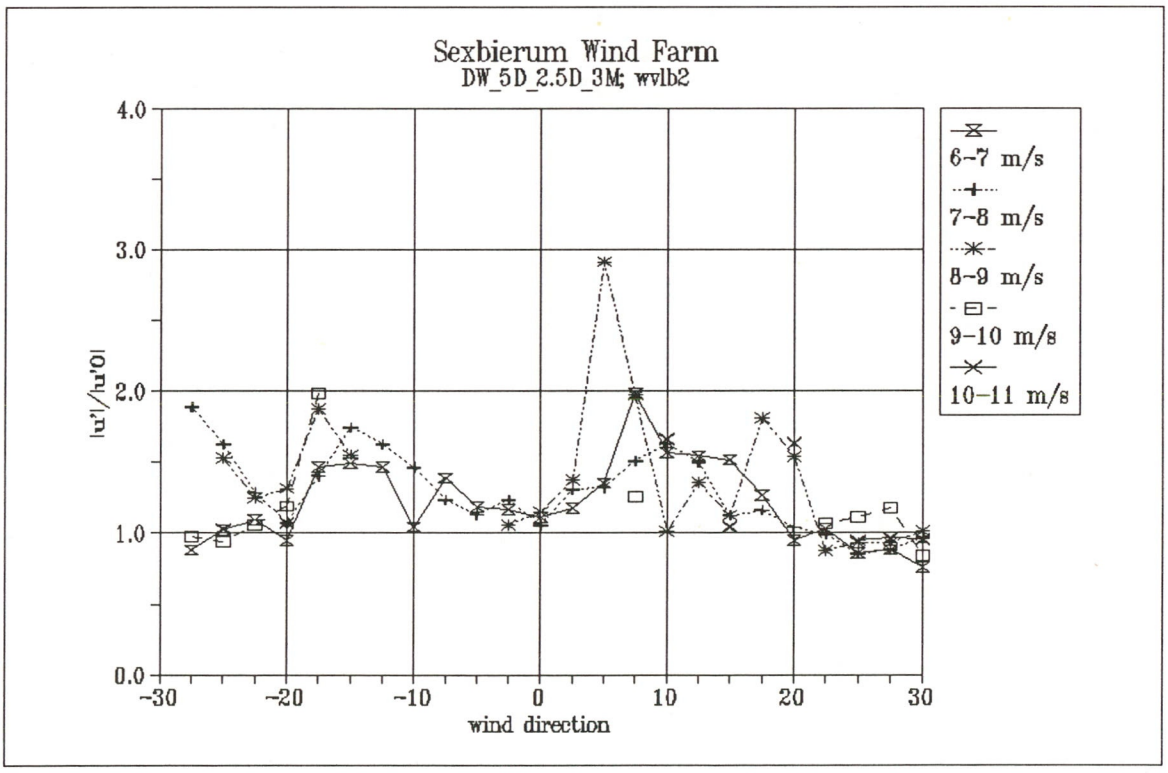

Figure 14 Longitudinal turbulence enhancement u'/u'_0 as a function of wind direction and wind speed bin

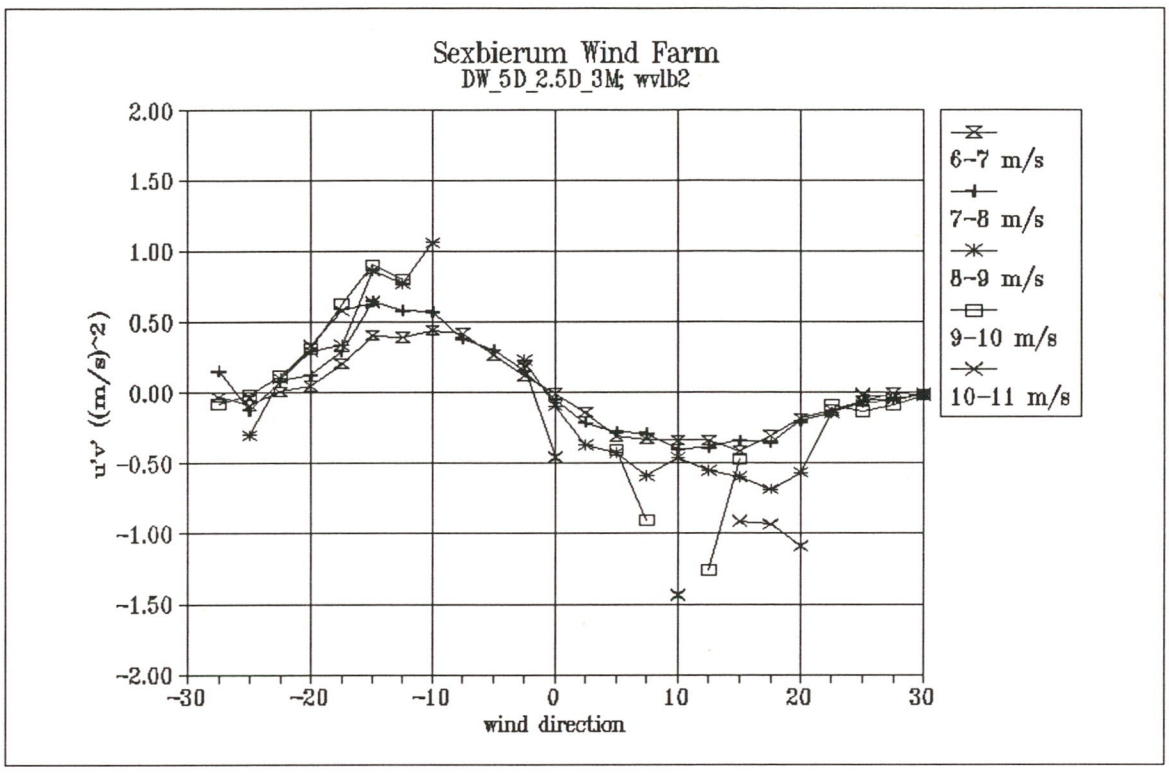

Figure 15 Shear stress u'v' as a function of wind direction and wind speed bin

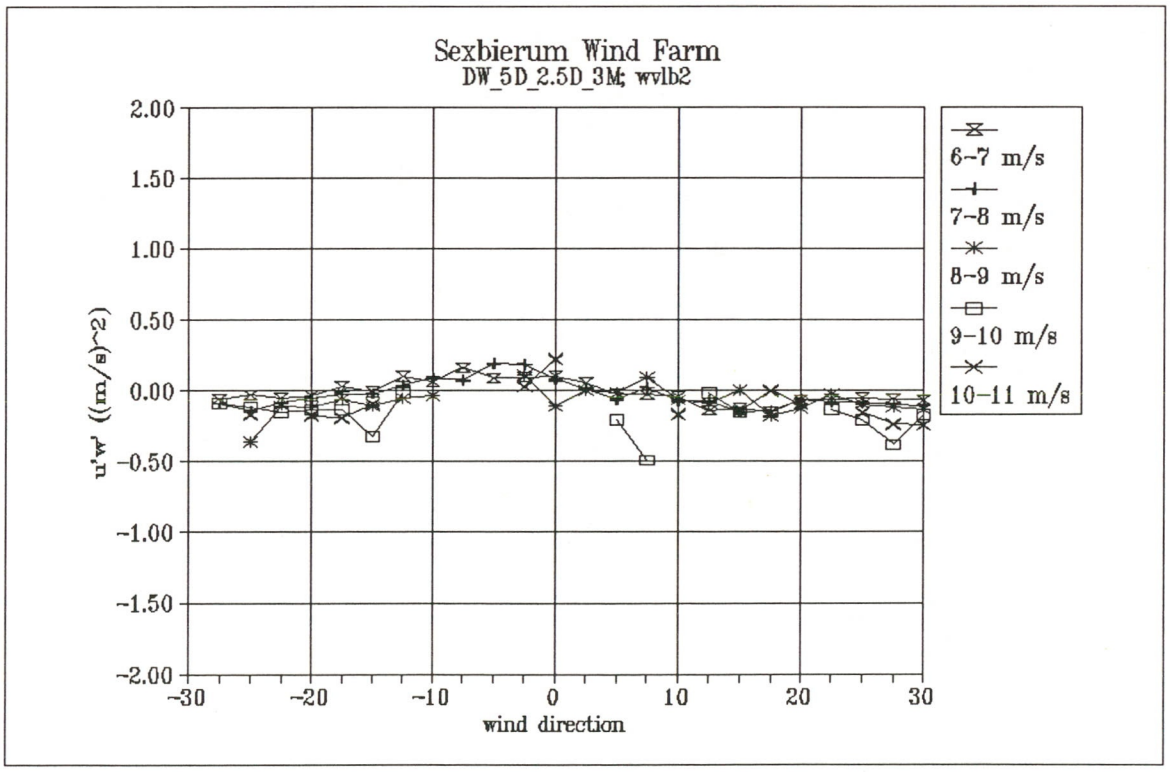

Figure 16 Shear stress u'w' as a function of wind direction and wind speed bin

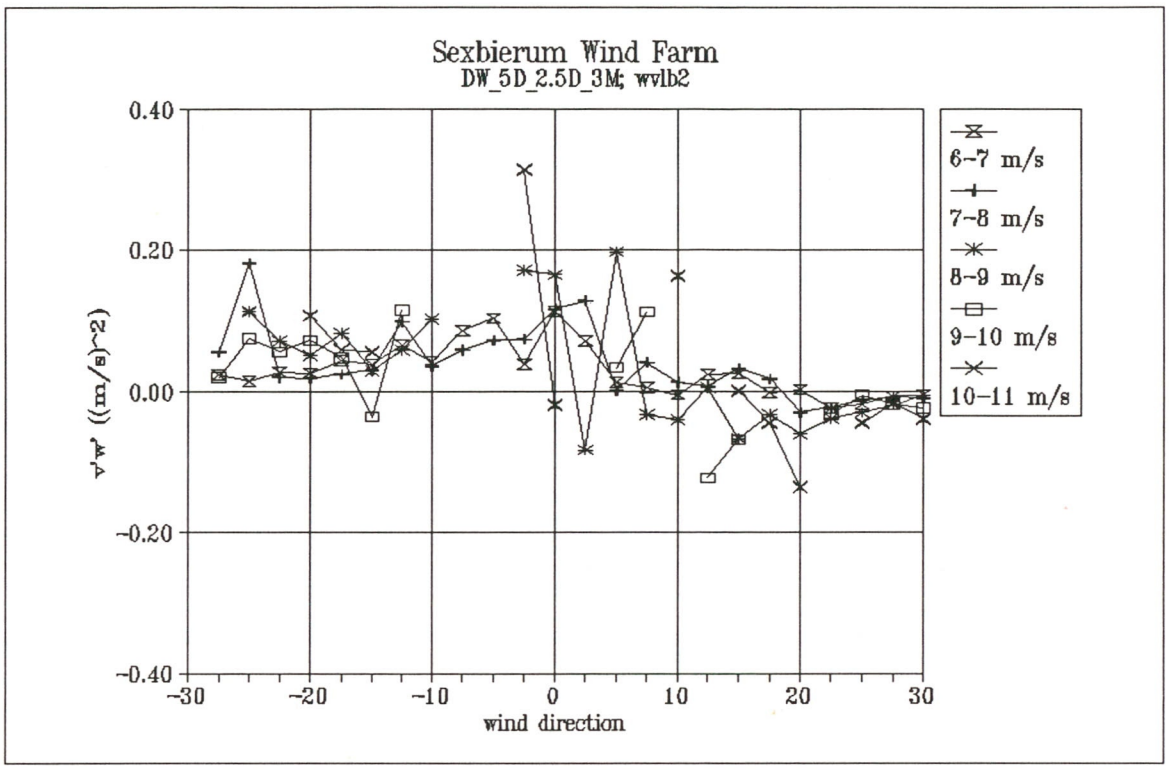

Figure 17 Shear stress v'w' as a function of wind direction and wind speed bin

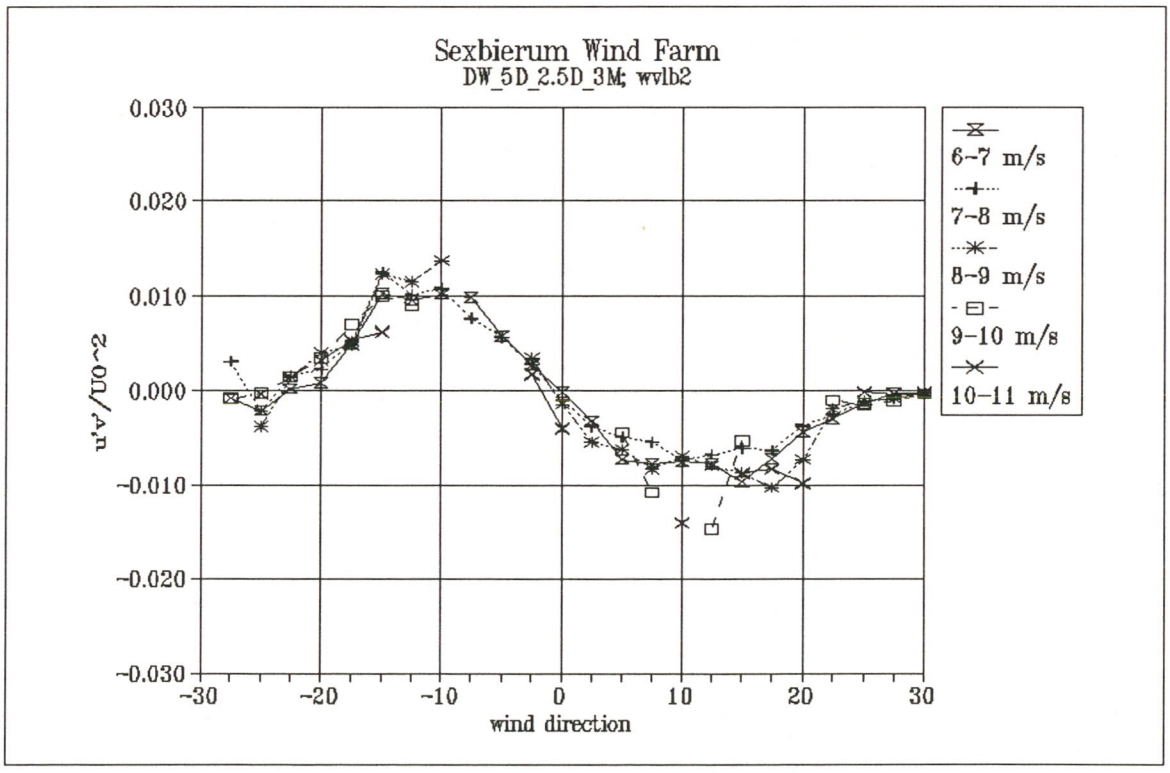

Figure 18 Non-dimensionalized shear stress $u'v'/U_0^2$ as a function of wind direction and wind speed bin

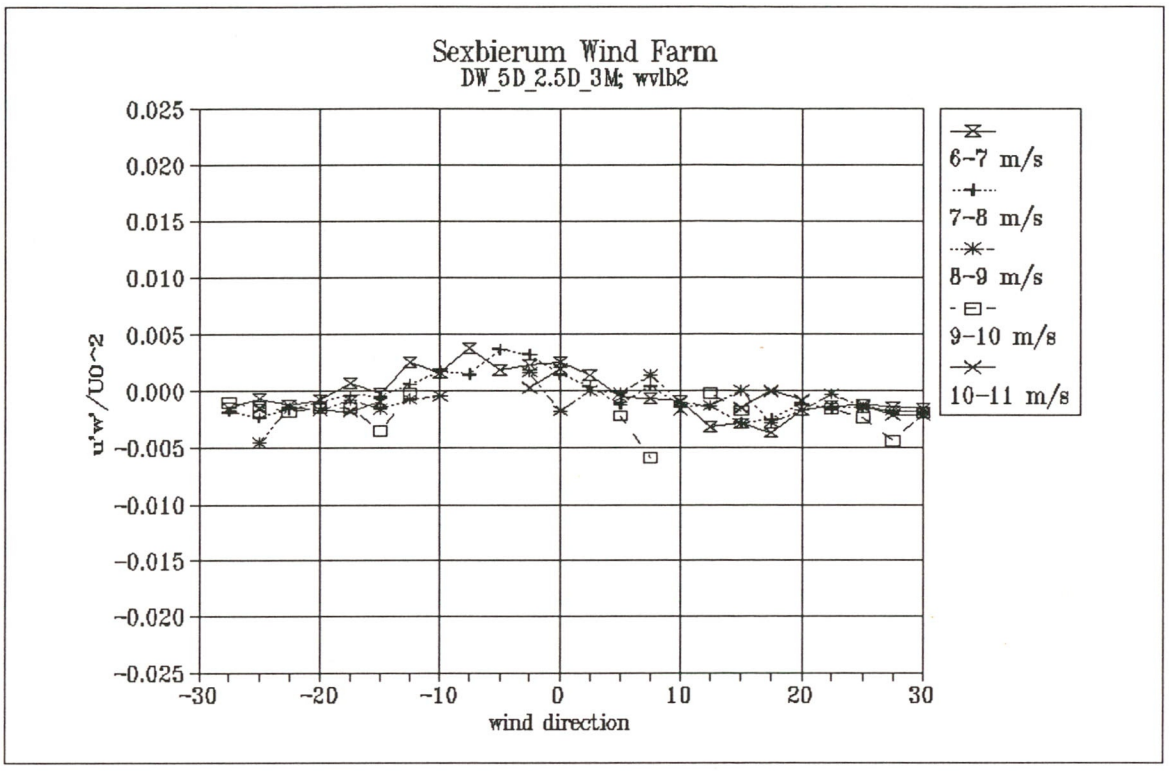

Figure 19 Non-dimensionalized shear stress $u'w'/U_0^2$ as a function of wind direction and wind speed bin

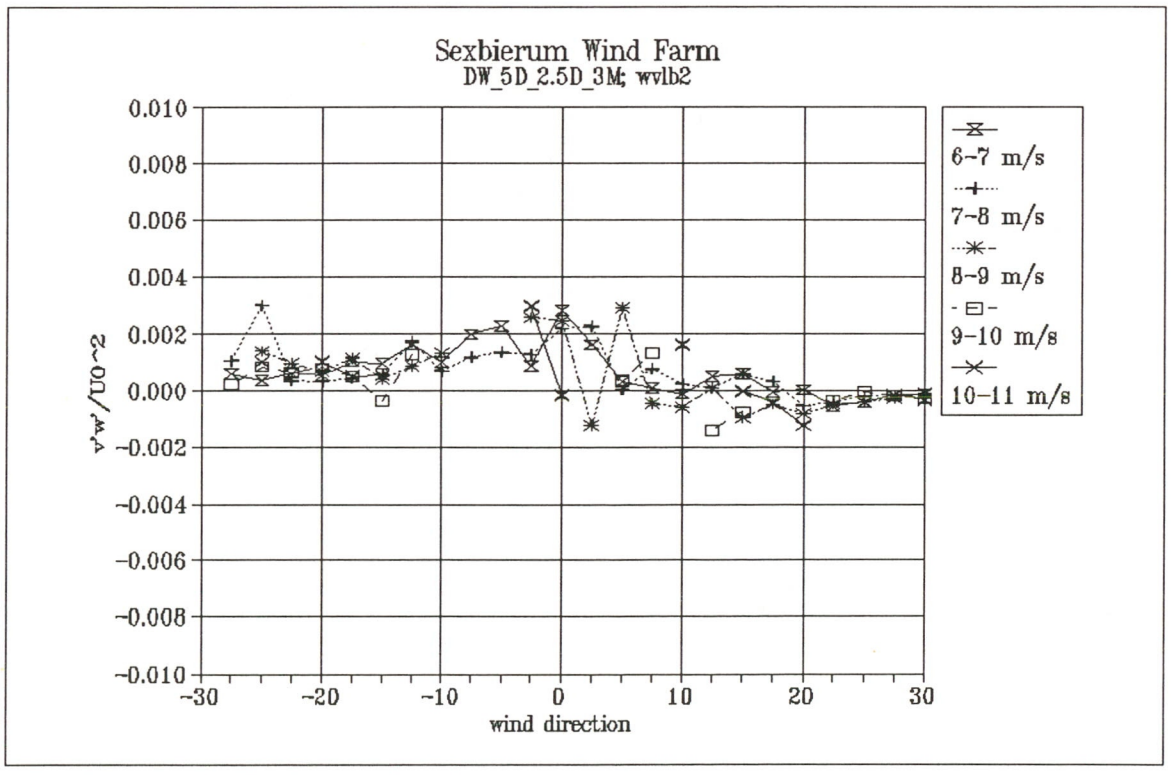

Figure 20 Non-dimensionalized shear stress $v'w'/U_0^2$ as a function of wind direction and wind speed bin

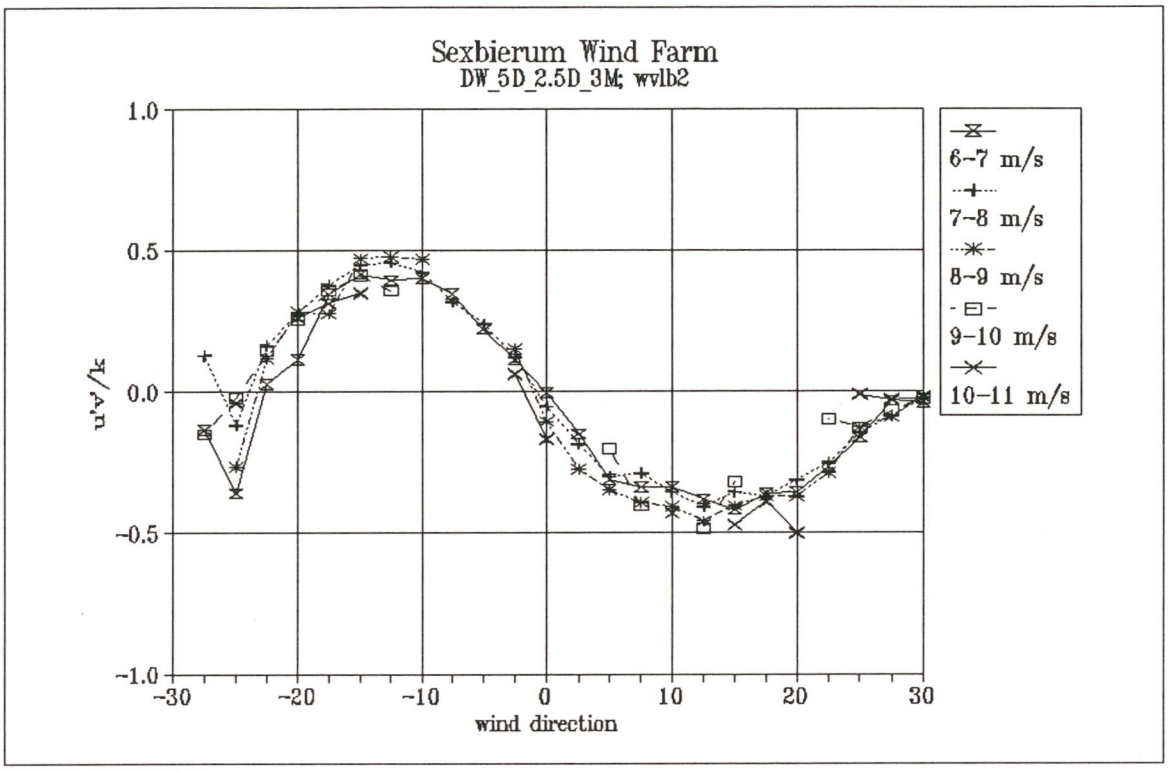

Figure 21 Non-dimensionalized shear stress u'v'/k as a function of wind direction and wind speed bin

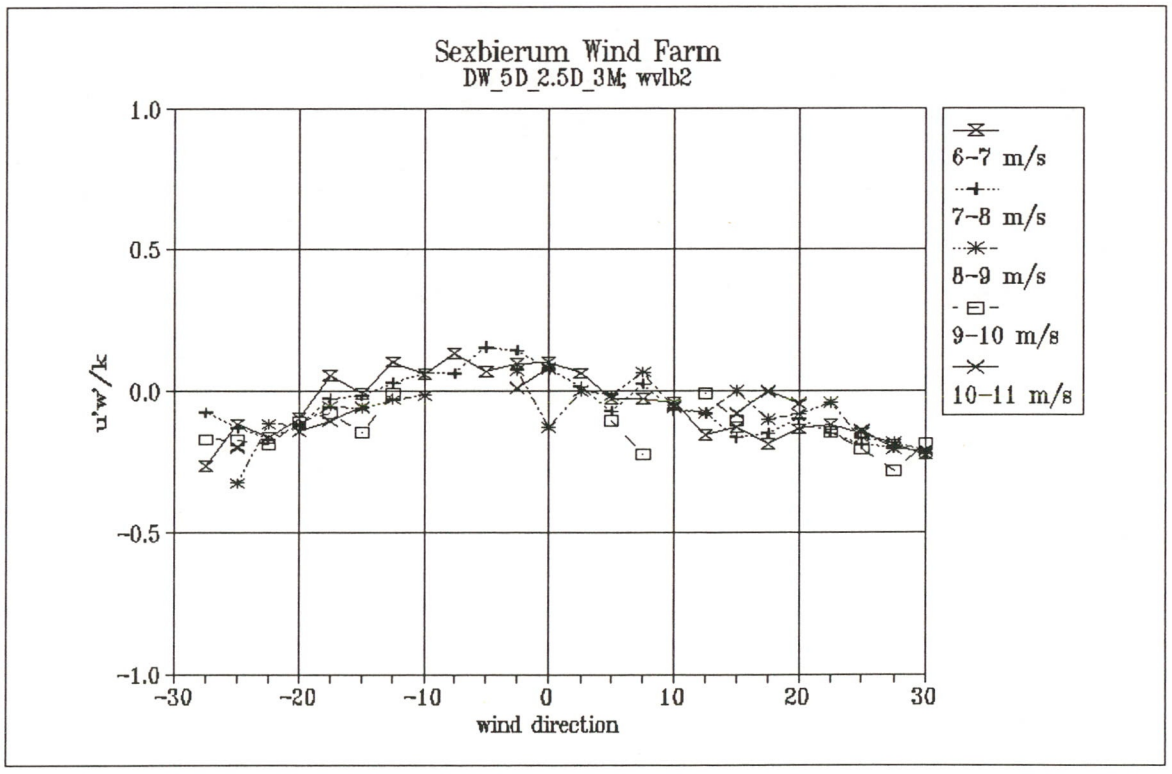

Figure 22 Non-dimensionalized shear stress u'w'/k as a function of wind direction and wind speed bin

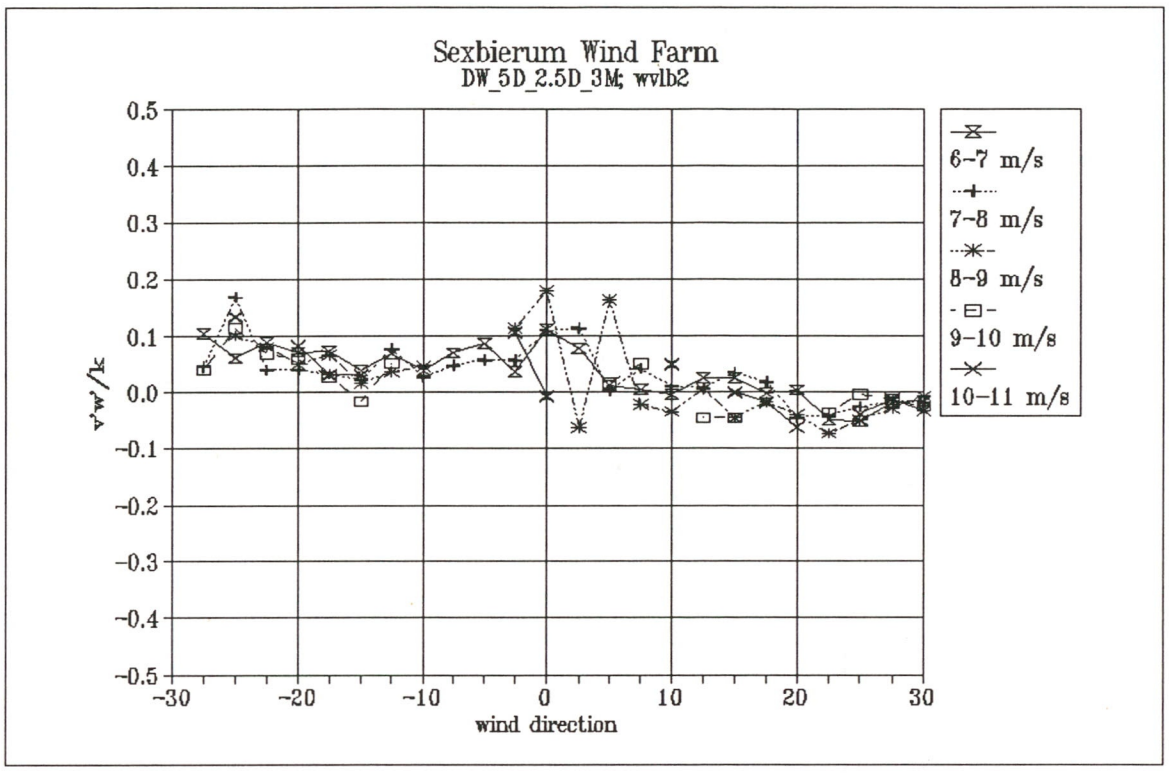

Figure 23 Non-dimensionalized shear stress v'w'/k as a function of wind direction and wind speed bin

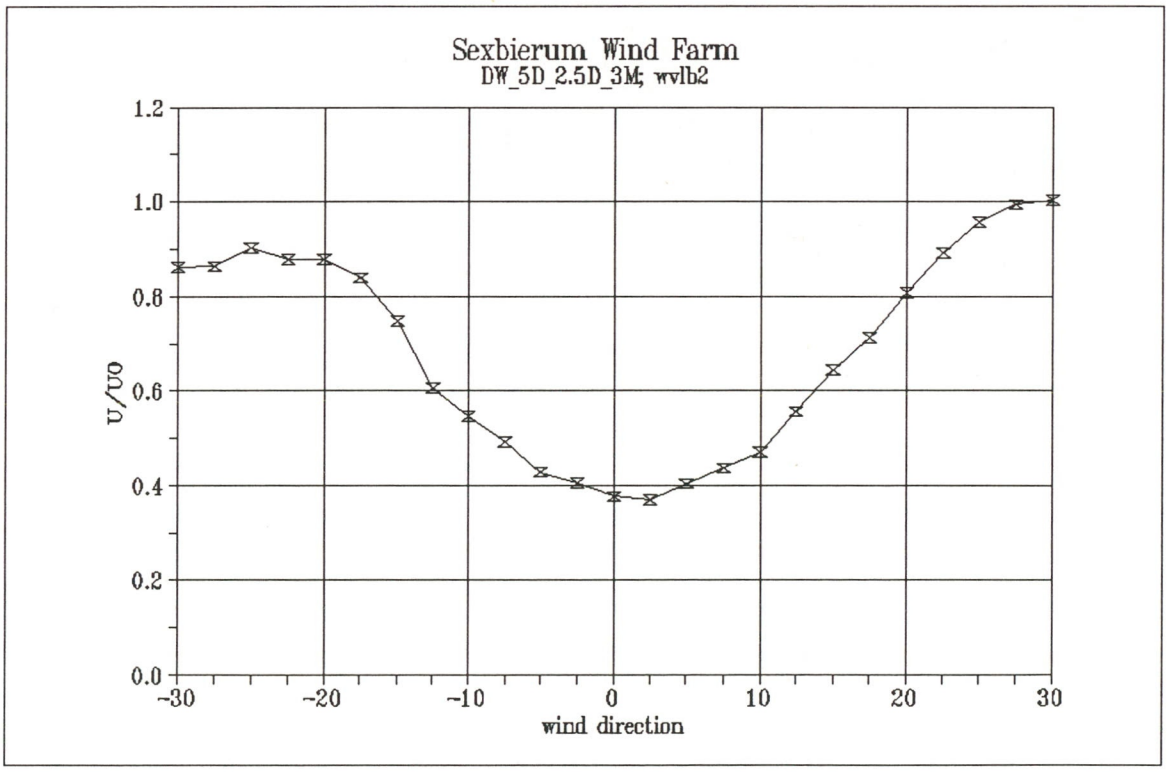

Figure 24 Wake deficit U/U_0 as a function of wind direction in the wind speed bin 5-10 m/s

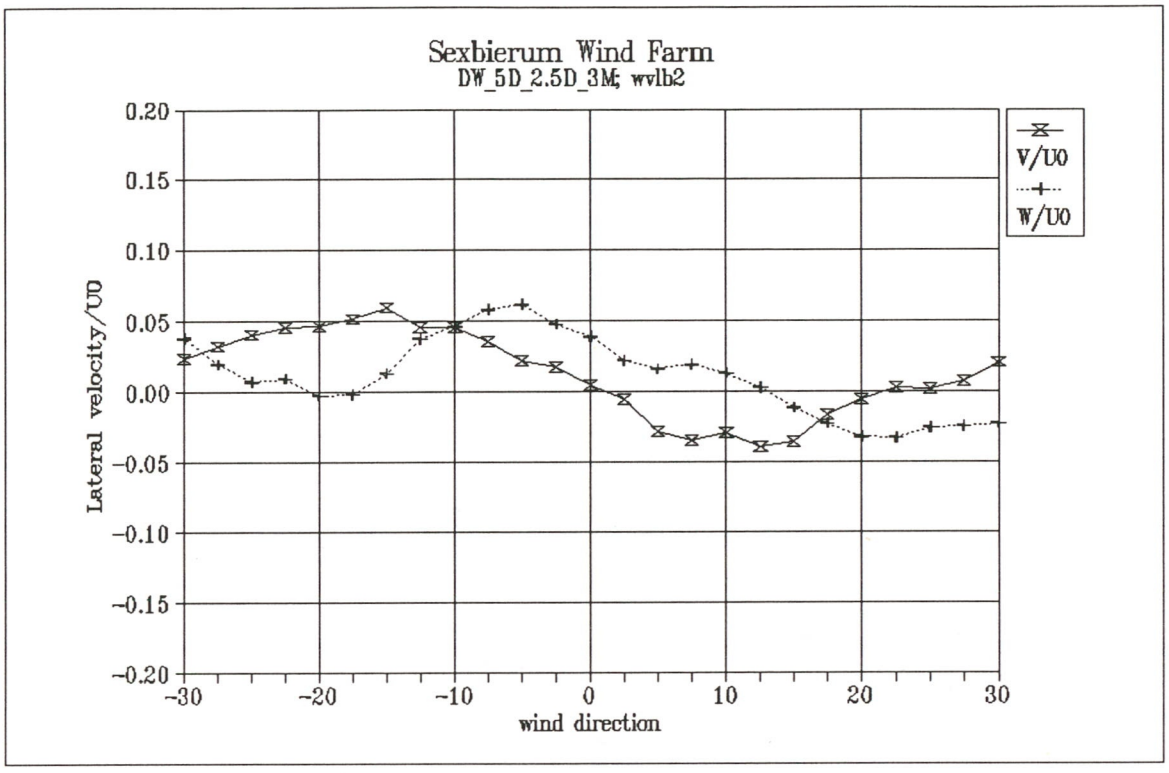

Figure 25 Lateral and vertical wind speed V/U_0 and W/U_0 as a function of wind direction in the wind speed bin 5-10 m/s

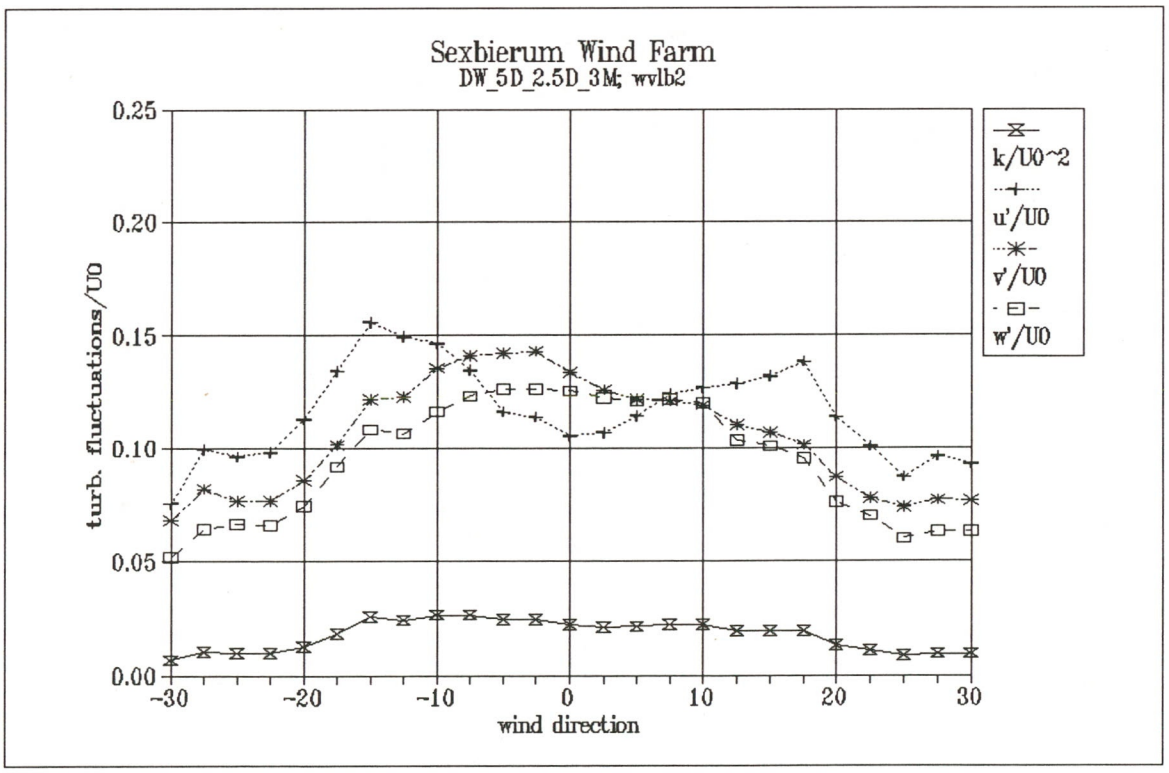

Figure 26 Turbulent fluctuations as a function of wind direction in the wind speed bin 5-10 m/s, non-dimensionalized with U_0

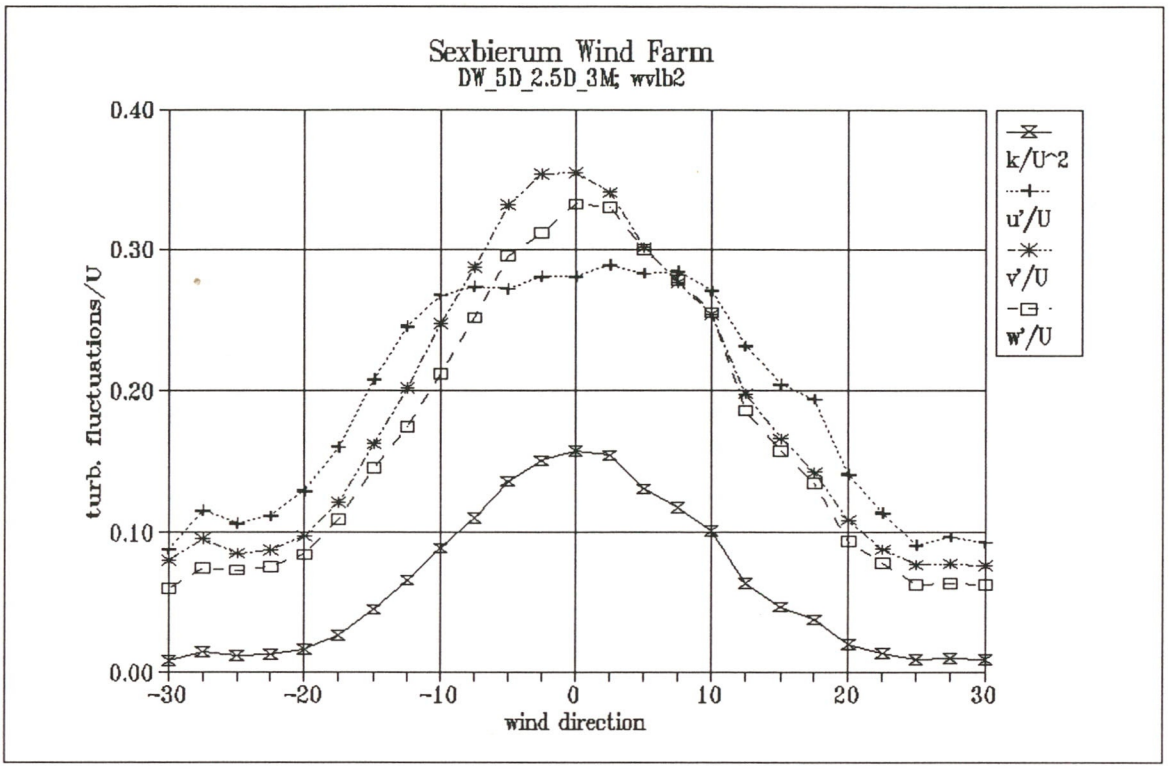

Figure 27 Turbulent fluctuations as a function of wind direction in the wind speed bin 5-10 m/s, non-dimensionalized with U

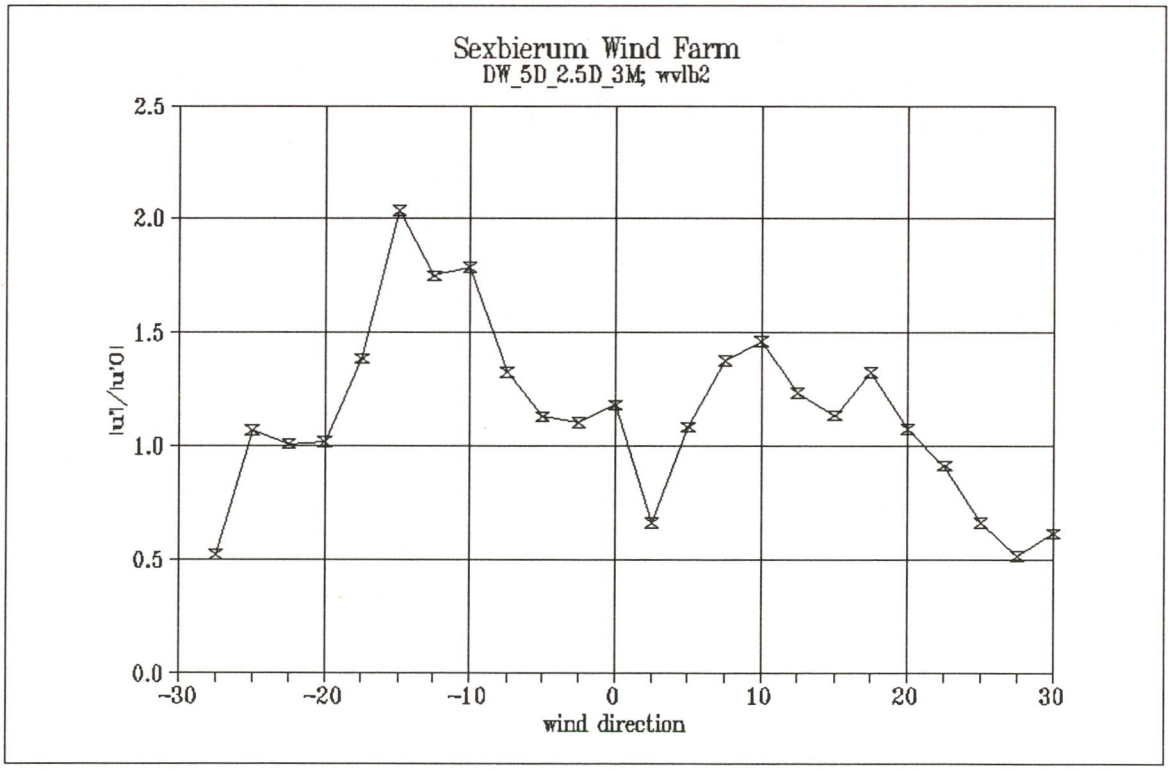

Figure 28 Longitudinal turbulence enhancement u'/u'_0 as a function of wind direction in the wind speed bin 5-10 m/s

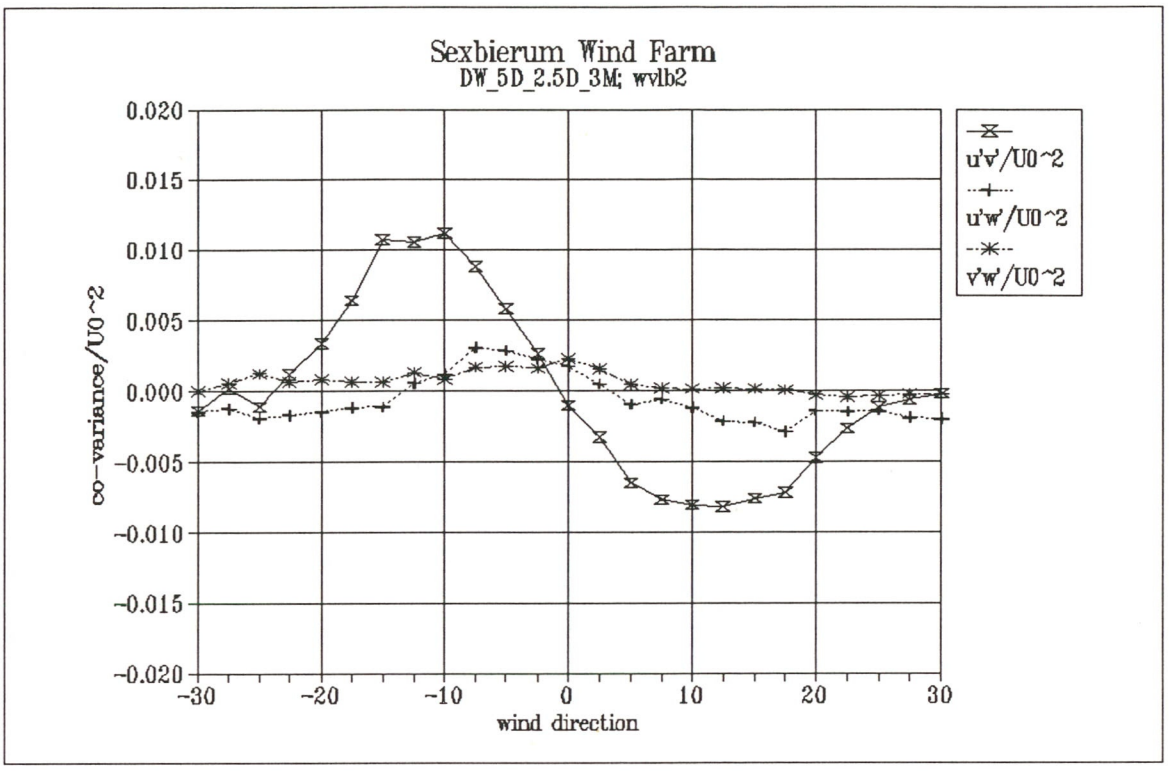

Figure 29 Non-dimensionalized shear stresses $u'v'/U_0^2$; $u'w'/U_0^2$; $v'w'/U_0^2$ as a function of wind direction in the wind speed bin 5-10 m/s

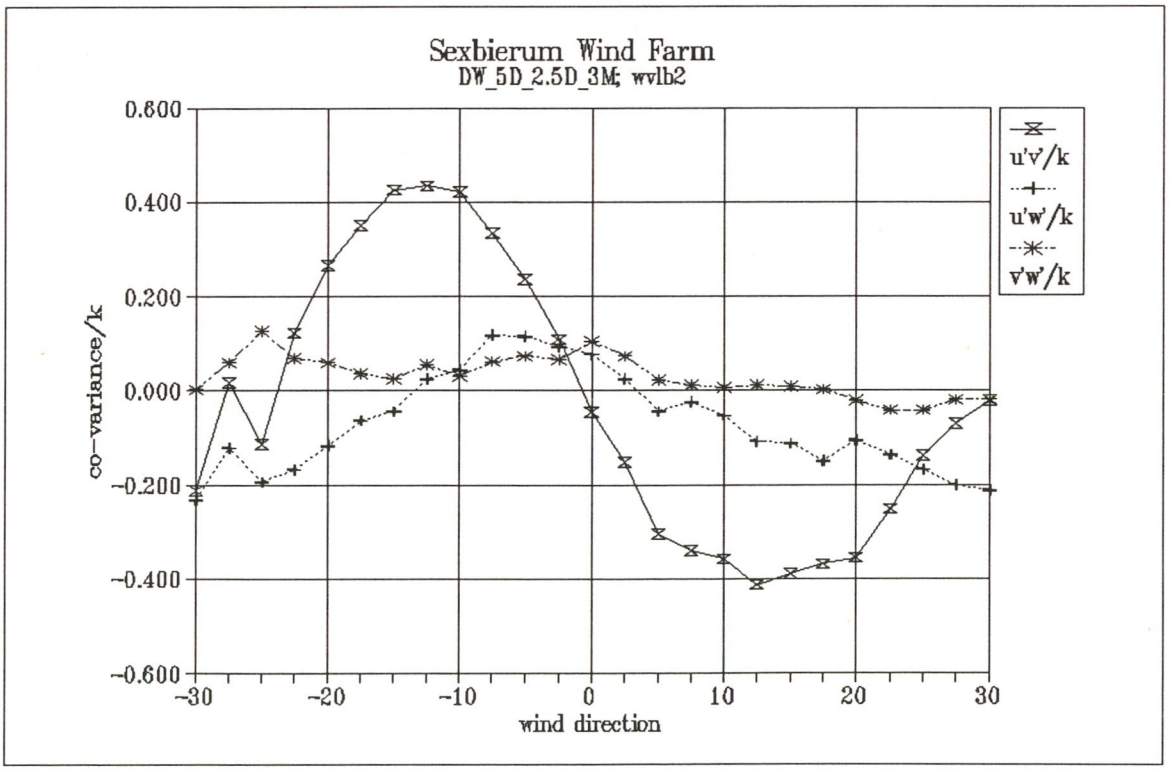

Figure 30 Non-dimensionalized shear stresses u'v'/k; u'w'/k; v'w'/k as a function of wind direction in the wind speed bin 5-10 m/s

A4.5 Sensor b2l

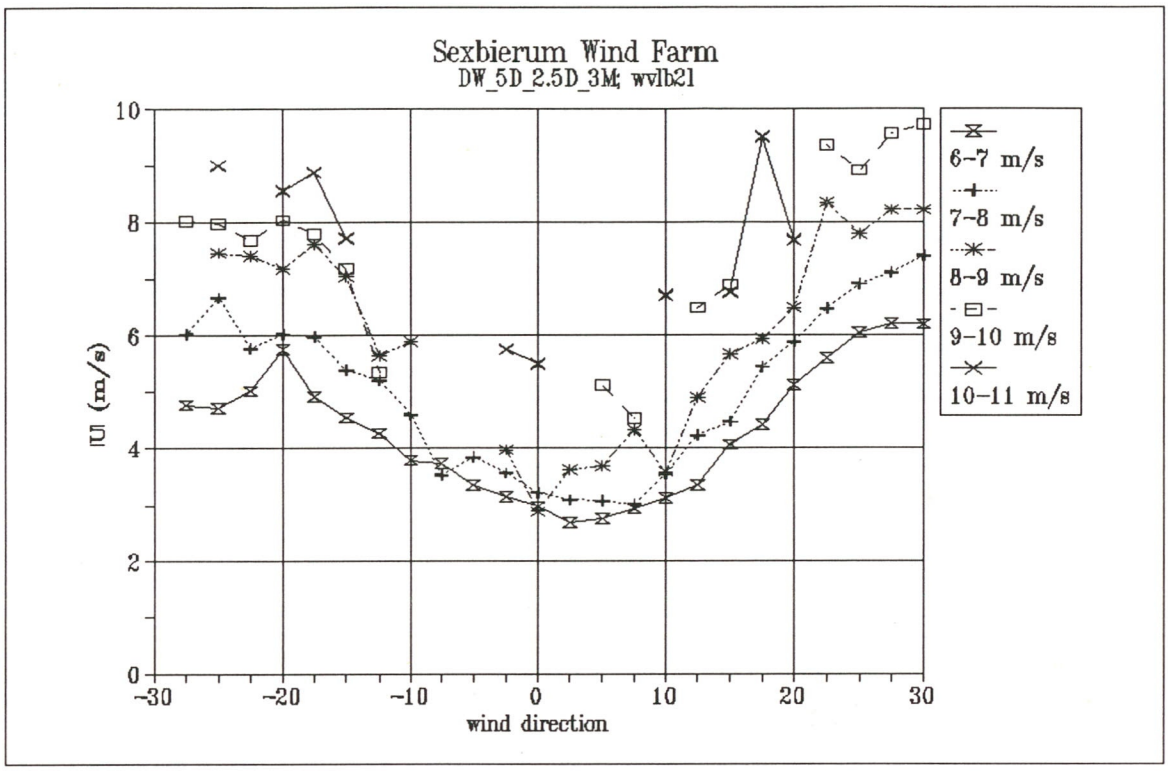

Figure 1 *Wind speed U as a function of wind direction and wind speed bin*

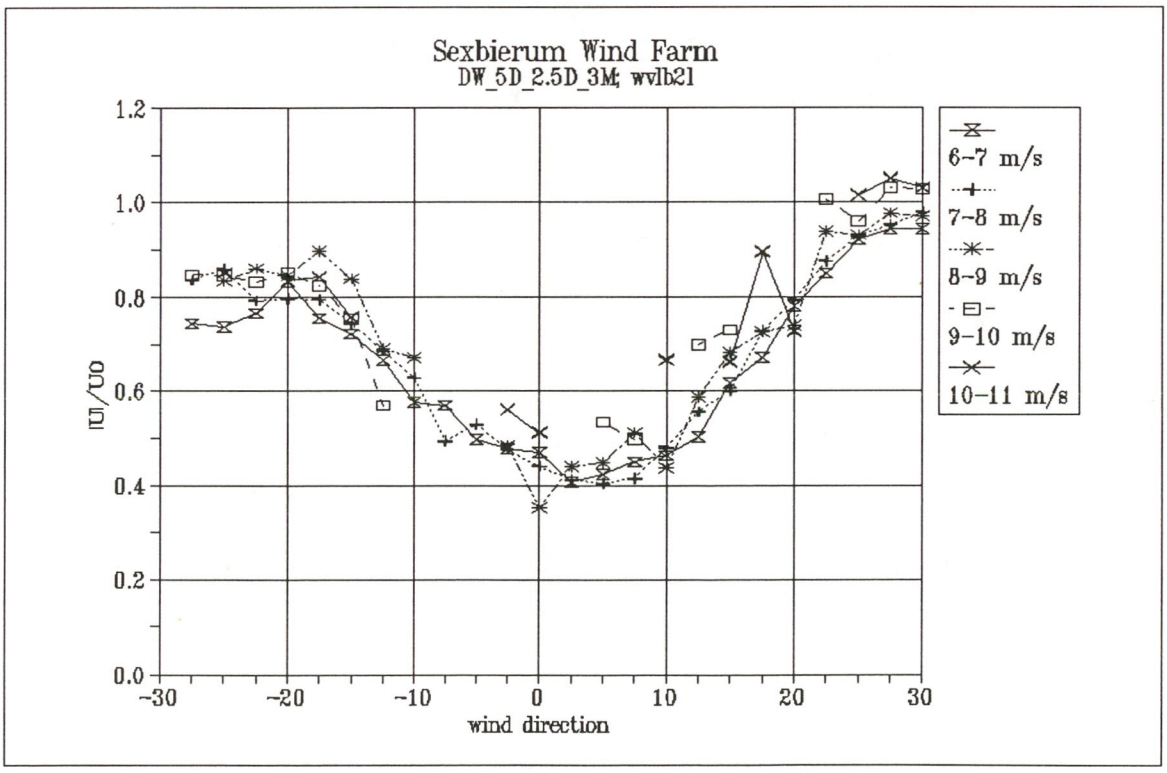

Figure 2 *Wake deficit U/U_0 as a function of wind direction and wind speed bin*

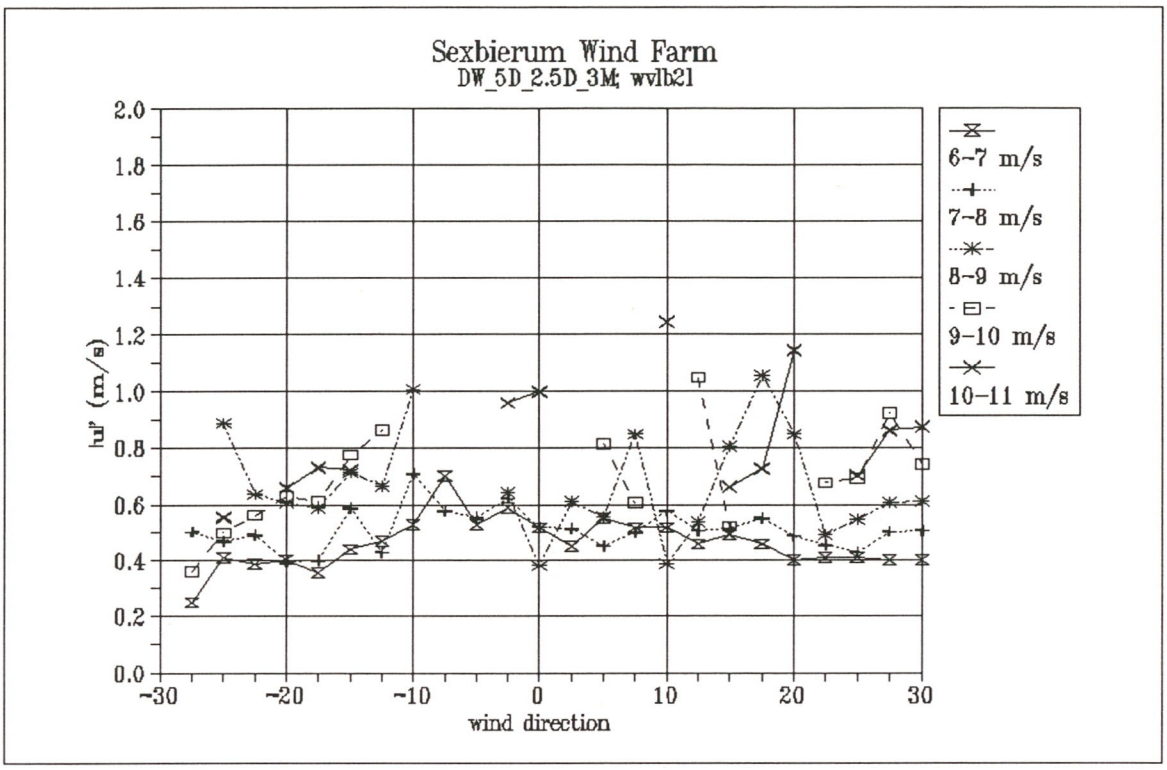

Figure 3 Turbulent fluctuations u' as a function of wind direction and wind speed bin

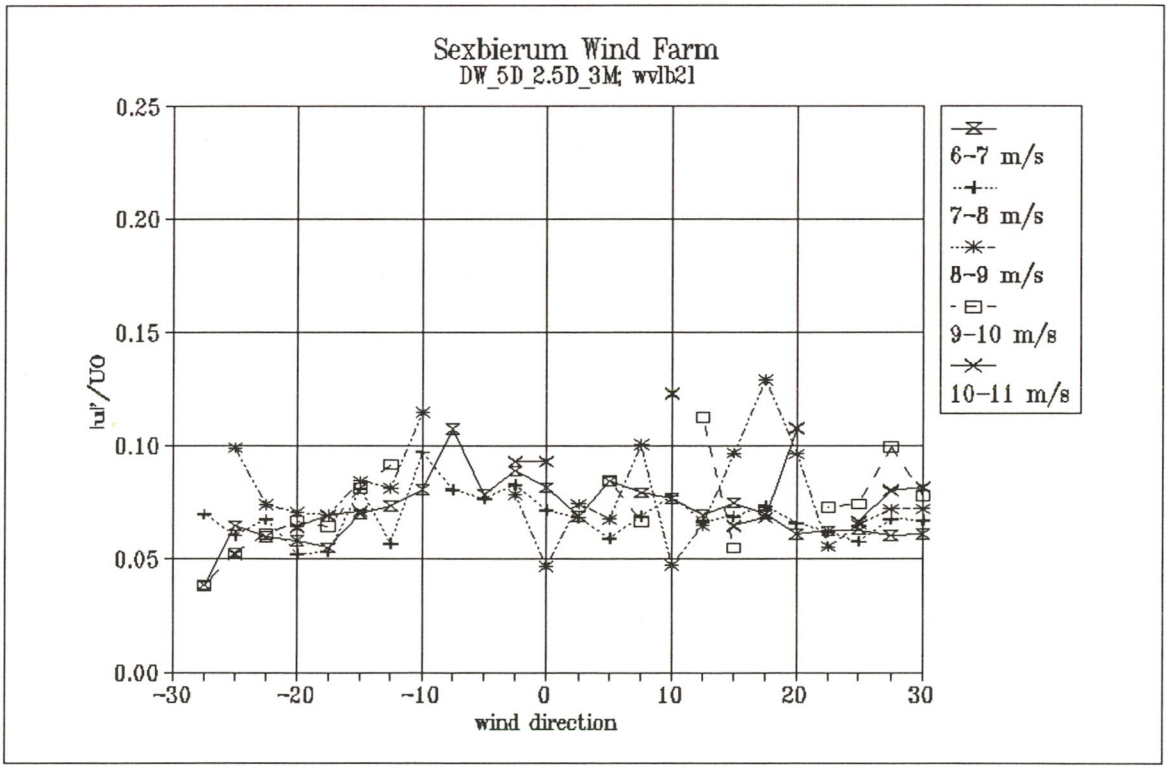

Figure 4 Non-dimensionalized turbulent fluctuations u'/U_0 as a function of wind direction and wind speed bin

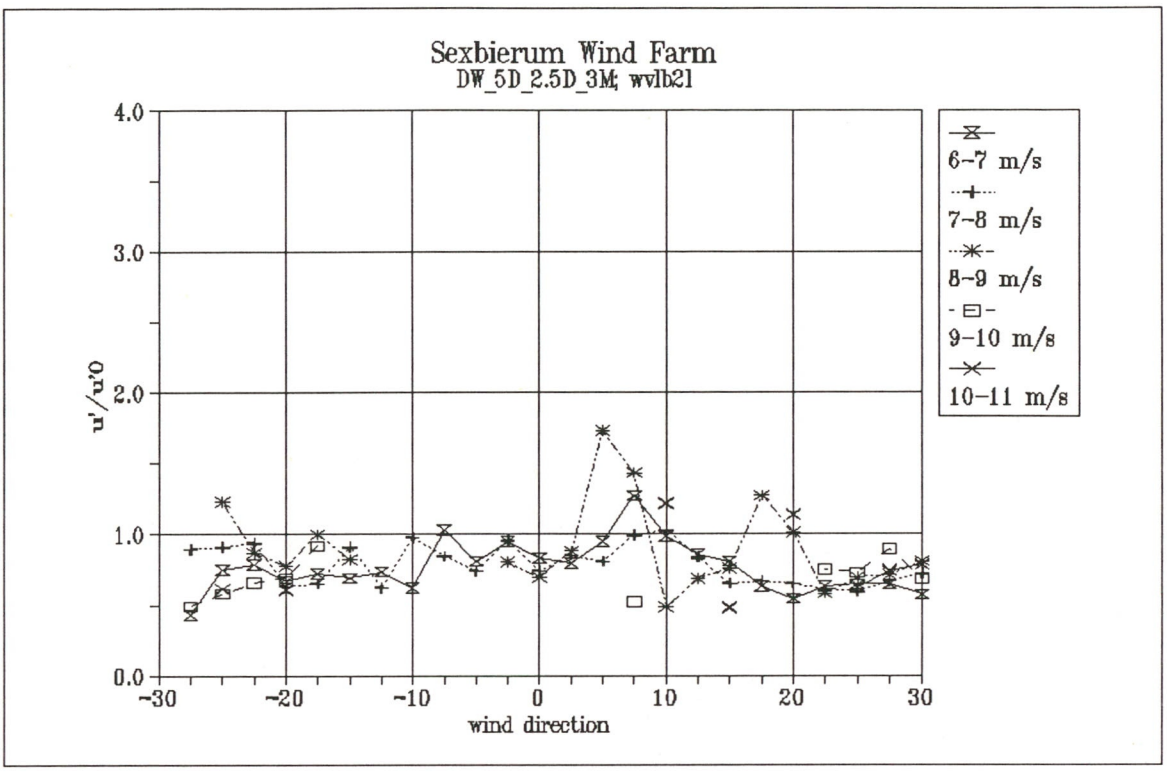

Figure 5 Turbulence enhancement u'/u'_0 as a function of wind direction and wind speed bin

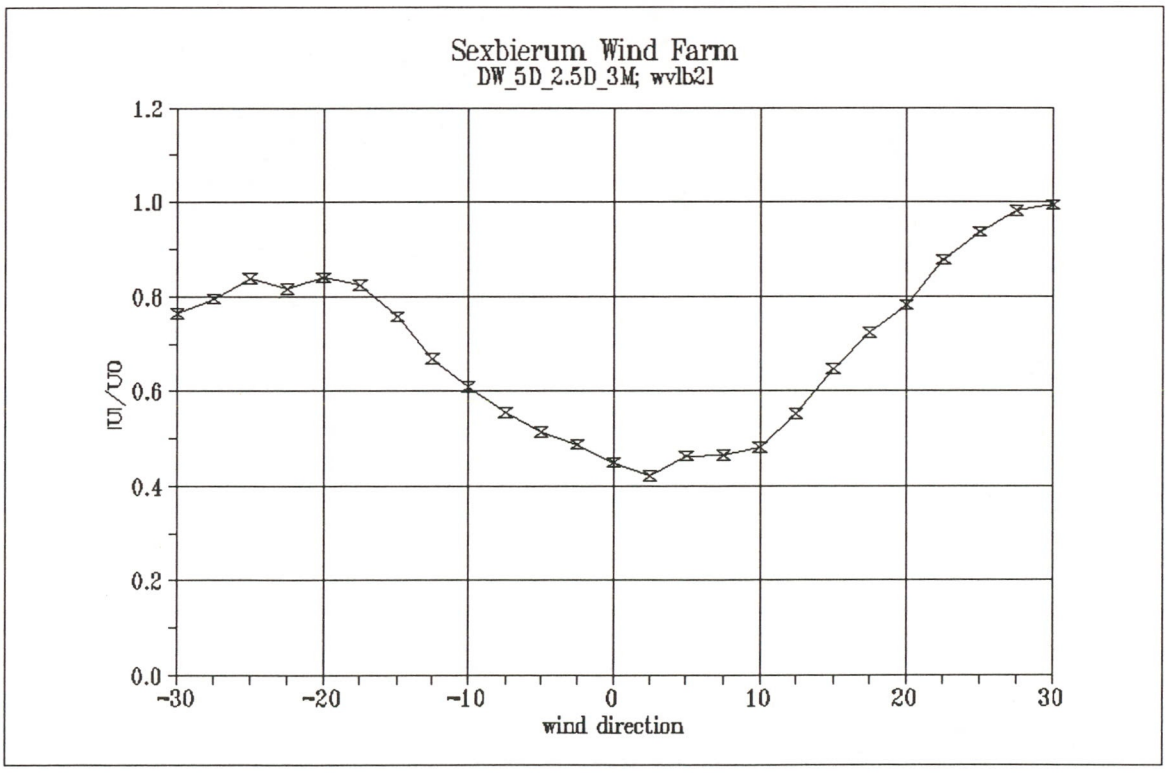

Figure 6 Wake deficit U/U_0 as a function of wind direction in the wind speed bin 5-10 m/s

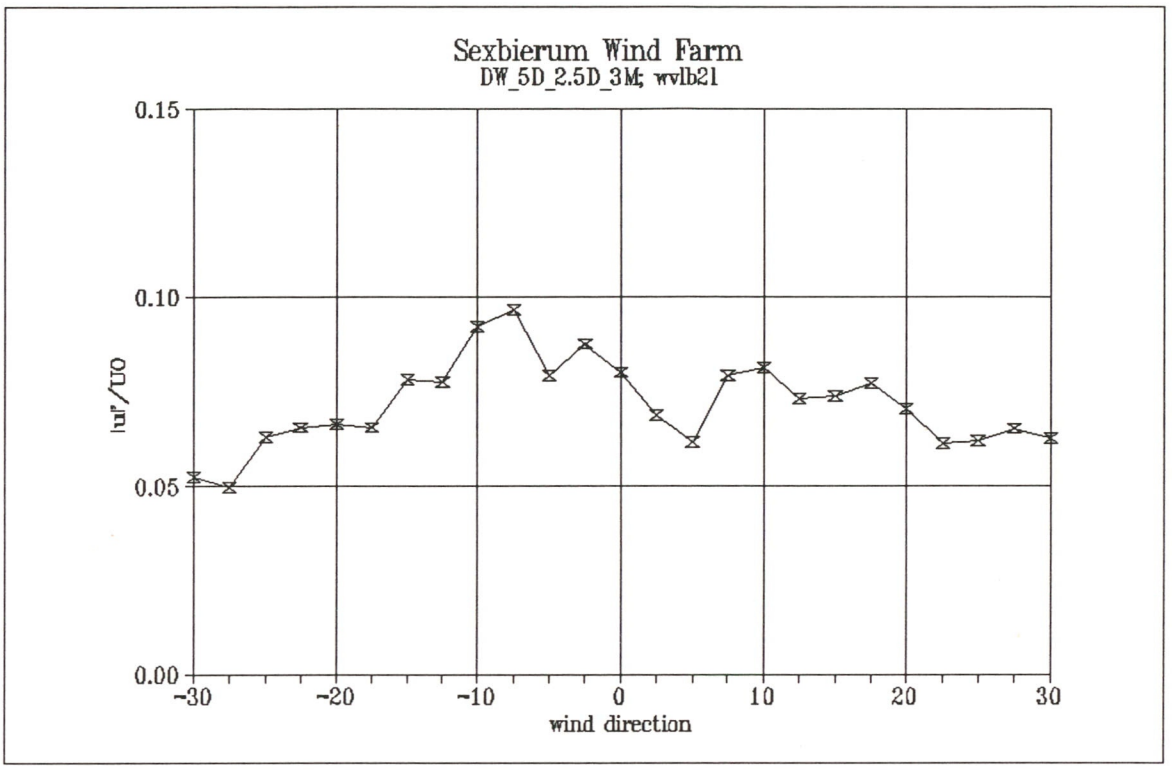

Figure 7 *Non-dimensionalized turbulent fluctuations u'/U_0 as a function of wind direction in the wind speed bin 5-10 m/s*

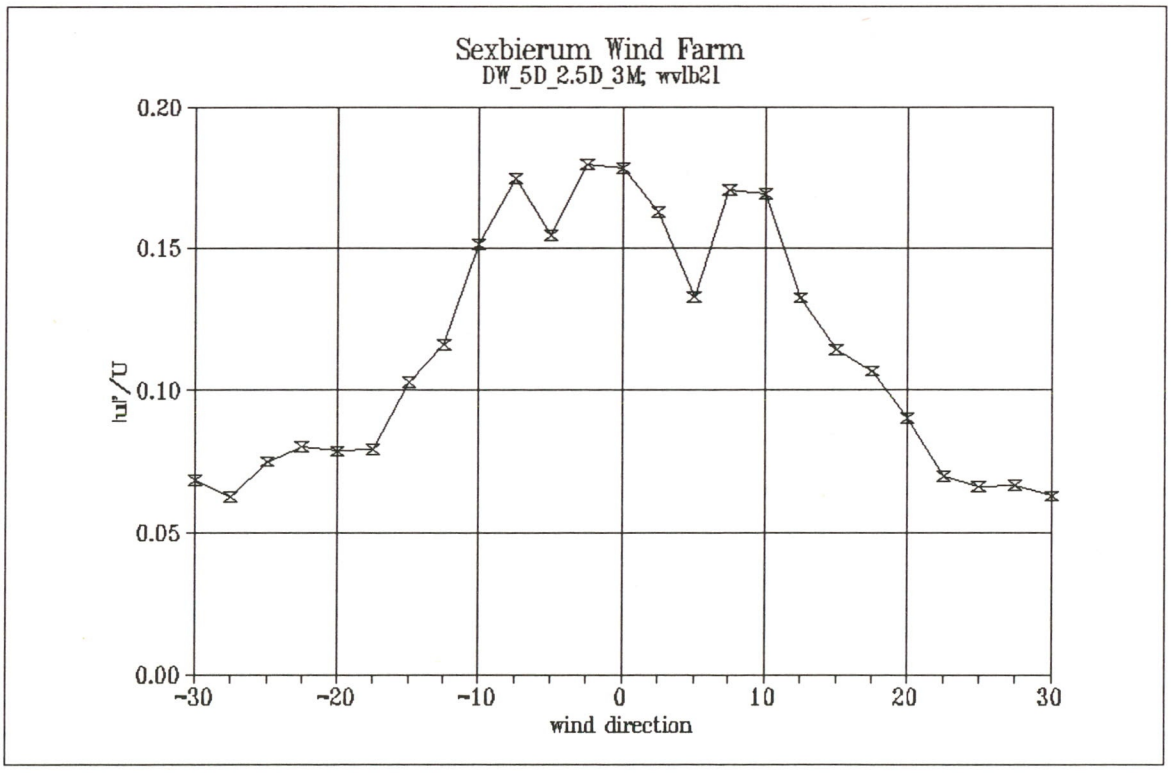

Figure 8 *Non-dimensionalized turbulent fluctuations u'/U as a function of wind direction in the wind speed bin 5-10 m/s*

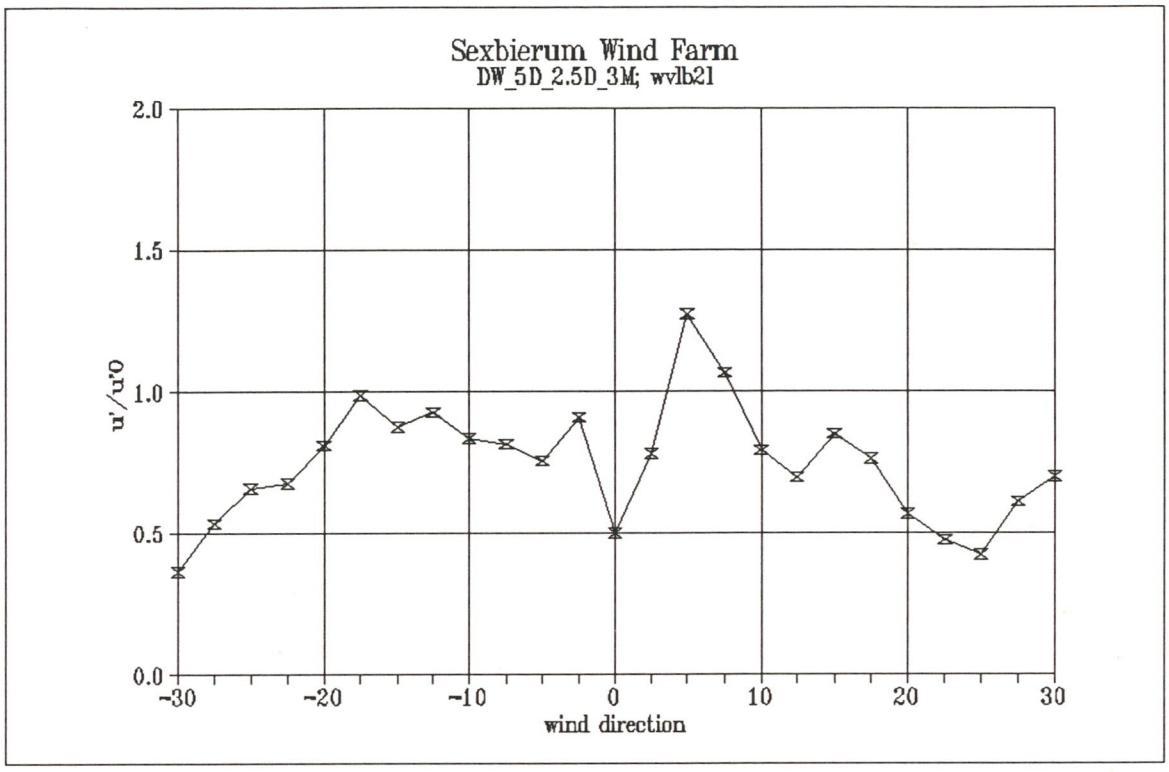

Figure 9 Turbulence enhancement u'/u'_0 as a function of wind direction in the wind speed bin 5-10 m/s

A4.6 Sensor b3

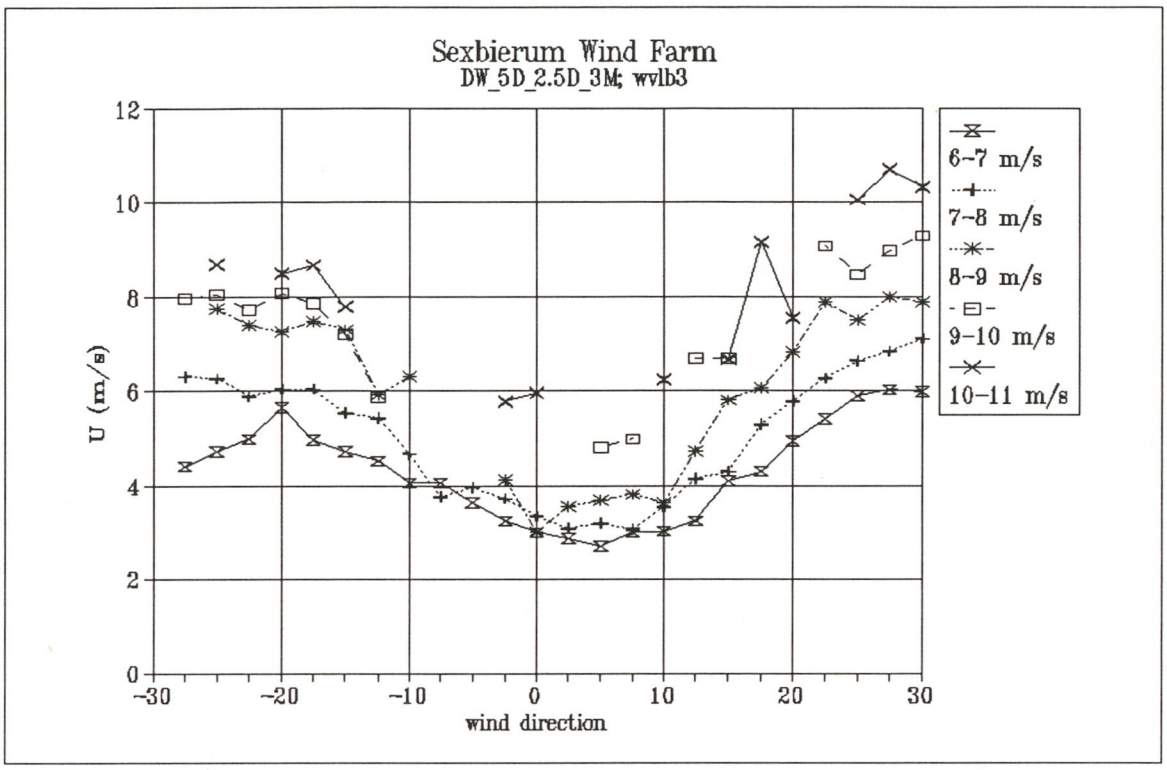

Figure 1 Horizontal wind speed U as a function of wind direction and wind speed bin

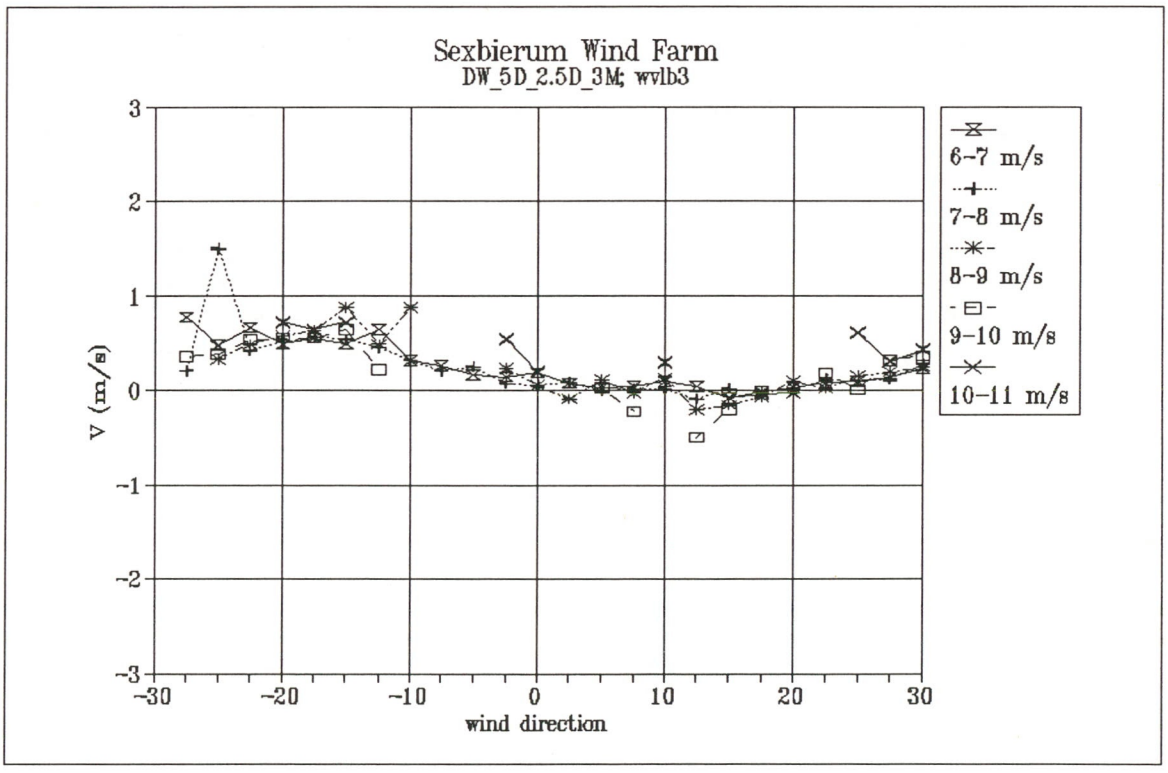

Figure 2 Lateral wind speed V as a function of wind direction and wind speed bin

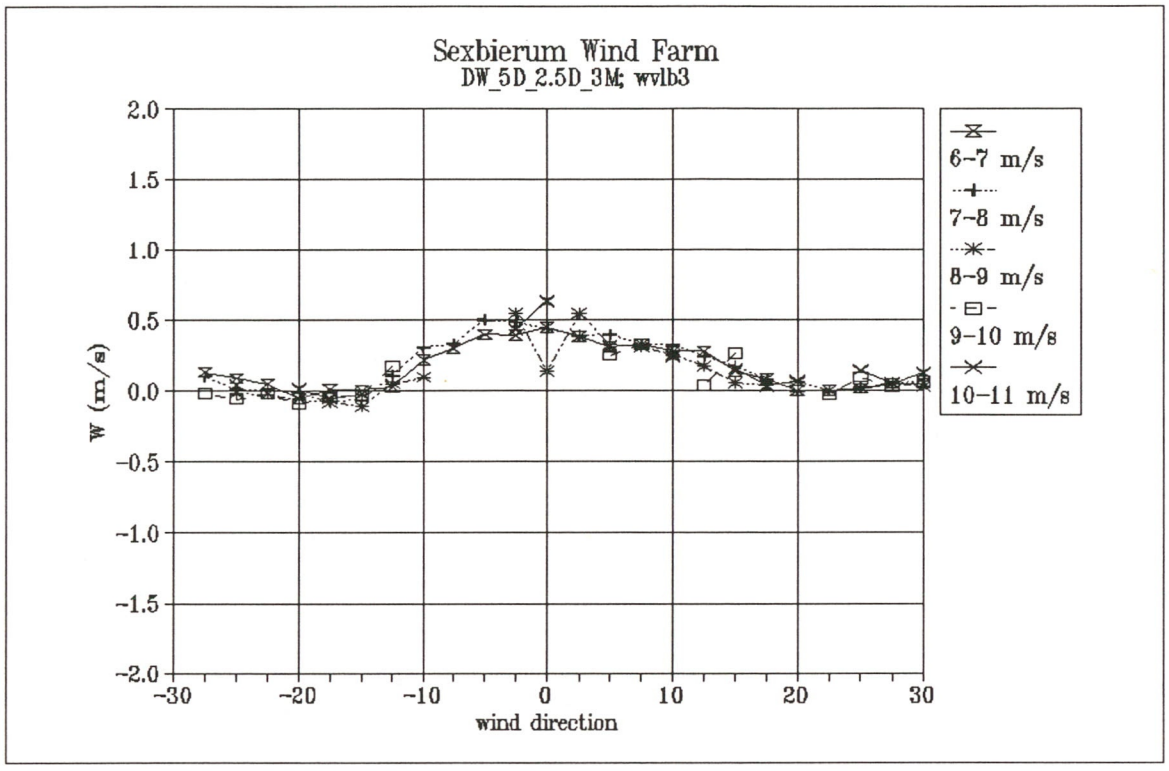

Figure 3 *Vertical wind speed W as a function of wind direction and wind speed bin*

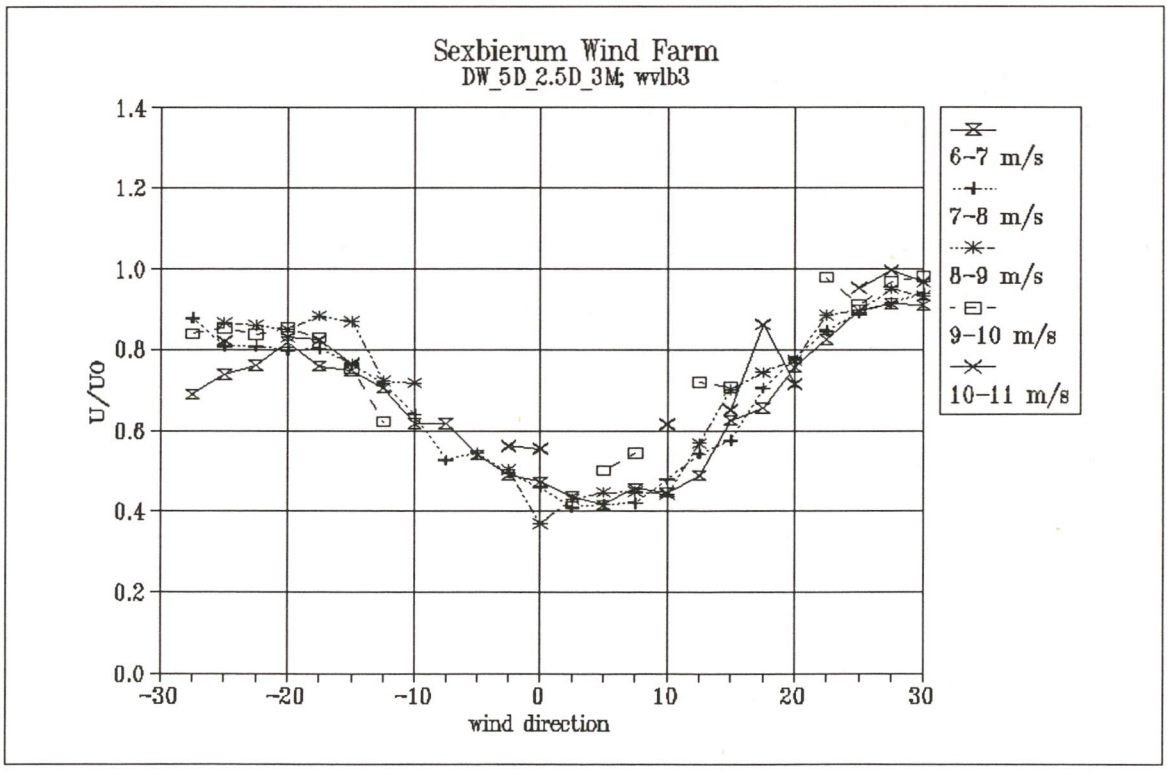

Figure 4 *Wake deficit U/U_0 as a function of wind direction and wind speed bin*

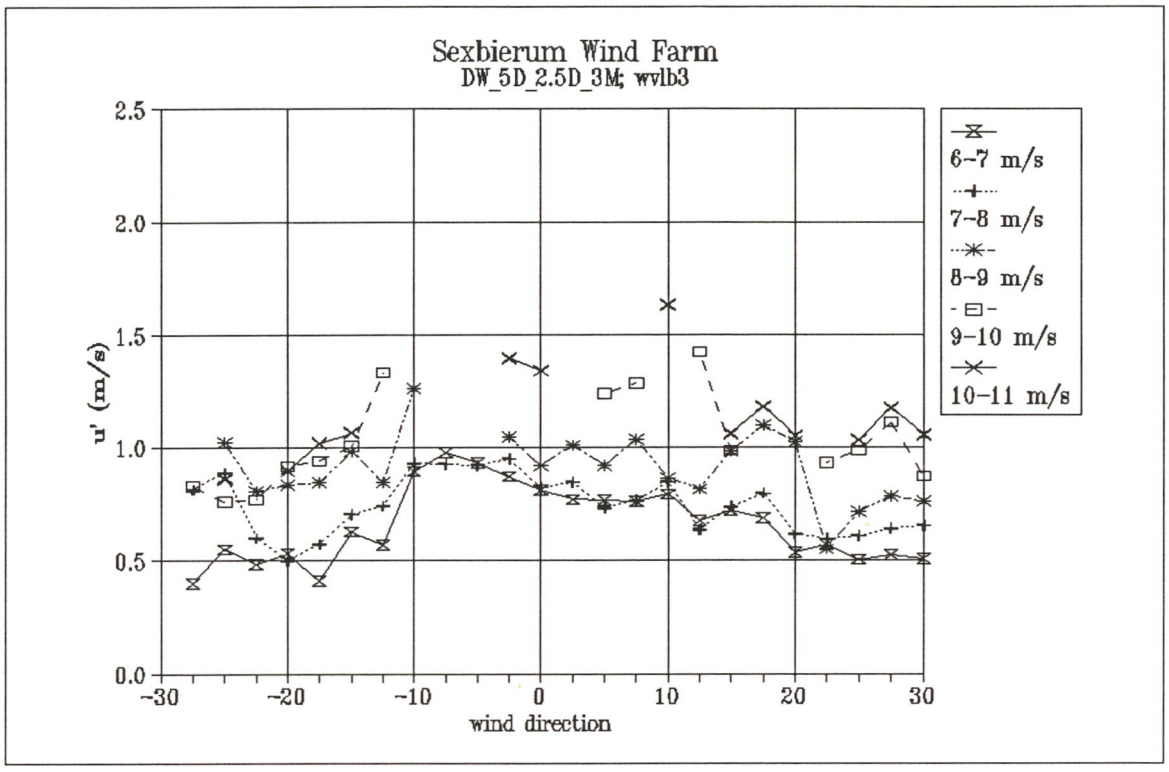

Figure 5 Longitudinal turbulent fluctuations u' as a function of wind direction and wind speed bin

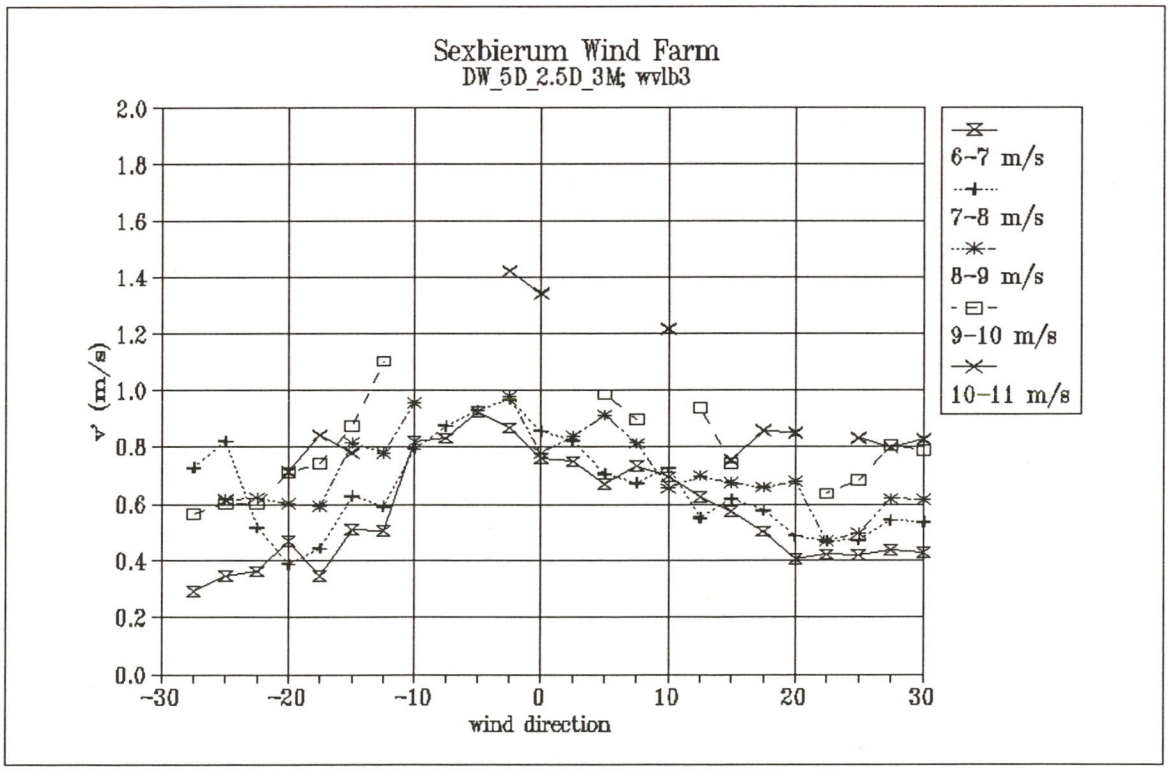

Figure 6 Lateral turbulent fluctuations v' as a function of wind direction and wind speed bin

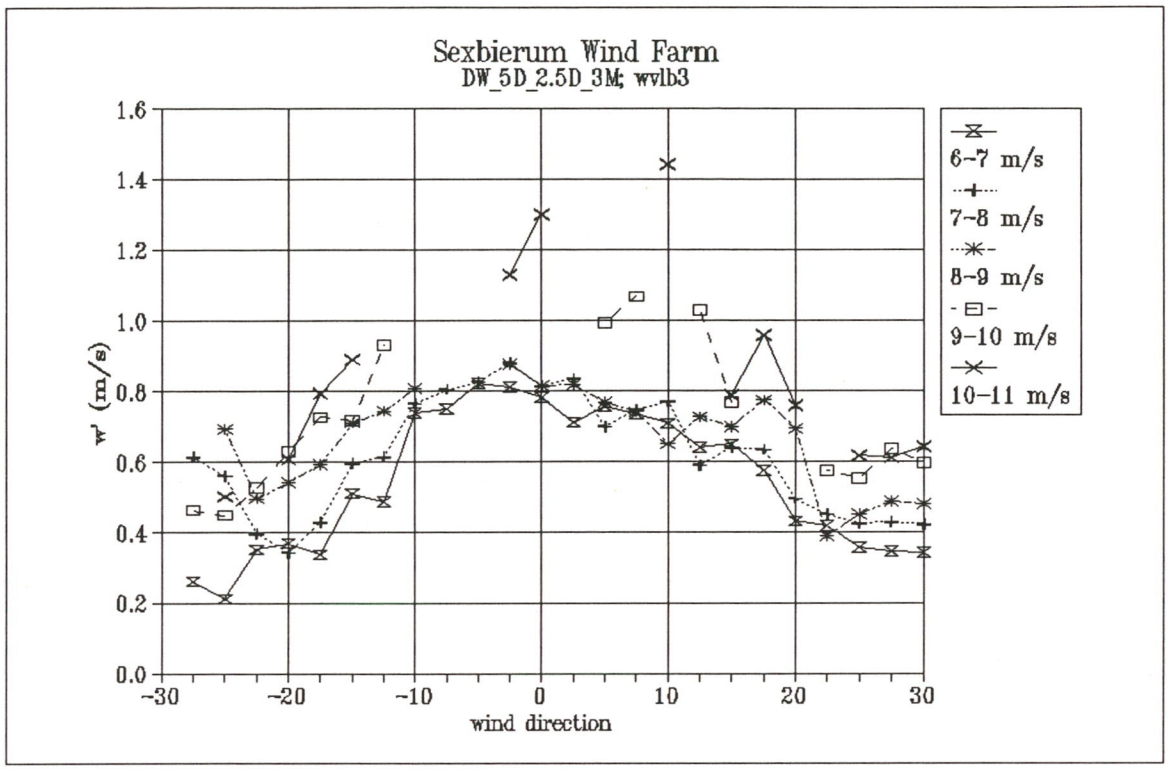

Figure 7 Vertical turbulent fluctuations w' as a function of wind direction and wind speed bin

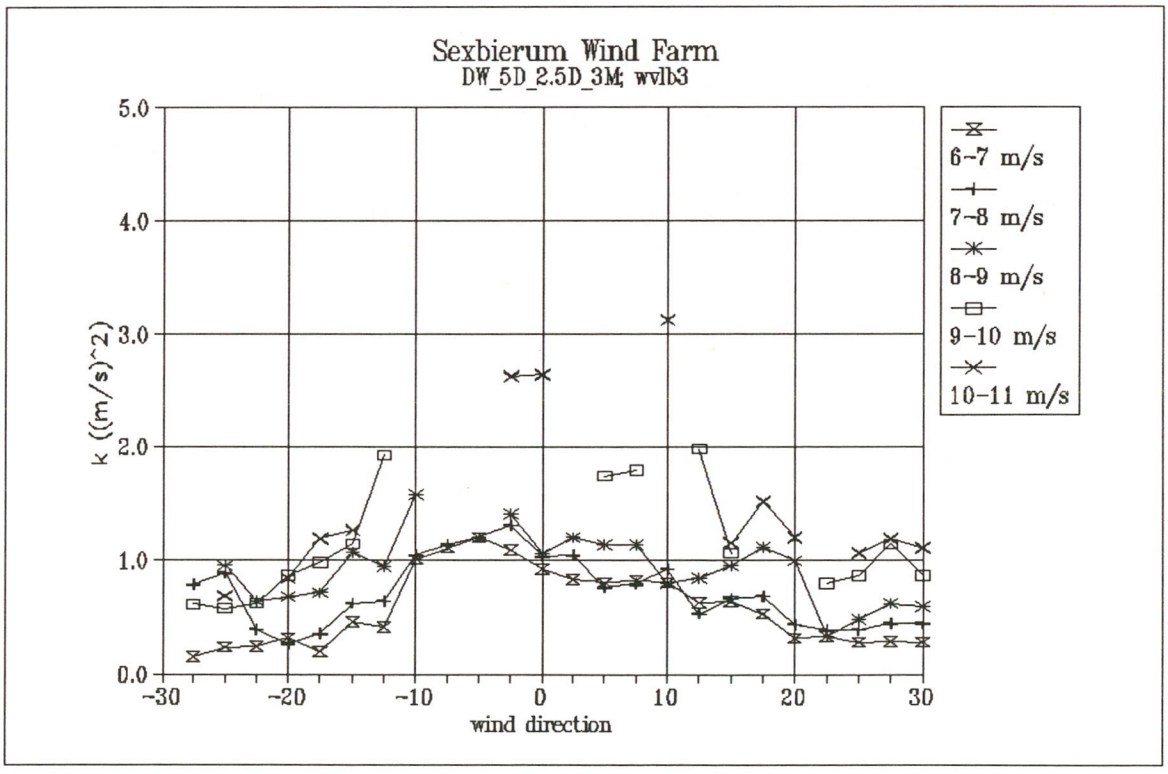

Figure 8 Turbulent kinetic energy per unit mass as a function of wind direction and wind speed bin

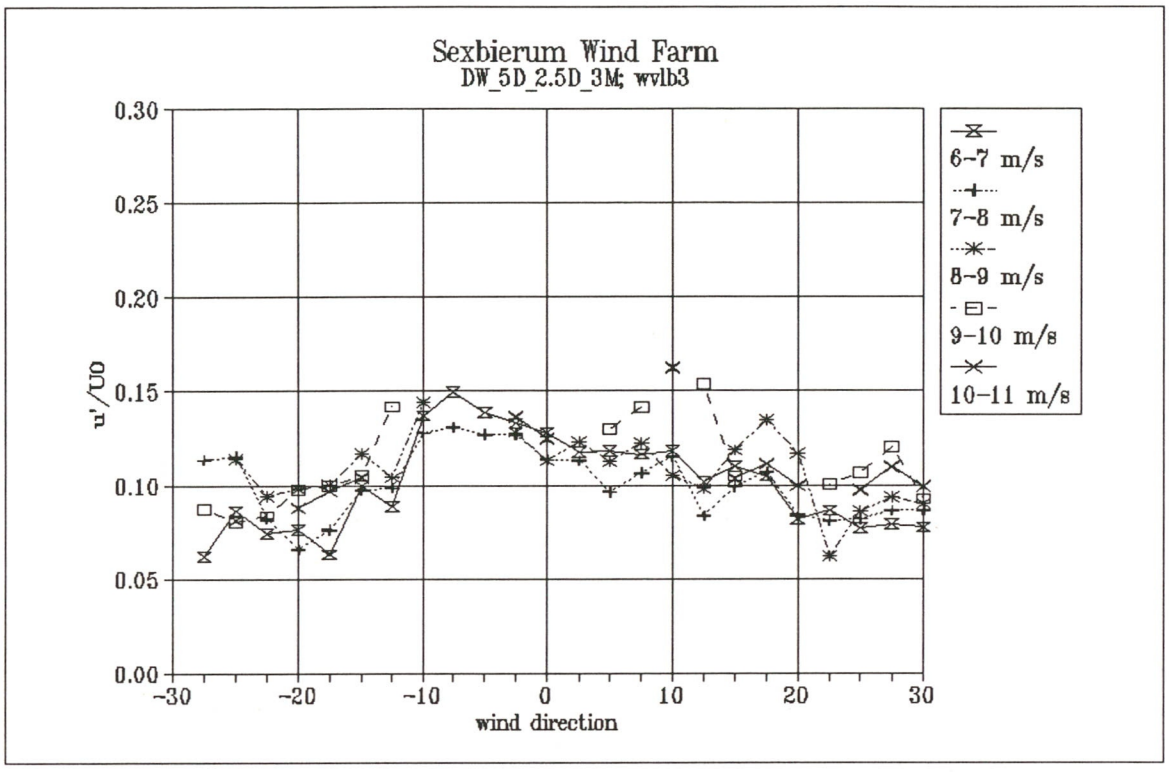

Figure 9 *Non-dimensionalized longitudinal turbulent fluctuations u'/U_0 as a function of wind direction and wind speed bin*

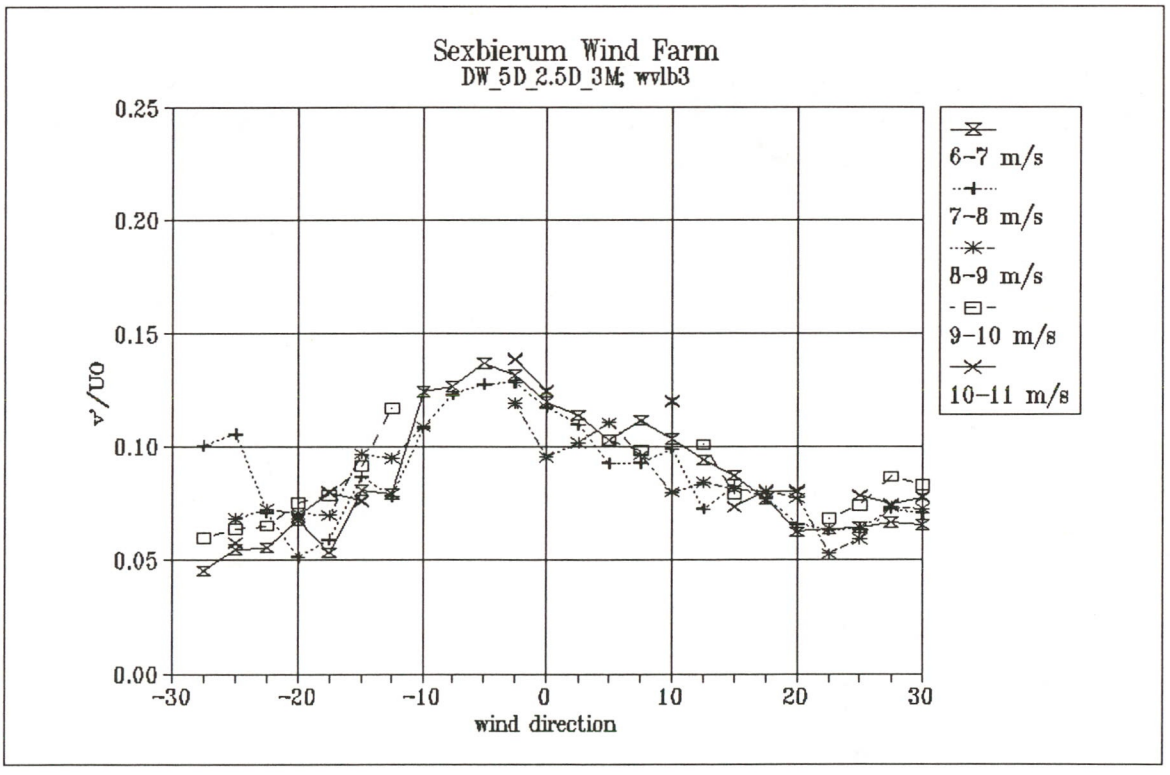

Figure 10 *Non-dimensionalized lateral turbulent fluctuations v'/U_0 as a function of wind direction and wind speed bin*

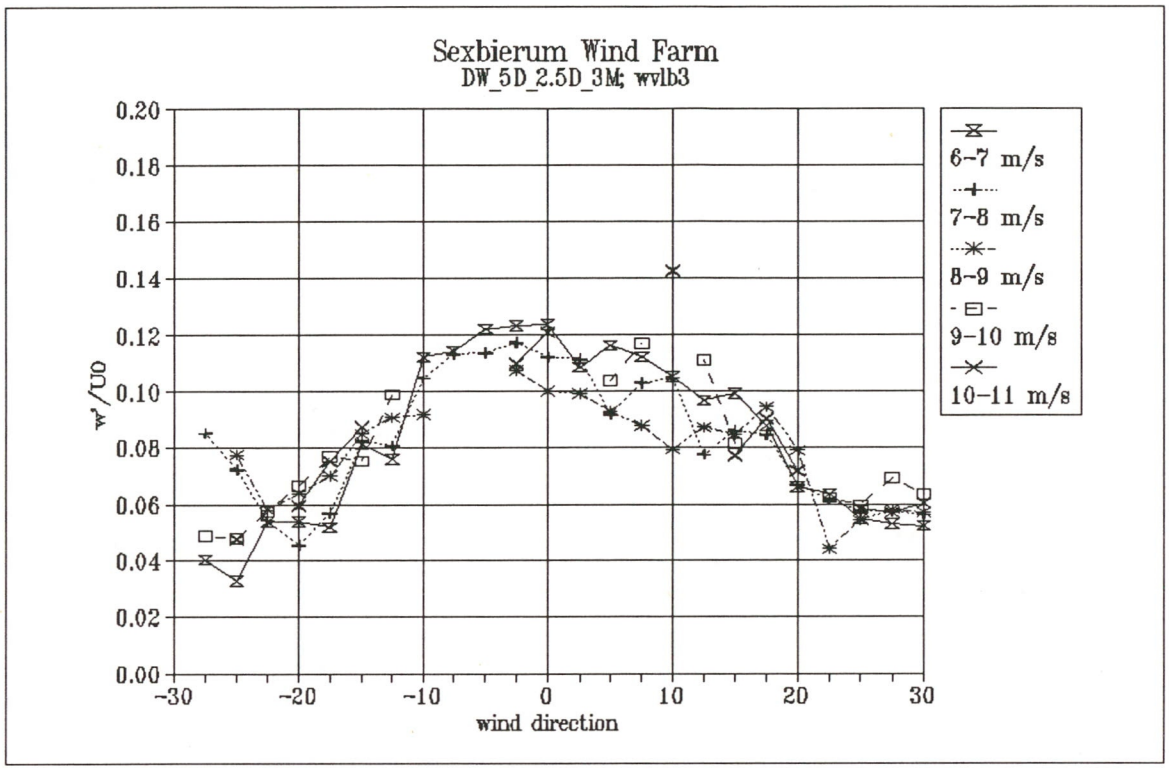

Figure 11 *Non-dimensionalized vertical turbulent fluctuations w'/U_0 as a function of wind direction and wind speed bin*

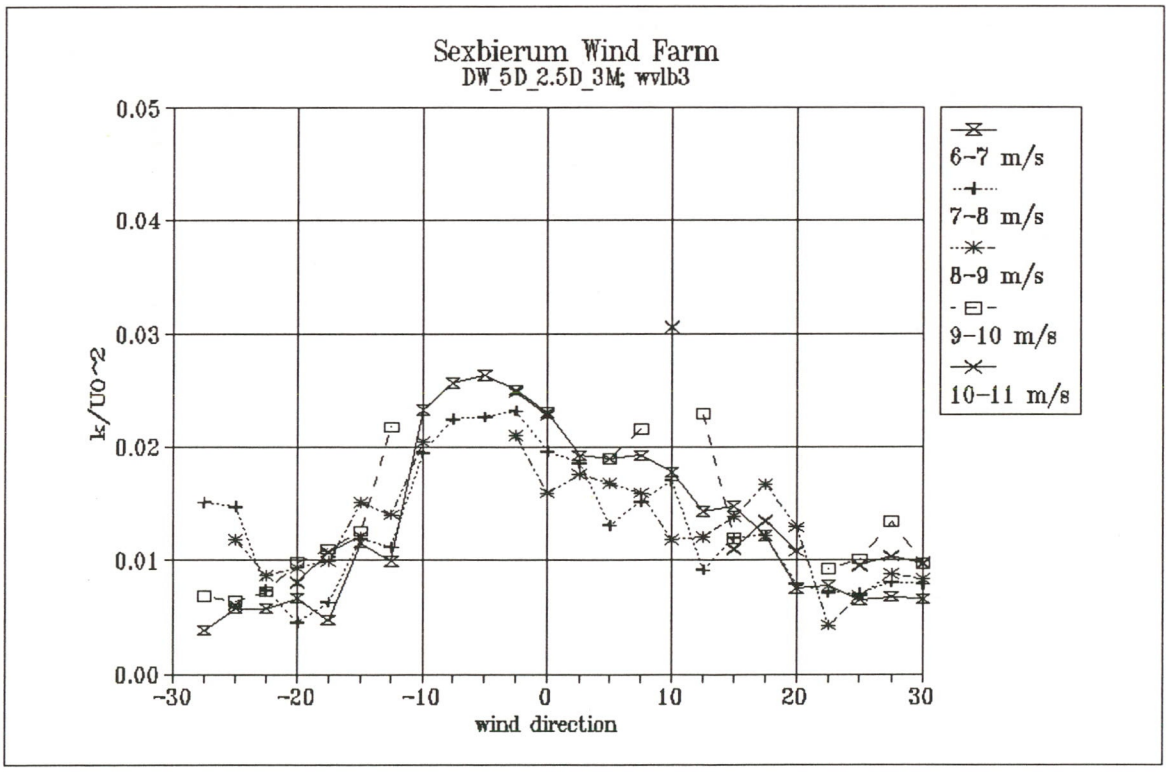

Figure 12 *Non-dimensionalized turbulent kinetic energy k/U_0^2 as a function of wind direction and wind speed bin*

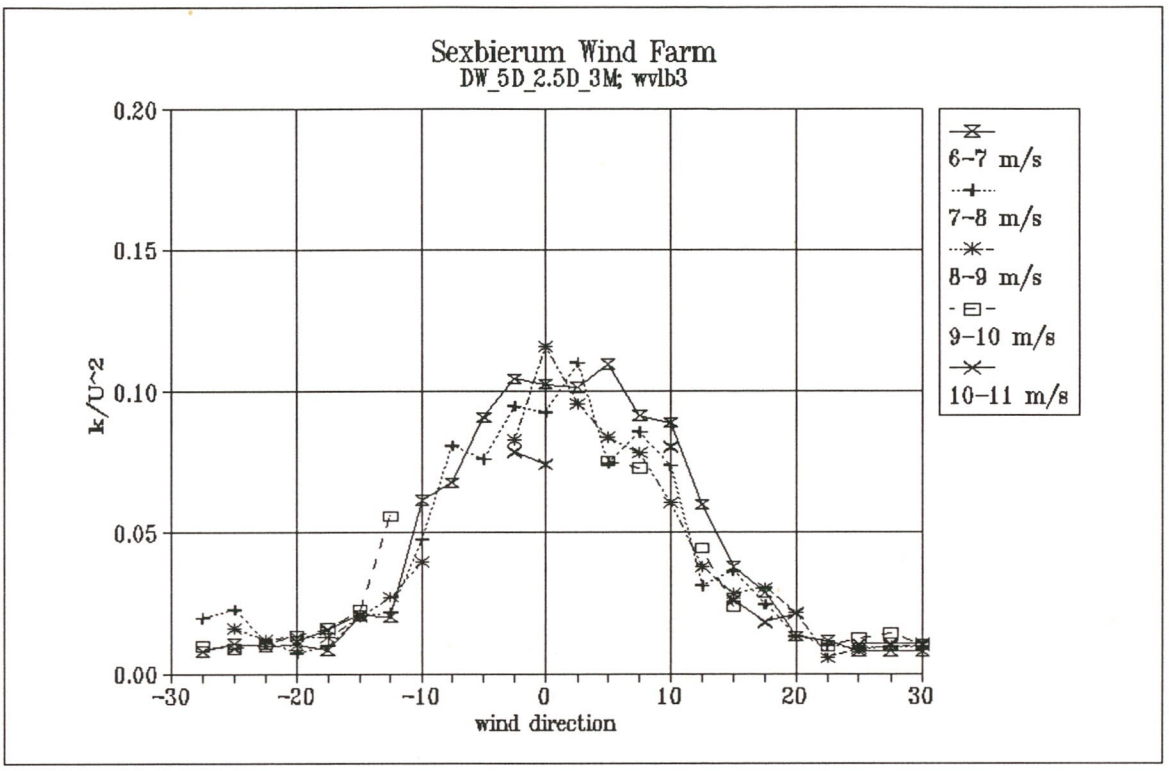

Figure 13 Non-dimensionalized turbulent kinetic energy k/U^2 as a function of wind direction and wind speed bin

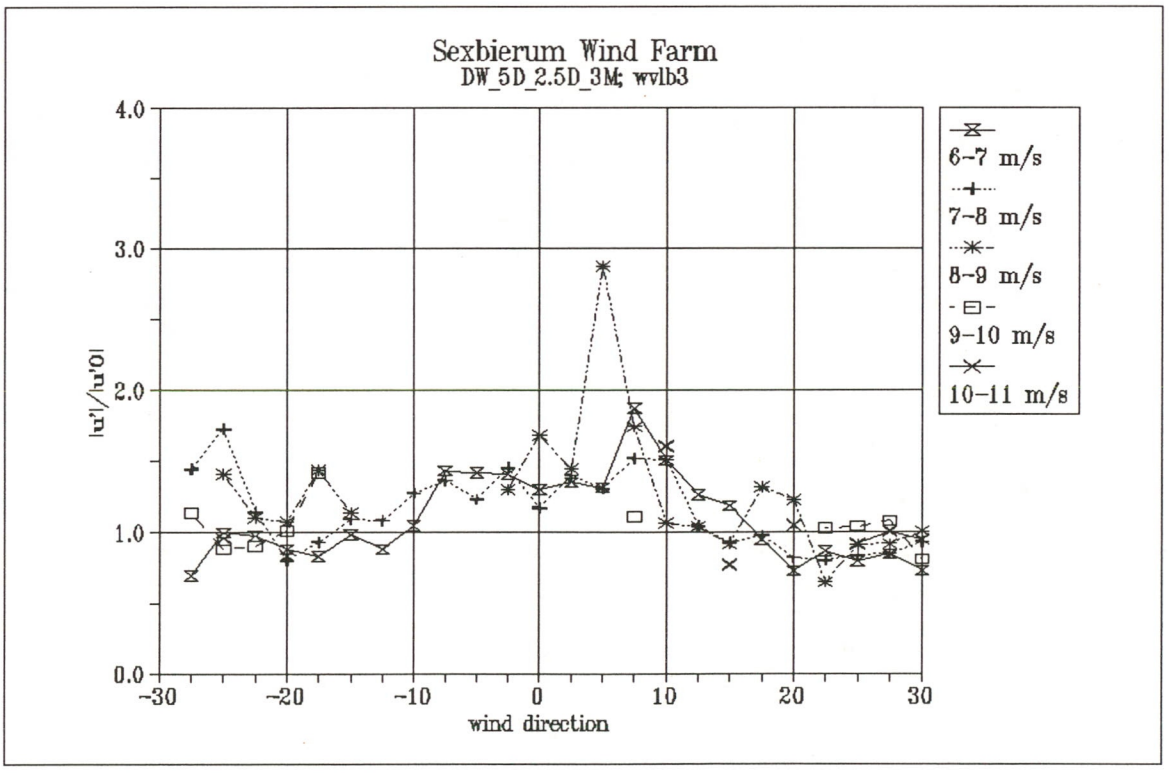

Figure 14 Longitudinal turbulence enhancement u'/u'_0 as a function of wind direction and wind speed bin

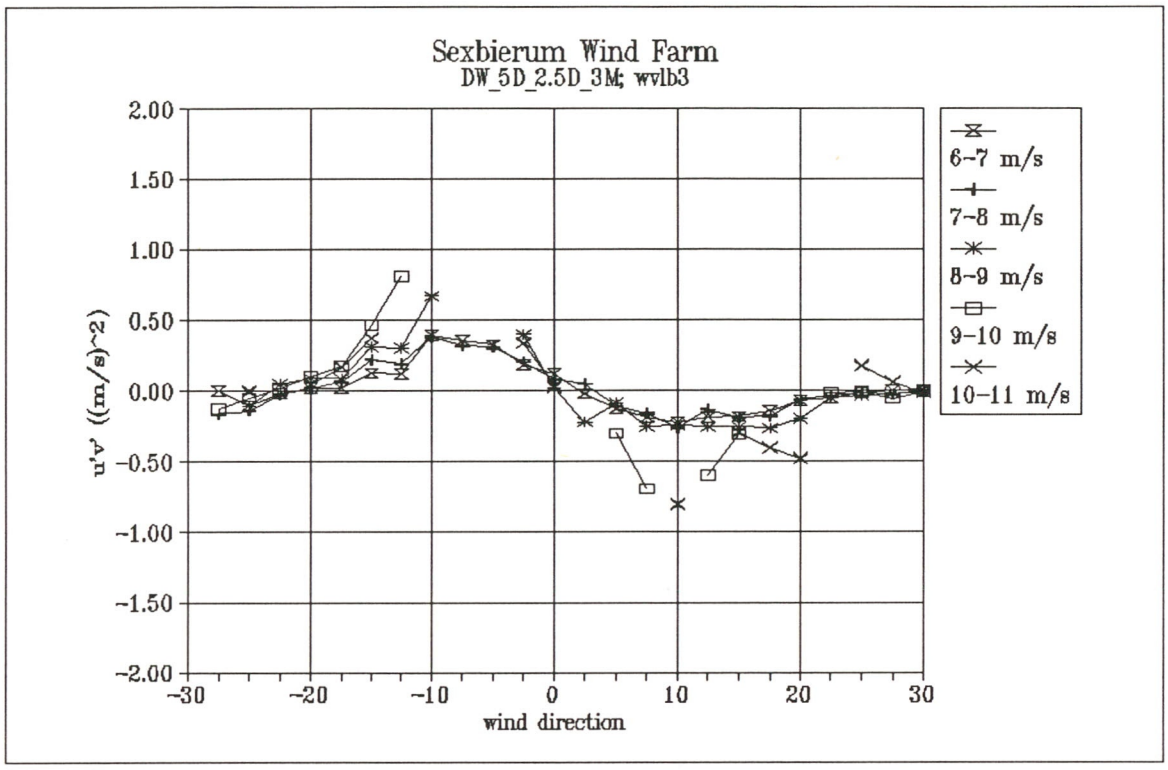

Figure 15 Shear stress u'v' as a function of wind direction and wind speed bin

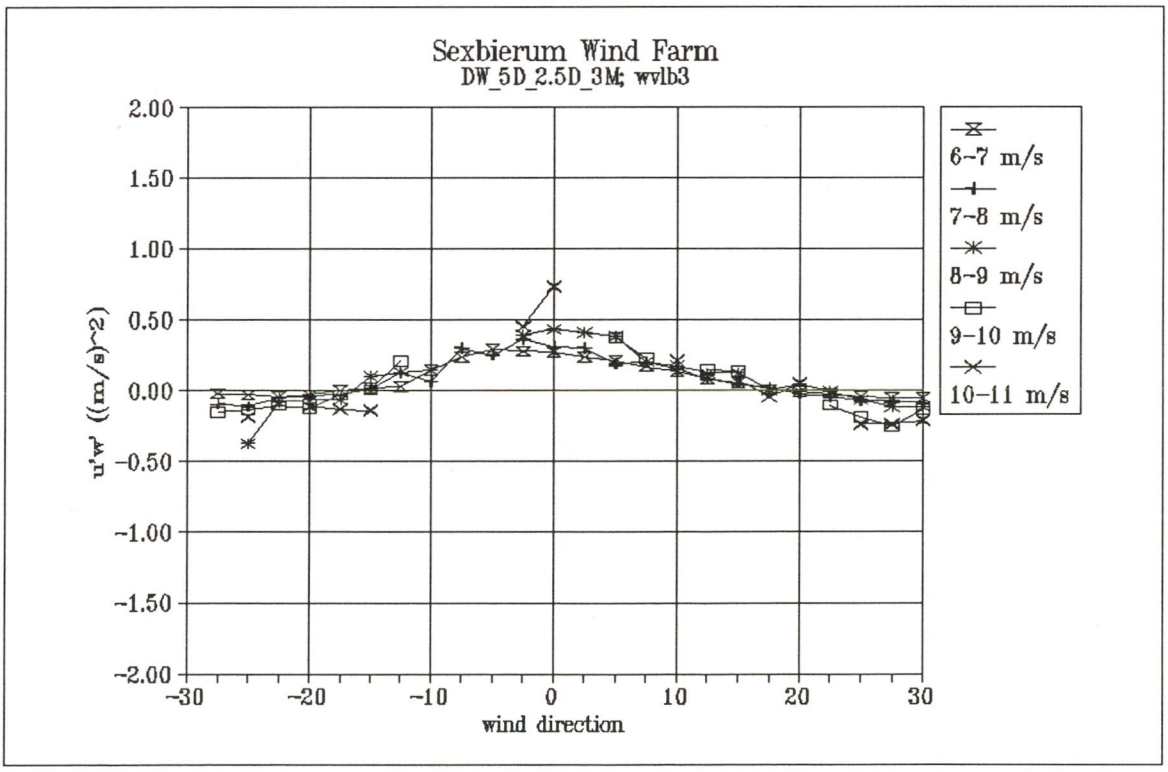

Figure 16 Shear stress u'w' as a function of wind direction and wind speed bin

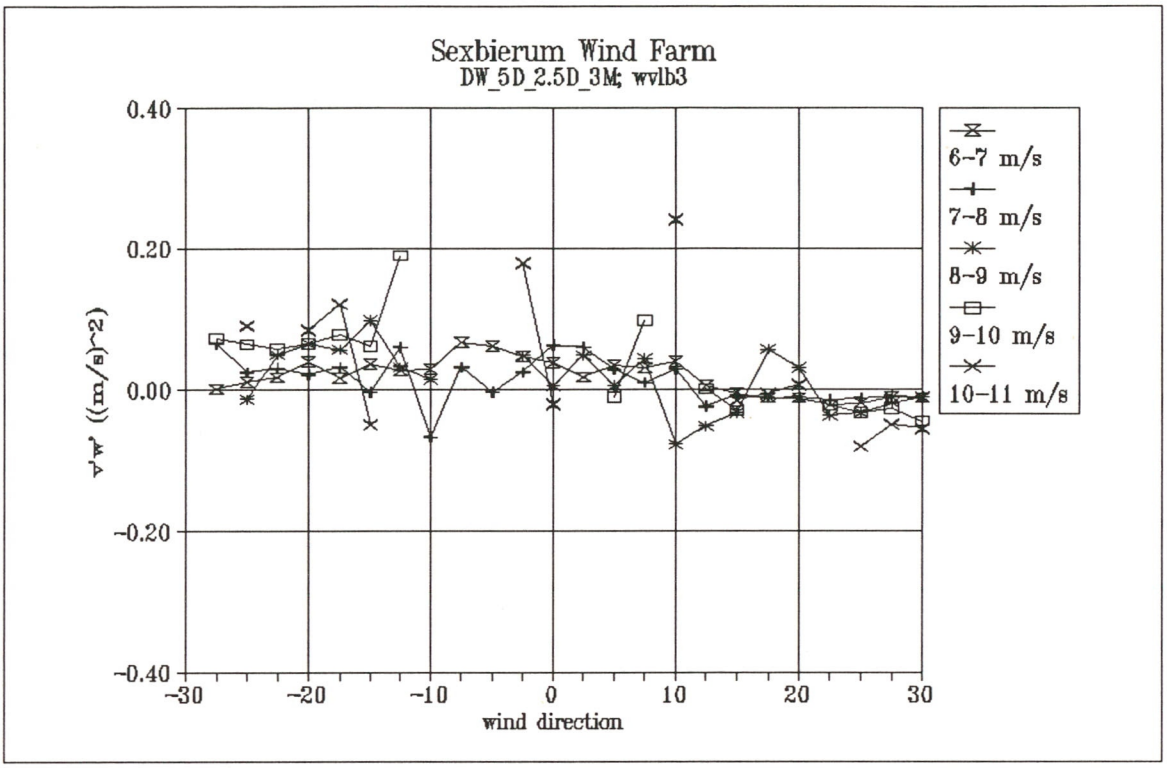

Figure 17 Shear stress v'w' as a function of wind direction and wind speed bin

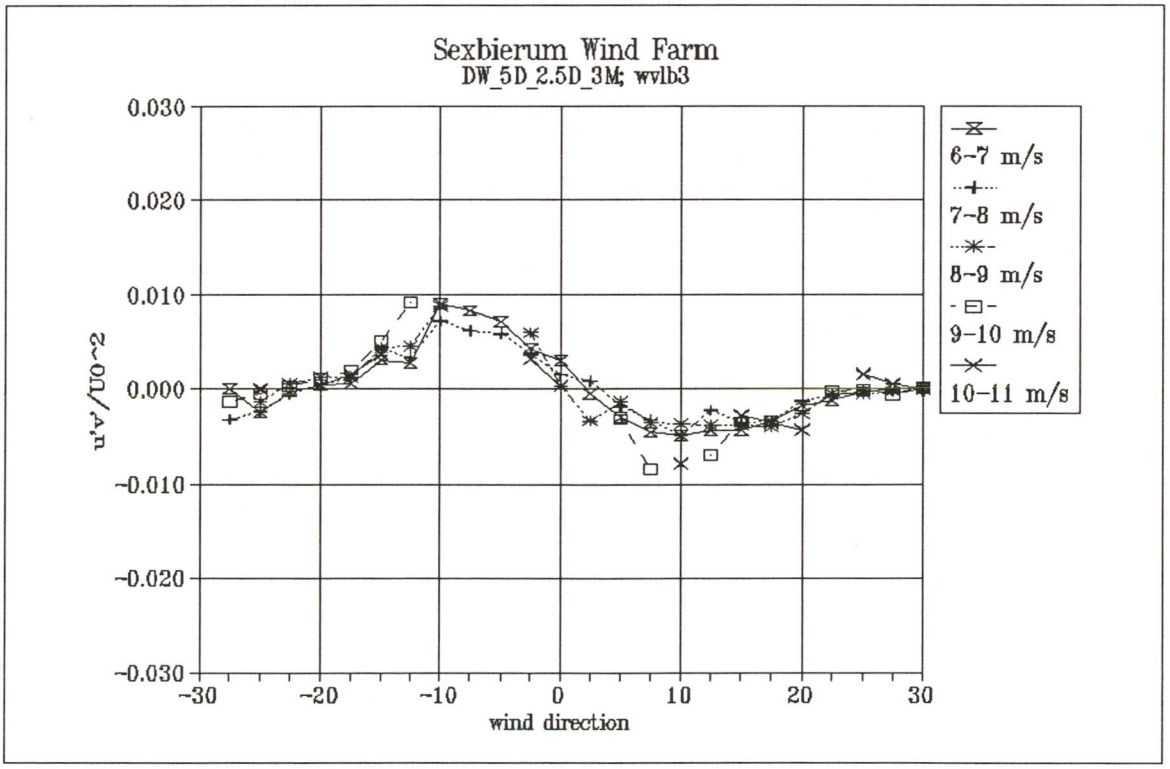

Figure 18 Non-dimensionalized shear stress $u'v'/U_0^2$ as a function of wind direction and wind speed bin

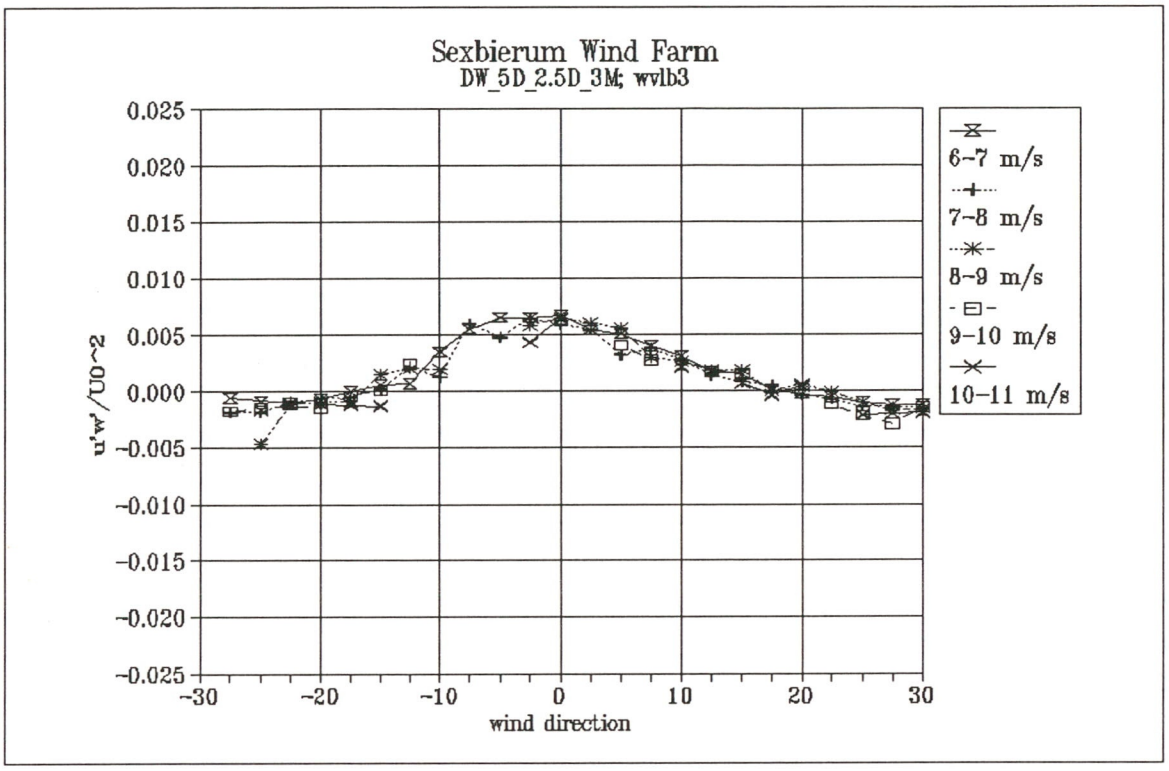

Figure 19 Non-dimensionalized shear stress $u'w'/U_0^2$ as a function of wind direction and wind speed bin

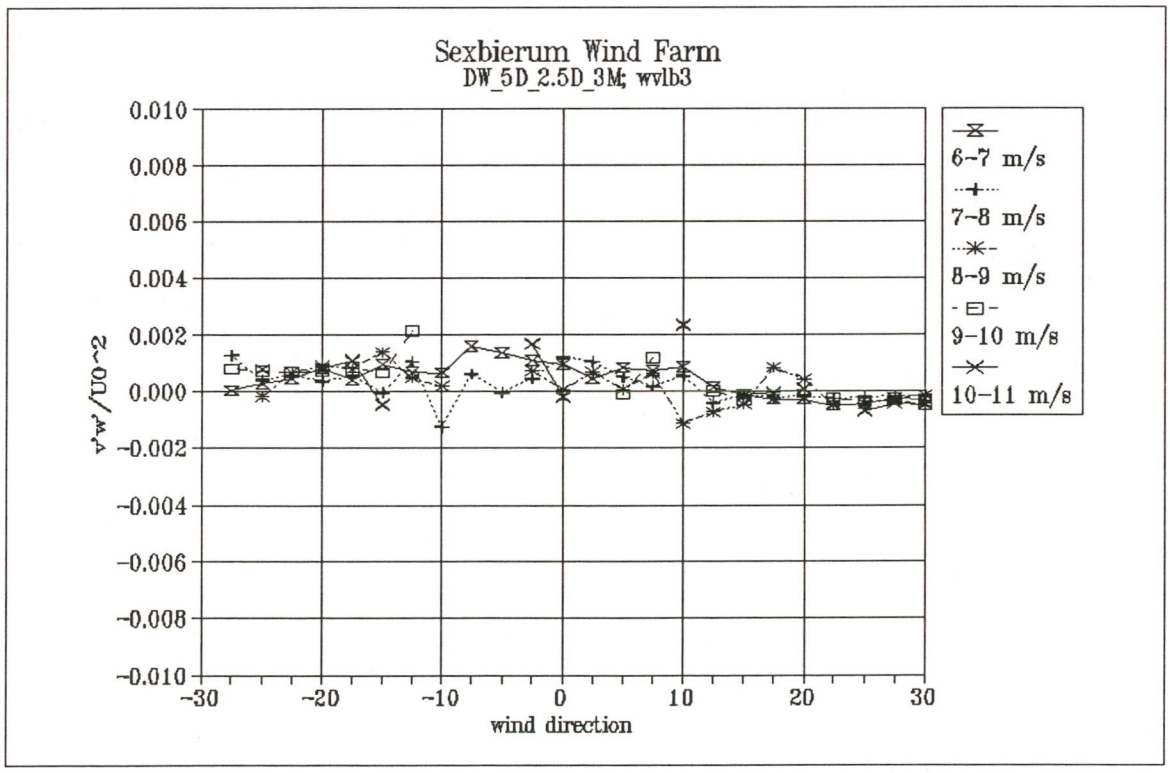

Figure 20 Non-dimensionalized shear stress $v'w'/U_0^2$ as a function of wind direction and wind speed bin

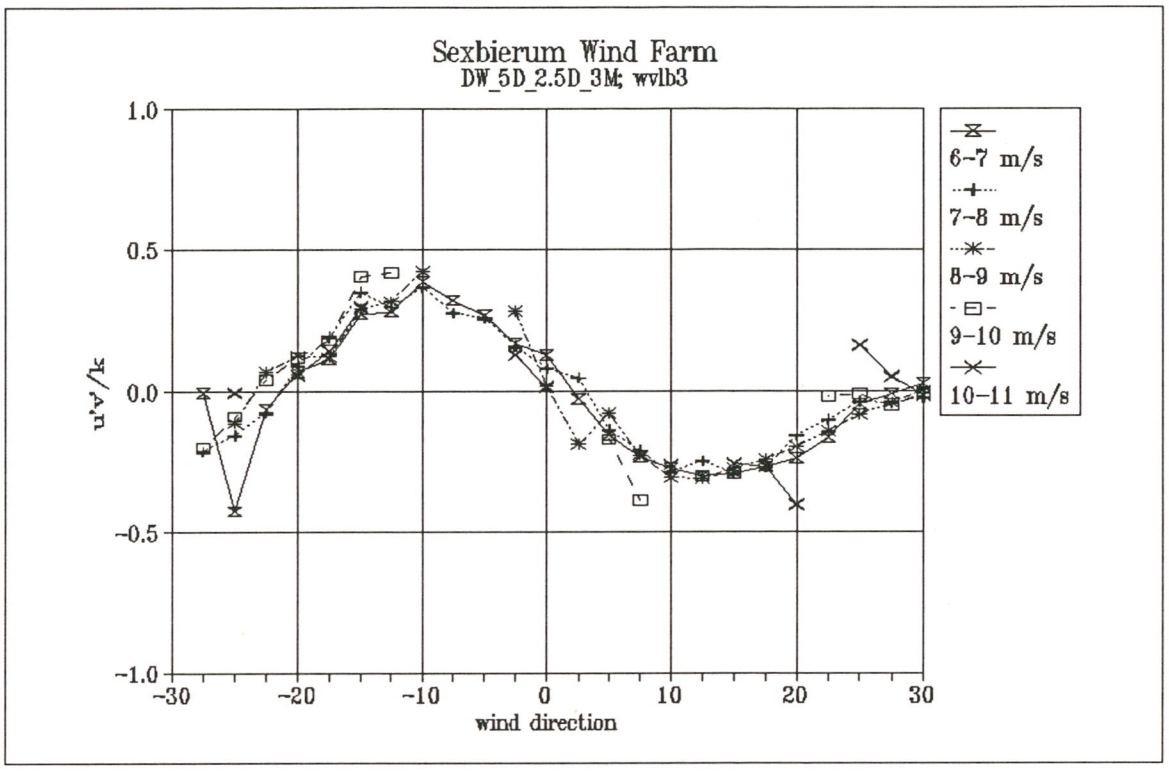

Figure 21 Non-dimensionalized shear stress u'v'/k as a function of wind direction and wind speed bin

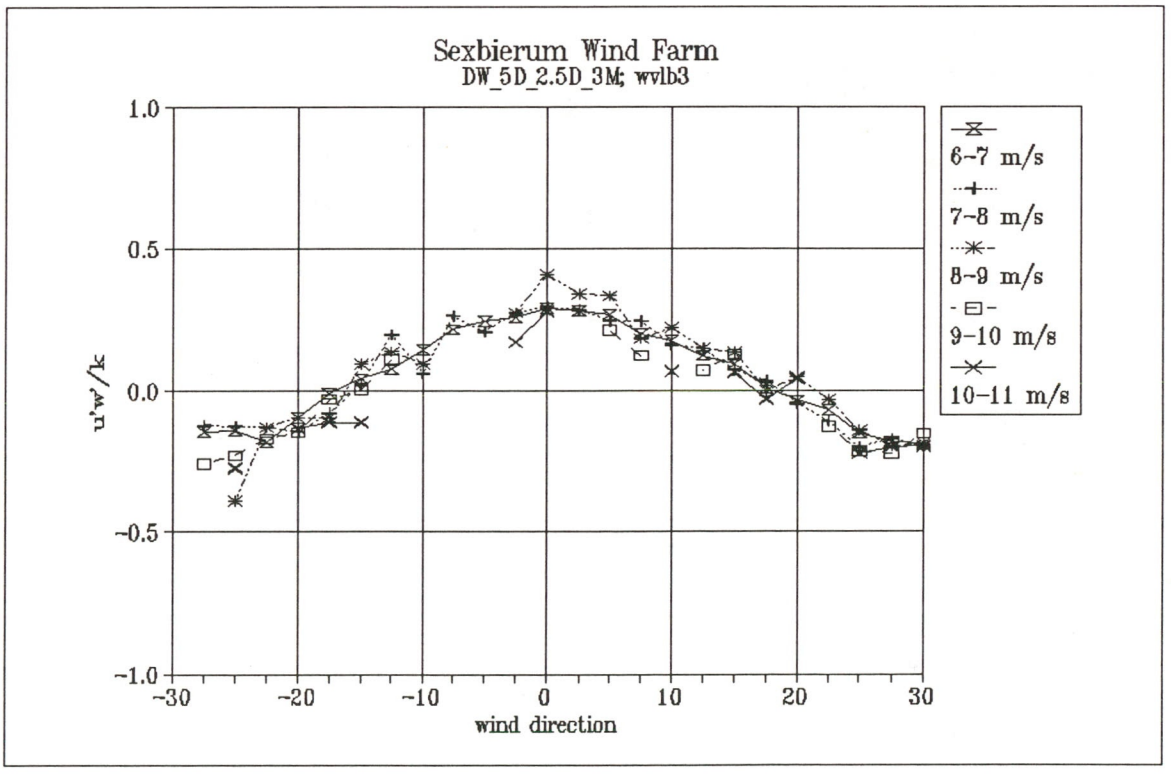

Figure 22 Non-dimensionalized shear stress u'w'/k as a function of wind direction and wind speed bin

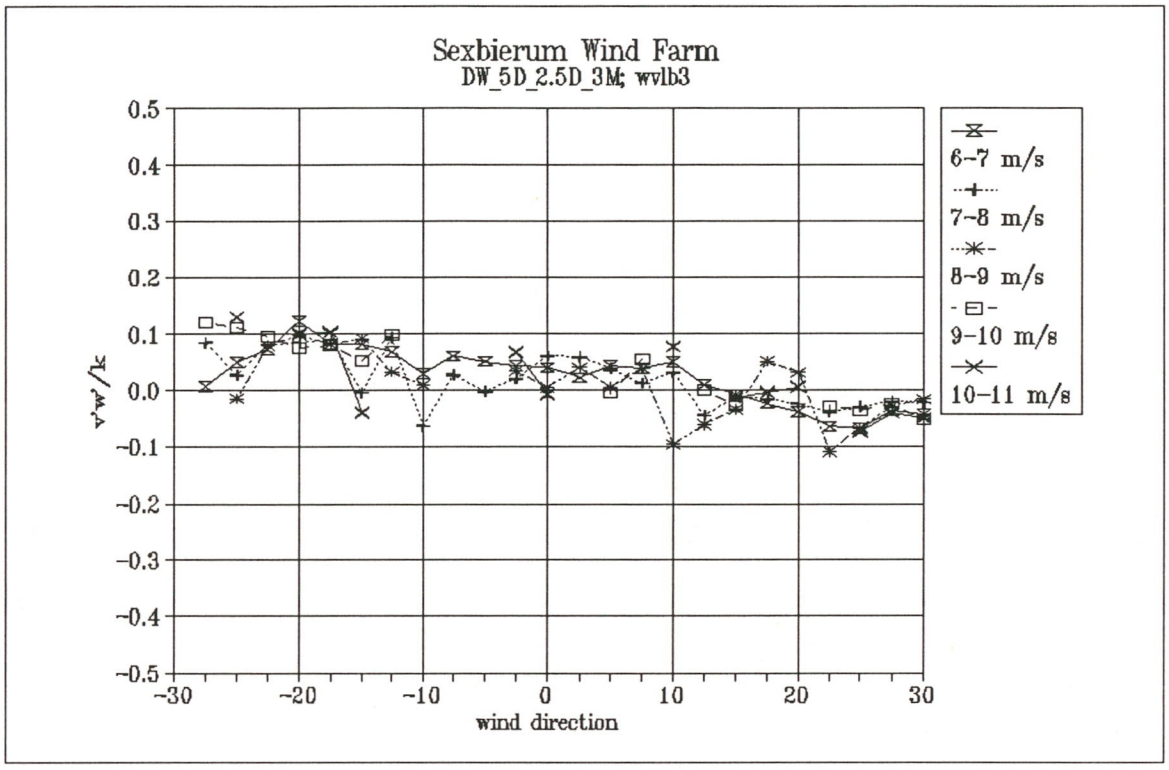

Figure 23 Non-dimensionalized shear stress v'w'/k as a function of wind direction and wind speed bin

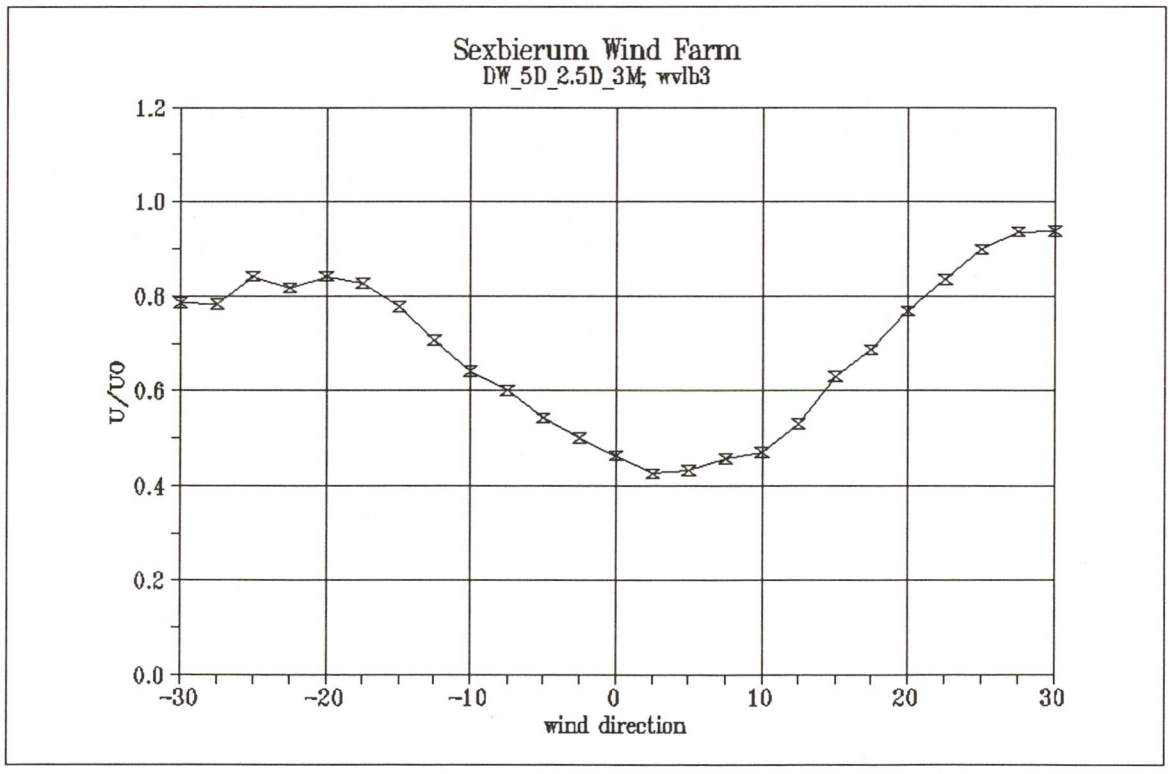

Figure 24 Wake deficit U/U_0 as a function of wind direction in the wind speed bin 5-10 m/s

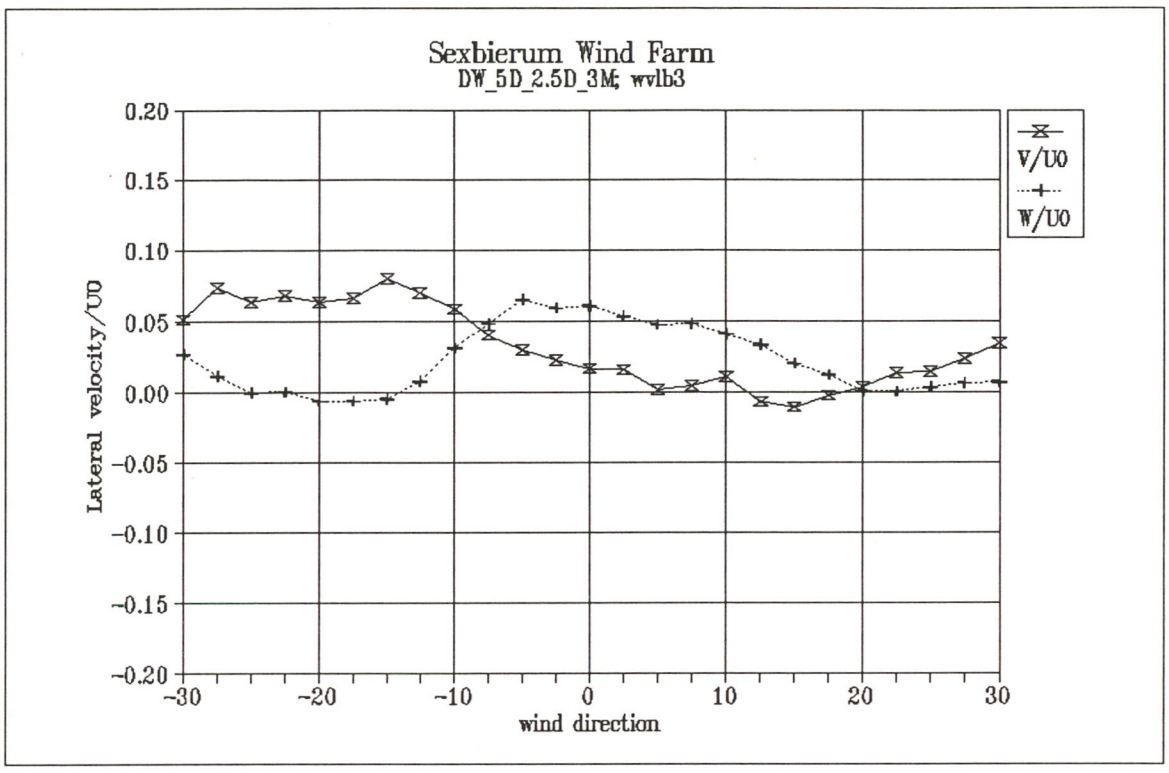

Figure 25 Lateral and vertical wind speed V/U_0 and W/U_0 as a function of wind direction in the wind speed bin 5-10 m/s

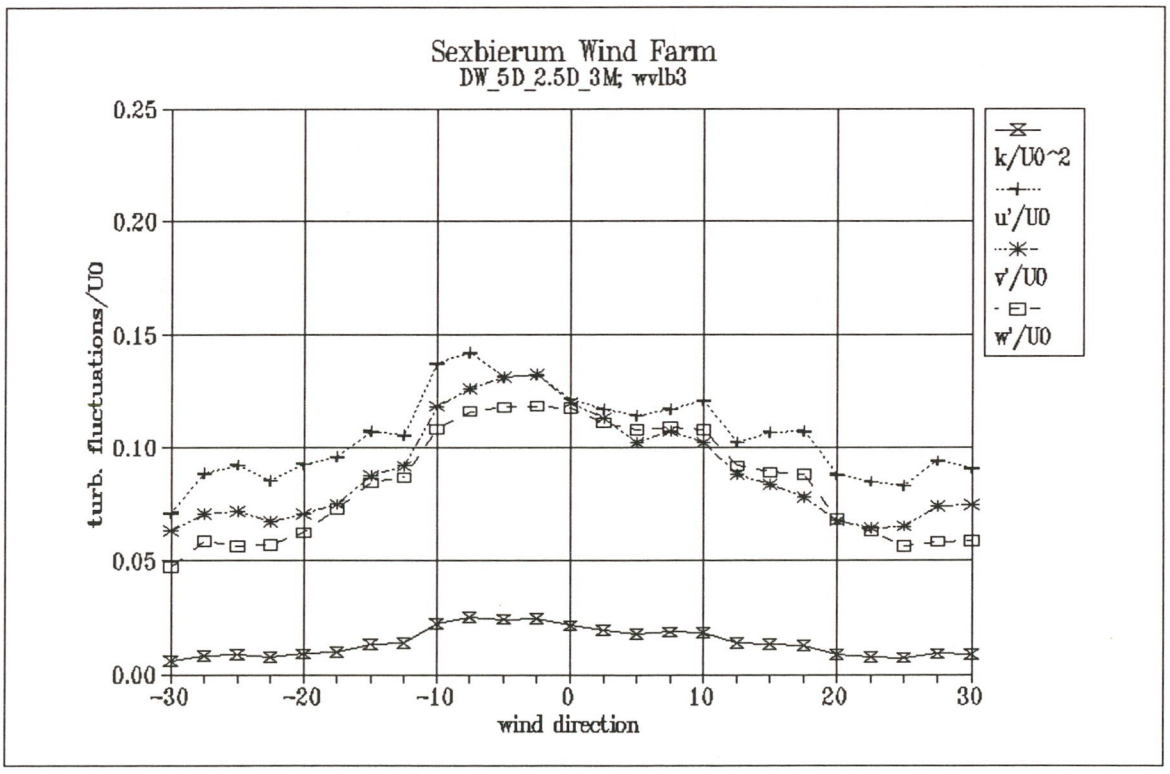

Figure 26 Turbulent fluctuations as a function of wind direction in the wind speed bin 5-10 m/s, non-dimensionalized with U_0

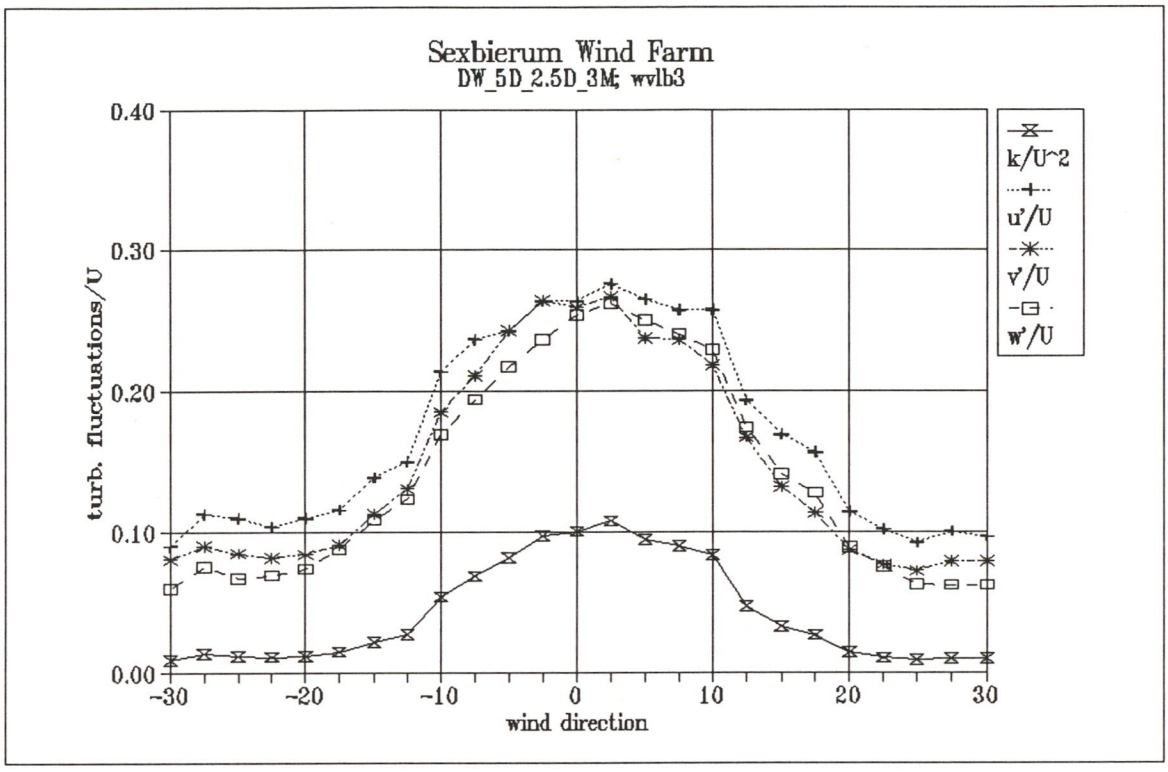

Figure 27 Turbulent fluctuations as a function of wind direction in the wind speed bin 5-10 m/s, non-dimensionalized with U

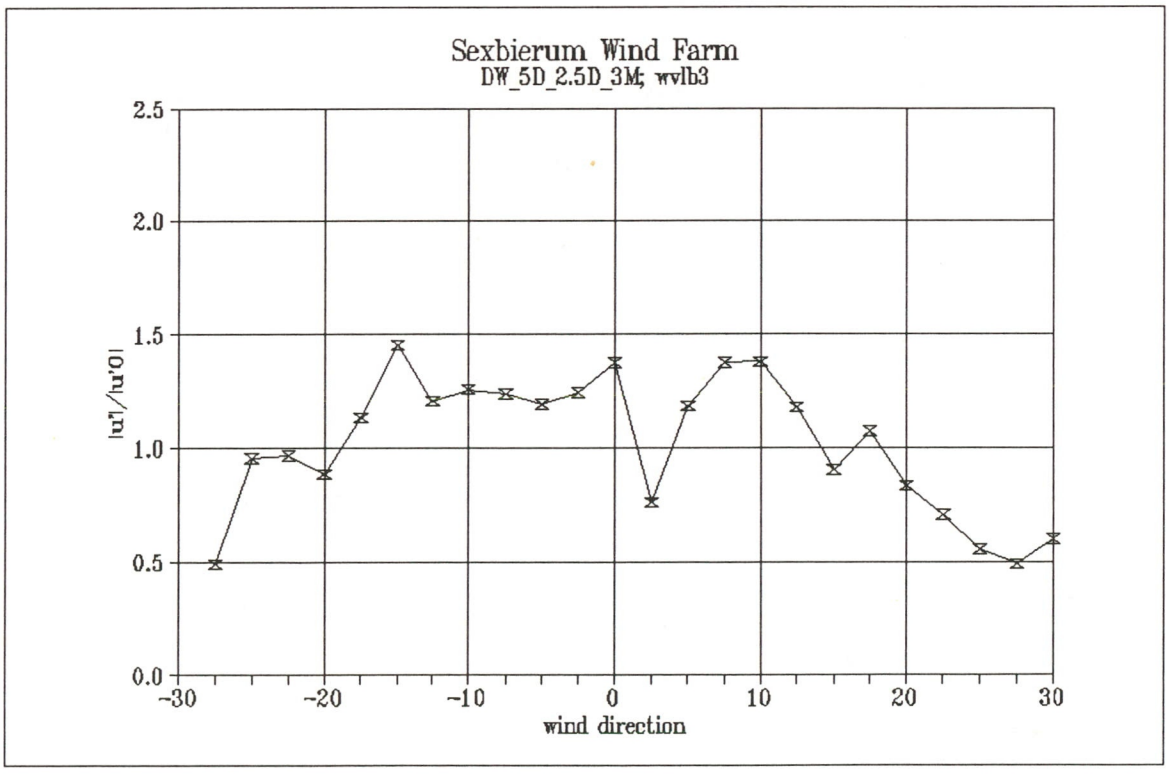

Figure 28 Longitudinal turbulence enhancement u'/u'_0 as a function of wind direction in the wind speed bin 5-10 m/s

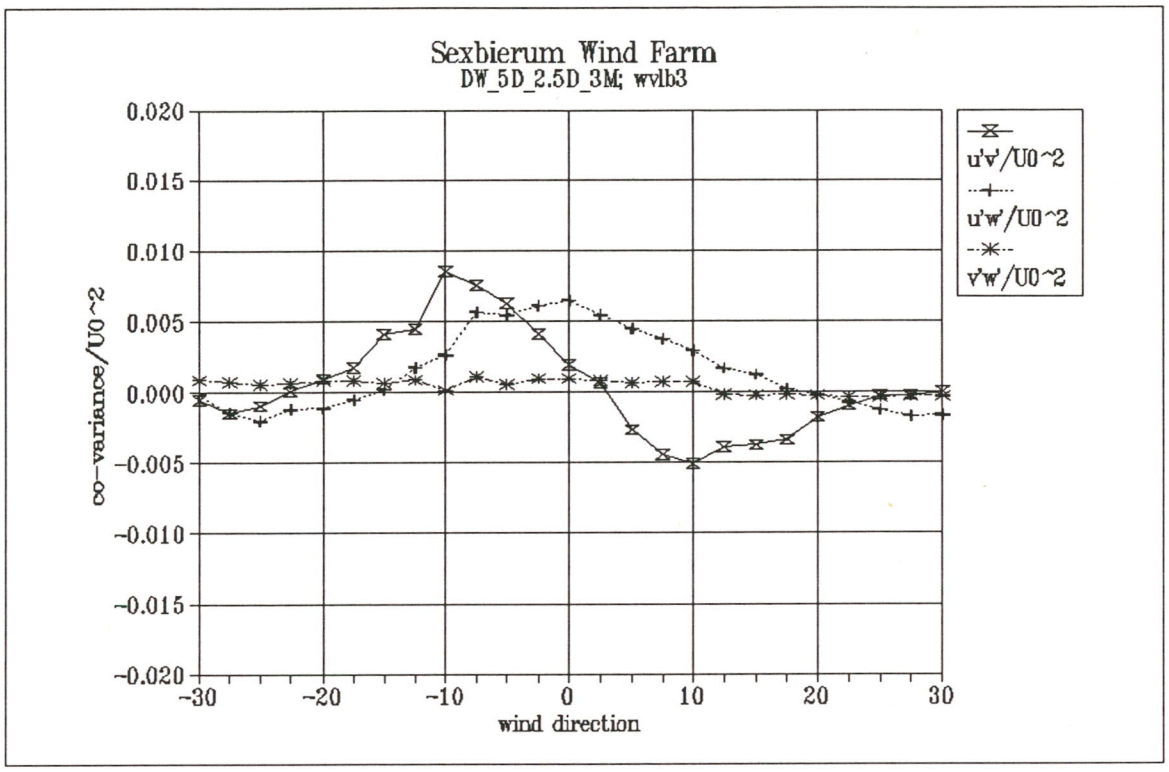

Figure 29 Non-dimensionalized shear stresses $u'v'/U_0^2$; $u'w'/U_0^2$; $v'w'/U_0^2$ as a function of wind direction in the wind speed bin 5-10 m/s

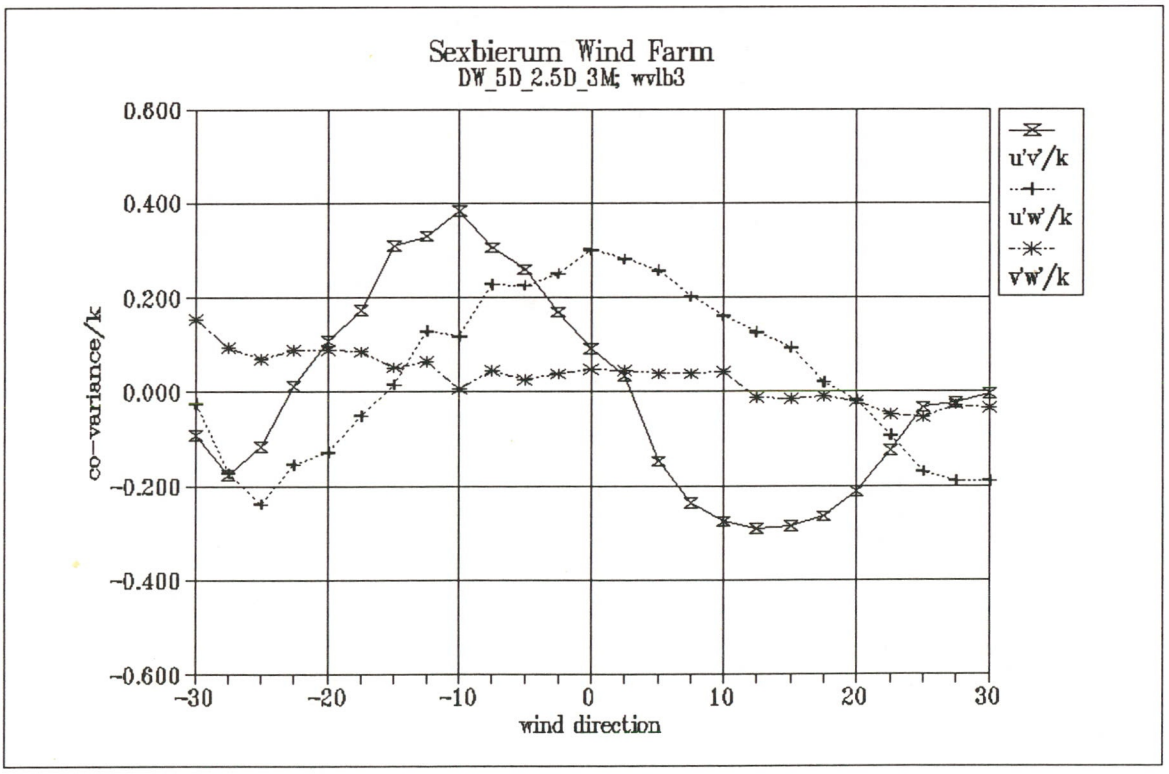

Figure 30 Non-dimensionalized shear stresses u'v'/k; u'w'/k; v'w'/k as a function of wind direction in the wind speed bin 5-10 m/s

A4.7 Sensor c2

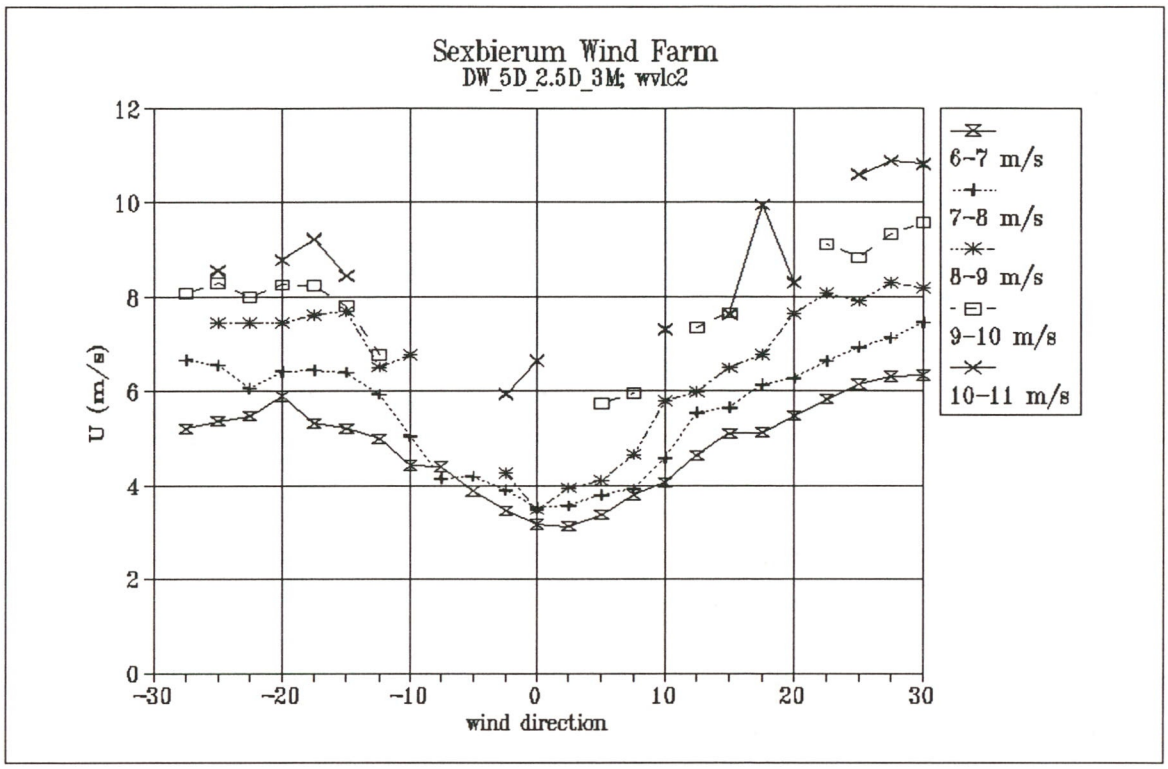

Figure 1 Horizontal wind speed U as a function of wind direction and wind speed bin

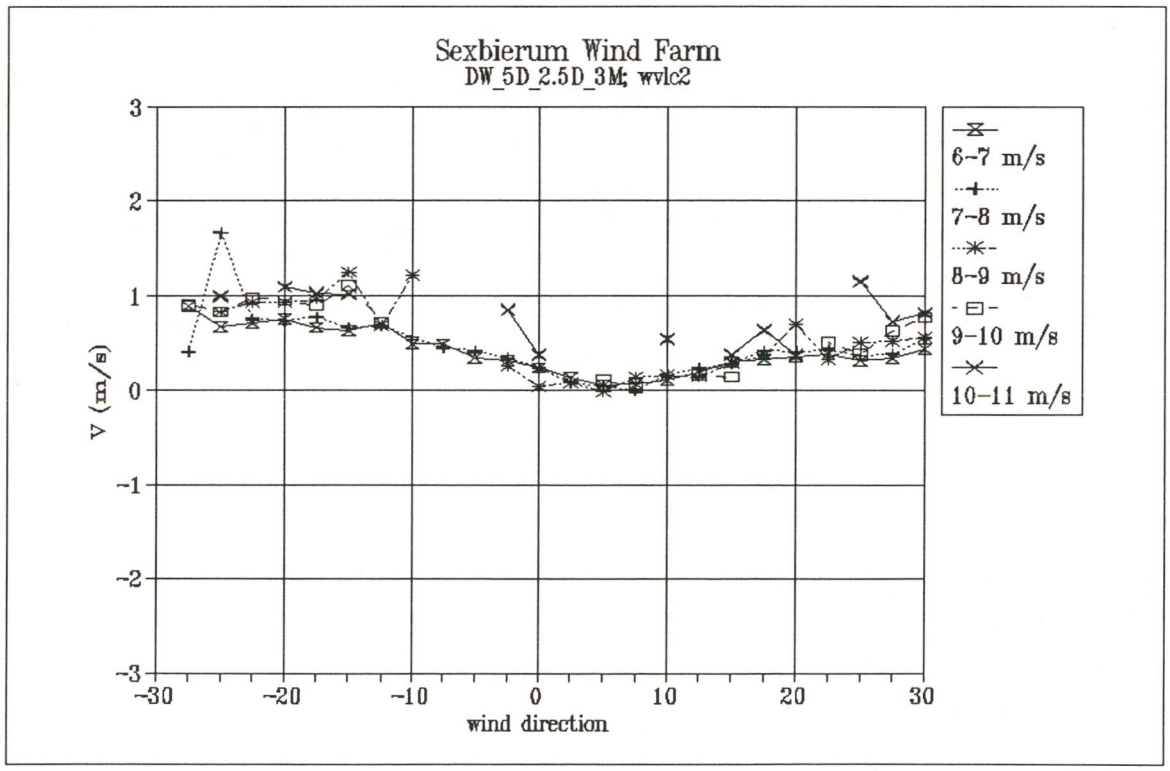

Figure 2 Lateral wind speed V as a function of wind direction and wind speed bin

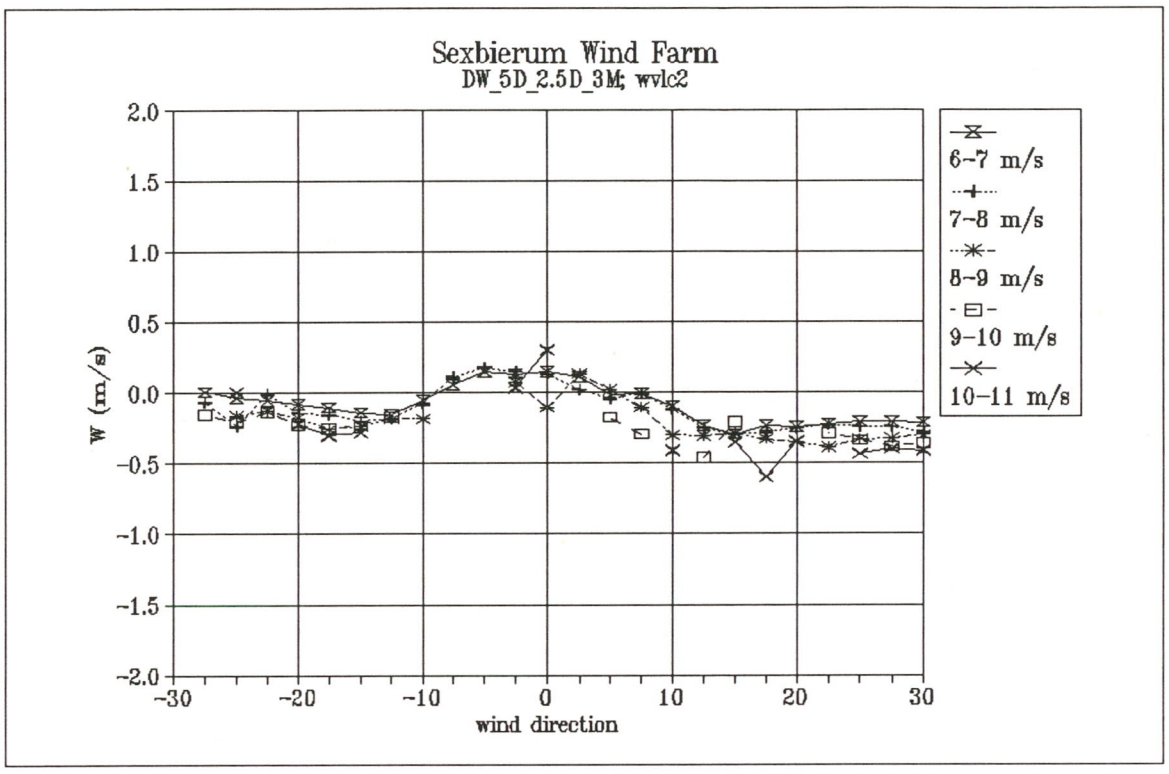

Figure 3 *Vertical wind speed W as a function of wind direction and wind speed bin*

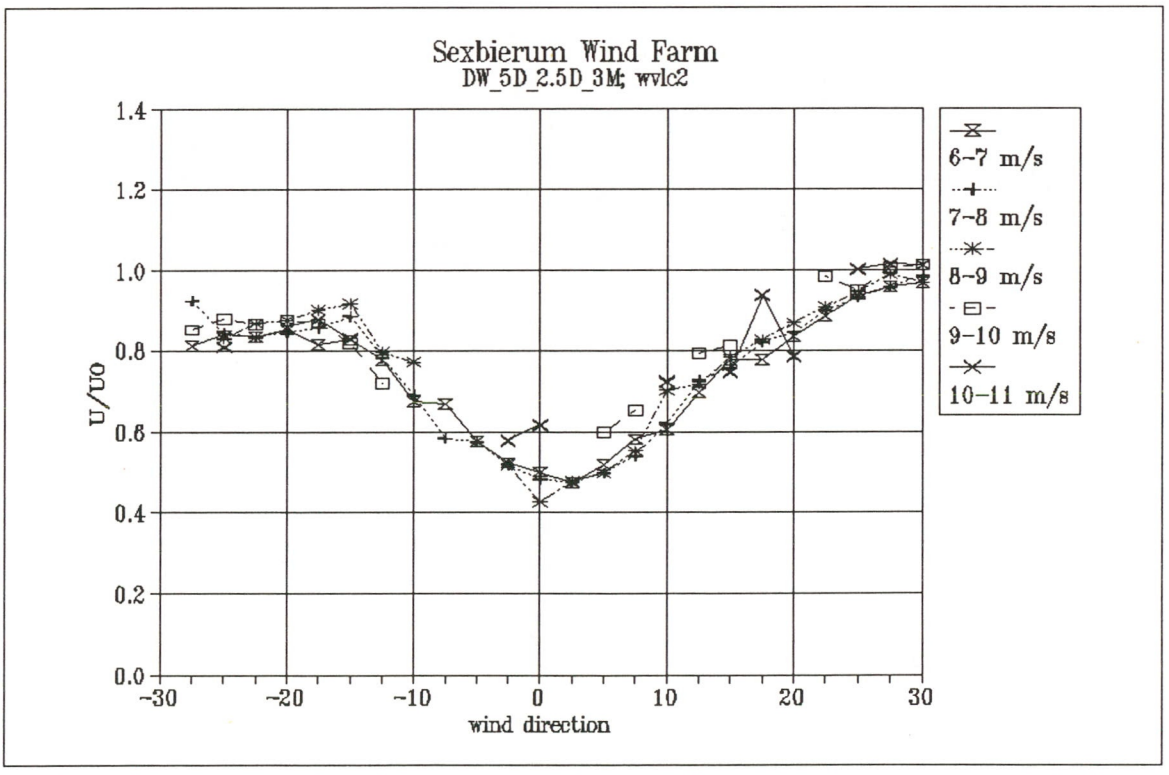

Figure 4 *Wake deficit U/U_0 as a function of wind direction and wind speed bin*

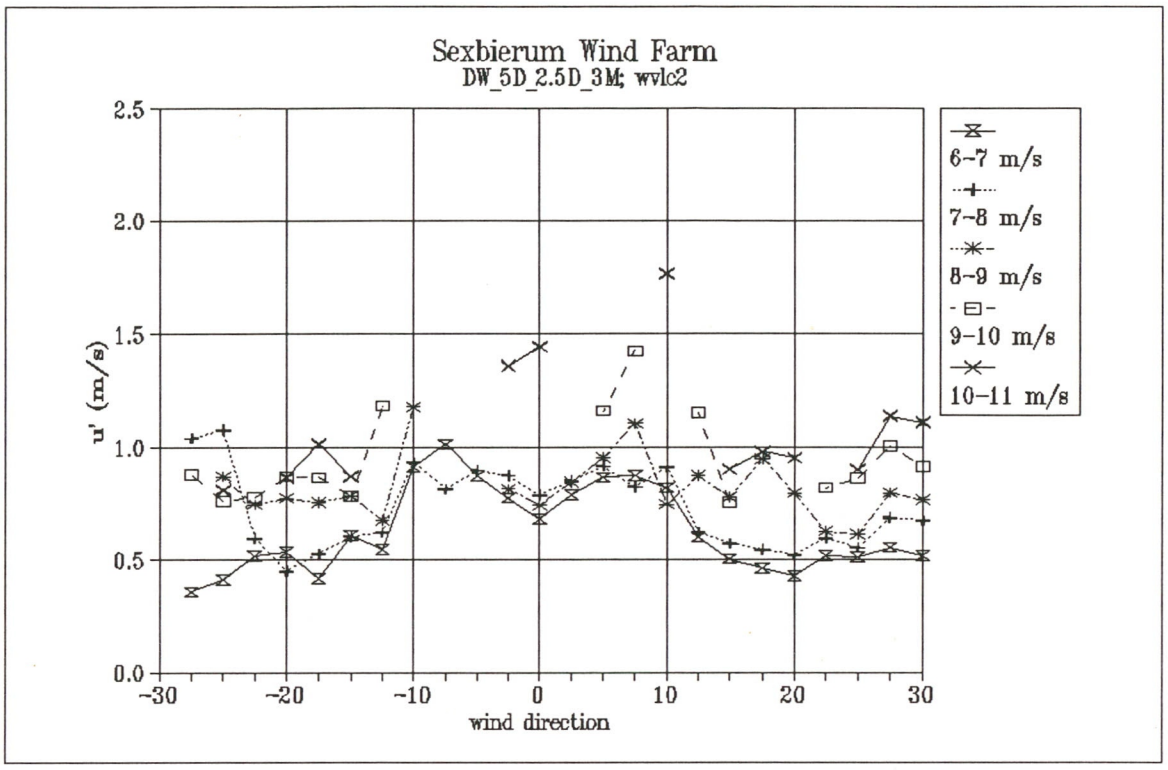

Figure 5 Longitudinal turbulent fluctuations u' as a function of wind direction and wind speed bin

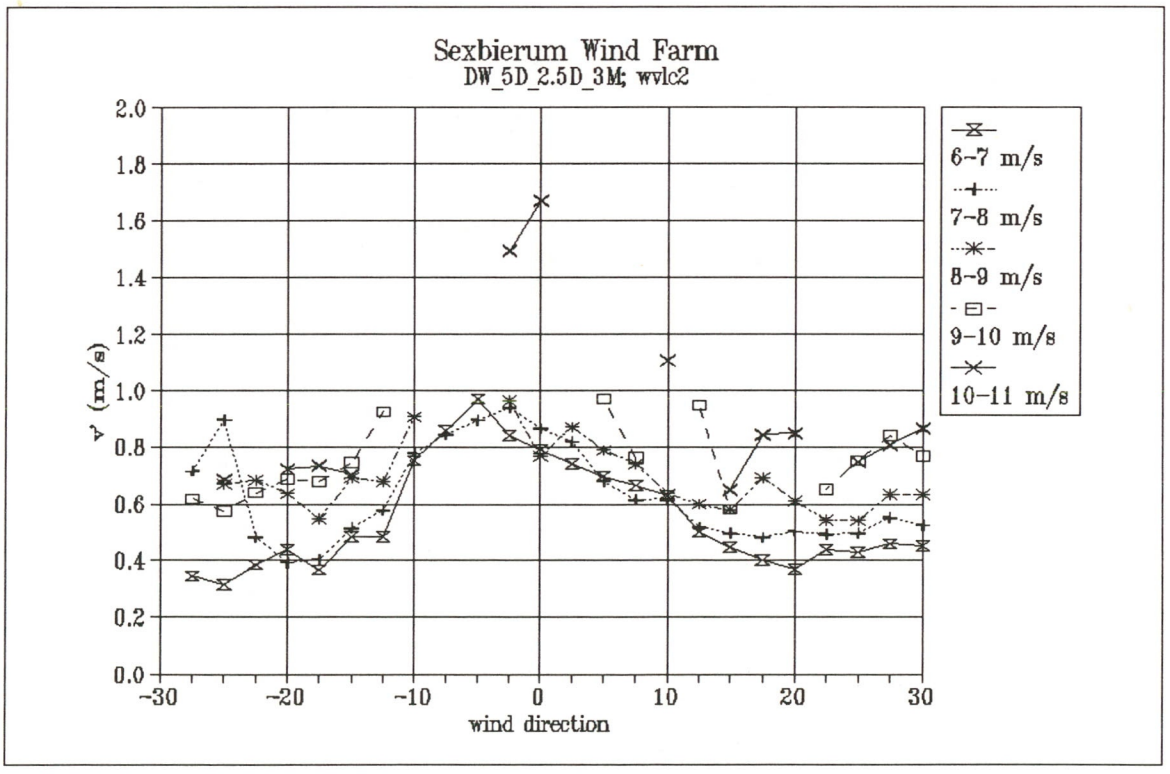

Figure 6 Lateral turbulent fluctuations v' as a function of wind direction and wind speed bin

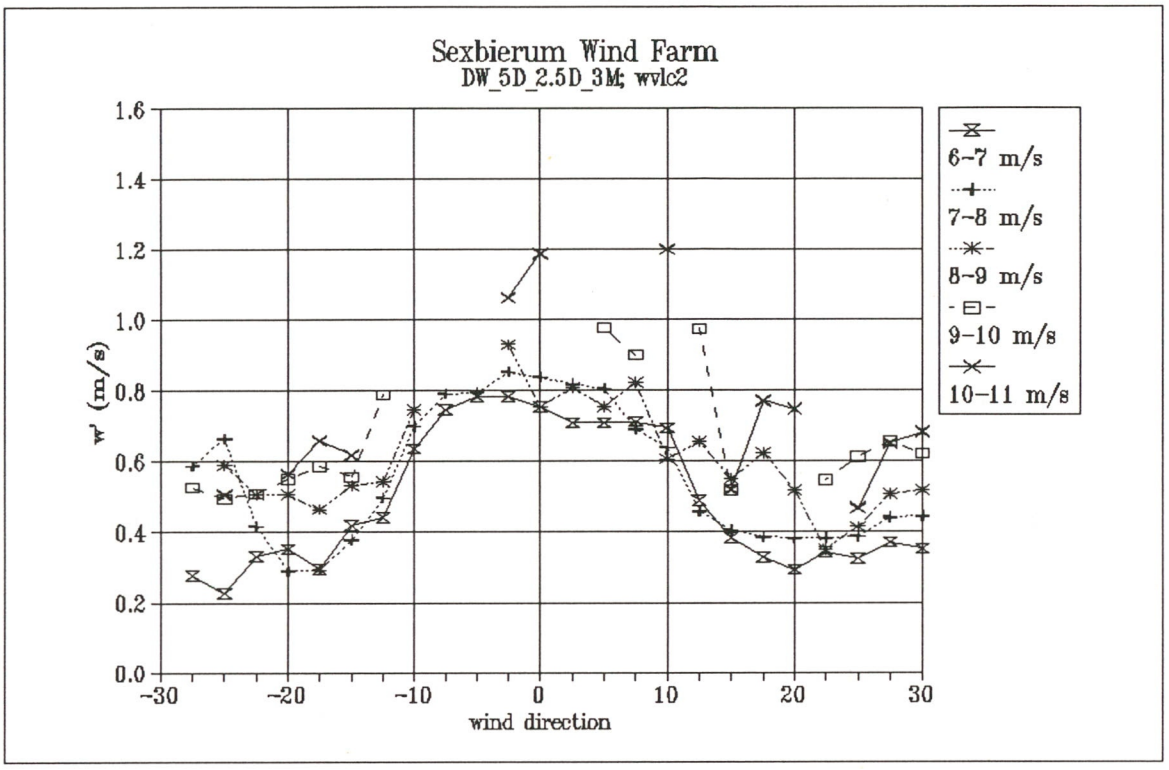

Figure 7 Vertical turbulent fluctuations w' as a function of wind direction and wind speed bin

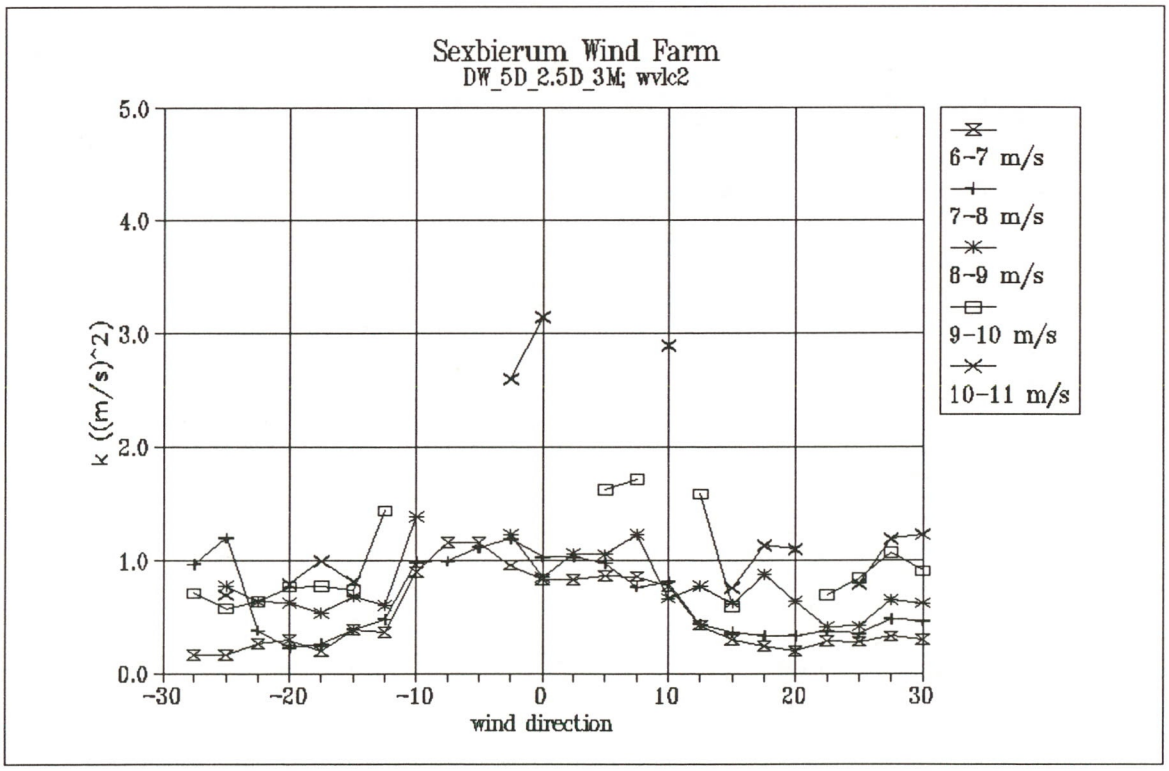

Figure 8 Turbulent kinetic energy per unit mass as a function of wind direction and wind speed bin

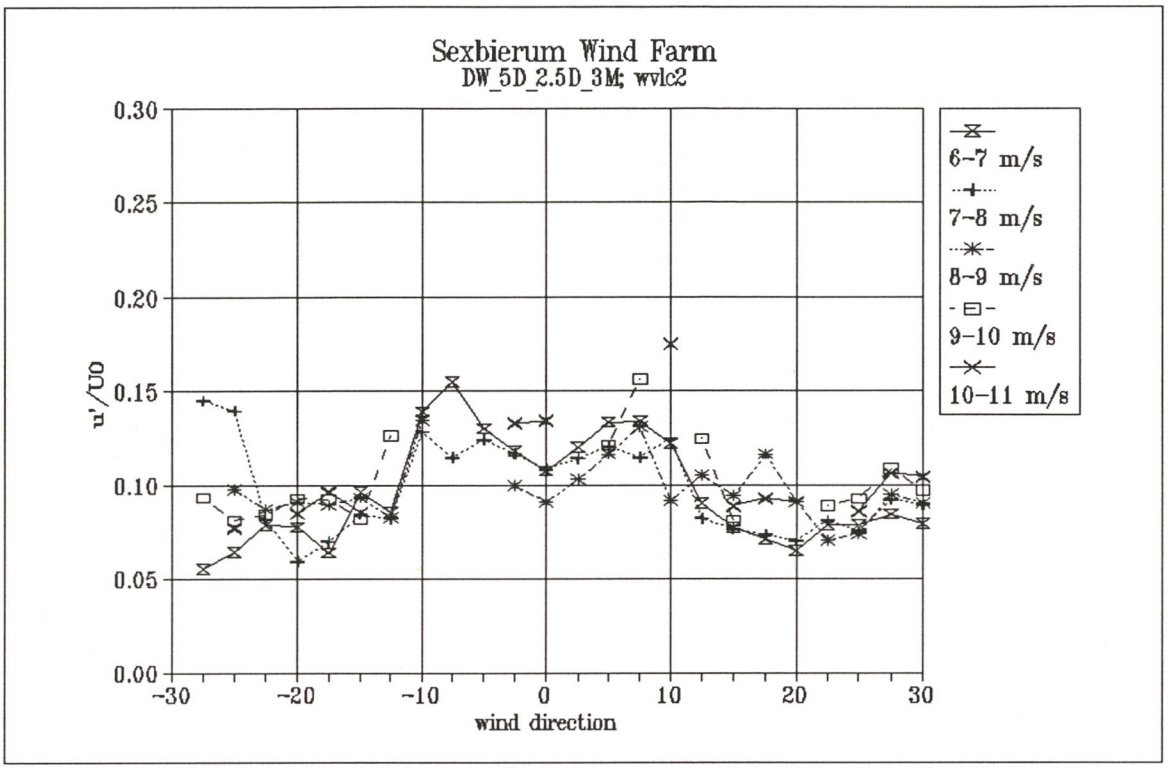

Figure 9 *Non-dimensionalized longitudinal turbulent fluctuations u'/U_0 as a function of wind direction and wind speed bin*

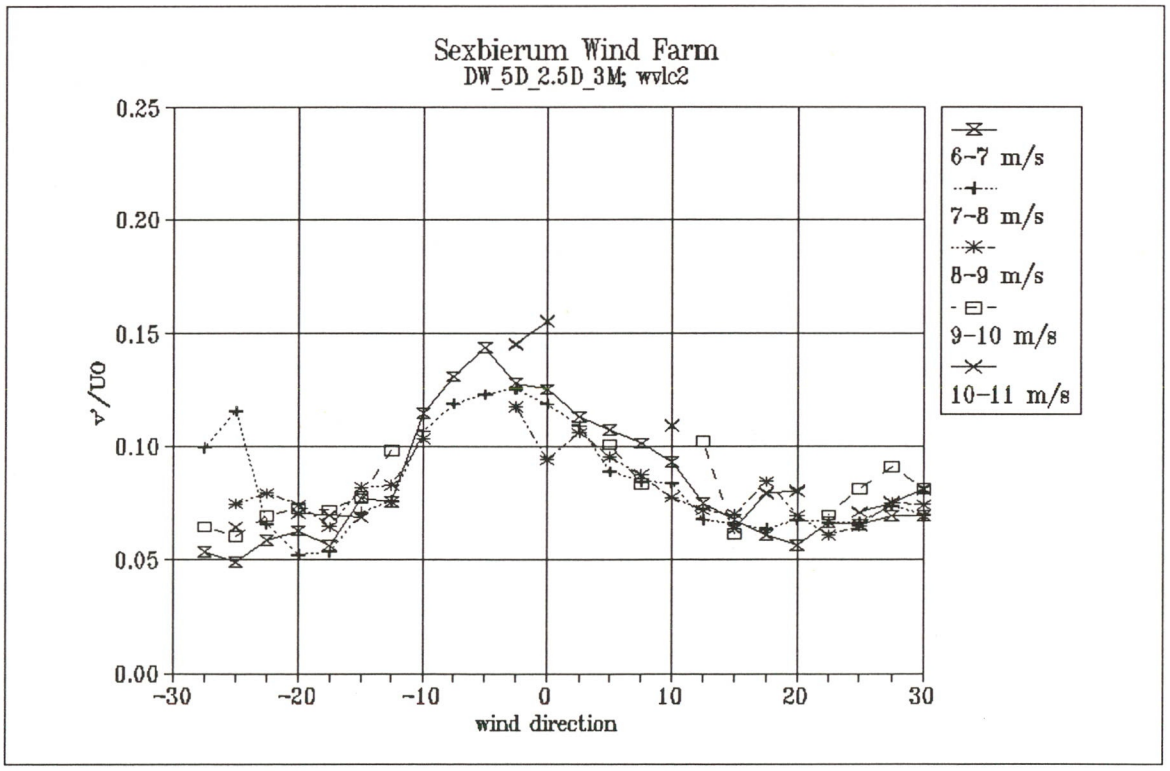

Figure 10 *Non-dimensionalized lateral turbulent fluctuations v'/U_0 as a function of wind direction and wind speed bin*

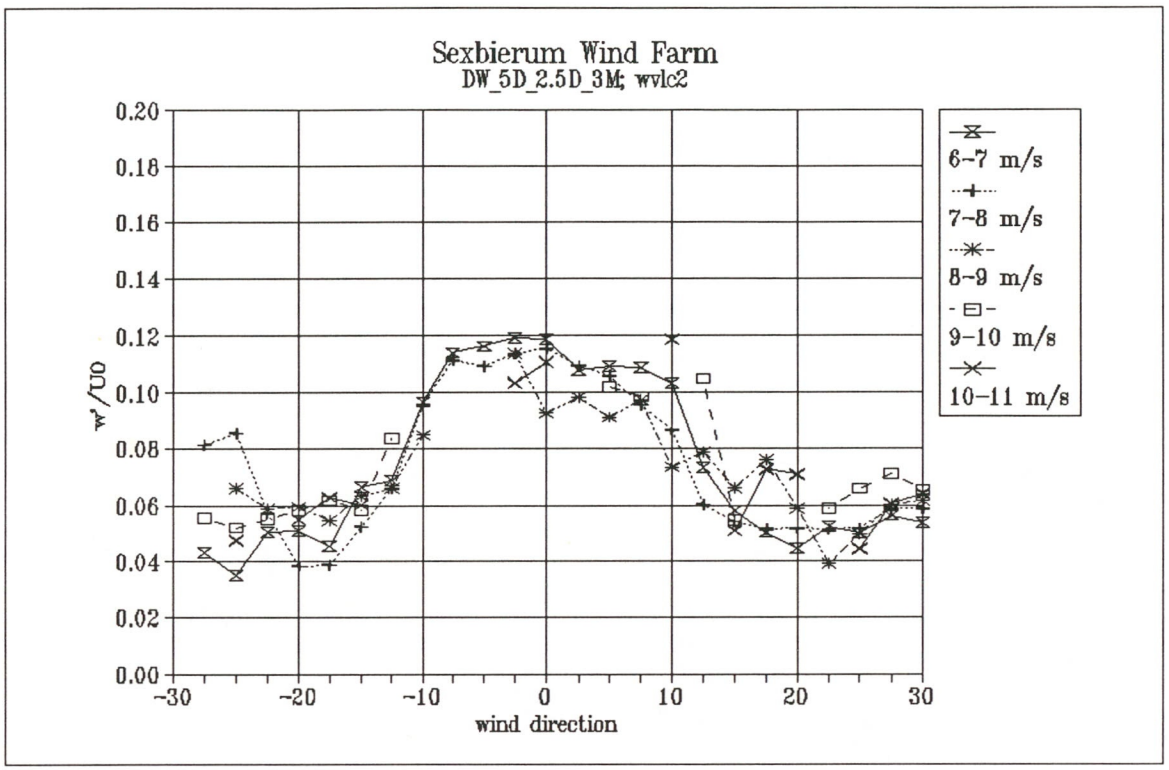

Figure 11 *Non-dimensionalized vertical turbulent fluctuations w'/U_0 as a function of wind direction and wind speed bin*

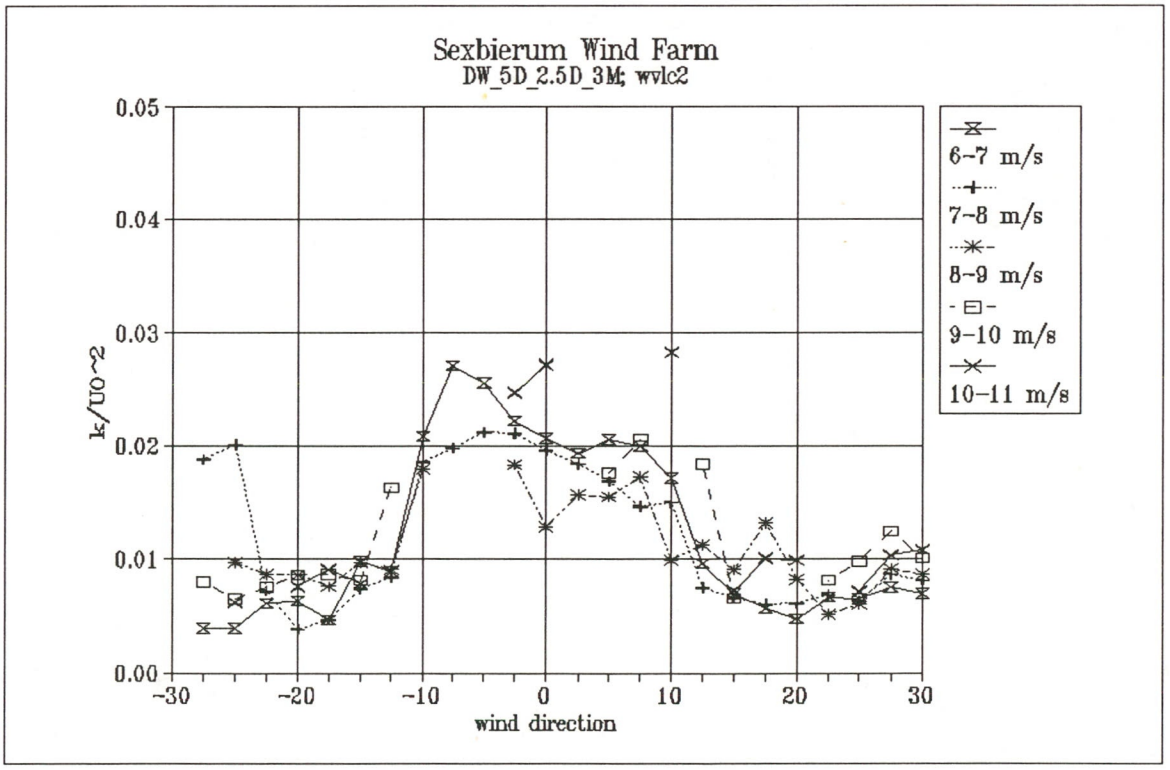

Figure 12 *Non-dimensionalized turbulent kinetic energy k/U_0^2 as a function of wind direction and wind speed bin*

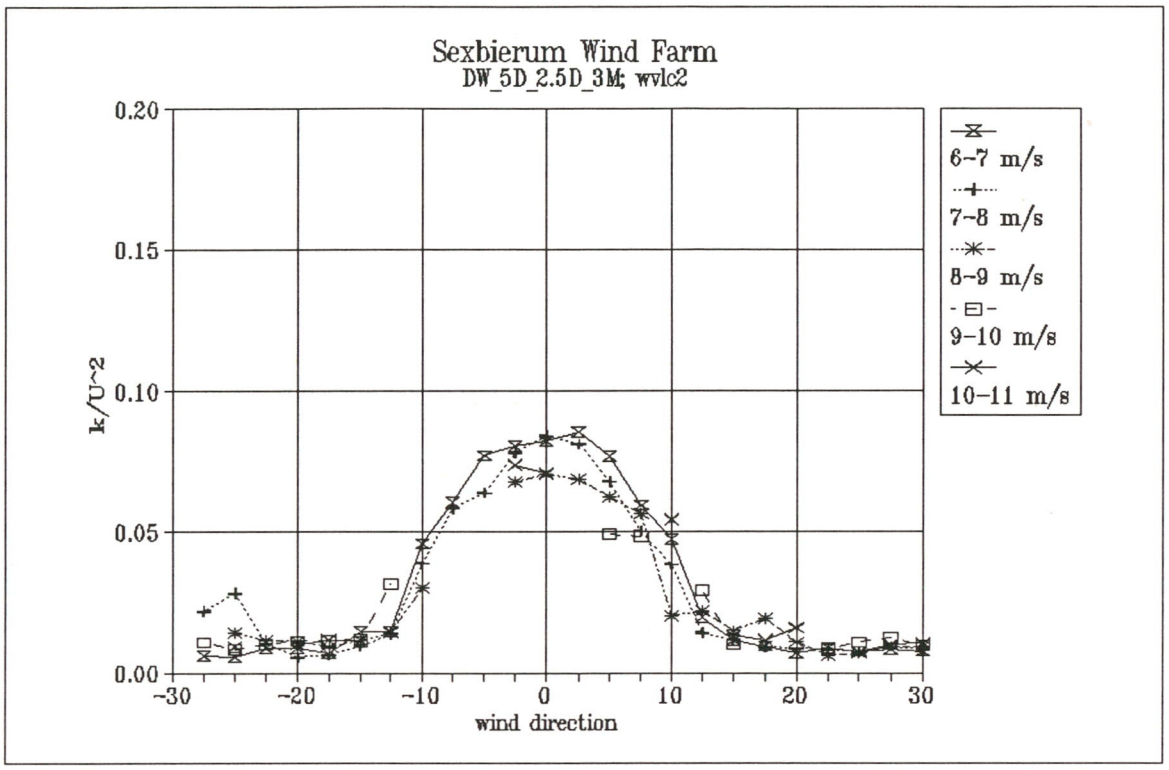

Figure 13 Non-dimensionalized turbulent kinetic energy k/U^2 as a function of wind direction and wind speed bin

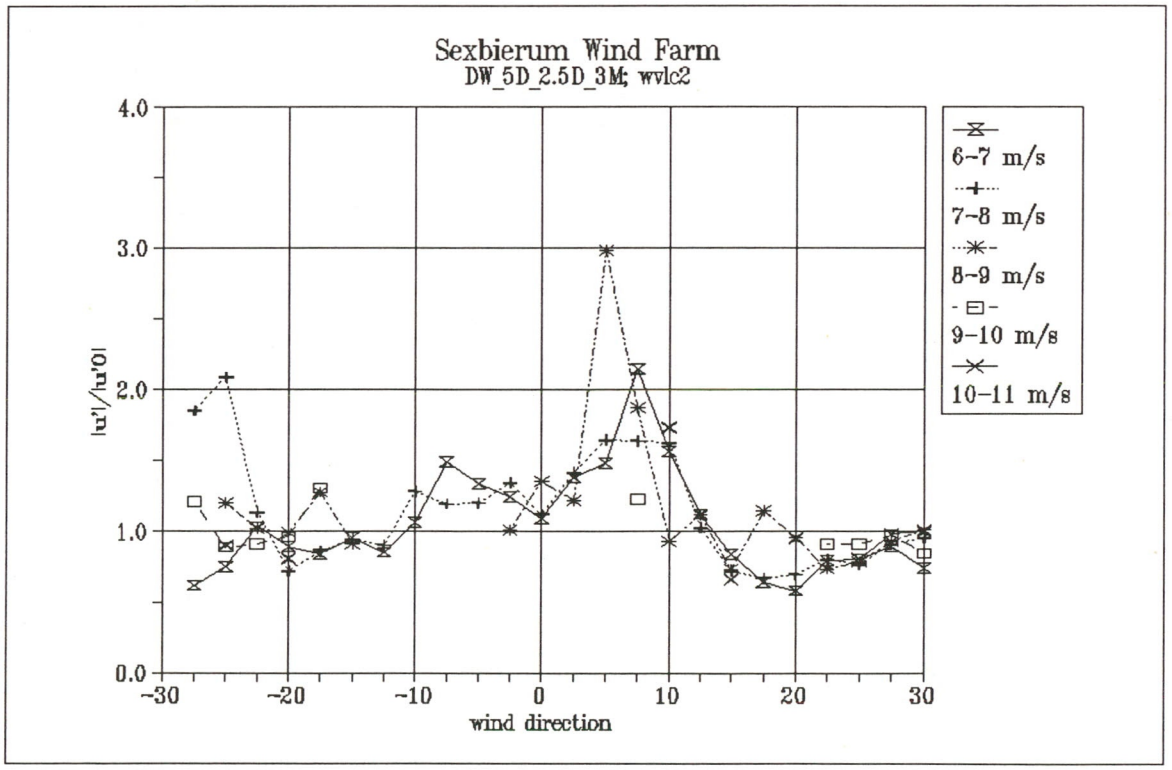

Figure 14 Longitudinal turbulence enhancement u'/u'_0 as a function of wind direction and wind speed bin

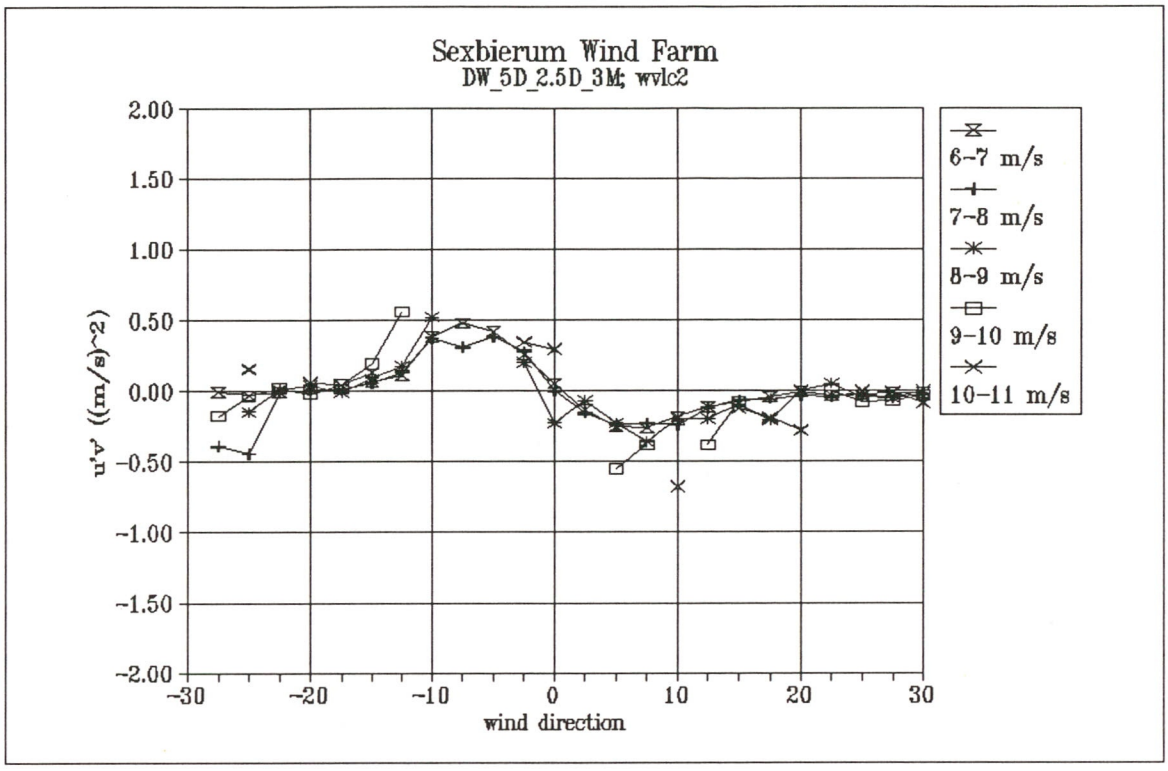

Figure 15 Shear stress u'v' as a function of wind direction and wind speed bin

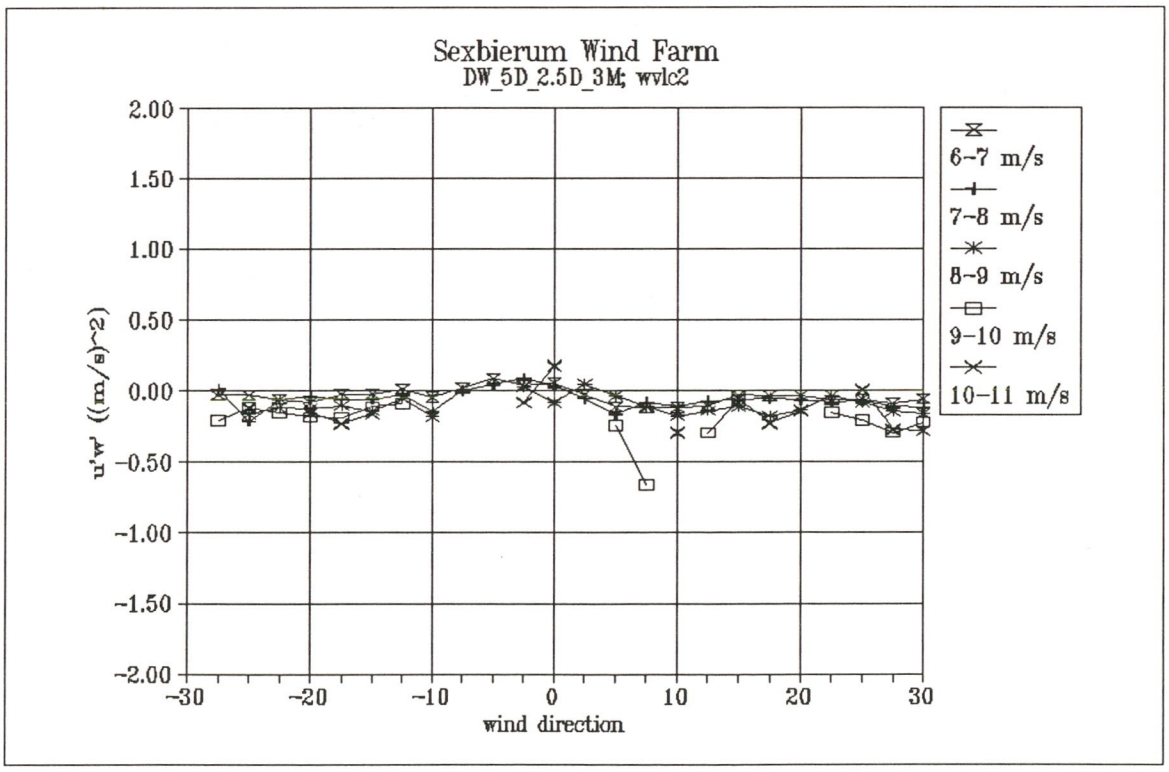

Figure 16 Shear stress u'w' as a function of wind direction and wind speed bin

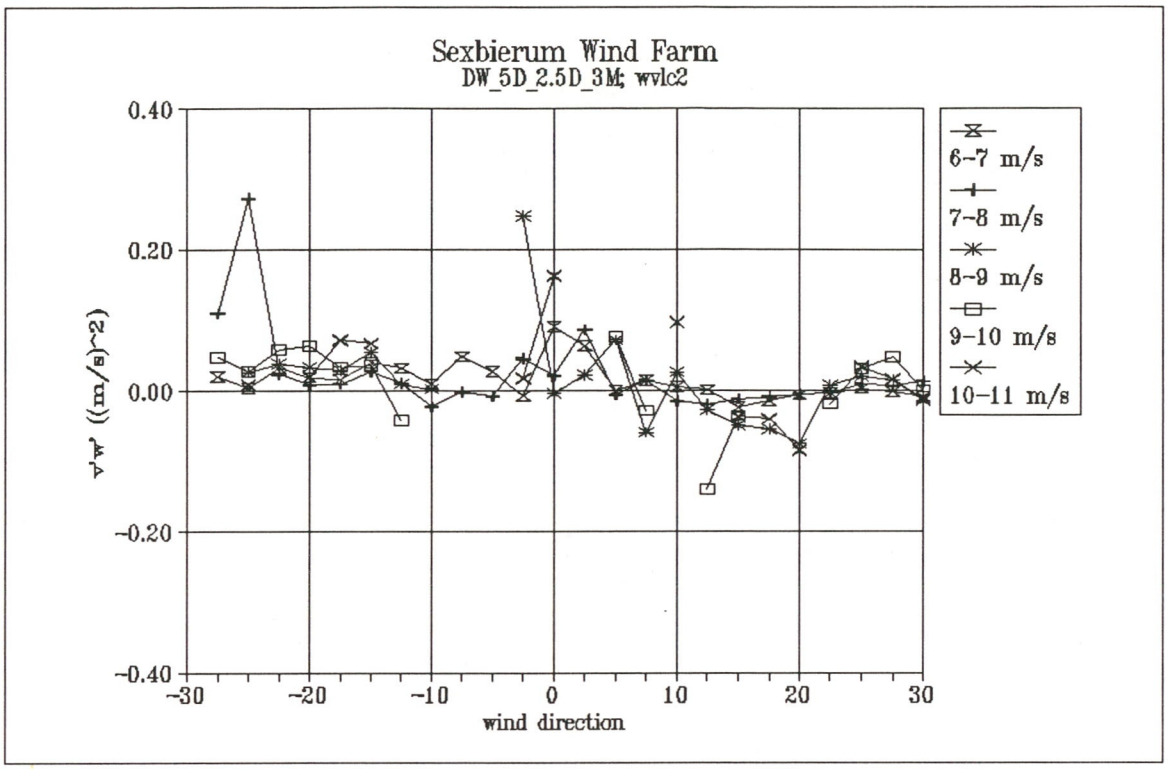

Figure 17 Shear stress v'w' as a function of wind direction and wind speed bin

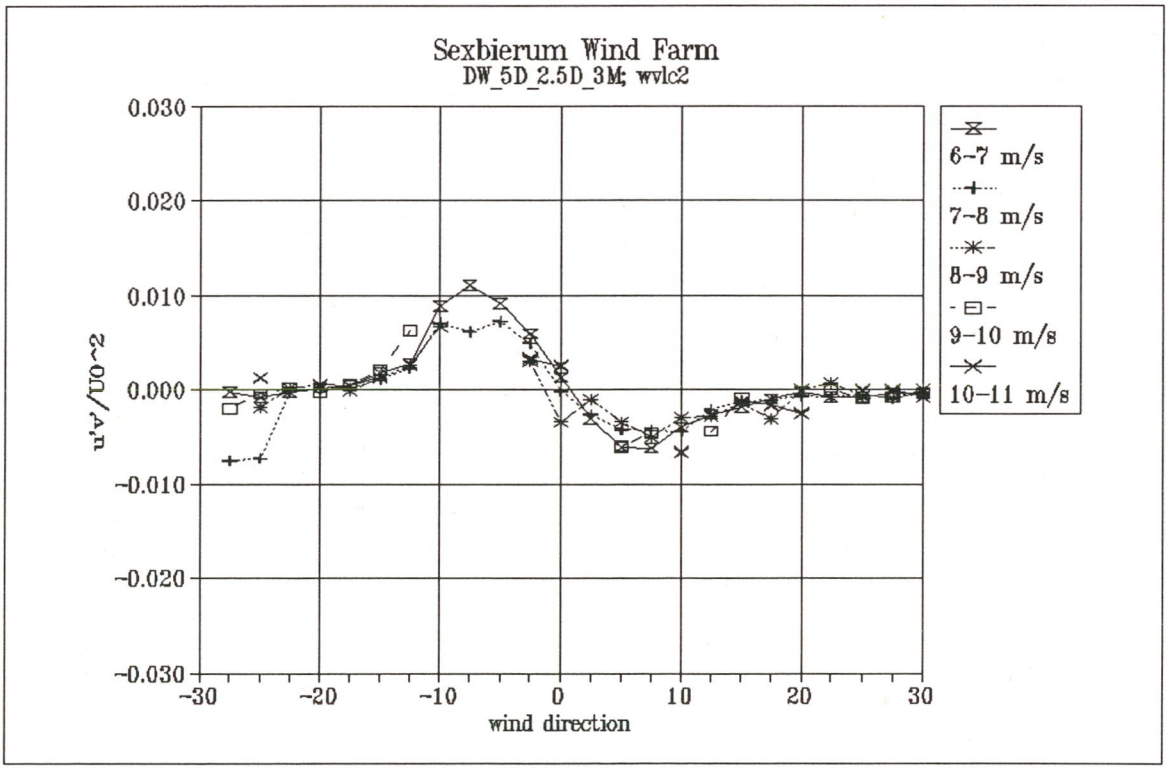

Figure 18 Non-dimensionalized shear stress $u'v'/U_0^2$ as a function of wind direction and wind speed bin

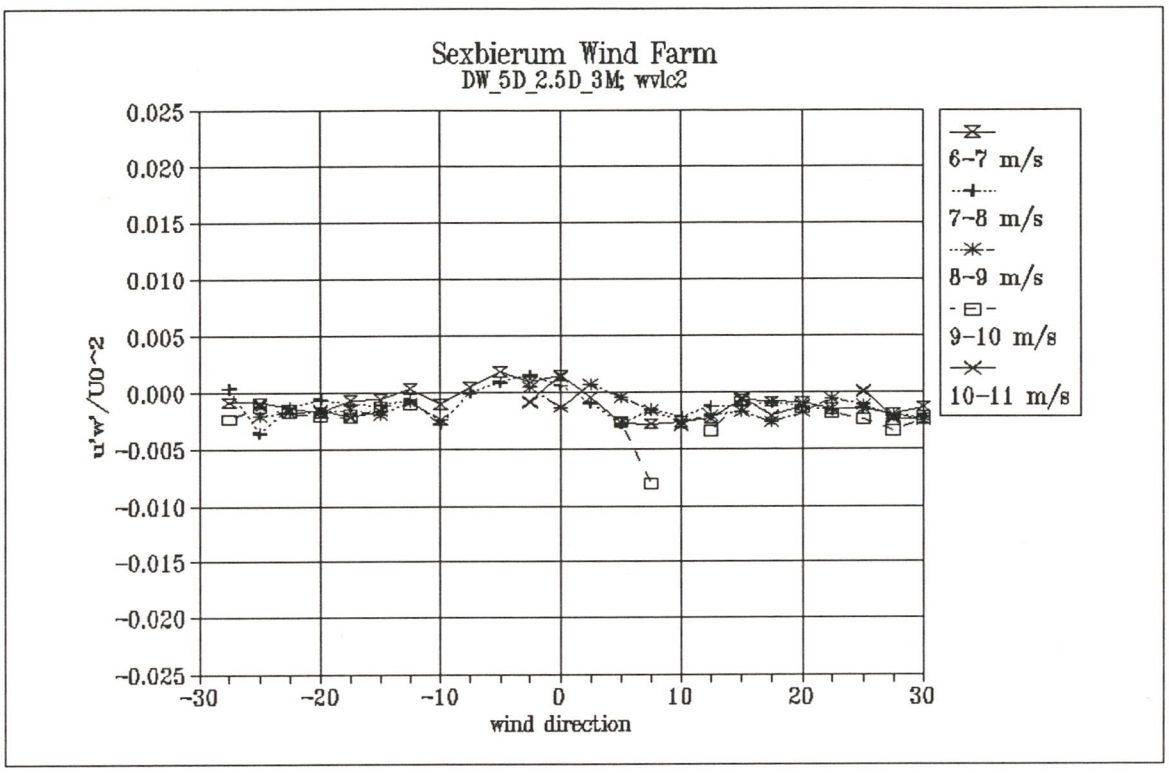

Figure 19 Non-dimensionalized shear stress $u'w'/U_0^2$ as a function of wind direction and wind speed bin

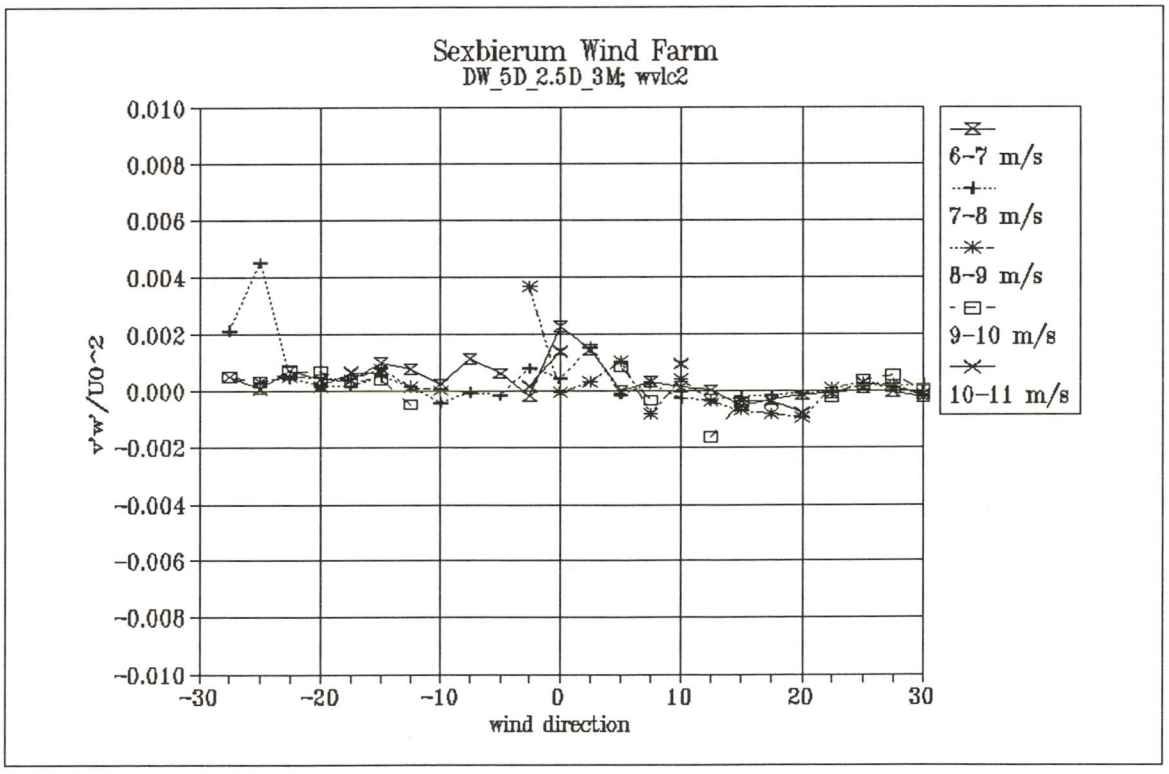

Figure 20 Non-dimensionalized shear stress $v'w'/U_0^2$ as a function of wind direction and wind speed bin

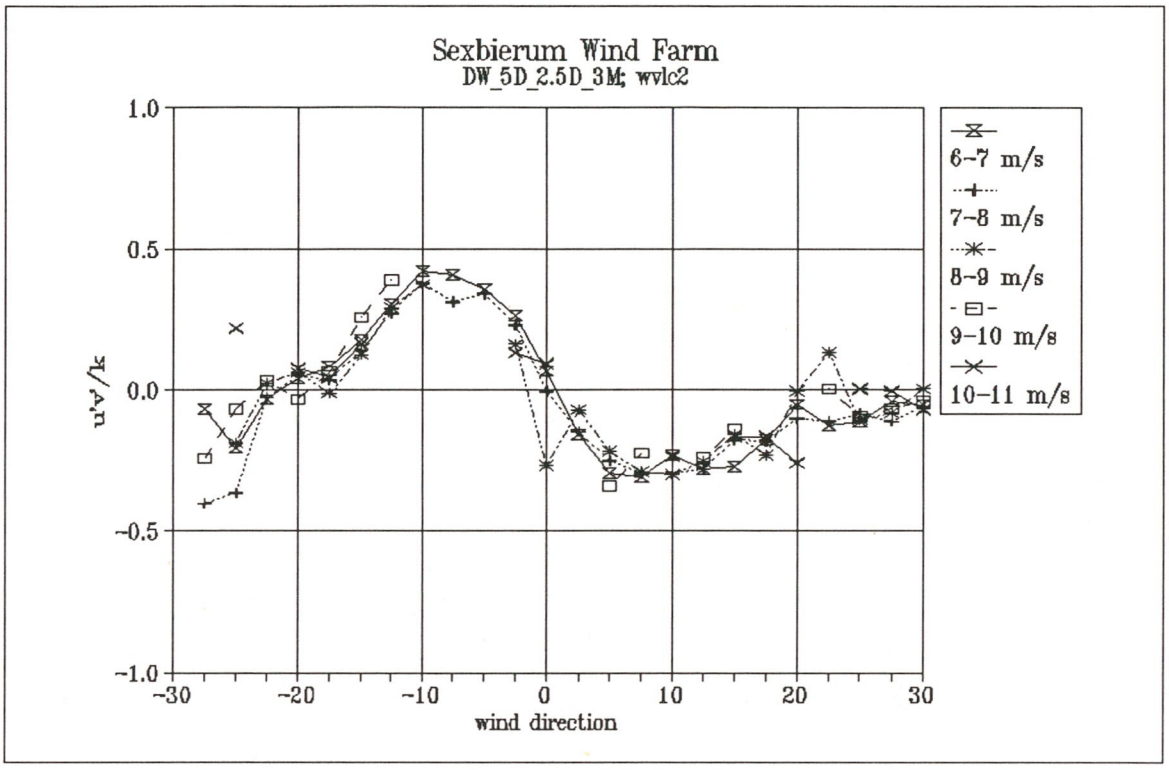

Figure 21 Non-dimensionalized shear stress u'v'/k as a function of wind direction and wind speed bin

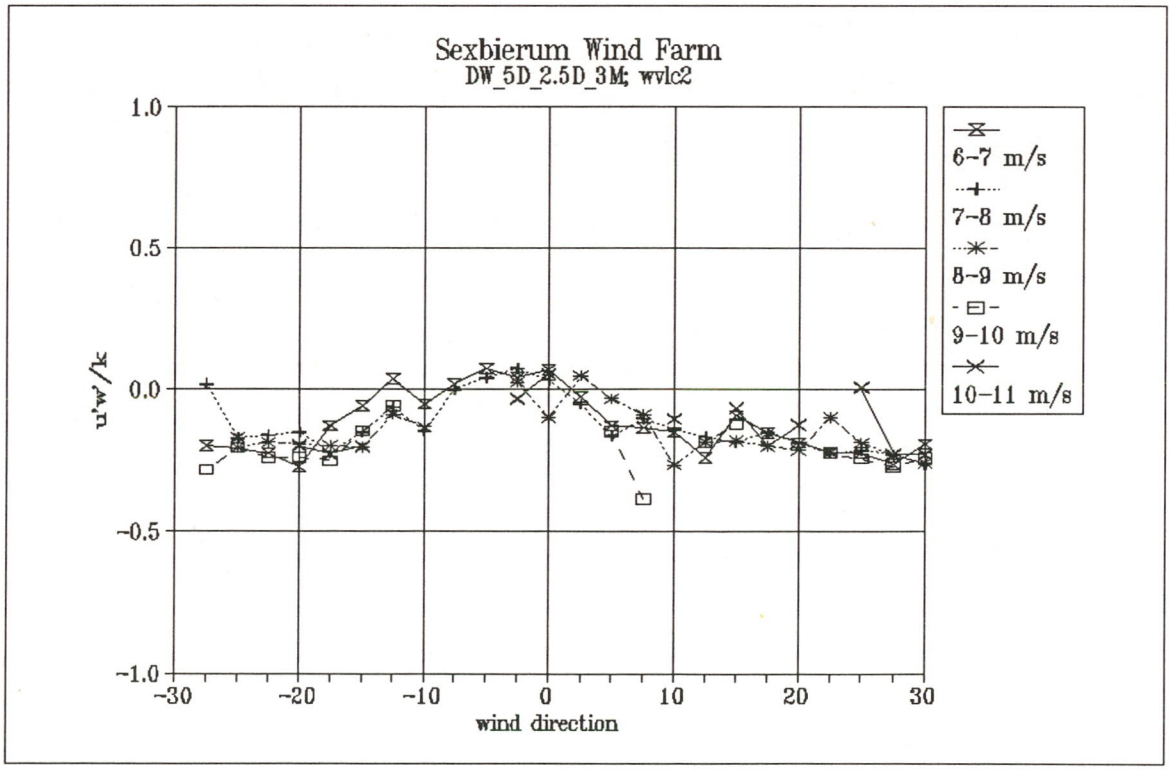

Figure 22 Non-dimensionalized shear stress u'w'/k as a function of wind direction and wind speed bin

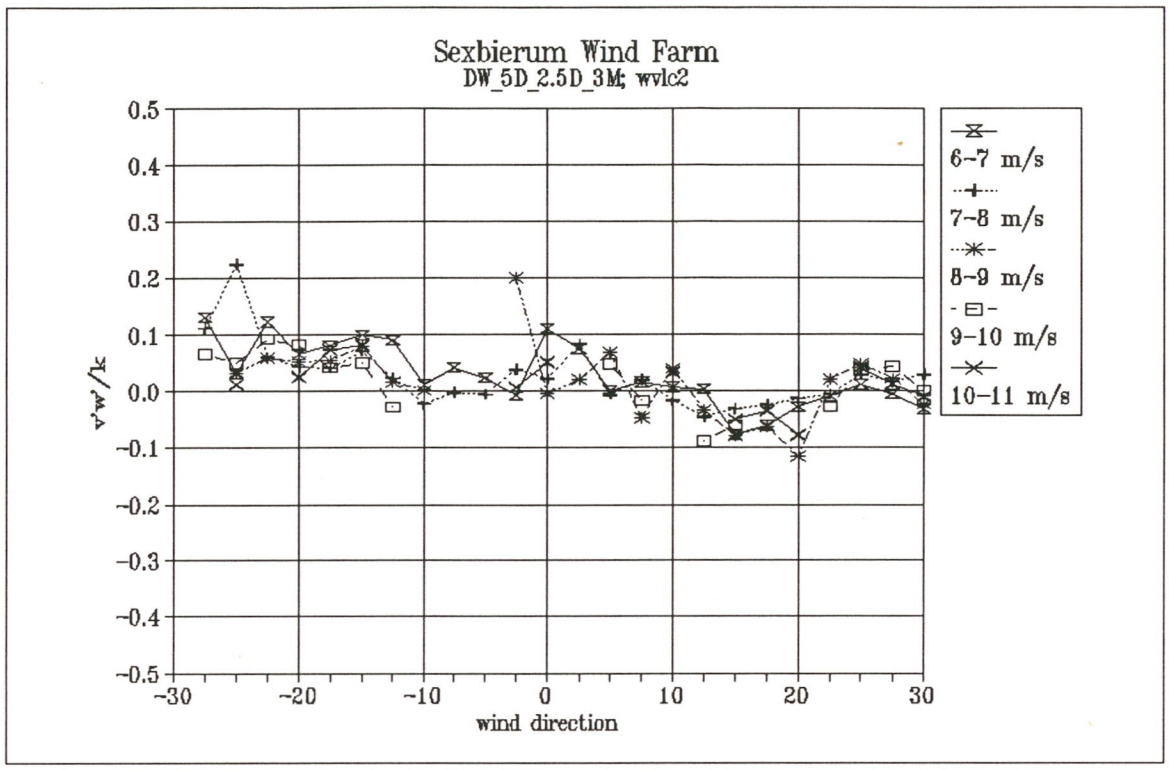

Figure 23 Non-dimensionalized shear stress v'w'/k as a function of wind direction and wind speed bin

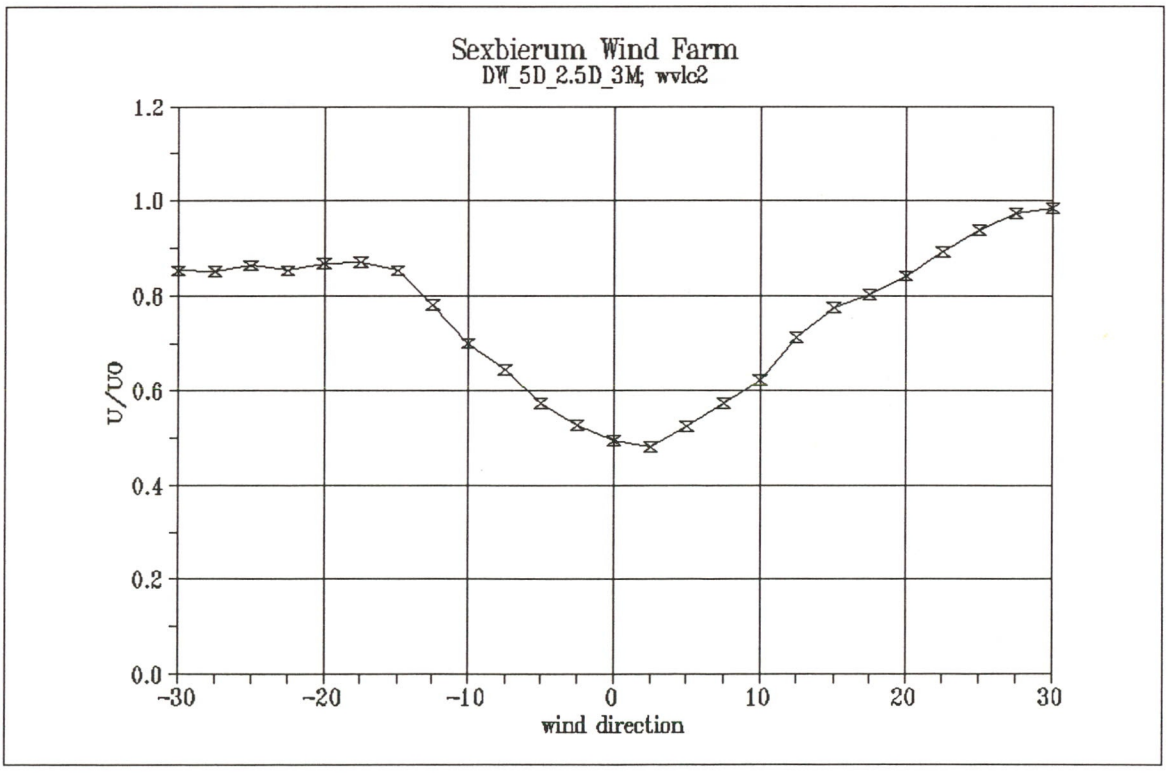

Figure 24 Wake deficit U/U_0 as a function of wind direction in the wind speed bin 5-10 m/s

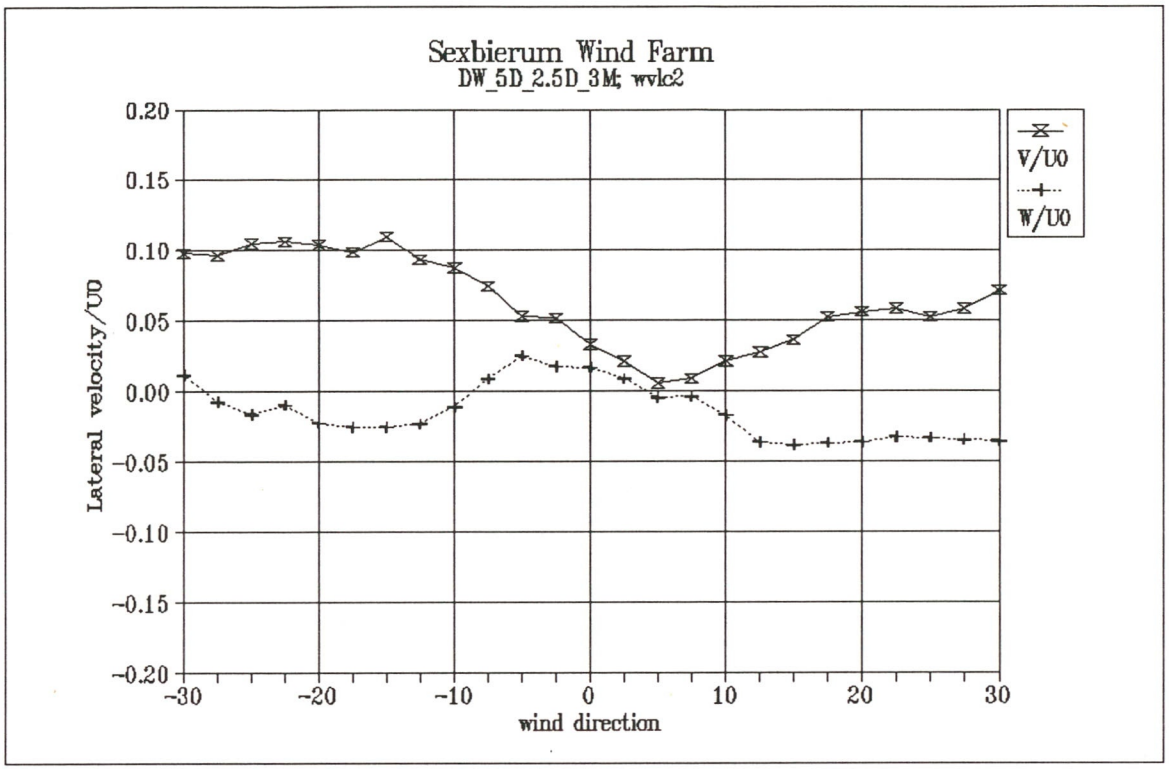

Figure 25 Lateral and vertical wind speed V/U_0 and W/U_0 as a function of wind direction in the wind speed bin 5-10 m/s

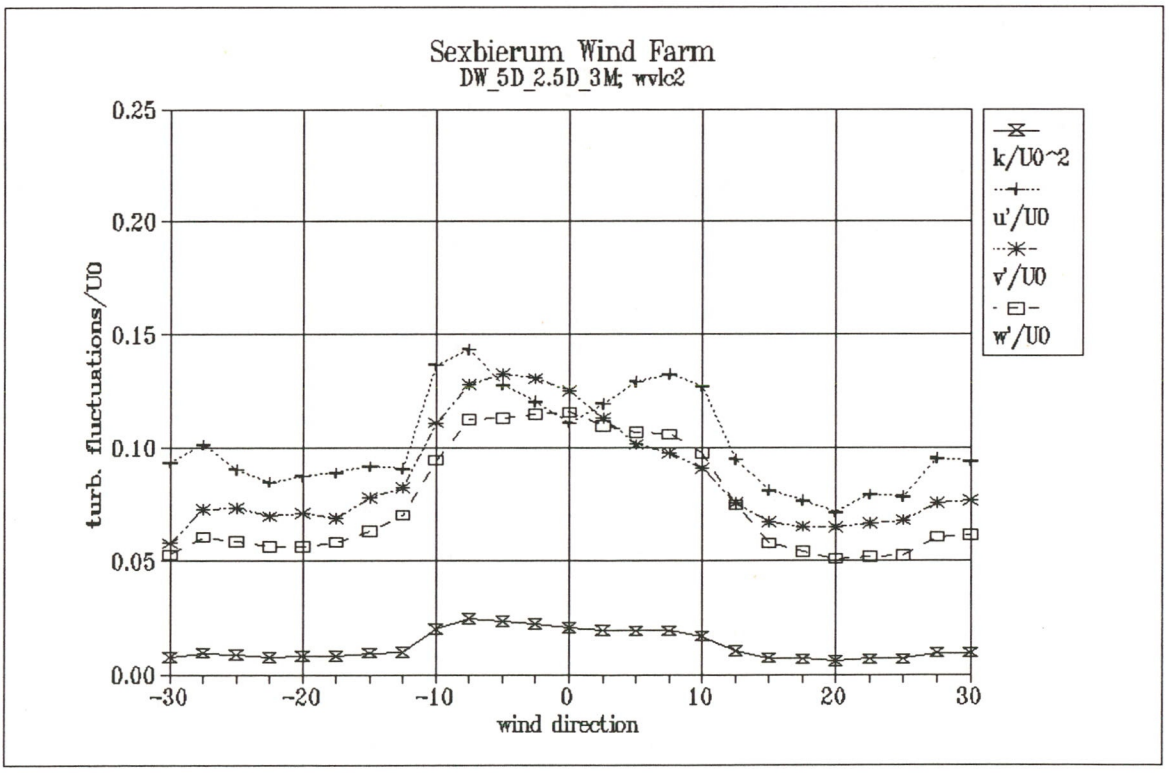

Figure 26 Turbulent fluctuations as a function of wind direction in the wind speed bin 5-10 m/s, non-dimensionalized with U_0

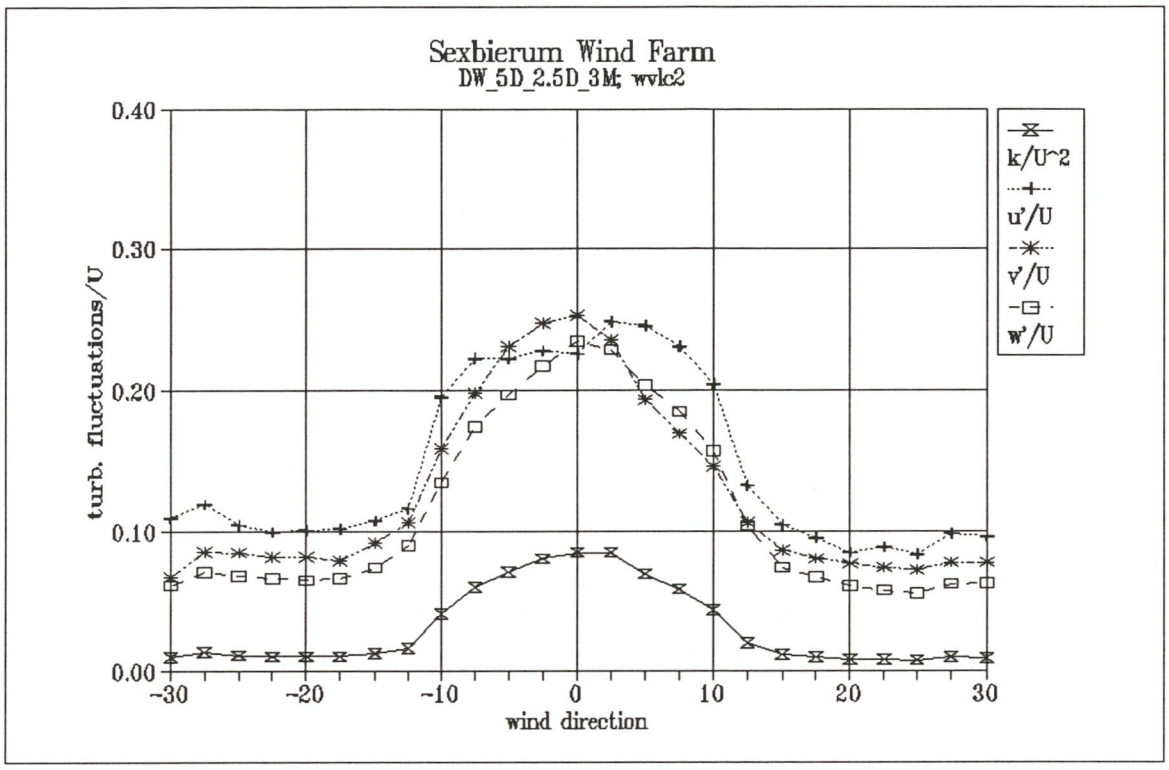

Figure 27 Turbulent fluctuations as a function of wind direction in the wind speed bin 5-10 m/s, non-dimensionalized with U

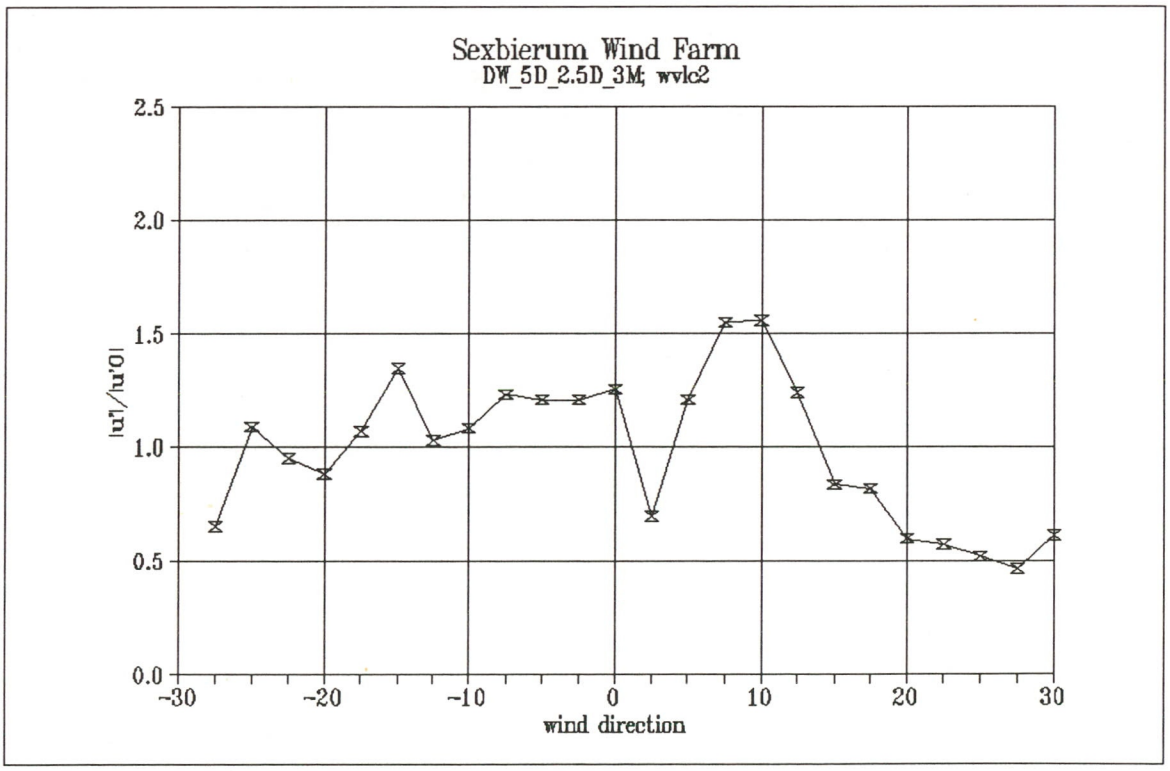

Figure 28 Longitudinal turbulence enhancement u'/u'_0 as a function of wind direction in the wind speed bin 5-10 m/s

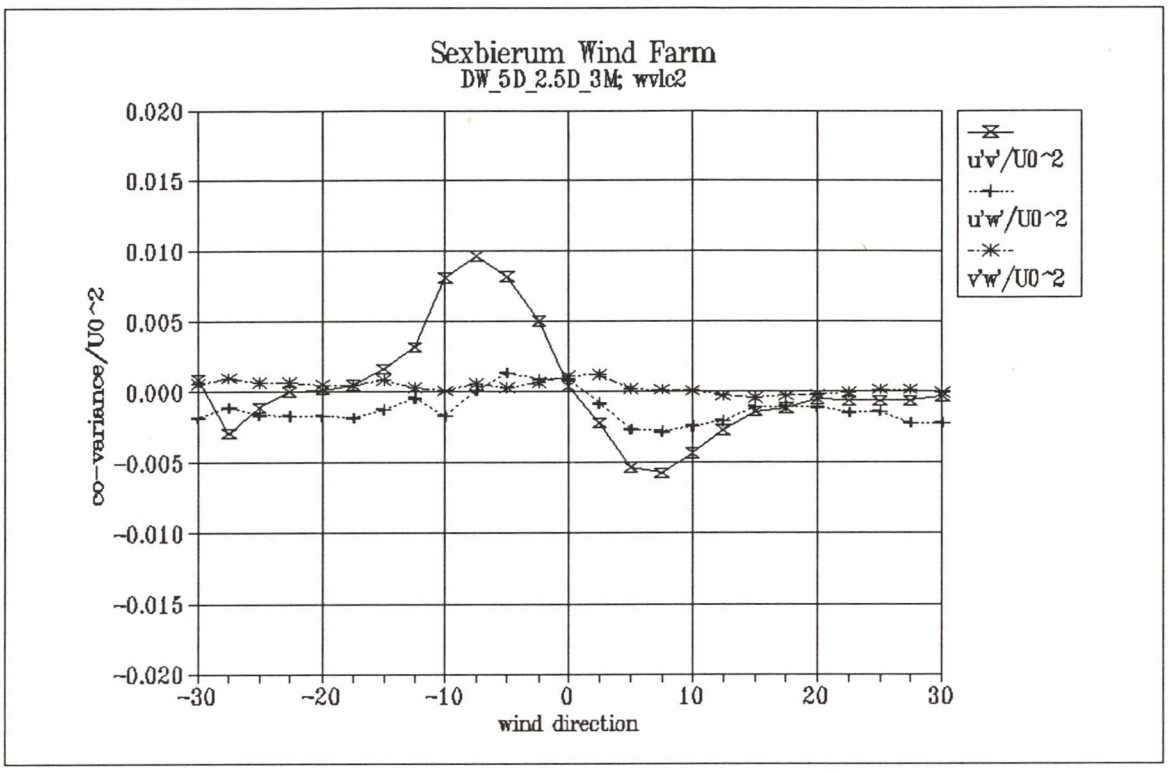

Figure 29 Non-dimensionalized shear stresses $u'v'/U_0^2$; $u'w'/U_0^2$; $v'w'/U_0^2$ as a function of wind direction in the wind speed bin 5-10 m/s

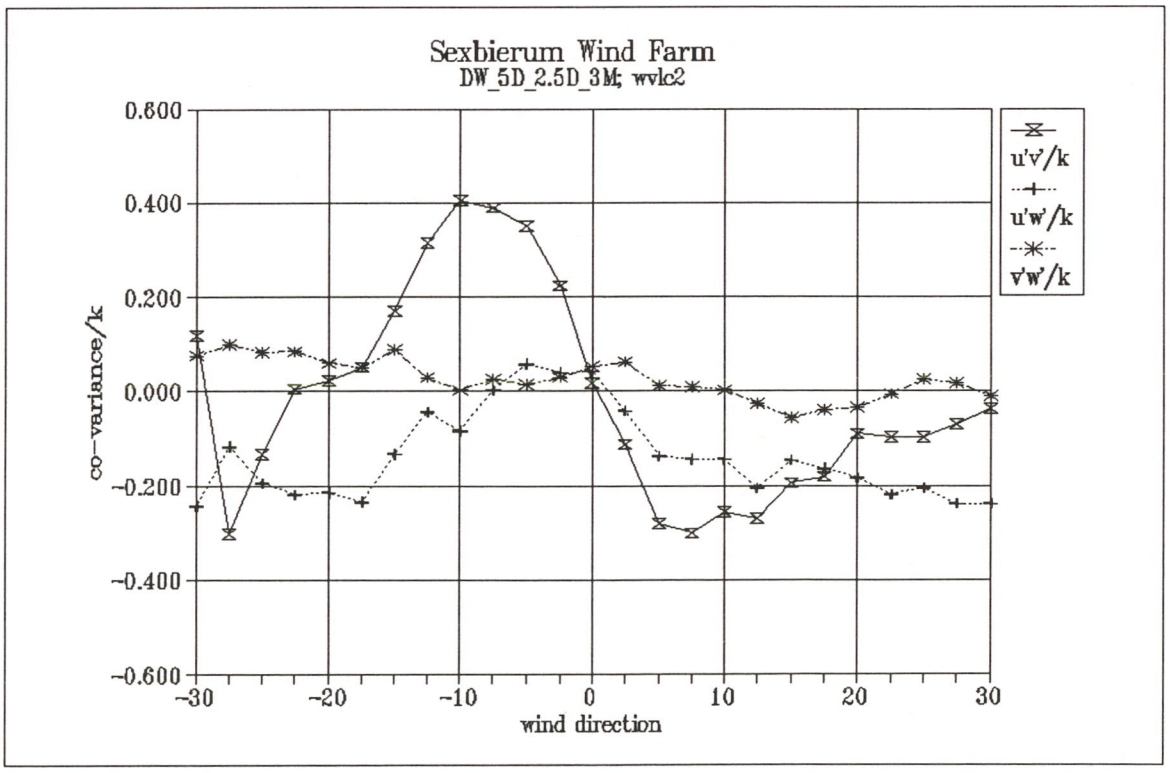

Figure 30 Non-dimensionalized shear stresses u'v'/k; u'w'/k; v'w'/k as a function of wind direction in the wind speed bin 5-10 m/s

A4.8 Vertical profiles

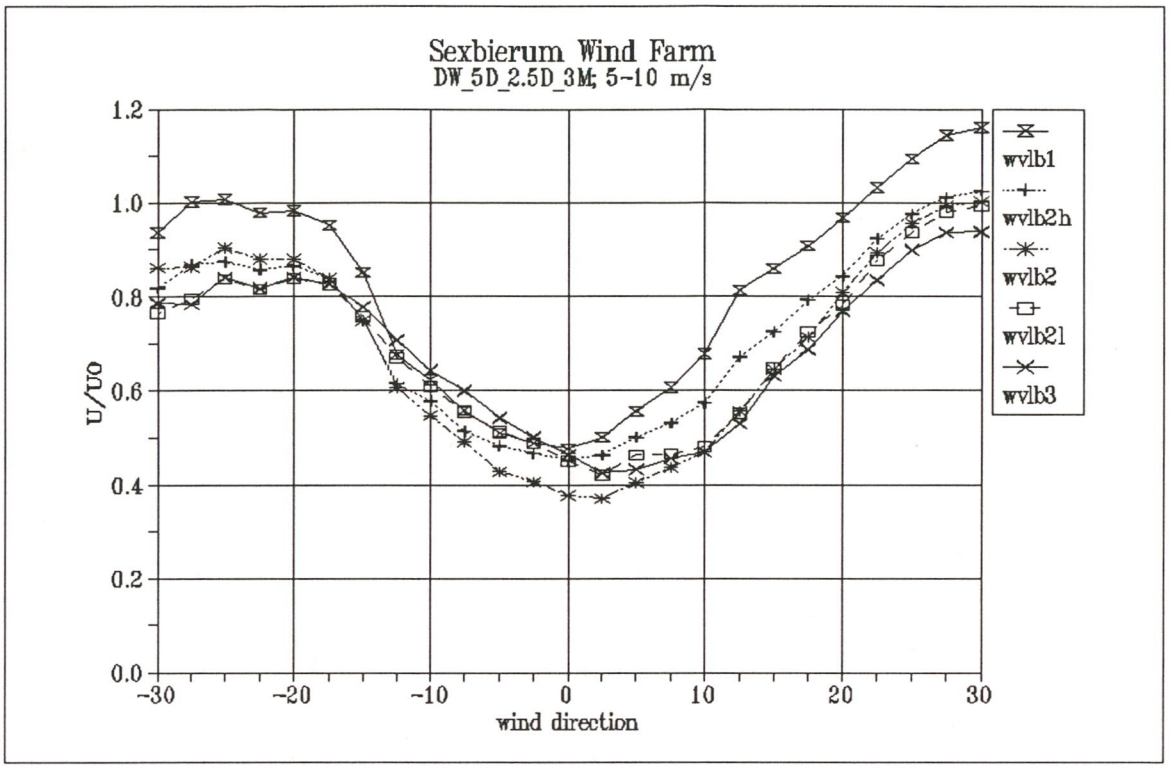

Figure 1 Wake deficit U/U_0 as a function of wind direction in the wind speed bin 5-10 m/s

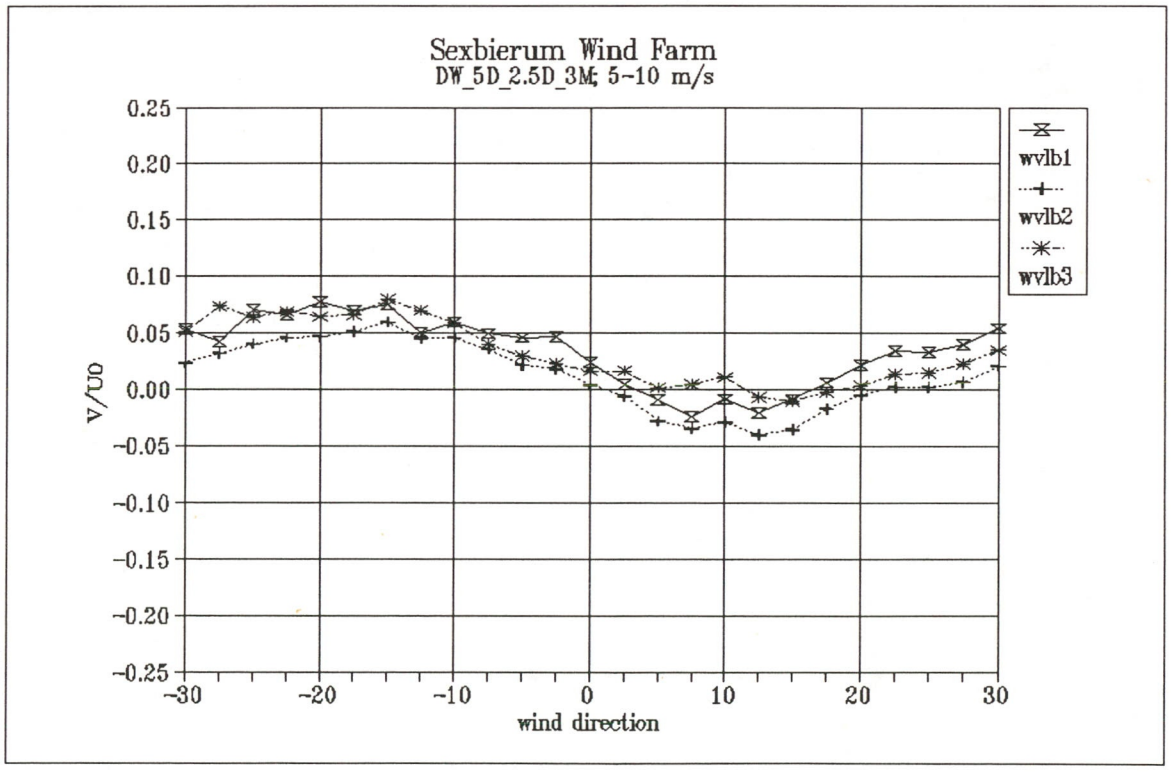

Figure 2 Lateral wind speed V/U_0 as a function of wind direction in the wind speed bin 5-10 m/s

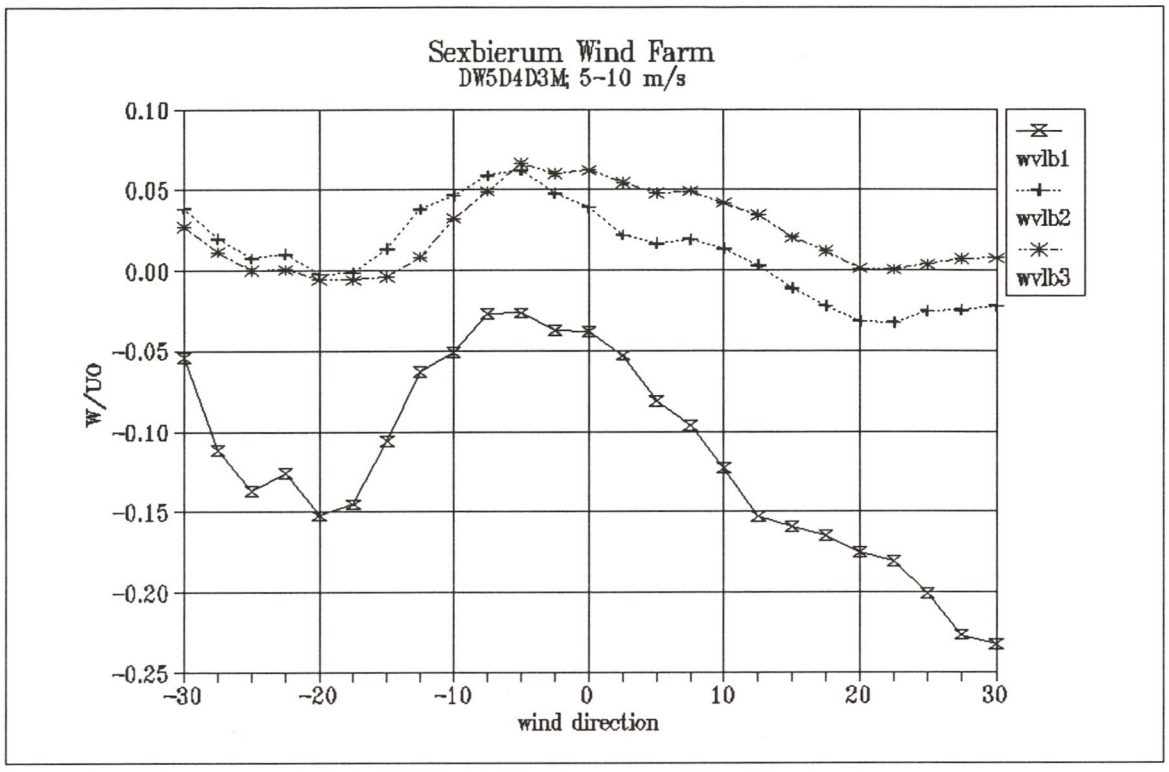

Figure 3 *Vertical wind speed W/U_0 as a function of wind direction in the wind speed bin 5-10 m/s*

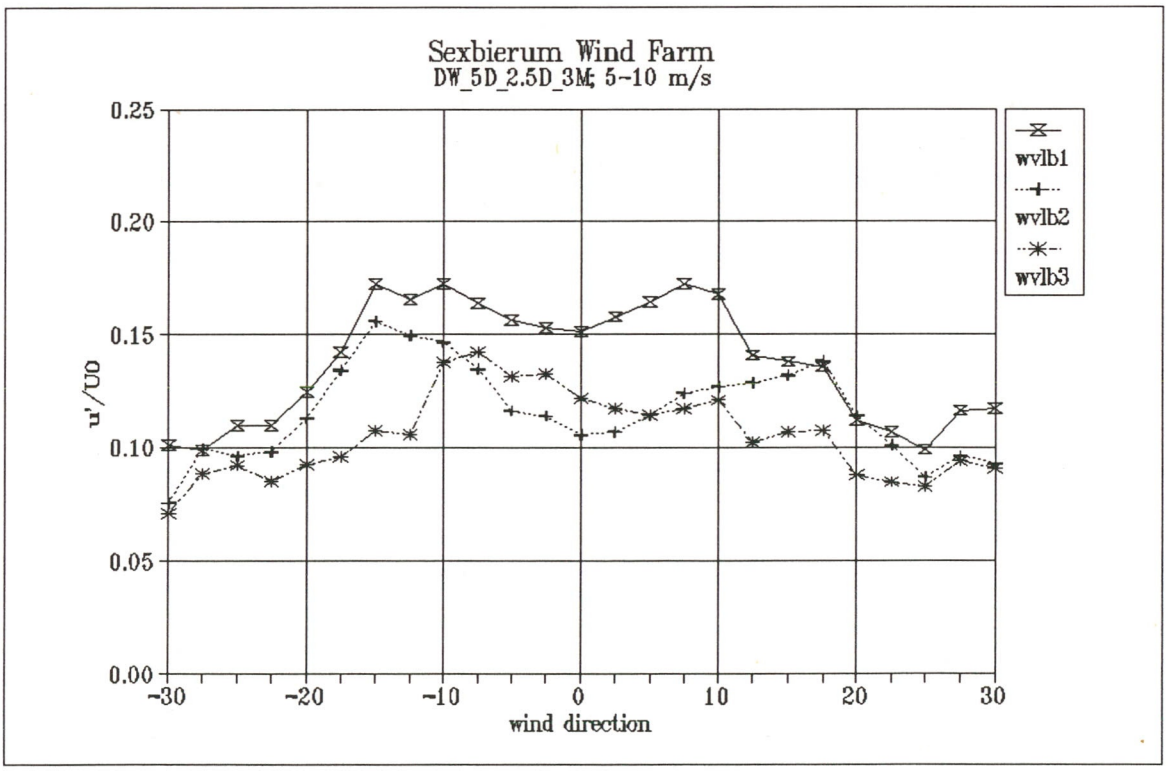

Figure 4 *Non-dimensionalized longitudinal turbulent fluctuations u'/U_0 as a function of wind direction in the wind speed bin 5-10 m/s*

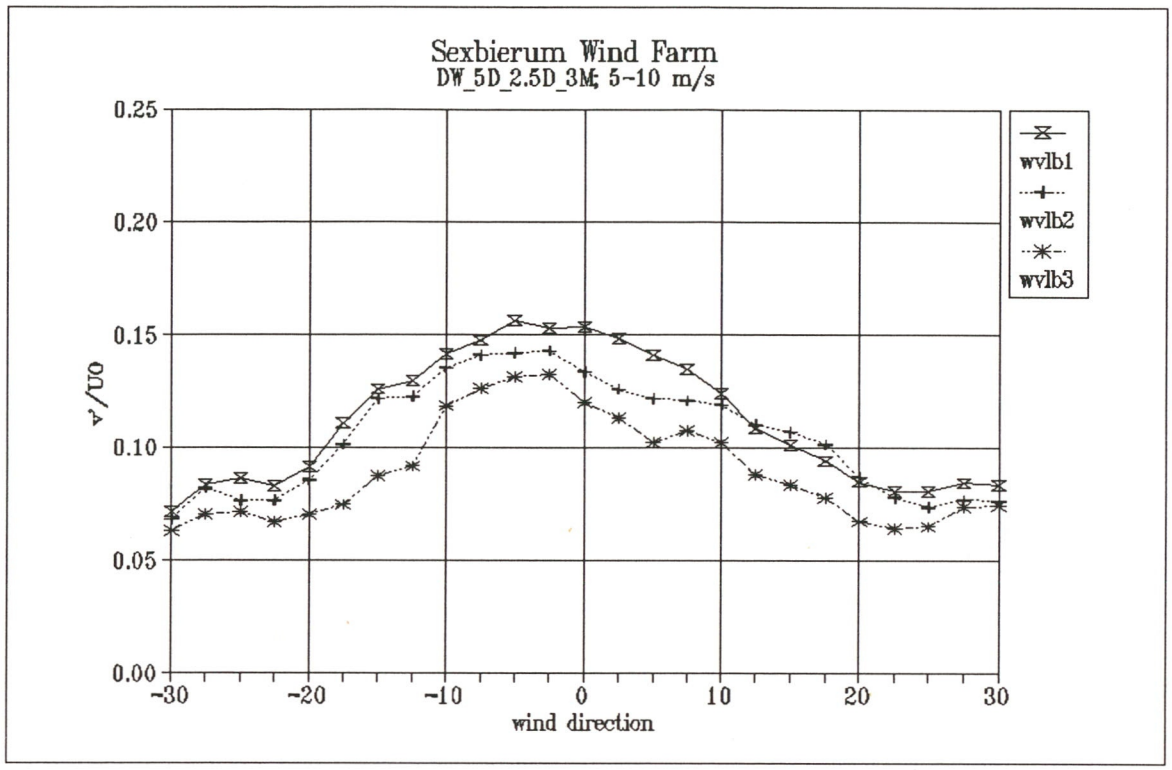

Figure 5 *Non-dimensionalized lateral turbulent fluctuations v'/U_0 as a function of wind direction in the wind speed bin 5-10 m/s*

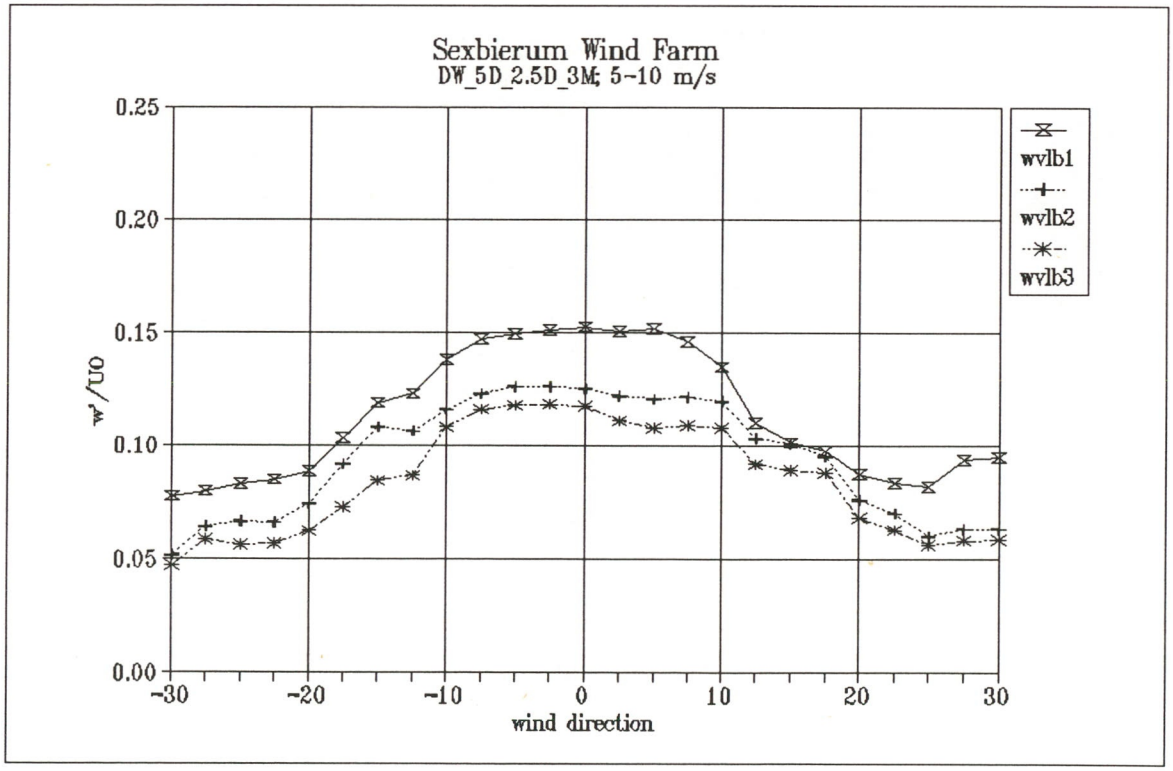

Figure 6 *Non-dimensionalized vertical turbulent fluctuations w'/U_0 as a function of wind direction in the wind speed bin 5-10 m/s*

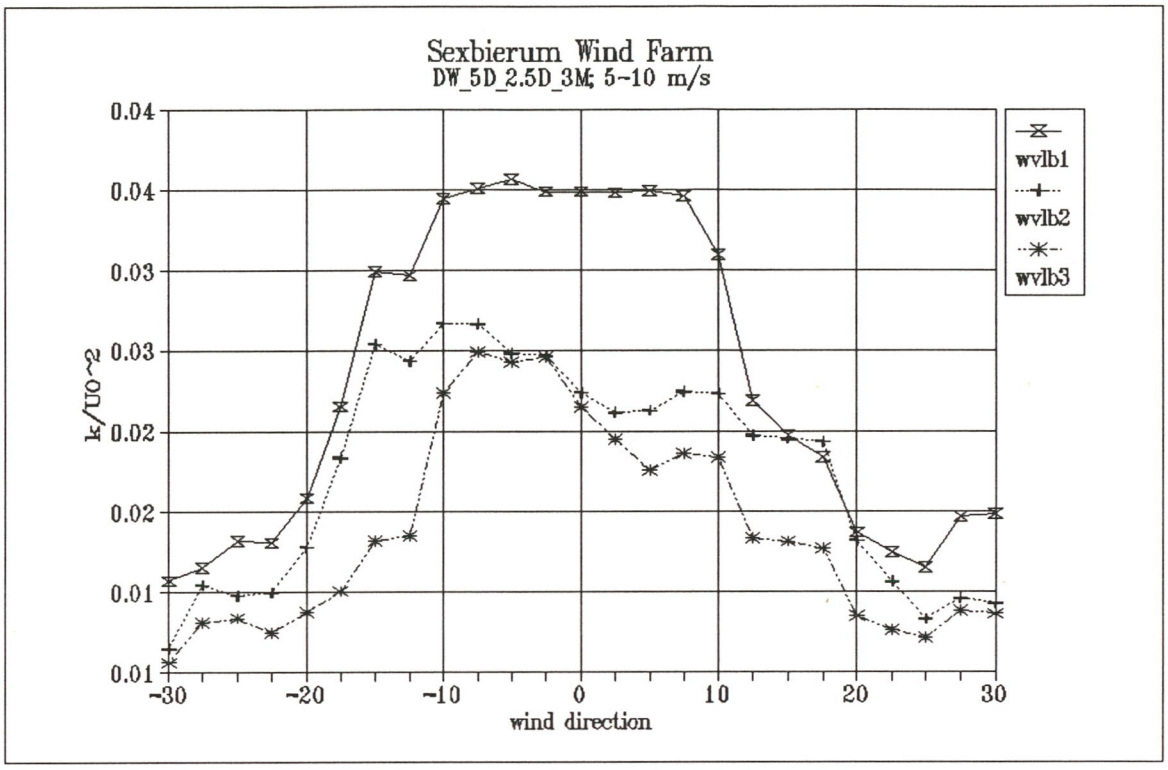

Figure 7 *Non-dimensionalized turbulent kinetic energy k/U_0^2 as a function of wind direction in the wind speed bin 5-10 m/s*

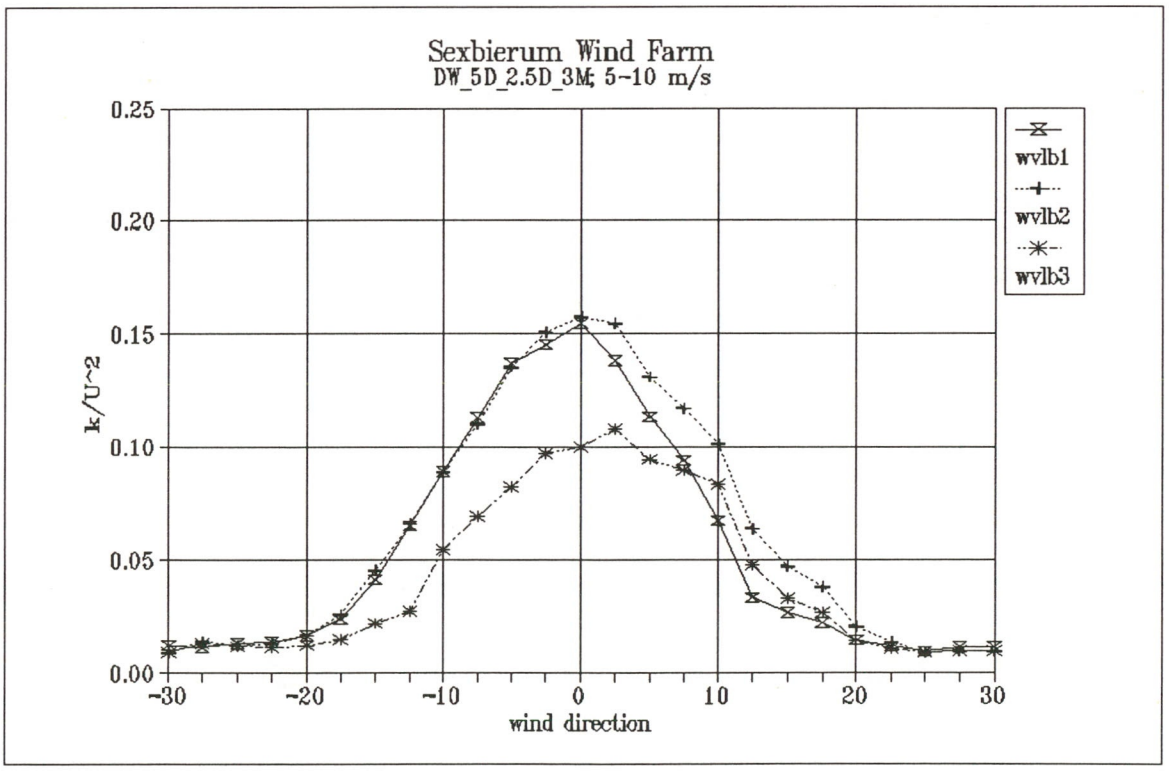

Figure 8 *Non-dimensionalized turbulent kinetic energy k/U^2 as a function of wind direction in the wind speed bin 5-10 m/s*

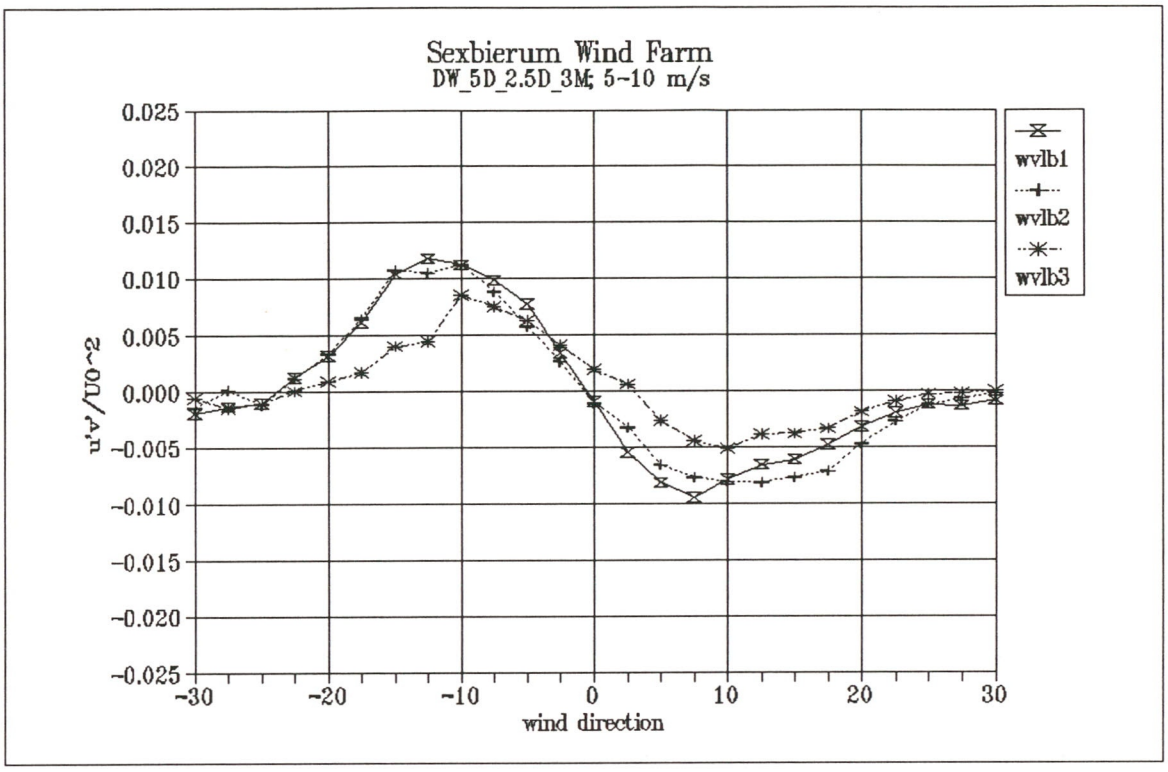

Figure 9 *Non-dimensionalized shear stresses $u'v'/U_0^2$ as a function of wind direction in the wind speed bin 5-10 m/s*

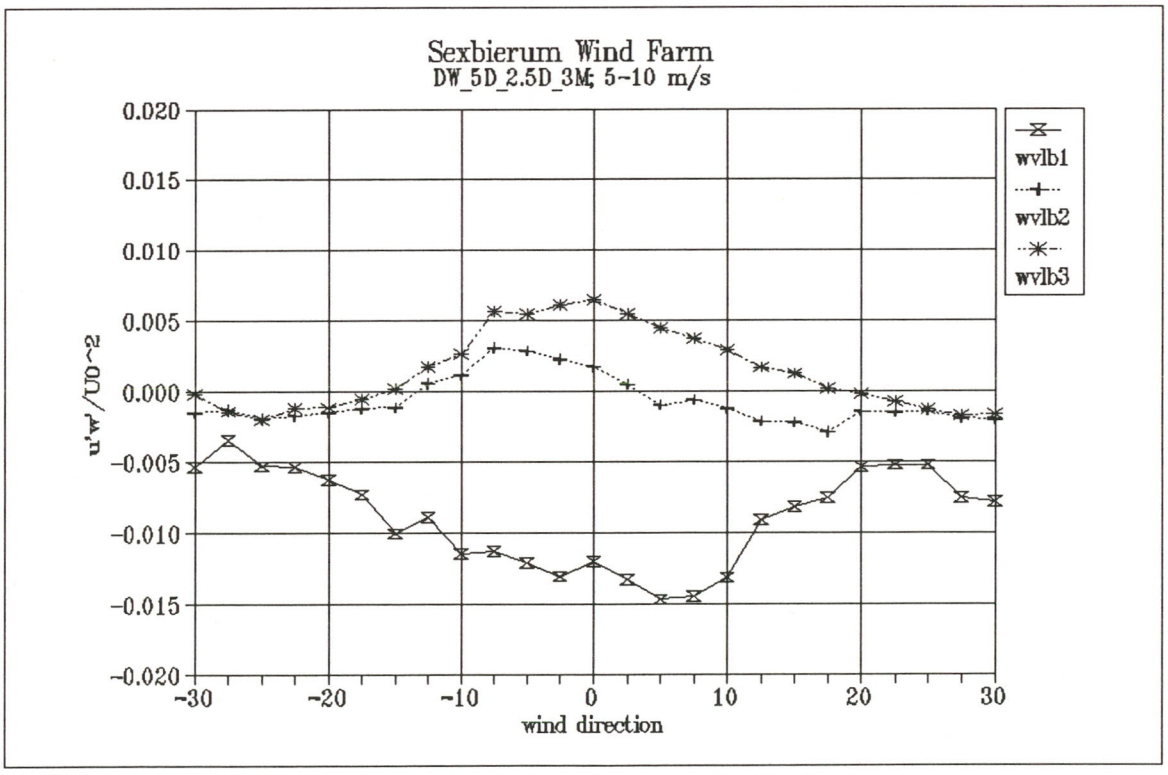

Figure 10 *Non-dimensionalized shear stresses $u'w'/U_0^2$ as a function of wind direction in the wind speed bin 5-10 m/s*

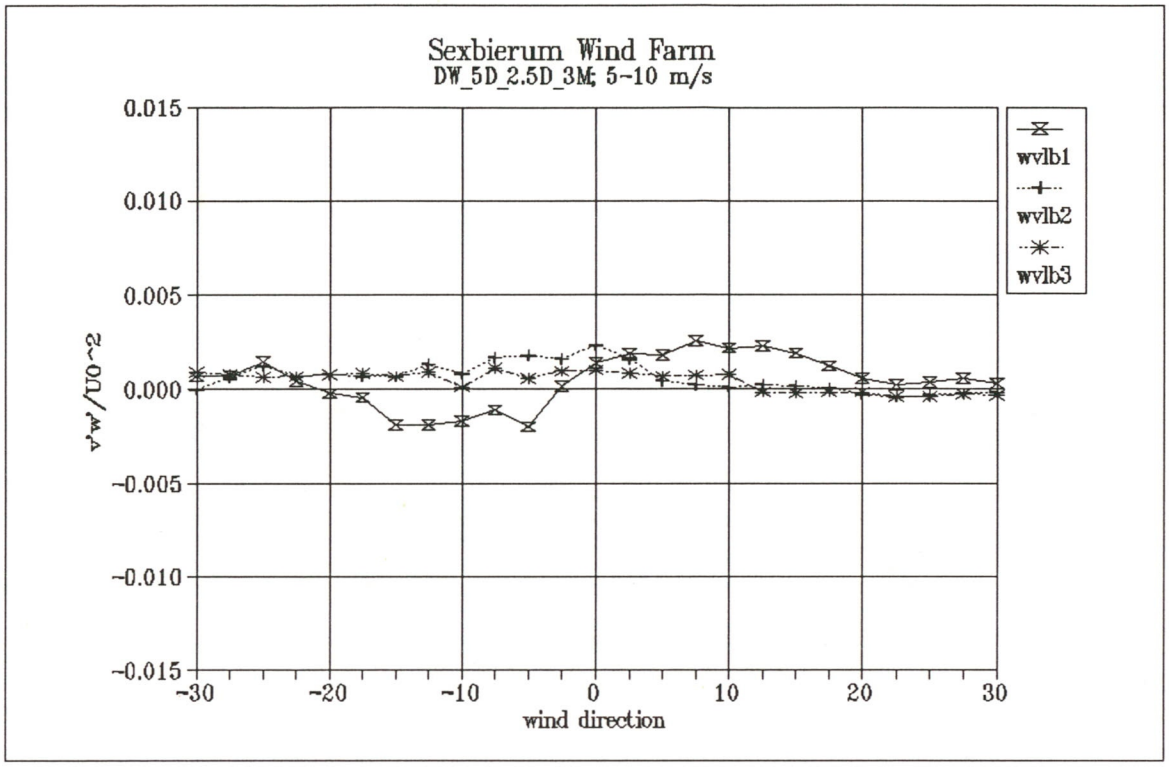

Figure 11 *Non-dimensionalized shear stresses $v'w'/U_0^2$ as a function of wind direction in the wind speed bin 5-10 m/s*

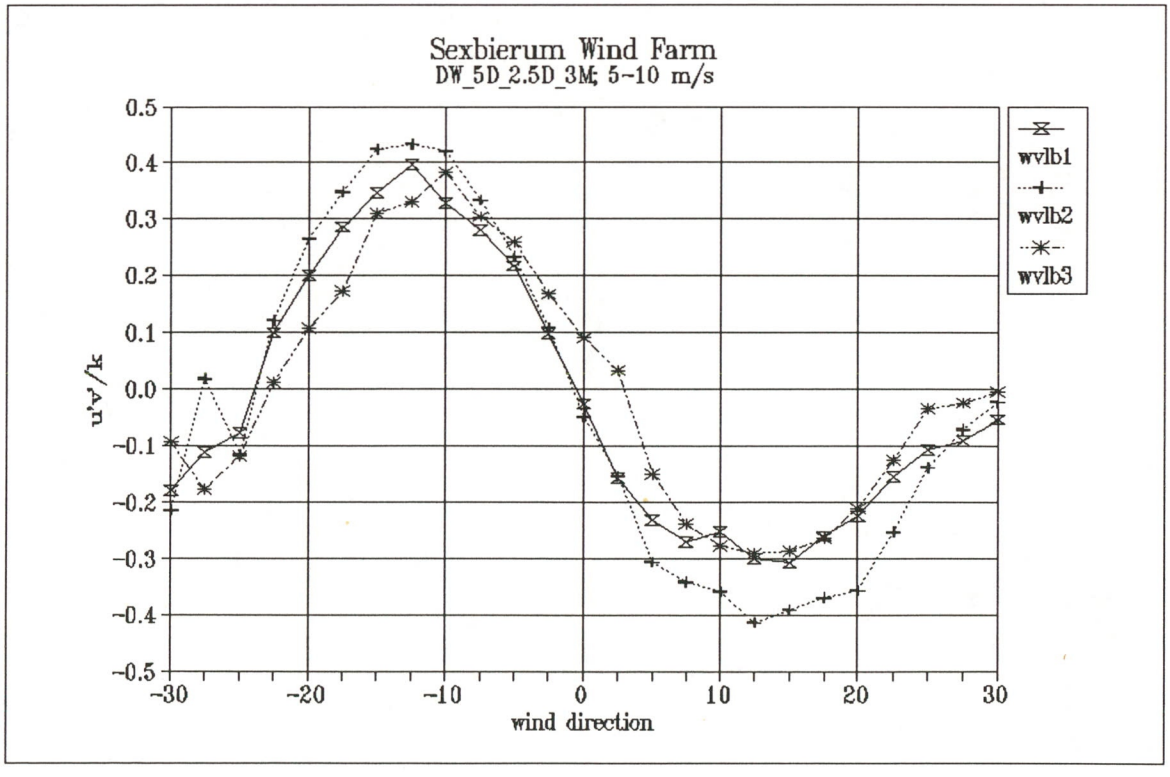

Figure 12 *Non-dimensionalized shear stresses u'v'/k as a function of wind direction in the wind speed bin 5-10 m/s*

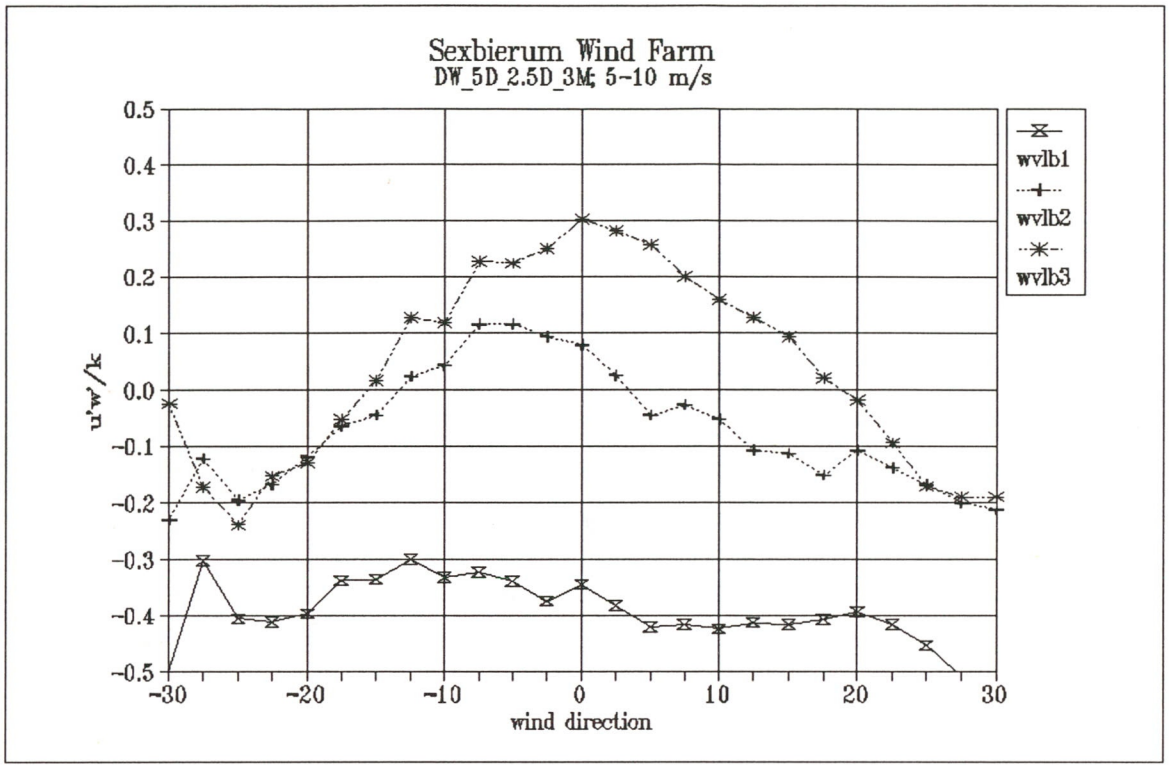

Figure 13 Non-dimensionalized shear stresses u'w'/k as a function of wind direction in the wind speed bin 5-10 m/s

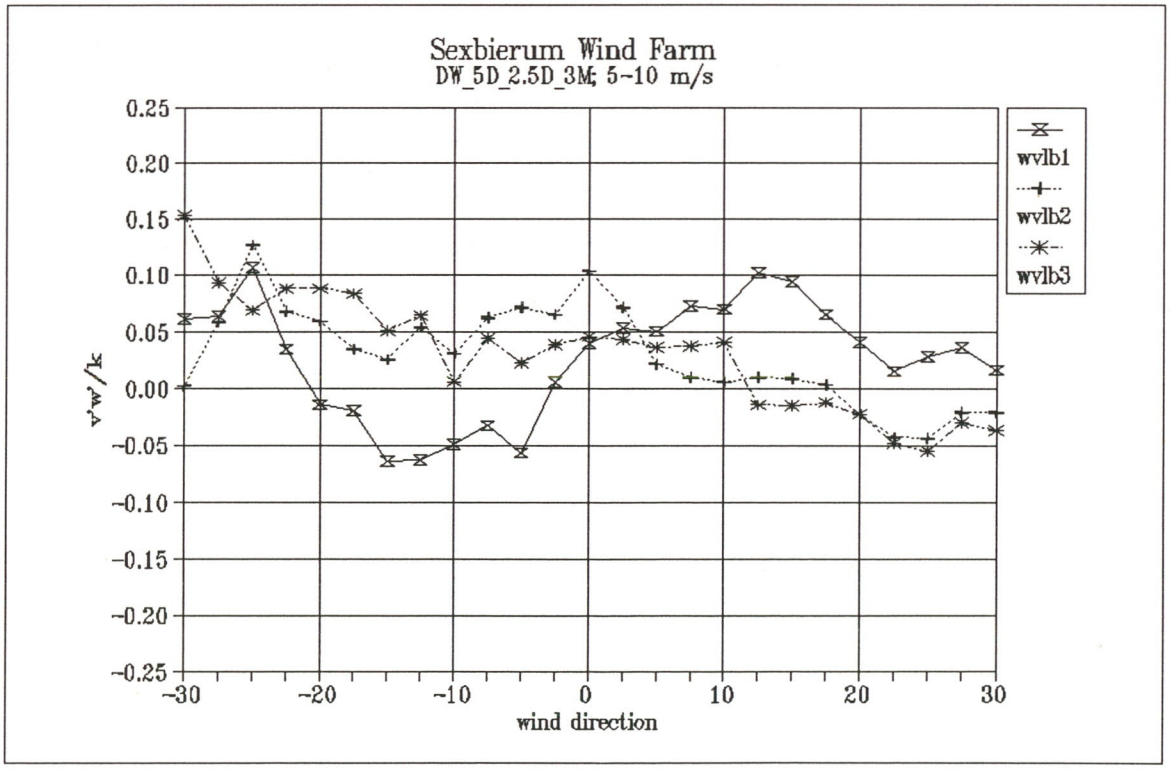

Figure 14 Non-dimensionalized shear stresses v'w'/k as a function of wind direction in the wind speed bin 5-10 m/s

A4.9 Horizontal profiles

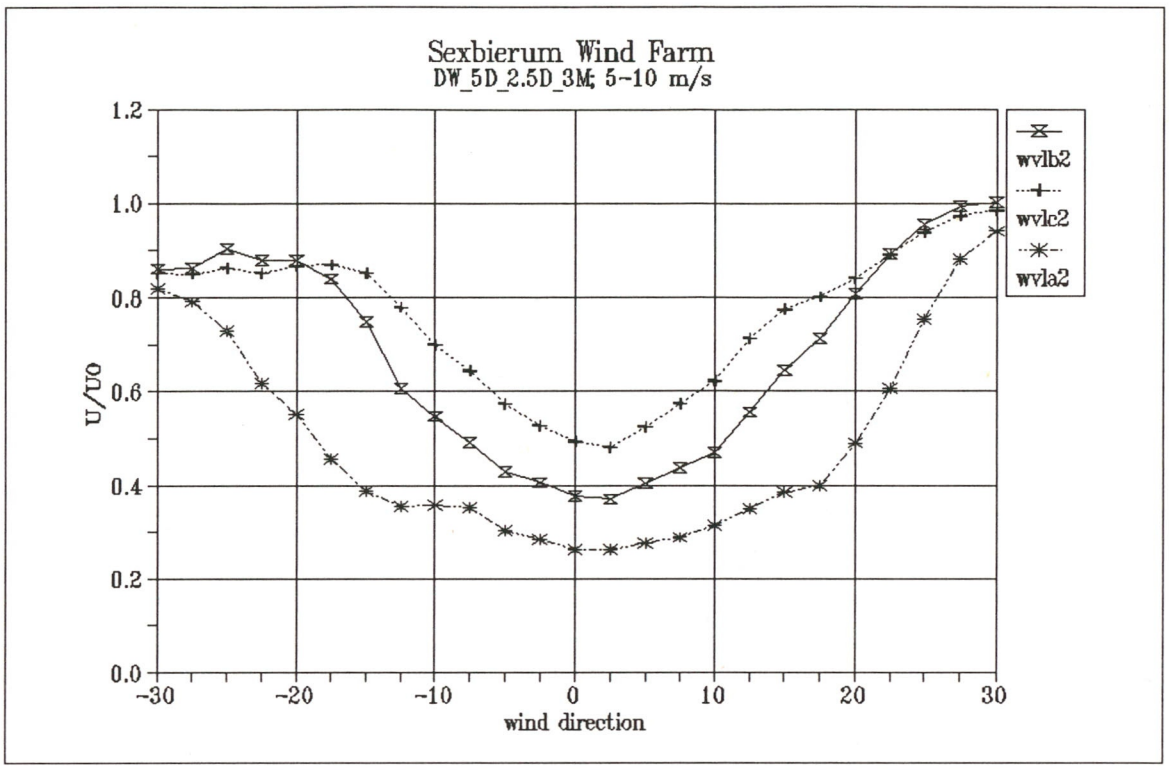

Figure 1 *Wake deficit U/U_0 as a function of wind direction in the wind speed bin 5-10 m/s*

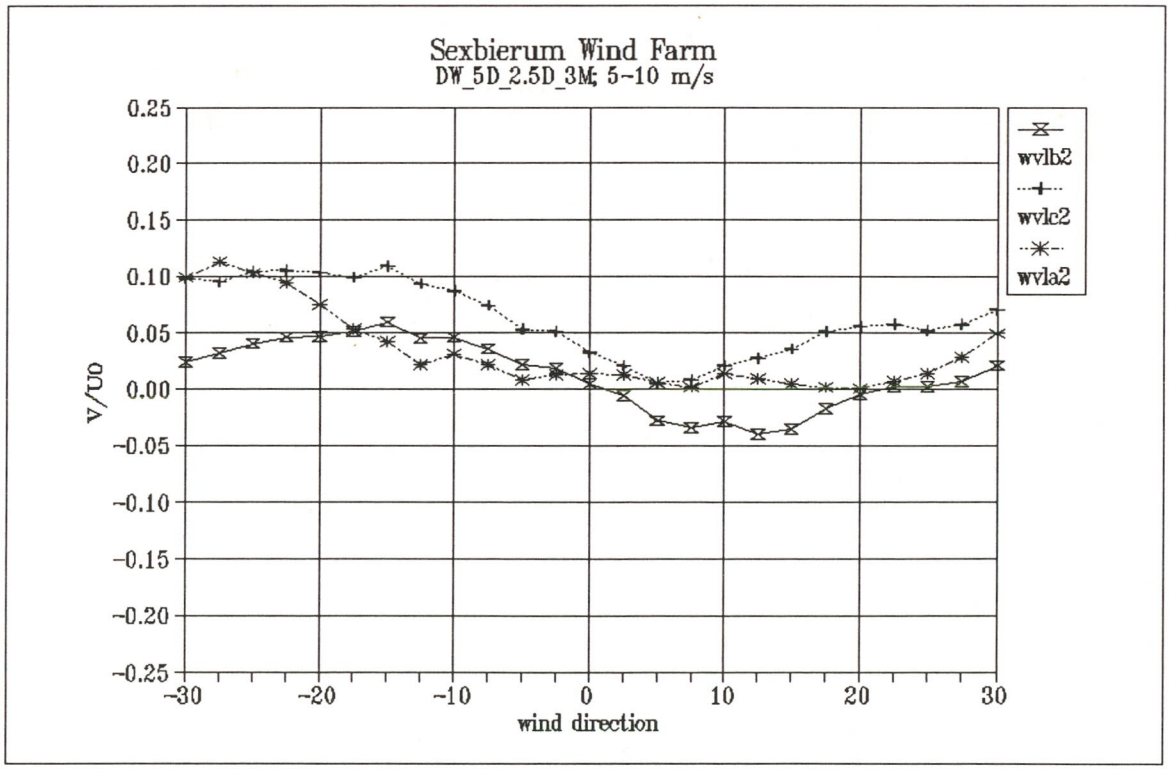

Figure 2 *Lateral wind speed V/U_0 as a function of wind direction in the wind speed bin 5-10 m/s*

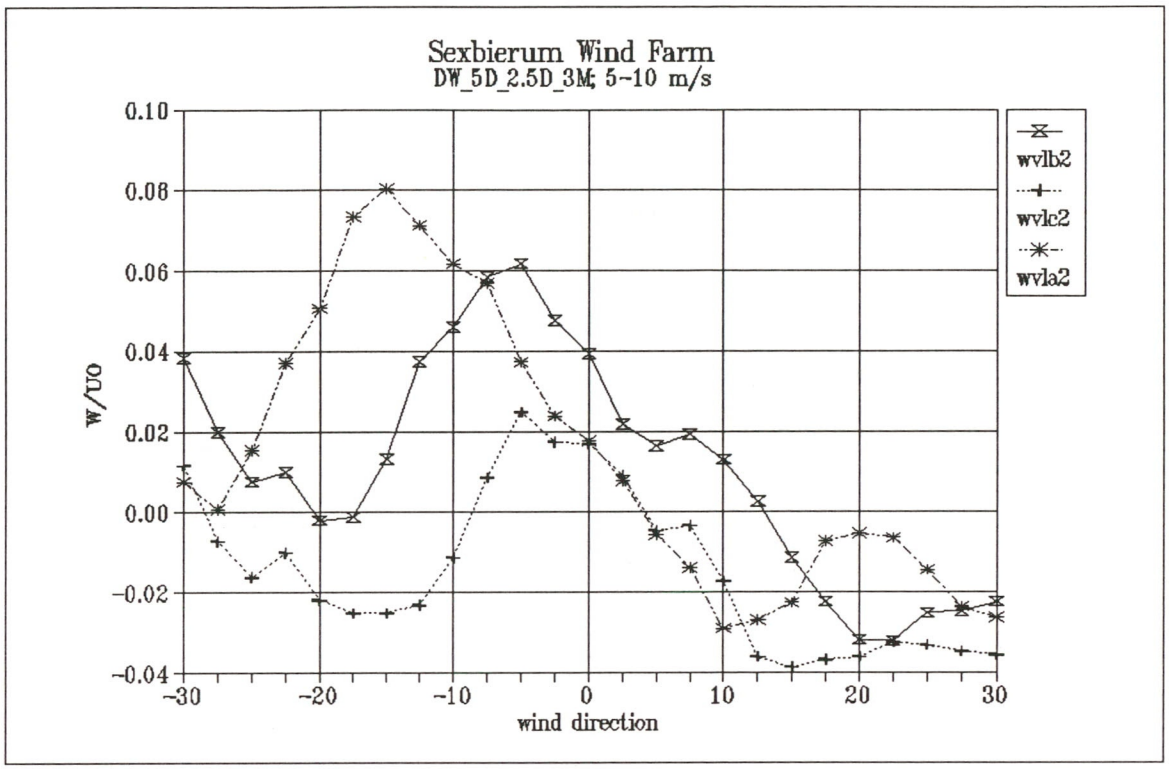

Figure 3 *Vertical wind speed W/U_0 as a function of wind direction in the wind speed bin 5-10 m/s*

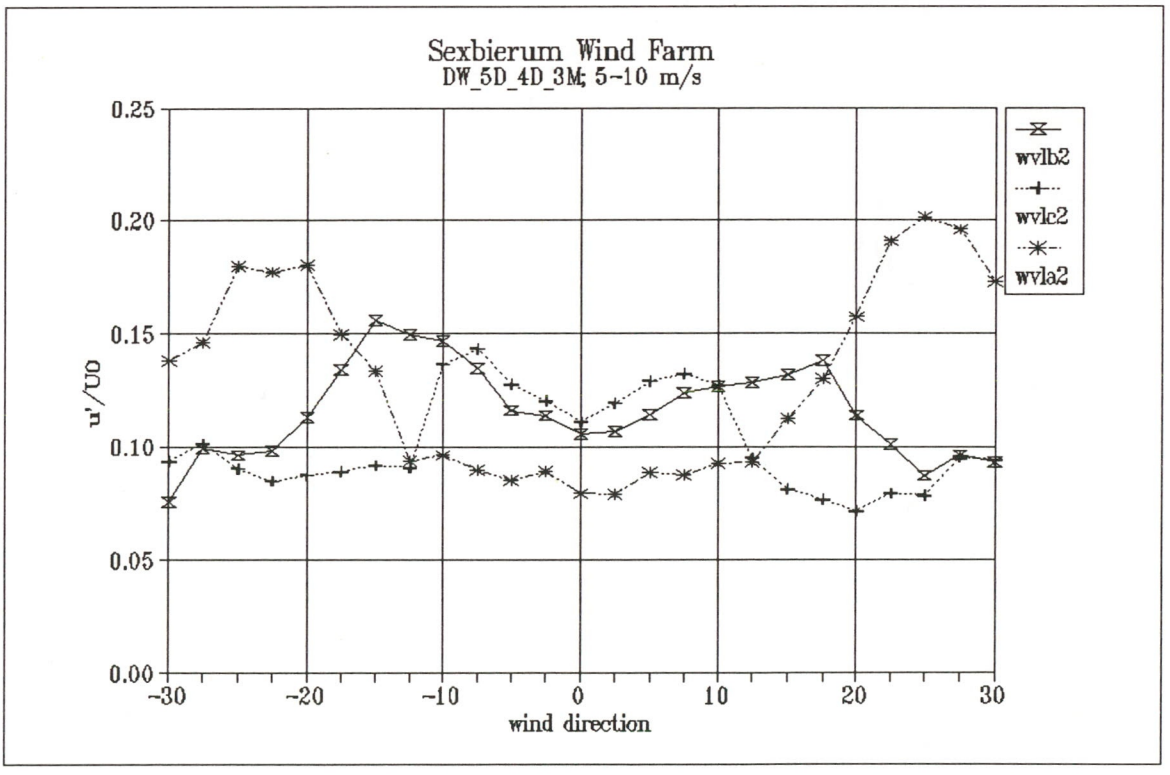

Figure 4 *Non-dimensionalized longitudinal turbulent fluctuations u'/U_0 as a function of wind direction in the wind speed bin 5-10 m/s*

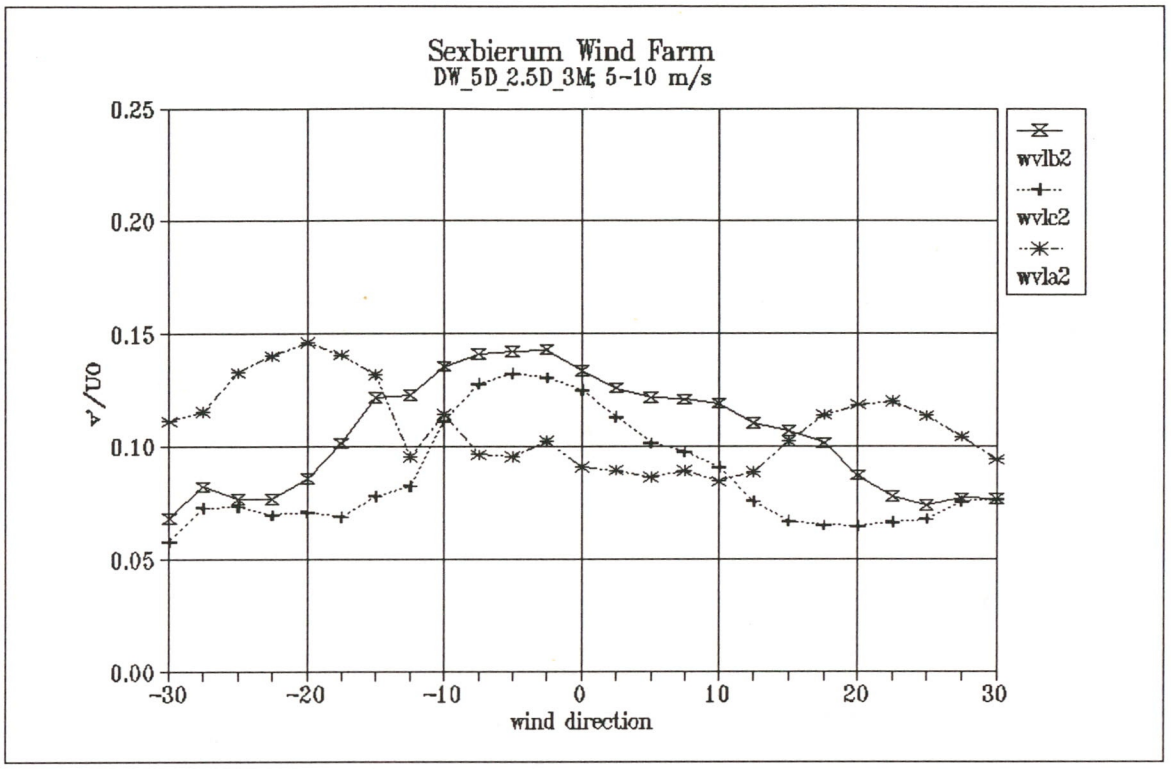

Figure 5 *Non-dimensionalized lateral turbulent fluctuations v'/U_0 as a function of wind direction in the wind speed bin 5-10 m/s*

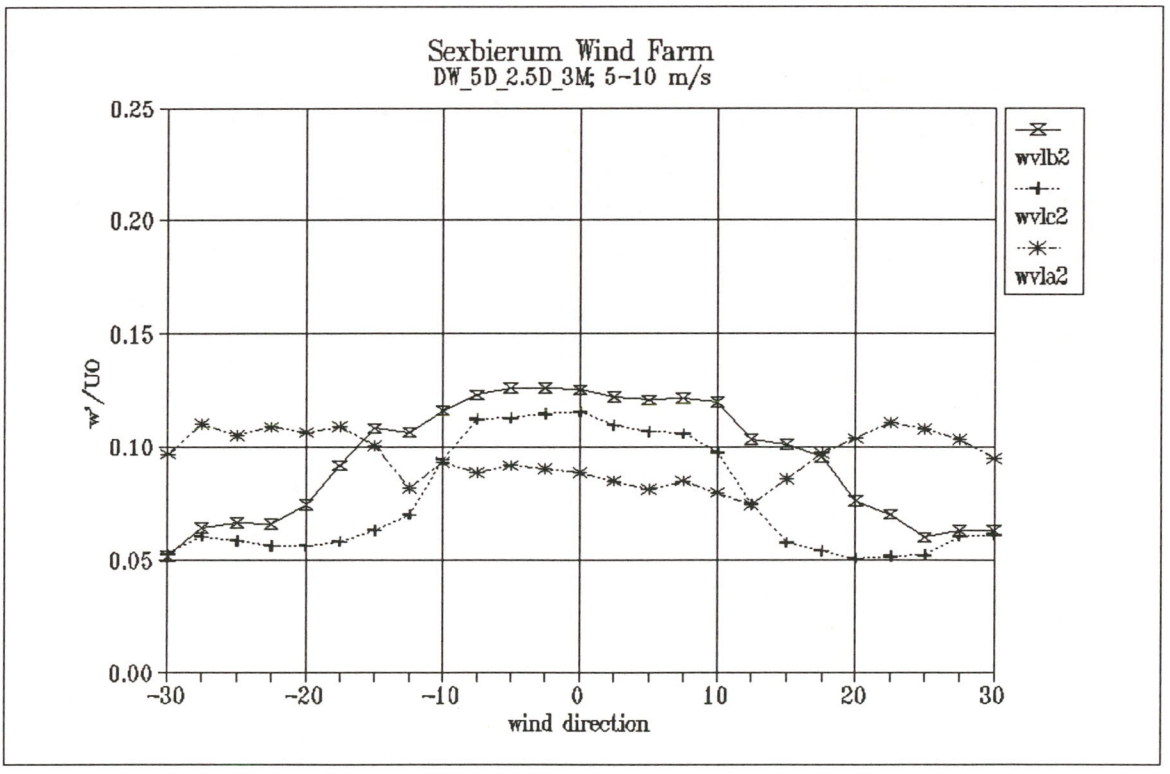

Figure 6 *Non-dimensionalized vertical turbulent fluctuations w'/U_0 as a function of wind direction in the wind speed bin 5-10 m/s*

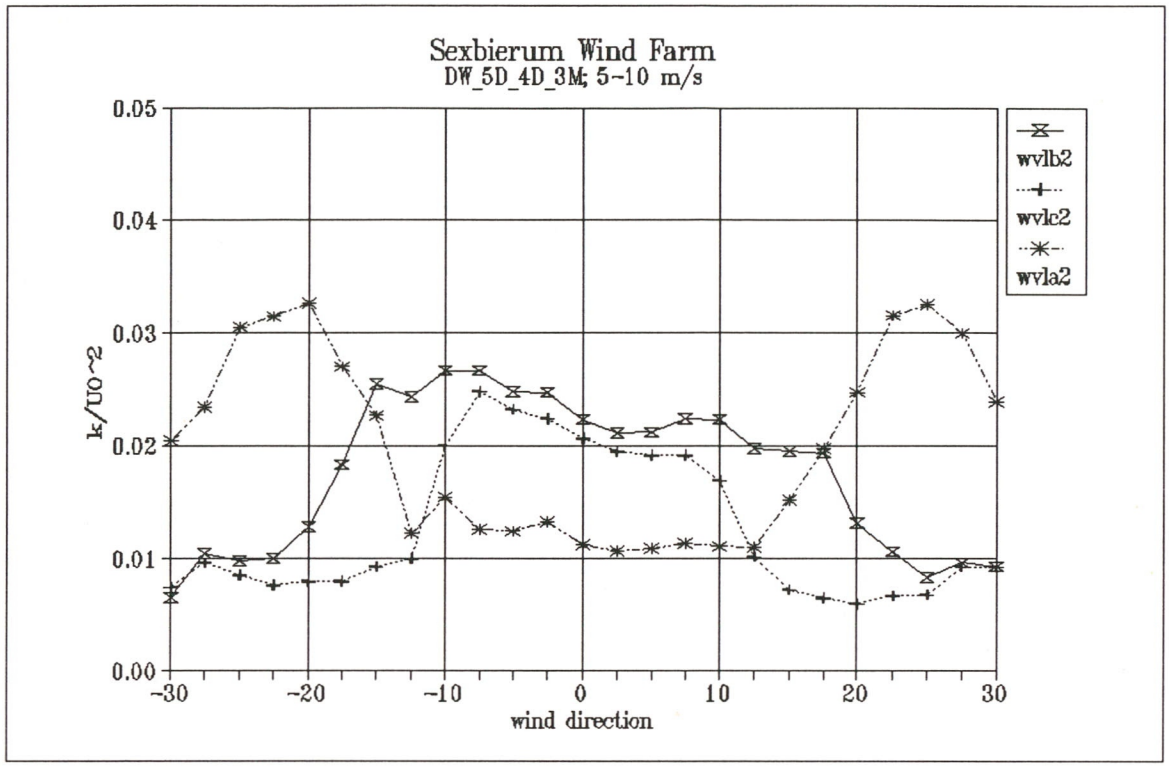

Figure 7 *Non-dimensionalized turbulent kinetic energy k/U_0^2 as a function of wind direction in the wind speed bin 5-10 m/s*

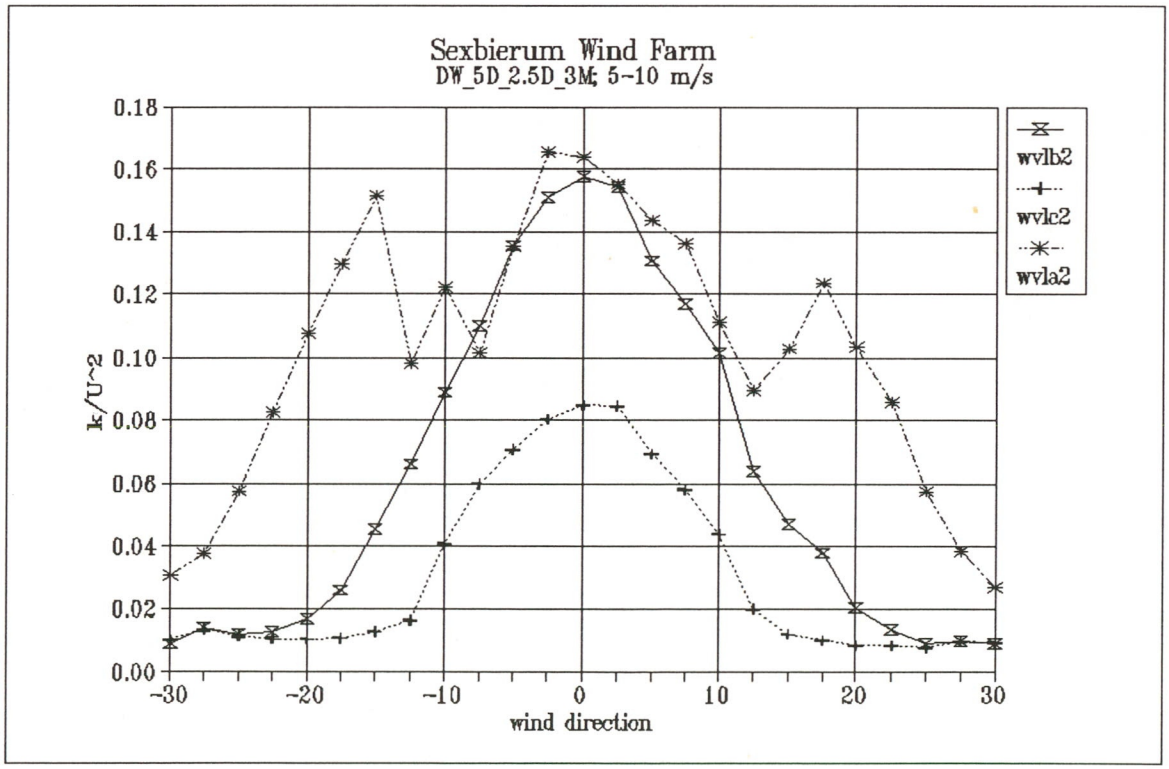

Figure 8 *Non-dimensionalized turbulent kinetic energy k/U^2 as a function of wind direction in the wind speed bin 5-10 m/s*

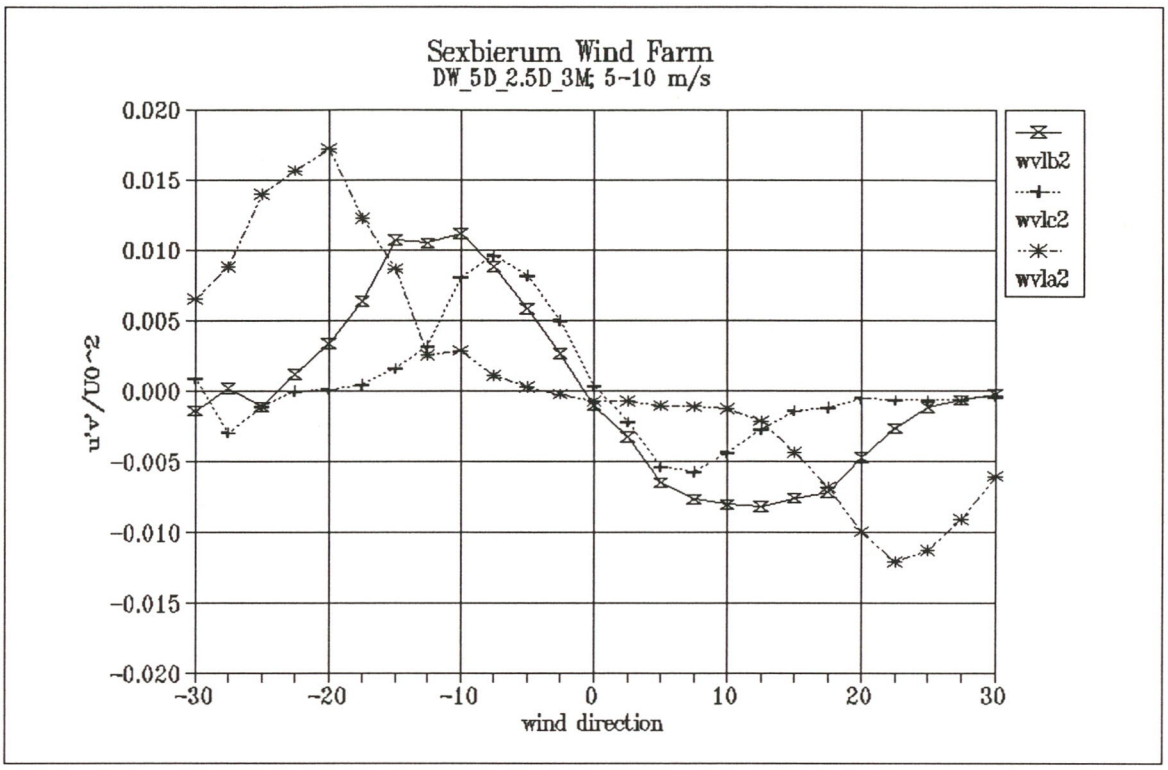

Figure 9 *Non-dimensionalized shear stresses $u'v'/U_0^2$ as a function of wind direction in the wind speed bin 5-10 m/s*

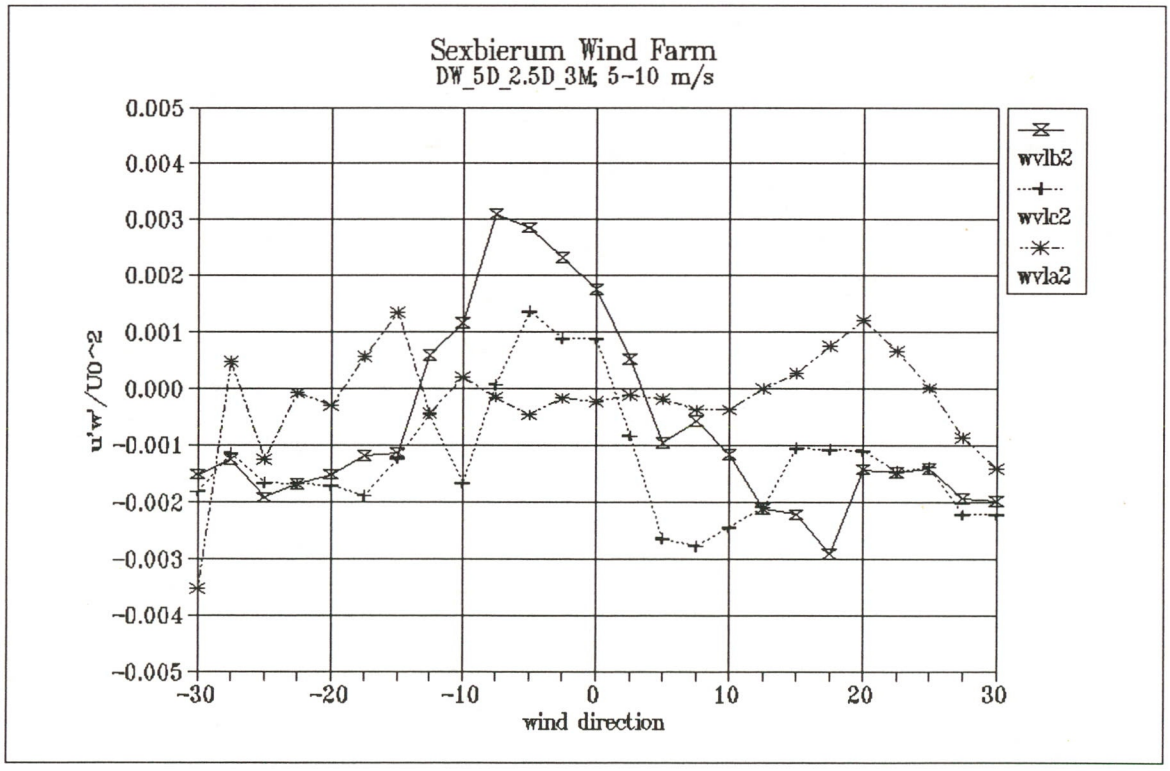

Figure 10 *Non-dimensionalized shear stresses $u'w'/U_0^2$ as a function of wind direction in the wind speed bin 5-10 m/s*

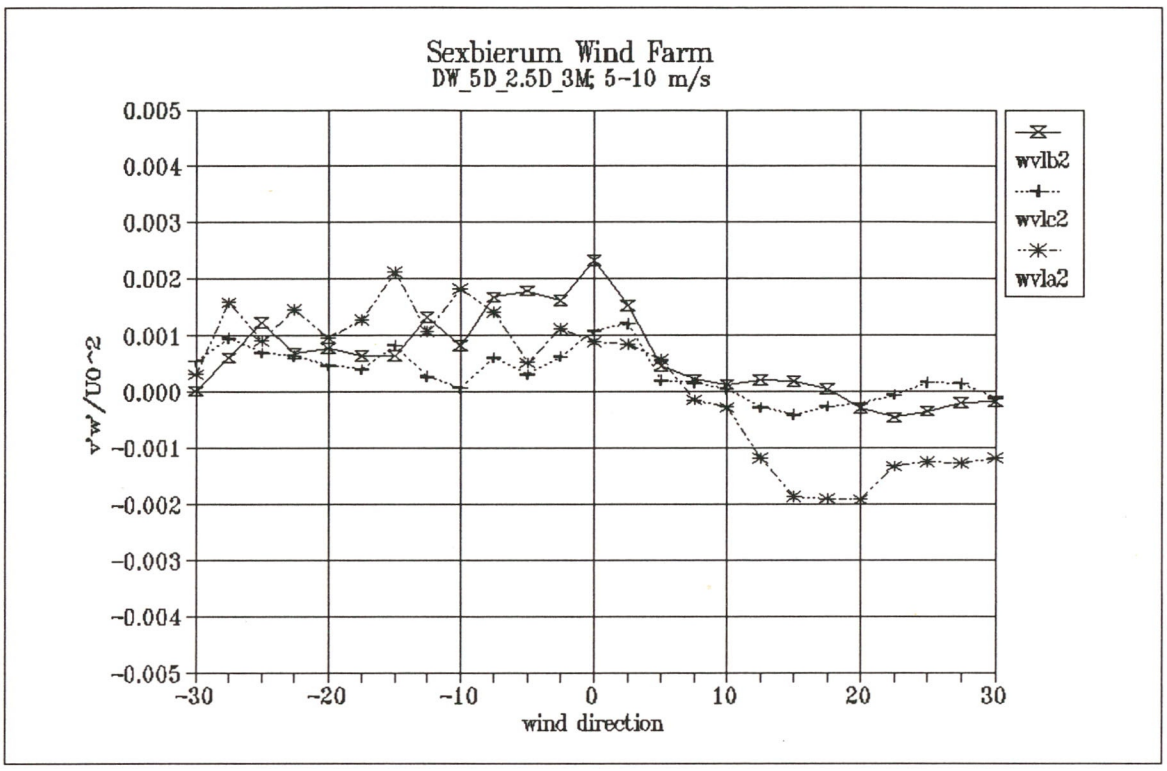

Figure 11 Non-dimensionalized shear stresses $v'w'/U_0^2$ as a function of wind direction in the wind speed bin 5-10 m/s

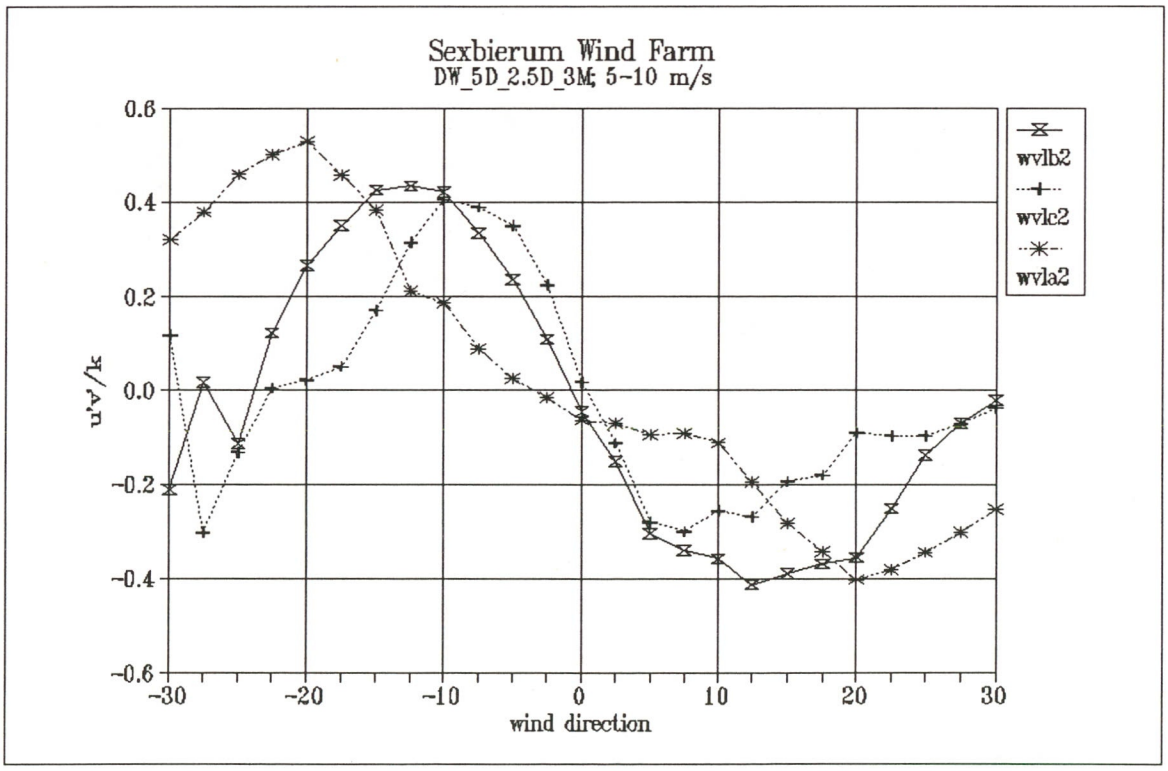

Figure 12 Non-dimensionalized shear stresses u'v'/k as a function of wind direction in the wind speed bin 5-10 m/s

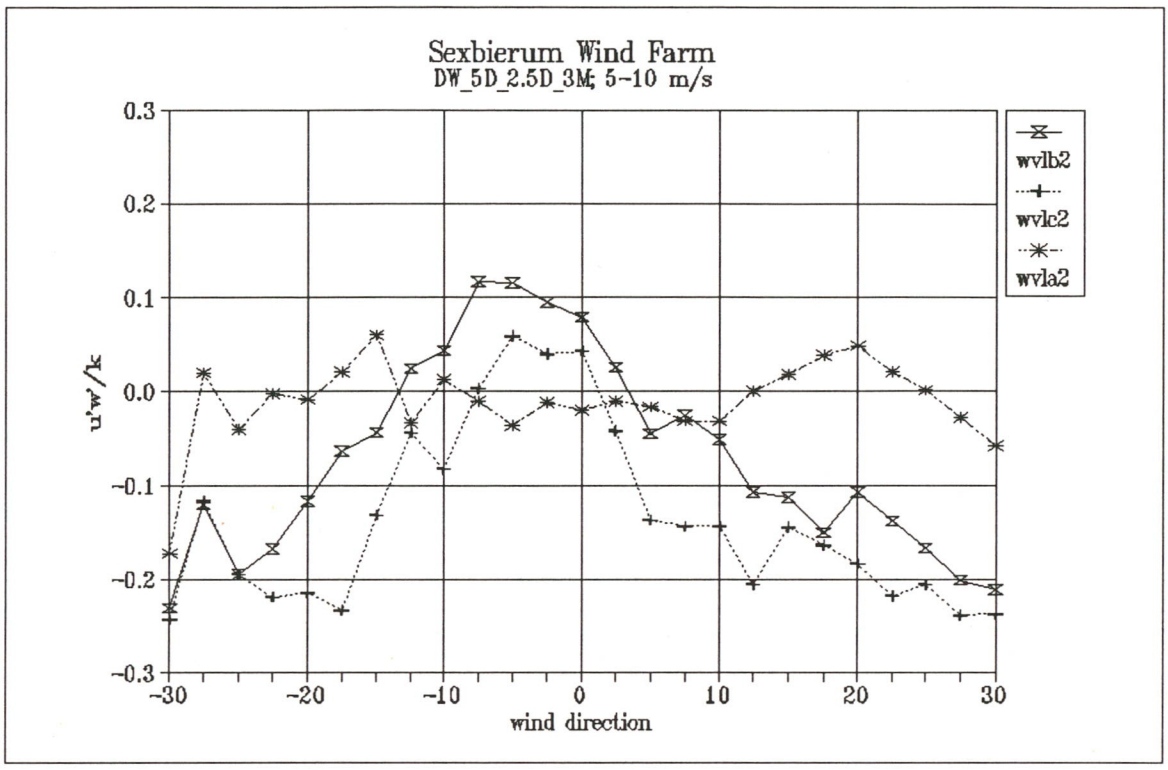

Figure 13 Non-dimensionalized shear stresses u'w'/k as a function of wind direction in the wind speed bin 5-10 m/s

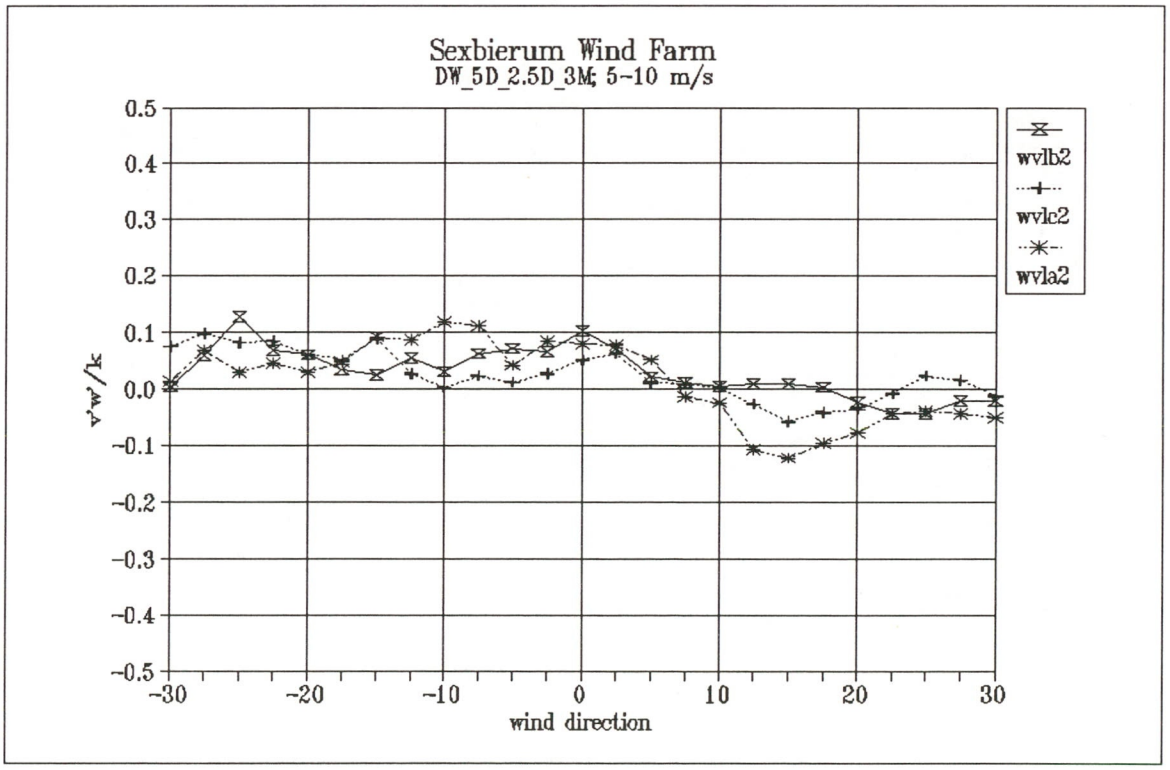

Figure 14 Non-dimensionalized shear stresses v'w'/k as a function of wind direction in the wind speed bin 5-10 m/s